



McGinley & Associates

**Reno**

815 Maestro Drive  
Reno, Nevada 89511  
Ph: 775.829.2245

**Las Vegas**

1915 N. Green Valley Parkway  
Suite 200  
Henderson, Nevada 89074  
Ph: 702.260.4961

[www.mcgin.com](http://www.mcgin.com)

- | Site Remediation
- | Soil & Groundwater Investigations
- | Geochemistry
- | Hydrogeology
- | Groundwater Modeling
- | Biological Services
- | Closure Optimization
- | Air Quality Permitting & Modeling
- | Brownfields Redevelopment
- | Permitting & Compliance
- | NEPA Studies
- | Phase I Assessments
- | Indoor Air Quality
- | Storm Water & Spill Plans
- | Underground Tank Services
- | Geographic Information Systems
- | Litigation Support & Expert Witness
- | Mining Plans of Operations
- | Mining Exploration Notices
- | Abandoned Mine Lands

# NUMERICAL GROUNDWATER FLOW MODEL REPORT

## Fort Cady Project San Bernardino County California

*Prepared for:*

***Fort Cady California Corporation  
16195 Siskiyou Rd, #210  
Apple Valley, CA 92307***

***November 11, 2019***

***Amended April 7, 2020***

## TABLE OF CONTENTS

EXECUTIVE SUMMARY .....	I
1. INTRODUCTION .....	1
1.1 Objective .....	1
1.2 Project Location .....	1
1.3 Solution Mining Plan.....	1
1.3.1 Process Solution Injection and Recovery .....	1
1.3.2 Process Water Supply.....	1
1.4 Purpose of the Groundwater Model.....	2
2. HYDROGEOLOGY.....	2
2.1 Geological Setting .....	2
2.1.1 Regional Geology.....	2
2.1.2 Local Geology .....	3
2.2 Hydrogeologic Setting .....	4
2.2.1 Groundwater Basins.....	4
2.2.2 Watersheds .....	4
2.2.3 Nearest Wells and Groundwater Uses.....	4
2.2.4 Springs and Streams of Significance .....	5
2.3 Groundwater Depths and Elevations .....	5
2.3.1 Project Area Wells.....	5
2.3.2 Surrounding Area Wells .....	5
2.3.3 Groundwater Flow Directions and Gradient.....	5
2.4 Hydraulic Properties of Subsurface Materials.....	7
2.4.1 Ore Body and Evaporates.....	7
2.4.2 Mudstone and Claystone Sediments .....	7
2.4.3 Local Alluvial Aquifers West of Pisgah Fault and East of Fault B.....	7
2.5 Conceptual Water Budget .....	10
2.5.1 Recharge Estimation.....	10
2.5.2 Subsurface Inflow.....	10
2.5.3 Subsurface Outflow.....	10
2.6 Groundwater Quality .....	11
3. SIMULATION OF THE GROUNDWATER FLOW SYSTEM.....	12
3.1 Conceptual Model .....	12
3.2 Modeling Approach .....	12
3.3 Modeling Codes .....	13
3.4 Steady-State Model Construction .....	13
3.4.1 Spatial Discretization.....	13
3.4.2 Model Layering.....	13
3.4.3 No-Flow Boundaries.....	15
3.4.4 General Head Boundaries .....	15
3.4.5 Horizontal Flow Barriers.....	15
3.4.6 Recharge (Specified Flux) Boundaries .....	16
3.4.7 Hydraulic Conductivity Properties .....	17
3.4.8 Potentiometric Head (Water Level) Targets used for Calibration .....	18
3.4.9 Calibration Technique .....	19
3.4.10 Simulated Heads and Calibration Quality .....	20
3.4.11 Simulated Steady-State Flow of Groundwater.....	20
3.4.12 Parameter Sensitivity Testing .....	21

4.	PREDICTIVE MODELING .....	22
4.1	Transient Modeling Parameters .....	22
4.1.1	Specific Storage Values .....	22
4.1.2	Effective Porosity .....	22
4.1.3	Pumping and Injection Wells.....	22
4.1.4	Daily Test Modeling Injection and Pumping Cycle.....	23
4.1.5	Long-Term Mining Simulation .....	25
4.1.6	Solute Transport Parameters.....	26
4.1.7	Land Subsidence Parameters.....	27
4.2	Transient Long-term Modeling Results.....	29
4.3	Development and Refinement of the AOR and ZEI Boundaries .....	32
5.	SUMMARY AND CONCLUSIONS.....	33
6.	LIMITATIONS.....	35
7.	CLOSING .....	36
8.	REFERENCES .....	37

## TABLES

Table 1	Project Area Groundwater Elevations and TDS Measurements
Table 2	Regional Groundwater Elevations Outside Model Domain
Table 3	Subsurface Hydraulic Properties Summary
Table 4	Historical Baseline Water Quality Information
Table 5	Summary of Model Layering
Table 6	Descriptions of General Head Boundaries
Table 7	Summary of Modeled Hydrologic Flow Barriers
Table 8	Summary of Modeled Recharge Zones
Table 9	Summary of Hydraulic Conductivity Attributes
Table 10	Steady-State Model Calibration Summary Statistics
Table 11	Daily Injection and Pumping Cycles in the Stress Testing Model
Table 12	Hydraulic Property Changes for Daily Stress Testing Model
Table 13	Simulated Pumping and Injection in Stress Test Modeling
Table 14	Pumping Simulation in the Long-Term Model
Table 15	Predicted Potentiometric Water Level Change at Modeled Observation Points
Table 16	Predicted Solute Transport Detection at Modeled Observation Wells

## FIGURES

Figure 1	Project Location Map
Figure 2	Site Map Showing Fort Cady Project Area and Groundwater Well Locations
Figure 3	Project Area Geologic Setting
Figure 4	Geologic Cross Sections
Figure 5	Project Area Groundwater Basins and Surrounding Area Wells
Figure 6	Project Area Watershed Boundaries
Figure 7	Groundwater Elevations in the Project Area and Vicinity
Figure 8	Groundwater Model Domain
Figure 9	Representative Model Layers
Figure 10	Model Boundary Conditions
Figure 11	Modeled Potentiometric Groundwater Surface
Figure 12	Simulated versus Measured Water Levels at Head Targets

Figure 13	Results of Horizontal and Vertical Conductivity Sensitivity Analysis
Figure 14	Results of GHB and Hydraulic Flow Barrier HFB Sensitivity Analysis
Figure 15	Results of Recharge Rate Sensitivity Analysis
Figure 16	Proposed Well Field Areas and Daily Stress Test Well Locations
Figure 17	Extent of Layer 6 Drawdown in after 100 days Under Low K and Ss
Figure 18	Extent of Layer 6 Drawdown in after 100 days under Mid K and Ss
Figure 19	Extent of Layer 6 Drawdown in after 100 days under High K and Ss
Figure 20	Mining Simulation Well Locations
Figure 21	Simulated Drawdown at Model Observation Points
Figure 22	Simulated Extent of Solute Transport, Area of Review Boundary, and Proposed Monitoring Wells
Figure 23	Cross-Section Showing Vertical and Lateral Extent of Predicted Solute Transport at Mine Year 25
Figure 24	Simulated Particle Concentrations at Model Observation Points
Figure 25	Predicted Land Subsidence at Mine Year 25

## **APPENDICES**

Appendix A	Model Layer Hydraulic Conductivity Distributions
Appendix B1	Potentiometric Head Change in Model Layers at Mine-Year 25
Appendix B2	Potentiometric Head Change in Layer 7 at 3-year Mine Progression Intervals
Appendix C1	Solution Concentration in Model Layers at Mine-Year 25
Appendix C2	Solution Concentration in Model Layer 7 at 3-year Mine Progression Intervals
Appendix D	Predicted Concentrations and Potentiometric Head Changes at AOR and ZEI Monitoring Wells and Observation Wells



## EXECUTIVE SUMMARY

A numerical groundwater flow model has been developed by McGinley and Associates, Inc. (MGA) of Reno, Nevada, and Interflow Hydrology, Inc. of Truckee, California (Interflow) to simulate the effects of solution mining of borate from the Fort Cady deposit (the Project). MGA and Interflow have prepared this report for Fort Cady California Corporation (FCCC) to summarize the methodology and results of the groundwater flow model and support the underground injection control (UIC) permit that is being evaluated by the US Environmental Protection Agency (EPA). The Project is located 35 miles east of Barstow, California, in the Mojave Desert.

The project is geographically situated in the Hector Basin, a NW-SE trending valley comprised of Tertiary fine-grained lacustrine (lake bed) and playa deposits that is bounded to the southwest and northeast by the Quaternary faults of the Eastern California shear zone, which have been previously demonstrated to be groundwater flow barriers. The ore body is comprised of borate-rich evaporite mineral beds situated between 1,300 and 1,500 feet below ground surface. Surface and groundwater recharge to the fault-bounded block of lakebed sediments is extremely limited, such that ore zone formation water contains elevated total dissolved solids (TDS) concentrations between 23,300 and 31,000 mg/L in formation water samples. Due in part to the lack of groundwater resources in the Project area, the nearest drinking water well is located approximately seven miles to the northwest of the Project, at the eastern outskirts of Newberry Springs, California.

The solution mining process involves injection of a dilute hydrochloric acid solution (<5% HCl) into the evaporite ore body, followed by pumping to recover the pregnant solution containing dissolved borate. Mining will be conducted in three (3) blocks, which for purposes of modeling, were divided into 16 mining areas. This model was developed for the ultimate ore body, to inform and construct the mining Zone of Endangering Influence (ZEI) and Area of Review (AOR). Based on the modeling results, the extent of the ore body in the UIC permit application was contracted on the northwestern and southeastern sides to ensure the ZEI from the proposed activity remains within the EIS boundary.

The modeled injection-recovery cycles occur daily and proceed through the sixteen modeled well-field areas in sequence, ultimately recovering borate solution from an approximate 495-acre subsurface ore body. Sequential cycles of injection and recovery from the well field areas were simulated in a transient groundwater flow model, developed from a calibrated steady-state model of existing conditions. The results were then used to determine the extent of the ZEI and associated AOR for UIC permitting.

The groundwater model was used to conservatively estimate that the potential for solution migration outside the well fields is limited to a ZEI boundary that extends an average of approximately 1,100 feet from the ore body and is generally 1,300 feet from the downgradient (eastern) boundary of the wellfield and 800 feet from the upgradient (western) boundary of the ore body. The ZEI boundary was defined in the groundwater model as the 0.01% relative concentration contour of the solute transport simulation (effectively zero). The AOR boundary was established at 100 to 300 feet outside the AOR boundary, based on the extent of simulated post-mining solute transport.

No third-party wells are located within the AOR, and no known underground sources of drinking water (USDWs) occur within the fault bounded wedge where the Project is located. The solution mining injectate is not predicted to migrate into alluvial materials outside the Pisgah Fault or Fault B, nor is it predicted to reach those faults. Injectate is not predicted to migrate into the deep basal conglomerate layer below the sequence of lacustrine deposits and on top of the andesite bedrock.

The groundwater model demonstrates that solution migration in the surrounding formation is limited to the immediate vicinity of the ore body. Furthermore, the solute transport modeling includes advection and dispersion, but does not include natural decay, reaction or absorption factors, and is therefore believed to be a conservative representation of potential transport of injectate in the

surrounding formation. Monitoring of pressures and concentrations in the ore body and adjacent formation during project operations will enable future versions of the numerical flow model to be calibrated to include these variables. Eight observation wells (OW-1 to OW-8) are situated within the AOR boundary to collect data on pressure and injectate solution migration. Twelve additional monitoring wells (MW-1 to MW-5, MW-7, AOR-1 to AOR-5, AOR-7) are situated on and directly outside the AOR boundary, to serve as verification that injectate solution is not migrating beyond the established AOR boundary.

# 1. INTRODUCTION

## 1.1 Objective

A numerical groundwater flow model has been developed by McGinley and Associates, Inc. (McGinley) of Reno, Nevada, and Interflow Hydrology, Inc. of Truckee, California (Interflow) to simulate the effects of solution mining of borate from the Fort Cady deposit (the project). McGinley and Interflow have prepared this report for Fort Cady California Corporation (FCCC) to summarize the methodology and results of the groundwater flow model and support the underground injection control (UIC) permit that is being evaluated by the US Environmental Protection Agency (EPA).

## 1.2 Project Location

The project is located in the eastern part of the Mojave Desert region in San Bernardino County, California. The project lies approximately 115 miles northeast of Los Angeles near the town of Newberry Springs and is approximately 35 miles east of the city of Barstow (Figure 1). The deposit is situated in the fault-bounded Hector evaporite basin at an elevation of approximately 2,000 feet above mean sea level (amsl), and is adjacent the Hector lithium clay open-pit mine owned by Elementis PLC. The project has a similar geological setting as Rio Tinto's boron operations and Nirma Limited's Searles Lake (Trona) operations, situated approximately 70 miles west-northwest and 80 miles northwest of the Project, respectively.

The Fort Cady borate ore body is located in Sections 25, 26 and 36 of T8N, R5E, in San Bernardino County, California. The ore body consists of colemanite and colemanite-rich anhydrite evaporite beds situated at depths between 1,300 feet and 1,500 feet below ground surface (bgs). The ore body is part of a larger vertical sequence of sub-horizontal, laminated, fine-grained lakebed and playa deposits comprised predominately of mudstone and clay. The total area of the modeled solution mining well field covers approximately 436 acres within an orebody area estimated at 495 acres. A site map showing the ore body and additional site features relevant to the groundwater model is provided in Figure 2.

## 1.3 Solution Mining Plan

### 1.3.1 Process Solution Injection and Recovery

The solution mining process involves injection of a dilute hydrochloric acid solution (<5% HCl) into the ore body, followed by pumping to recover the solution containing dissolved borate. The injection-recovery cycle will occur daily. Injection pressures will not exceed 250 psi and are expected to average 150 psi. Injection rates will vary over time based on the ore body permeability, which will increase over time as the colemanite is dissolved. Likewise, the number of wells and manner of injection and recovery will change over time. Initially, a push-pull process will occur, with injection and recovery pumping occurring from the same well. As mining continues, the process may change to injection and adjacent recovery in the well network. Five (5) wells will be drilled and mined during years 1 and 2. The number of wells will then be increased to approximately 35, and approximately 500 wells may be utilized sequentially over the mine life. The projected mine life is 25 years.

### 1.3.2 Process Water Supply

Borate-enriched solution (pregnant solution) that is pumped to the surface will be concentrated to precipitate borate crystals. The barren process solution will be regenerated for reuse in the injection wells. Since the fault-bounded basin containing the ore body does not produce water at a quantity or quality that is acceptable for industrial use, process water will be obtained from project water wells located outside of fault boundaries. Specifically, the process water will be pumped from well MWW-

1, located 3,000 feet southwest of the Pisgah Fault, and well PW-1, located 900 feet east of Fault B (Figure 2).

## 1.4 Purpose of the Groundwater Model

The numerical groundwater flow model has been developed to assess the degree to which process solution will be confined to the ore body during and after mining. The modeling is based on existing data and information of pre-mining material properties and the results of pilot testing. The predictive modeling has also been used to choose locations of observation well and monitoring well networks to compliment the Project. As solution mining takes place, the additional data produced from operations monitoring will be used to refine the model, as needed, to maintain an up-to-date tool for environmental management and potentially for mining optimizations.

## 2. HYDROGEOLOGY

### 2.1 Geological Setting

The following descriptions of Regional and Local Geology were excerpted from a geologic summary of the Fort Cady project prepared by E. G. Deal (1985) and Terra Modelling Services Inc. (TMS, 2017).

#### 2.1.1 Regional Geology

The project area is located in the Hector Basin of the Barstow Trough of the central Mojave. The Mojave comprises a structural entity commonly referred to as the Mojave block, and is bounded on the southwest by the San Andreas fault zone and the Transverse Ranges, on the north by the Garlock fault zone, and on the east by the Death Valley and Granite Mountain faults.

The central Mojave region is made up of a number of relatively low mountain ranges separated by intervening basins which are floored primarily by alluvium. The central Mojave area is cut by numerous faults of various orientations, but which predominantly trend to the northwest (Figure 3). The Barstow Trough, which is a structural depression, extends northwesterly from Barstow toward Randsburg and east-southeasterly toward Bristol. It is characterized by thick successions of Cenozoic sediments, including borate bearing lacustrine deposits (i.e., ancient lake sediments), with abundant volcanism along the trough flanks. The northwest-southeast trending trough initially formed during Oligocene through Miocene times, between 30 and 5 million years ago. As the basin was filled with sediments and the adjacent highland areas were reduced by erosion, the areas receiving sediments expanded, and playa lakes, characterized by fine-grained clastic and evaporitic chemical deposition, formed in the low areas at the center of the basins.

The colemanite-bearing beds at the Fort Cady deposit are Miocene in age and it has been suggested that they are part of a lacustrine facies (i.e., ancient lake sediments) of the Miocene Barstow Formation. By mid-Miocene time the Barstow Basin had become an elongated trough about 10 miles wide by 60 miles long that was the depositional site for several thousand feet of alluvial, fluvial, and lacustrine sediments which form the Barstow Formation.

The Fort Cady deposit lies within the eastern end of the Barstow Basin. In the vicinity of the City of Barstow, the basin appears to bifurcate, and the southern fork may have connected with the Kramer Basin to the west. The Kramer Basin contains the well-known U.S. Borax sodium borate deposit.

Faulting associated with movement on the Garlock and San Andreas fault systems has since disrupted the Mojave block. In the region of the Fort Cady deposit, regional faults are dominantly northwest-trending with a right-lateral strike-slip component of movement.

## 2.1.2 Local Geology

Surface exposures are mostly Quaternary in age (less than 2.5 million years). Alluvial fan sediments and valley fill comprise the surface in the north and west portions of the project area. The alluvium is overlain by recent (~20,000 years ago) basaltic lava flows in the southern part of the project area. Pisgah Crater, a cinder cone associated with these flows, is located about 2 miles east of the Fort Cady deposit. Other outcrops include sparse exposures of zeolitized tuff and claystone.

There are three prominent geologic features in the project area (Figure 2 and Figure 3):

- Pisgah Fault, which transects the southwest portion of the project area west of the ore body;
- Pisgah Crater located 2 miles east of the site; and
- Fault B, an unnamed fault, located east of the ore-body.

The Pisgah Fault is a right-lateral slip fault that exhibits at least 600 feet of vertical separation in the project area (Simon Hydro-Search, 1993). The east side of the fault is upthrown relative to the west side. Fault B is located east of the ore body and also exhibits at least 360 feet of vertical separation, based on most recent drilling and stratigraphic interpretations by Terra Modeling Services (TMS, 2018), using correlation of volcanic ash units in borings on each side of Fault B. Vertical separation on Fault B was previously interpreted by Simon Hydro-Search (1993) as approximately 700 ft. The borate ore body is situated within a thick area of fine-grained, predominantly lacustrine (lakebed) mudstones, east of the Pisgah Fault and west of Fault B. The central project area has been uplifted along both faults, forming an uplifted block or wedge, thus isolating the formations containing the orebody from the other sediments in the Mojave block in this area.

Drilling shows that the surface deposits are underlain by a dominantly mudstone sequence ranging from 1400 ft to over 1900 ft thick, which in turn overlies andesitic lava flows. The Oligocene-Miocene age mudstone sequence can be subdivided into four major units (TMS, 2018). Contacts between these units are gradational, making exact thicknesses difficult to determine. Typical thicknesses based on available drill hole data are provided below. From top downward the stratigraphic units are:

- Unit 1 is characterized by a 500 to 650-foot thick sequence of red-brown mudstones with minor sandstone, zeolitized tuff, limestone clasts, and rarely hectorite clay beds. Unit 1 is intersected immediately below the alluvium and surface basaltic lavas.
- Unit 2 is a green-grey mudstone that contains minor anhydrite, limestone, and zeolitized tuffs. Unit 2 has a similar thickness (300 to 500 feet) as the overlying Unit 1. Unit 2 is interpreted as lakebed sediments.
- Unit 3 is a 250 to 500-foot thick evaporite section which consists of rhythmic laminations of anhydrite, clay, calcite, and gypsum. Thin beds of air fall tuff were also intercepted which provide time continuous markers for interpretation of the sedimentation history. These tuffs have variably been altered to zeolites or clays. Unit 3 contains the colemanite deposit, which is generally 80 to 200 feet thick and dips to the southwest. Anhydrite is the dominant evaporite mineral, and the ore deposit itself is made up mostly of an intergrowth of anhydrite, colemanite, celestite, and calcite with minor amounts of gypsum and howlite.
- Unit 4 is characterized by clastic sediments made up of red and grey-green mudstones and siltstones, with locally abundant anhydrite and limestone clasts. The unit is approximately 150 feet thick and rests directly on the irregular surface of andesitic lava flows. Where drill holes intersect this boundary, it has been noted that an intervening sandstone or basal conglomerate composed mostly of coarse volcanic debris is usually present. Most drill holes did not extend to this depth.

Geologic cross sections through the project area and the groundwater model domain are provided in Figures 4a and 4b. The orientation of cross-sections is shown in Figures 2 and 3.

## 2.2 Hydrogeologic Setting

### 2.2.1 Groundwater Basins

California Department of Water Resources (DWR) Bulletin 118 provides delineations of the boundaries of groundwater basins throughout the State of California. Groundwater basin boundaries in the region of the Project are shown in Figure 5. Groundwater wells in the region from which representative static groundwater levels were obtained are also shown on Figure 5. The Fort Cady borate ore body is situated in the Lavic Valley Groundwater Basin, which extends for approximately 30 miles in a NNW-SSE direction and is approximately seven miles wide in the project area. The basin is bounded to the west by the Pisgah Fault, beyond which is the Lower Mojave River Valley Groundwater Basin, and is bounded to the east by a topographic divide, beyond which is the Broadwell Valley Groundwater Basin. There are no groundwater basins bordering the Lavic Valley basin to the north and south of the project area, due the presence of the Fort Cady Mountains (north) and Rodman Mountains and Lava Bed Mountains (south). Groundwater flow in the Lavic Valley basin is poorly defined, and outflow is interpreted to occur to the east to Broadwell Valley, with no localized groundwater discharge such as evapotranspiration or discharge to springs or a river.

The spatial domain of the numerical groundwater flow model for the project incorporates the northern portion of the Lavic Lake Groundwater Basin, extending south to Lavic Lake, a dry playa bed, and east to the topographic divide. The model domain extents west across the Pisgah Fault to the eastern edge of Troy Lake, a dry playa bed, incorporating the southeastern-most part of the Lower Mojave River Valley Groundwater Basin. Groundwater flow in the portion of the Lower Mojave River Valley basin is northwesterly toward Mojave Valley.

The northeastern-most model domain also incorporates the upper-most portion of the Broadwell Valley Groundwater Basin. Groundwater in this portion of the model domain flows easterly to Broadwell Valley.

### 2.2.2 Watersheds

The project area is located in the eastern portion of the Troy Lake watershed, a USGS hydrologic unit code (HUC)-10 watershed. Although rarely present in the vicinity of the project, surface water flows in a northwesterly direction past the project area from the Rodman Mountains to the south and the Pisgah Crater topographic divide to the east. The project groundwater model domain covers most of the eastern portion of the Troy Lake watershed, and extends eastward to include a portion of the neighboring Sunshine Peak-Lavic Lake HUC-10 watershed (Figure 6).

### 2.2.3 Nearest Wells and Groundwater Uses

The nearest groundwater well outside of the immediate project area is a non-potable water well located 5.6 miles northwest of the project ore body and 0.4 miles southeast of the I-40 rest area (Well 1807, Figure 2). Private drinking water wells associated with rural residences are located greater than 6.5 miles west of the project ore body, at the eastern edge of the town of Newberry Springs. Irrigation wells are located further west, in Newberry Springs, the closest of which is approximately 10 miles west of the project. The Pisgah Fault separates these residential and irrigation wells from the project area, such that they are not within the same regional groundwater flow system and are not hydraulically connected.

Except for an industrial well owned by Candeo Lava Products located 3.5 miles east of the project ore body, there are no known water wells located in the vicinity of the project to the north, south, or east. Water level measurements from the Candeo Lava Products well were not available for this study. The next closest water well to the north, south, or east is in the town of Ludlow, 14 miles east of the project. The location of groundwater wells that provide representative static groundwater elevations for the region surrounding the project are provided in Figure 5.

## 2.2.4 Springs and Streams of Significance

There are no springs or streams of significance in the vicinity of the project. Surface water-related features consist of unnamed dry washes that may carry water during heavy storm events. These washes generally drain west through the project area toward the Troy Lake playa in Newberry Springs.

The nearest spring included in the USGS National Hydrography Dataset (NHD) is an unnamed spring located in the Lava Bed Mountains, 5.9 miles southeast of the project (Figure 2), at an elevation of 3,150 feet amsl. This spring is located west of the Pisgah Fault and would be fed by local meteoric water infiltration, such that it would not be affected by project activities. The next-closest spring to the project is Sheep Spring, located in the Rodman Mountains, at an elevation of 3,040 feet. The Sheep Spring is located west of the Pisgah Fault and west of the Calico Fault Zone, which combined with its mountain location, indicate that it will not be affected by project activities.

## 2.3 Groundwater Depths and Elevations

Available static groundwater depths and elevations for project area and surrounding area wells are provided in Table 1 and Table 2, respectively, and are summarized below. The potentiometric surface elevations are also provided in Figure 7.

### 2.3.1 Project Area Wells

The static depths to groundwater in the project area are 230–390 feet below ground surface (bgs). The depths to groundwater in the project area are generally shallower at lower elevation wells and deeper at higher elevation wells. In the fault bounded wedge between the Pisgah Fault and Fault B, static groundwater is 230–260 feet bgs (1,748–1,755 ft amsl). Groundwater to the west of the Pisgah Fault is present in quaternary alluvial fan sediments of the Lower Mojave River Valley Groundwater Basin at depths of 200–265 feet bgs (1,783–1,787 ft amsl) in project wells MWW-1, MWW-S1, and MWW-2. There is approximately a 30 to 40 ft water level differential on the east and west sides of the Pisgah Fault, which is regionally recognized as a barrier to groundwater flow, and forms a groundwater basin boundary. Groundwater in the vicinity of Fault B at project wells TW-1, PW-1, and PW-2, is found at depths of 350–390 feet bgs (1,720–1,725 ft amsl) in coarser alluvial sediments to the east of Fault B (PW-1 and PW-2) and a mix of alluvial and fine playa sediments to the west of Fault B (TW-1).

### 2.3.2 Surrounding Area Wells

The depth to groundwater to the west of the project, in the vicinity of Newberry Springs, is 50–150 feet bgs (1,690–1,735 ft amsl). Depth to groundwater to the east of the project, at the nearest well in the town of Ludlow, is approximately 500 feet bgs (1,238 ft bgs).

### 2.3.3 Groundwater Flow Directions and Gradient

To the west of the Pisgah Fault, the gradient is to the northwest, toward the Troy Lake playa and Newberry Springs. To the east of the Pisgah Fault (a groundwater flow barrier), the gradient is to the east, toward Fault B. To the east of Fault B, the gradient is assumed to be east, toward Ludlow.

These gradients indicate an eastward groundwater flow direction through the project area on the east side of the Pisgah Fault and a northwesterly flow direction on the west side of the Pisgah Fault. An interpretation of the groundwater potentiometric surface elevation contours for the project area are provided in the discussion of Steady State Model Results (Section 3.4.8).

Well ID	Latitude	Longitude	Top of Casing Elevation (ft amsl)	Well Depth (ft)	Screened Interval (ft)	Lithologic Formation	Depth to Water (ft)	Groundwater Elevation (ft amsl)	Total Dissolved Solids (mg/L)
MWW-1	34.73511	-116.43587	2058.0	700	296-696	Qa/Qao	271.7	1786.3	1500
MWW-S1	34.73511	-116.43442	2051.0	unknown	unknown	Qa/Qao	264.1	1786.9	1400
MWW-2	34.74831	-116.45273	1988.0	700	299-600	Qa/Qao	204.67	1783.33	NA
SMT-93-2	34.75604	-116.41706	2004.0	1450	1200-1335	Ore Body	256.0	1748	12000
P-5	34.75352	-116.41807	1988.0	1550	1200-1435	Ore Body	233.0	1755	NA
PW-1	34.76350	-116.39716	2083.92	1000	500-1000	Qa/Qao	359.48	1724.44	NA
PW-2	34.76304	-116.39818	2081.74	1000	500-1000	Qa/Qao	357.96	1723.78	3100
TW-1	34.76366	-116.40125	2111.14	1000	700-1010	Qa/Qao	387.9	1723.24	2900
Well 1807	34.79656	-116.51885	1813.0	unknown	unknown	Qa/Qao	54.75	1758.25	1000
Well 1823	34.81840	-116.51302	1832.0	unknown	unknown	Qa/Qao	72.8	1759.2	7900

Note: Measurements taken between November 2018 and July 2019; NA – Data not available

Well ID <sup>1</sup>	Latitude	Longitude	Reference Elevation (ft amsl)	Depth to Water (ft)	Groundwater Elevation (ft amsl)	Meas. Date	Location	Source
09N03E22R006S	34.85125	-116.64537	1828.351	133.591	1694.76	1Q 2019	Newberry Springs	DWR WDL
10N03E27J004S	34.92836	-116.64520	1750.295	59.455	1690.84	1Q 2019	Newberry Springs	DWR WDL
08N04E11K001S	34.79665	-116.51993	1809.897	53.76	1756.137	4/1/2019	Newberry Springs	DWR WDL
08N04E18Q003S	34.78098	-116.59894	1904.0	168.97	1735.03	3/7/2018	Newberry Springs	DWR WDL
WCR2015-001628	34.80395	-116.59779	1790	60	1730	6/15/2015	Newberry Springs	DWR WCRs
WCR2019-005265	34.80491	-116.62632	1820	112	1708	12/18/2018	Newberry Springs	DWR WCRs
WCR1990-020207	34.72667	-116.16314	1740	502	1238	12/5/1990	Ludlow	DWR WCRs
09N07E24H001S	34.8550	-116.1878	1301.24	101.6	1199.64	6/28/1979	Broadwell Valley	DWR WDL

<sup>1</sup> Well ID from California Department of Water Resources (DWR) Water Data Library (WDL) or DWR Well Completion Report (WCRs) Database (DWR 2019a, 2019b)



## 2.4 Hydraulic Properties of Subsurface Materials

Subsurface hydraulic properties for the project area, including the playa and lakebed sediments of the ore body, the alluvial sediments west of the Pisgah Fault, and the playa and alluvial sediments in the vicinity of Fault B are summarized in Table 3, and in the text below.

### 2.4.1 Ore Body and Evaporates

Testing for hydraulic properties of the colemanite and evaporates/claystones containing the colemanite have occurred on several occasions. Hydro-Engineering (1996) summarized some of the testing and provided interpretations of prior testing conducted in 1981 and 1990. The native ore body transmissivity (T) is estimated at 10 gal/day/ft, or 1.3 ft<sup>2</sup>/day. Assuming the colemanite ore body occurs over an approximate 300 ft thickness, then the native hydraulic conductivity (K) over this thickness is estimated at  $4.5 \times 10^{-3}$  ft/day. This K value is of a similar magnitude as estimated by Simon Hydro-Search (1993) of  $8.2 \times 10^{-3}$  to  $2.2 \times 10^{-2}$  ft/day (K converted from millidarcy units).

The storage coefficient (S) of the ore body was estimated by Hydro-Engineering (1996) at  $2.5 \times 10^{-6}$ . Increases in transmissivity / hydraulic conductivity and storage coefficient will occur as colemanite is dissolved from the formation. Hydro-Engineering (1996) estimated the end-point permeability of the ore body formation after colemanite dissolution will be approximately 30 times higher, and a long-term storage coefficient may be approximately  $1.1 \times 10^{-5}$ . The end-point hydraulic properties are still low, owing to the fact that a majority of the formation is evaporites (anhydrite) and claystone that will not be dissolved. The end-point porosity of the ore body formation after mining is predicted to be 15 percent (Simon Hydro-Search, 1993; Core Laboratories, 1981) based on the colemanite content within the sediments and laboratory core analyses.

Injection and pumping tests were conducted in 1981 by Duval Corporation, 1986-1987 by Mountain States Minerals, and between 1996-2001 by Fort Cady Minerals Corporation. Injection was conducted at 150-300 psi pressures in the 1982 testing, with injection flow rates mostly of 1.5-2.5 gpm, indicative of the hydraulically tight nature of the ore body formation. In the 1986-1987 testing, rates of 1.3 to 5.3 gpm were observed over testing periods lasting from 6 to 71 days.

### 2.4.2 Mudstone and Claystone Sediments

The mudstone and claystone sediments above and below the ore body evaporites are also understood to be of very low transmissivity. Pump test results provided by Confluence Water Resources (Confluence, 2019) provided an estimate of the hydraulic conductivity in the  $10^{-5}$  range, as described below in Section 2.4.3.

### 2.4.3 Local Alluvial Aquifers West of Pisgah Fault and East of Fault B

Confluence Water Resources (2019) conducted a step-drawdown pumping test and a 10-day constant-rate pumping test of well PW-1 located on the east side of Fault B (Figure 2). Wells PW-2 and TW-1 located on either side of Fault B were used as observation wells. The pumping rate was 250 gpm. Analyses of the pumping test results indicate a transmissivity in the alluvium on the east side of Fault B of 1,697–2,100 ft<sup>2</sup>/day, equaling a hydraulic conductivity of 2.6–3.2 ft/day. A storage coefficient (S) for the alluvium was estimated at  $2.6 \times 10^{-5}$ . No pumping drawdown was observed in well TW-1 on the west side of Fault B, located only 1,228 feet to the southwest. Well TW-1 was only observed to produce 0.1 gpm during construction and development, and a mild recovering water level trend from well development that occurred several months prior was still being observed in the well. Based on the recovery trend, a preliminary estimate of hydraulic conductivity of the mudstone and claystone in which TW-1 is completed is estimated by Confluence (2019) at  $6.4 \times 10^{-5}$  ft/day, a very low value.

In 1982, the Duval Corp conducted a pumping test of the MWW-1 well. A step-drawdown and two 12-hour constant-rate pumping tests were conducted. During the pumping tests, water level drawdown

was observed in well DHB-32. The location of DHB-32 is uncertain, but may be the water well that is currently called well MWW-S1 and is located approximately 430 ft east of MWW-1. The pumping and recovery data from the first 12-hour constant rate test were compiled and analyzed by McGinley and Interflow. Analyses of the pumping well data indicates a transmissivity of 260 to 310 ft<sup>2</sup>/day using the Hantush (1960) leaky confined aquifer solution, and 600 to 700 ft<sup>2</sup>/day using the Theis (1935) and Cooper-Jacob (1946) solutions. The Hantush (1960) leaky confined solution is interpreted to be the most representative solution, and when divided by a saturated thickness of approximately 425 ft at MWW-1, produces an estimated hydraulic conductivity of 0.6 to 0.7 ft/day. Similar analyses of the observation well data from DHB-32 produced values approximately an order of magnitude higher, however, it is not clear if the DHB-32 observation well is the same well as MWW-S1, and the distance from pumping well has significant bearing on the outcome of the solutions.

**Table 3 –Subsurface Hydraulic Properties Summary**

Unit	Transmissivity (T) (ft <sup>2</sup> /day)	Hydraulic Conductivity (K) (ft/day)	Storativity (S)	Porosity (u)	Source	Notes
Qa / Qoa - Alluvium East of Fault B	1,697 - 2,000	2.6 - 3.1	--	--	Confluence Water Resources, 2019	PW-1 pumping well data
Qa / Qoa - Alluvium East of Fault B	1835 - 2100	2.8 – 3.3	$2.6 \times 10^{-5}$	--	Confluence Water Resources, 2019	PW-2 observation well data from PW-1 pumping test
Ts (Unit 2)	$1.95 \times 10^{-2}$	$6.4 \times 10^{-5}$	--	--	Confluence Water Resources, 2019	Estimate from long-term recovery rate trend analysis for TW-1
Qa / Qoa - Alluvium West of Pisgah Fault	260 – 310	0.6 - 0.7	--	--	Duval Corp; McGinley-Interflow (2019)	Pumping test of MWW-1; step-drawdown test and two 12-hr constant rate tests; data collected in 1982 by Duval Corp analyzed by McGinley-Interflow
Qa / Qoa - Alluvium West of Pisgah Fault	600 - 700	1.4 – 1.6	--	--	Duval Corp; McGinley-Interflow (2019)	Pumping test of MWW-1 using observation well data from DHB-32; location of observation well is uncertain, assumed to be MWW-S1
Qa / Qoa - Alluvium West of Pisgah Fault	716	1.8	--	--	Howard Pump; McGinley-Interflow (2019)	Estimated T from 1987 well MWW-2 development specific capacity data from Howard Pump (SC = 2.23 gpm/ft)
Ore Body (Unit 3)	3.3	$2.8 \times 10^{-2}$	$1 \times 10^{-5}$ to $1 \times 10^{-4}$	--	In-Situ, 1987	Slug Testing over 118 ft interval
Ore Body (Unit 3)	0.88 – 0.94	$1.8 \times 10^{-2}$ (3 to 8 mD = $8.2 \times 10^{-3}$ to $2.2 \times 10^{-2}$ )	--	--	In-Situ, 1990	Multiple well constant rate injection test in seven area test wells – post leaching, assumed effective aquifer thickness of 50 ft
Ore Body (Unit 3)	--	$8.2 \times 10^{-3}$ – $2.2 \times 10^{-2}$	--	Increasing by 12% (end)	Simon Hydro-Search, 1993	Porosity predicted to increase to 12-15% at the end
Ore Body (Unit 3)	13.37	0.27	$4.3 \times 10^{-6}$	--	Hydro-Engineering, 1994	Assumed thickness of 50 ft, reinterpretations of 1983 and 1990 injection testing
Ore Body (Unit 3)	45 (acid effected) 1.3 (native)	$4.5 \times 10^{-3}$	$2.5 \times 10^{-6}$ $1.1 \times 10^{-5}$ long-term	--	Hydro-Engineering, 1996	Additional injection testing in 1995 with acid injectate; K value determined by McGinley-Interflow assuming 300 ft thickness; end point K of ore body expected to be 30 times higher
Ore Body	--	$7.94 \times 10^{-7}$ to 0.167	--	13.2 – 26.2	Core Laboratories, 1981 (presented in Respec, 2019)	Laboratory testing conducted on seven samples from the ore body for testing of acid extracts. Vertical versus horizontal permeability is not differentiated (assume results may be represented vertical K – injection through the length of the cores). The porosity values are bulk porosity (not effective porosity).

## 2.5 Conceptual Water Budget

The groundwater budget for the project area and model domain includes inputs from meteoric water recharge derived from the upper slopes of the Cady Mountains to the north, and the Rodman and Lava Bed Mountains to the south. Limited groundwater inflow may also occur from the Bullion Mountains watershed to the southeast of the project area, and within the Lavic Valley Groundwater Basin. Groundwater outflow is interpreted to occur to the east of the project area, toward Ludlow, as part of the Broadwell Valley Groundwater Basin flow system. Groundwater outflow also occurs to the northwest of the project area toward Newberry Springs, from the portion of Lower Mojave River Valley to the west of the Pisgah Fault. Precipitation falling on the alluvial fans below the mountains and on the valley bottom is assumed to return to the atmosphere by evapotranspiration. No surface water or shallow groundwater are present to enable evapotranspirative losses of groundwater.

### 2.5.1 Recharge Estimation

Groundwater recharge to the project area represented in the numerical groundwater flow model was estimated by determining the amount of precipitation falling on lands above 2,250 ft elevation in the local watersheds that feed the model domain. The elevation of 2,250 ft amsl was chosen as an approximate boundary for the zone of recharge based on the extent of vegetation and drainage channels observed in aerial imagery. The fraction of incipient precipitation that infiltrates to become groundwater recharge was further estimated to be low in this arid desert environment, between 0.5% to 1%.

Watershed boundaries from the National Hydrography Dataset (NHD) were used to determine that the upland (>2,250 ft amsl) watershed areas are approximately 26,800 acres and 42,960 acres for the north and south portions of the model domain, respectively (Figure 6). Annual average precipitation for these watersheds was determined using the PRISM 1981-2010 normal precipitation data product available at 800m spatial resolution (PRISM Climate Group, 2019). The area-weighted average precipitation for the upland watershed areas was determined to be 5.26 inches and 6.41 inches for the north and south areas, respectively.

The Cady Mountains watershed area to the north, with a peak elevation of 4,593 ft at Cady Peak, are estimated to receive 10,870 AFA of precipitation, of which is estimated to produce 54 to 109 AFA of groundwater recharge. The Lava Bed Mountains and Rodman Mountains to the south, with a peak at an elevation of 4,427 ft amsl at Sunshine Peak, are estimated to receive approximately 22,400 AFA of precipitation, of which approximately 112 to 224 AFA is estimated to become groundwater recharge. This estimated range of groundwater recharge compares similarly to, but is a little lower than, the estimate of recharge to the contributing area to the process water supply well MWW-1 (southwest of the Pisgah Fault) made by Simon HydroSearch (1993), which ranged between 163 to 405 AFA.

### 2.5.2 Subsurface Inflow

A small amount of subsurface inflow to the project area may additionally be occurring from the Bullion Range watershed that drains to Lavic Lake, located to the south of the Pisgah Crater. Upland elevations in this watershed area (Figure 6) are estimated to receive 27,136 AFA of precipitation, with an estimated groundwater water recharge of 135-271 AFA at the 0.5 to 1% rate. Lavic Lake is a dry playa, and is not a groundwater discharge area. Subsurface outflow from the watershed is likely to the east of the Pisgah Crater, but may also flow south of the Pisgah Crater into the project area.

### 2.5.3 Subsurface Outflow

All groundwater recharge and subsurface inflow to the project area results in subsurface outflow to either the east, out of the Lavic Valley Groundwater Basin area to the Ludlow portion of the Broadwell Valley Groundwater Basin, or to the west toward Newberry Springs and the Lower Mohave River Groundwater Basin (Figure 7). No other sources of groundwater outflow have been identified in the

project area, as there are no springs, areas of ET, or currently producing wells.

## 2.6 Groundwater Quality

Recent total dissolved solids (TDS) measurements in existing project groundwater wells are included in Table 1. Historical pH and TDS concentrations from project wells are summarized in Table 4.

Water quality on the east side of the Pisgah Fault, where the colemanite ore body and downgradient areas are located, is characterized by total dissolved solids (TDS) concentrations greater than 2,500 mg/L, which exceed the drinking water standard of 1,000 mg/L. Wells TW-1 and PW-2, located on either side of Fault B, had TDS concentrations of 2,900 mg/L and 3,100 mg/L, respectively, when sampled in November, 2018 (Confluence Water Resources, 2019). The water from PW-2 reportedly has a strong sulfur odor and elevated temperature of approximately 120 °F (C. Byrns, personal communication).

Well SMT-93-2, a test well that was rinsed post-closure and located within the ore body, had a TDS concentration of 12,000 mg/L when it was sampled in November 2018. Historical sampling of formation water from former well SMT-1 had an average TDS concentration of 24,300 mg/L in 1981, following well drilling and development and prior to any injection testing (Mann, 1981). A sample of formation water from DHB-34, located 1,500 feet southeast of SMT-1 had a reported TDS concentration of 31,200 mg/L prior to injection testing (Mann, 1981; Krier, 1981).

Groundwater west of the Pisgah Fault has lower TDS than groundwater east of the fault. TDS concentrations measured in November 2018 were 1,500 mg/L and 1,400 mg/L in wells MWW-1 and MWW-S1, respectively. The TDS concentration had a similar value of 1,620 mg/L after the well was drilled and developed in 1982. Well MWW-2 was drilled in 1987, and contained 867 mg/L of TDS in a sample collected in 1991.

Well ID	Latitude	Longitude	Meas. Year	TDS (mg/L)	pH	Source
SMT-1	34.7562	-116.4176	1981	24,300	8.49	Mann, 1981
DHB-34	34.7525	-116.4129	1981	31,200	na	Mann, 1981
MWW-1	34.7351	-116.4359	1982	1,630	7.7	Well Completion Records
MWW-2	34.7483	-116.4527	1991	867	8.9	Well Completion Records

na – not analyzed

### 3. SIMULATION OF THE GROUNDWATER FLOW SYSTEM

#### 3.1 Conceptual Model

The conceptual model for groundwater flow through the Fort Cady area can be summarized as follows, based on the hydrogeology presented in Section 2 of this report.

- The Fort Cady colemanite deposit is situated near a groundwater flow divide. Groundwater flow to the west of Pisgah Fault is westerly to the Newberry Springs area as part of the Lower Mohave River Groundwater Basin. Groundwater flow to the east of the Pisgah Fault is northeasterly within the Lavic Valley Groundwater Basin, likely outflowing to the Broadwell Valley Groundwater Basin flow system.
- There are no natural groundwater discharges in the Fort Cady area, except for subsurface outflows to the eastern and western hydrographic areas. There are no areas of shallow groundwater where discharges by phreatophyte evapotranspiration or playa evaporation may occur. There are no springs or streams in the area. Only ephemeral drainages exist.
- Recharge to the project area is modest in this arid and low-altitude region of the Mohave Desert, and occurs from small contributing watersheds to the north and south.
- No groundwater pumping, other than for testing purposes for the project and assumed minor industrial water at the adjacent hectorite mine, has occurred in the area, and the local groundwater flow system is in a state of natural equilibrium.
- Fault B together with the Pisgah Fault creates a “wedge” of uplifted earth, in which the colemanite deposit is situated. The colemanite occurs within evaporite beds contained in the lower portion of a thick sequence of predominantly mudstone (lakebed) deposits. The colemanite ore body exists at depths ranging from approximately 1,300 to 1,500 ft bgs.
- Both the evaporites and mudstone have a very low bulk hydraulic conductivity, based on reported lithologies and testing, in the range of  $10^{-2}$  to  $10^{-4}$  ft/day. These materials do not constitute an aquifer. The lakebed formations do not yield substantive volumes of water to wells, and even under injection pressures up to 300 psi, do not accept large volumes of water (1.5-2.5 gpm). Water yields to exploration and test wells within the colemanite deposit and mudstones within the “wedge” are very low, generally <1 gpm for a sustained period of time. Recovery of static water levels after modest flow testing can require months.
- By contrast, alluvial materials outside the “wedge” and on the opposite side of the bounding faults contain more granular alluvial materials that have hydraulic conductivities several orders of magnitude higher, in the range of  $10^{-1}$  to  $10^1$  ft/day. These materials can yield significant water to wells, tested up to 300 gpm, and represent the nearest known aquifers to the colemanite deposit. Process water supply for mining will be produced from wells within these alluvial units.

#### 3.2 Modeling Approach

A steady-state numerical groundwater flow model has been constructed and calibrated to represent the existing natural flow system. The model incorporates known and interpreted geology and associated hydraulic properties down to, within, and beneath the colemanite deposit. Measured water levels within the defined model area are used as calibration targets. Hydraulic conductivities, fault barrier conductance, outflow boundary conductance, and the local recharge magnitudes have all been calibration variables in the model. Where pumping tests have defined hydraulic properties, they have been used to guide calibration for consistency with testing data. The colemanite ore body hydraulic

properties are set at native conditions in the steady-state model, but are varied (increased) during transient simulations, to reflect conditions during and after acid-leaching of the colemanite.

The recharge to the model area is uncertain, but interpreted to be low. The recharge magnitudes as derived during calibration do not exceed a small fraction (<1%) of the average annual precipitation falling on higher elevation tributary watersheds. The outflow boundaries reflect down-gradient water level elevations outside the model domain, and the subsurface flow magnitude is governed by a calibrated conductance term at the boundary. Calibration successfulness is judged by review of common statistics related to comparison of simulated groundwater levels at water level targets to the measured levels.

Once the calibrated steady-state model was satisfactorily developed, it was then converted into a transient model. The goal of the transient modeling is to make preliminary estimates of long-term (mine life) potentiometric water level changes and injectate migration into the surrounding formation, under what is believed to be an initially conservative set of assumptions. Some attributes of the proposed mining, such as the long-term injection and extraction rates, and changes in hydraulic conductivity and porosity of the colemanite formation as solution mining occurs are based on testing results and interpretations, and are simplified to represent expected average conditions for this initial transient flow modeling. The potential migration of the acid solution injectate is assumed to take place under advection and dispersion solute transport without reactions, decay or absorption within the formation. Approaches and assumptions will be discussed in more detail in the transient modeling section of this report.

### **3.3 Modeling Codes**

The US Geological Survey (USGS) numerical groundwater flow modeling code MODFLOW was used for flow simulations, specifically the MODFLOW2000 version (Harbaugh et al, 2000). The MT3DMS code was used for contaminant transport simulations (Zheng and Wang, 1999), and links directly with MODFLOW. Potential land subsidence was simulated using the SUB Package of MODFLOW developed by Hoffman et al (2003).

The Groundwater Vistas (v7) pre- and post-processor for MODFLOW and MT3D was used for model construction and output visualization (Environmental Simulations Inc, 2018). The statistical parameter estimation code PEST (Doherty, 2015), as implemented in Groundwater Vistas, was used during model calibration.

### **3.4 Steady-State Model Construction**

#### **3.4.1 Spatial Discretization**

The model grid is composed of 83 rows and 102 columns, covering an area that extends approximately 5-6 miles in all directions from the ore body. The model orientation is rotated 35° west so that the northern and southern edges of the model are oriented with the bounding Cady and Lava Bed mountain ranges, and the ore body is elongated in the model east-west direction. The model origin (lower left corner) corresponds to UTM ft (NAD 83, Zone 11N) coordinates of: 1765891.6 N, 12613137.2 E. Model units are in feet and time units are days.

The outer cells are 1000 ft by 1000 ft square, transitioning to a cell size of 250 ft by 250 ft square over the area of the ore body. There is a total of 110,058 active cells in the model domain. Grid spacing reductions transition in steps not exceeding more than ½ of the dimensions of the neighboring cells. Figure 8 shows the grid layout and model domain.

#### **3.4.2 Model Layering**

There are 13 layers in the model. MODFLOW layer type 3, convertible confined-unconfined, was assigned to all layers. The layer thicknesses are roughly established to accommodate representation of

the primary geologic units. The highest vertical resolution (thinnest layering) was assigned to layers comprising the ore body and formation directly above and below.

The top of layer 1 is set at land surface, as interpolated from the USGS 10-meter resolution digital elevation model (DEM). The bottom of layer 13 is elevation 600 ft below mean sea level. The thickness of earth represented in the model ranges from approximately 2500 ft on the valley floor to up 4500 ft in the mountain ranges. Layer 1 has variable thickness, with a bottom elevation of 1650 ft amsl. All other layers are uniform and horizontal layers ranging in thickness from 100 ft to 500 ft.

Model layers 1-3 are used to represent Quaternary alluvial deposits to the west of the Pisgah Fault and east of Fault B. Water supply wells for the project have been drilled in these sediments. Logging for recent test wells near Fault B suggests up to 1000 ft of Quaternary sediments (Confluence, 2019), represented using model layers 1 to 3. Well logs for test wells west of the Pisgah Fault (MWW-1 and MWW-2) indicate up to 600-700 ft of possible Quaternary sediments (represented using model layers 1 and 2).

Model layers 4-10 are a uniform 100 ft in thickness, and used to represent the sedimentary layers (mudstones) in which the colemanite deposits occur. Layer 12 is also 100 ft in thickness and is used to represent a basal conglomerate layer encountered above andesite bedrock and beneath the ore body at some locations (RESPEC, 2019). Andesite bedrock in the uplifted wedge between the Pisgah Fault and Fault B is represented by layer 13.

Figures 9a and 9b provide an illustration of the grid layering and a summary of model layers is presented in Table 5.

<b>Table 5 – Summary of Model Layering</b>			
<b>Model Layer</b>	<b>Top Elevation (ft amsl)</b>	<b>Bottom Elevation (ft amsl)</b>	<b>Notes</b>
1	Variable, 1790-4241	1650	Upper alluvium, partially saturated, Unit 1 overlying ore body
2	1650	1350	Upper alluvium, saturated, Unit 1 mudstones overlying ore body, alluvium tapped by MWW-1 to the west of the Pisgah Fault
3	1350	1000	Deeper alluvium, Unit 2 mudstones above
4 - 5	1000 (each layer is a uniform 100 ft thick)	800	Unit 2 mudstones above the ore body, mudstone and claystone beneath alluvium tapped by PW-1 and MWW-1 outside the bounding faults
6 - 10	800 (each layer is a uniform 100 ft thick)	300	Unit 3 evaporates and mudstones, including the colemanite ore body within the bounding faults, and mudstones-claystones outside the faults
11	300	0	Older basin-fill mudstones-claystones beneath the ore body and elsewhere beneath the valley floor
12	0	-100	In the wedge bound by faults, used to represent a basal conglomerate on top of andesite bedrock; outside faults, older basin-fill mudstones-claystones
13	-100	-600	Within the wedge bound by faults, represents andesite bedrock; outside faults, older basin-fill mudstones-claystones



### 3.4.3 No-Flow Boundaries

It is implicitly assumed that groundwater outside of the model domain does not enter or leave the system, except as permitted to occur at General Head Boundaries (GHBs) described below. The base, top and sides of the model domain other than the at the GHBs are no-flow boundaries. Recharge occurs to portions of the upper model layer as specified fluxes, described in section 3.4.6.

### 3.4.4 General Head Boundaries

The majority of the active MODFLOW model area is bounded by no-flow boundaries, with three exceptions where groundwater may flow into or out of the model domain. These locations of inflow or outflow are associated with the groundwater basin delineations by CA DWR, as shown in Figure 7, and the interpreted directions of groundwater flow within the groundwater basins.

The movement of groundwater into or out of the model domain is simulated using MODFLOW General Head Boundaries. The GHBs are a head dependent boundary condition, whereby the flux (flow rate) into or out of the cell is computed by the model based upon the head calculated in the GHB cell, the head specified outside the boundary cell, and a conductance term. Groundwater inflow or outflow is dictated by a potentiometric gradient to or from a specified point outside the boundary, which is based on a fixed water level elevation at a defined distance beyond the cell. The groundwater gradients are defined by regional groundwater levels shown in Figure 7. Subsurface flow can be further regulated (constricted) by a conductance value in the GHB cell, which has been derived during calibration. Table 6 summarizes the GHB parameters in the calibrated steady-state model, and Figure 10 shows the locations of the GHBs. Information on preferential flow at varying depths or along the lateral extent of each GHB boundary does not exist. For simplicity, the GHBs are simulated to extend through all 13 model layers to reflect potential shallow and deep subsurface flow, and utilize the same gradient and conductance parameters spatially and at depth.

<b>Table 6 – Descriptions of General Head Boundaries</b>					
<b>GHB No.</b>	<b>Elevation of Water Level outside of boundary (ft amsl)</b>	<b>Distance to point of water level elevation (ft)</b>	<b>Note / Reference for Gradient Control</b>	<b>Calibrated Conductance (ft<sup>2</sup>/day)</b>	<b>Magnitude of Outflow (-) or Inflow (+) (AFA)</b>
1	1730	16,900	Allows for outflow to Newberry Springs area	2.78	-63.1
2	1238	39,300	Allows for outflow toward Ludlow	0.317	-143.2
3	1800	23,800	Assumes groundwater inflow from to the Bullion Mountains watershed to the southeast.	0.434	+37.9

### 3.4.5 Horizontal Flow Barriers

The MODFLOW Horizontal Flow Barrier (HFB) package was used to represent the Pisgah Fault and Fault B in the model. Other faults are mapped in the model domain, but evidence of the faults functioning as potential impediments to groundwater flow is not available. These faults are therefore not explicitly represented in the model. Both the Pisgah Fault and Fault B have demonstrated flow impediment properties, based on lithologic differences on either side of the faults (juxtaposition of

mudstones with younger alluvium), water level differences on either side of the Pisgah Fault, groundwater chemical differences across the faults, and as documented in the pumping test of PW-1 near Fault B. Locations of HFBs are shown in Figure 10. Each HFB is applied to all model layers, with uniform conductance property. A summary of the HFBs in the model is presented in Table 7.

The HFB operates between model cells, applying a resistance to the movement of flow between adjacent cells, but are not impermeable barriers to flow. The HFB conductance term controls the permeability of the barrier, which has been derived during model calibration to achieve a match to static water levels near the faults. Initial HFB conductance terms were set at approximately  $10^{-6}$  ft/day, but were adjusted to be less restrictive to groundwater flow across the faults during model calibration, to achieve a match to water level elevations on each side of the fault. Water level differentials are summarized in Table 1, indicating approximately 31 to 42 feet of water level difference across the Pisgah Fault near the ore body, and only about 1 foot of water level difference across Fault B. The water level difference across Fault B would not be sufficient by itself to justify impediment of groundwater flow, but the lithologic differences observed in PW-1 as contrasted with PW-2 and TW-1, along with the absence of pumping response in TW-1 during the pumping test of PW-1 define a hydraulic barrier condition. The magnitude of northeastward groundwater flow through the hydraulically tight mudstone and across Fault B is likely very low, and in a natural state of equilibrium, the water level difference across the fault is corresponding low, suggesting that the condition is not one of fault gauge restricting flow, but more likely the result of juxtaposition of sedimentary units along with a limited flux of groundwater through the mudstone lithology.

For clarity, groundwater flow still occurs across the represented fault zones, based on the groundwater gradient on either side of the structure. As such, the faults are not represented as impermeable barriers, rather as impediments to lateral flow. The higher the calibrated conductance term, the lower the degree of impediment of flow across the fault. For example, the calibrated conductance of Fault B ( $6.62 \times 10^{-4}$ ) is near to the calibrated hydraulic conductive of the mudstone deposits ( $6.43 \times 10^{-3}$ ), and therefore creates less of an impediment to groundwater flow, as contrasted with the calibrate conductance for the Pisgah Fault, which is approximately 1 order of magnitude lower.

<b>Table 7 – Summary of Modeled Hydrologic Flow Barriers</b>		
<b>HFB No.</b>	<b>Represents</b>	<b>Calibrated Conductance (ft/day)</b>
0	Pisgah Fault	$2.81 \times 10^{-5}$
1	Fault B	$6.62 \times 10^{-4}$

### 3.4.6 Recharge (Specified Flux) Boundaries

Recharge by precipitation to the model area is assumed to occur in the upland areas within the model domain, and the tributary area to these mountains outside the model domain. Recharge in the model is simulated using the MODFLOW Recharge package, and is a specified flux of water. Recharge is applied only to the upper-most active model layer (layer 1). Locations of recharge zones are shown in Figure 10. The recharge applied to the Cady Range (zone 2) provides a source of groundwater north of Fault B and at the upper portion of the Broadwell Valley Groundwater Basin. Recharge applied to the Lava Bed Range provides a source of groundwater to the upper-most portion of the Lower Mojave River Valley Groundwater Basin, situated west of the Pisgah Fault, which through leakage across the Pisgah Fault provides a modest source of groundwater to the wedge area within the Lavic Valley Groundwater Basin.

The recharge applied to these areas was adjusted during calibration, but within constraints of the conceptual model that the recharge is low, being < 1% of the precipitation occurring within the watershed (Section 2.5). Table 8 summarizes the calibrated recharge rates.

<b>Table 8 - Summary of Modeled Recharge Zones</b>				
<b>Recharge Zone No.</b>	<b>Rate of Recharge (ft/day)</b>	<b>Note</b>	<b>Conceptual Range for Recharge (AFA)</b>	<b>Simulated Recharge Volume (AFA)</b>
1	0	Valley floor - majority of model domain.	0	0
2	$1.689 \times 10^{-5}$	Fort Cady Range	54 - 109	58.6
3	$2.758 \times 10^{-5}$	Lava Bed Range	112 - 224	110.4

### 3.4.7 Hydraulic Conductivity Properties

Hydraulic properties for the model were input on a cell-by-cell basis, with each cell having a defined hydraulic conductivity (K) value. In the model, groups of cells with equivalent values are lumped into 13 discrete zones. K zone distributions for each model layer are shown in Appendix A figures, along with vertical K distribution cross-section figures. Most hydraulic properties assigned to these zones were adjusted during the model calibration process.

Initial values for hydraulic conductivities for lithologic units represented were derived from pumping tests conducted in the alluvium, and hydraulic properties testing for the ore body, as summarized in Table 3. Small amounts of variation were tolerated during calibration of the alluvium. The ore body is assumed to have a hydraulic conductivity of  $4.5 \times 10^{-3}$  which was held constant for the steady-state (pre-mining) model calibration. The ore body value is based on pre-leaching ore body permeability testing and evaluations, as summarized by Hydro-Engineering (1996). The initial hydraulic properties of bedrock were assumed based on the general rock type. The basal conglomerate unit represented beneath the mudstone deposits and ore body, and on top of andesite bedrock, is assumed to have a high hydraulic conductivity of 1 ft/day, relative to the mudstone sediments. The conglomerate K value was not adjusted during model calibration.

Initial vertical conductivities for sedimentary units were assumed to be one-tenth the horizontal values. The vertical to horizontal ratio was adjusted during model calibration. The resulting vertical hydraulic conductivities (K<sub>z</sub>) were approximately one to three orders of magnitude lower than horizontal hydraulic conductivities (K<sub>x-y</sub>) in depositional formations (Table 9). Bedrock materials were allowed to have a 1:1 K<sub>x-y</sub> to K<sub>z</sub> ratio. The model area weighted mean K<sub>x-y</sub> is 0.1145 ft/day, and the mean K<sub>z</sub> is 0.0186 ft/day.

**Table 9 – Summary of Hydraulic Conductivity Attributes.**

K Zone No.	Formation Representing	Kx-y (ft/day)	Kz (ft/day)	Ratio Kx-y to Kz	Ss*	Sy*	Porosity**
1	Mudstones and Claystones	6.43E-03	1.74E-05	370.6	9.00E-08	0.05	0.50
2	Intermediate Depth Alluvium East of Fault B (tapped by Well PW-1)	2.00E+00	2.86E-01	7.0	9.00E-08	0.15	0.35
3	Granitic Bedrock	1.00E-01	1.00E-02	10.0	9.00E-08	0.02	0.05
4	Pisgah Crater Volcanic Rock	1.00E-02	1.00E-02	1.0	9.00E-08	0.02	0.05
5	Volcanic Rocks	1.00E-01	1.00E-01	1.0	9.00E-08	0.05	0.15
6	Upper Alluvium west of Pisgah Fault	1.76E-02	2.75E-03	6.4	6.00E-07	0.15	0.35
7	Upper Alluvium east of Fault B	1.87E-01	4.08E-02	4.6	9.00E-08	0.15	0.35
8	Intermediate Depth Alluvium East of Fault B (above screened interval for Well PW-1)	3.03E-01	2.39E-01	1.3	9.00E-08	0.15	0.35
9	Intermediate Depth Alluvium West of Pisgah Fault (tapped by Well MWW-1)	5.00E-01	5.19E-02	9.6	6.00E-07	0.15	0.35
12	Basal Conglomerate on top of Andesite	1.00E+00	1.00E-01	10.0	2.60E-07	0.15	0.35
13	Andesite Bedrock beneath Ore Body	1.00E-01	1.00E-02	10.0	1.00E-08	0.05	0.15
20	Colemanite Ore Body	4.50E-03	1.00E-04	45.0	2.50E-08	0.01	0.01-0.15
21	Evaporites - Anhydrite	4.50E-03	1.00E-04	45.0	2.50E-08	0.01	0.01

\* Ss and Sy are computationally only used in transient model runs

\*\* The porosity value used in modeling is effective porosity, not total void space porosity, and is computationally only used in solute transport model runs

### 3.4.8 Potentiometric Head (Water Level) Targets used for Calibration

Ten wells with accurate potentiometric water level elevations are available for the model domain. These water level data are summarized in Table 1, and locations are shown in Figure 7. These water levels are used as steady-state water level elevation (head) targets. The targets are assigned to model layers based on well depths. All water level target values are given equal weight in the model calibration.

### 3.4.9 Calibration Technique

Model calibration is an iterative process of adjusting model parameters and boundary conditions to obtain a reasonable match between field measurements and model-computed values. Calibration was conducted for the steady-state model, which is assumed to represent natural and pre-mining conditions.

During calibration, refinements were made to the recharge rates,  $K_{x-y}$  and  $K_z$  values, GHB conductance, and HFB conductance. Model calibration progressed toward increasing model complexity and desired simulation capabilities while maintaining numerical stability.

In some cases, calibration was achieved through manual trial and error methods whereby a single input parameter is adjusted and the model is subsequently run to observe the effects of the change. This process is repeated until an acceptable value for the parameter is achieved, as gaged by the improvement in matching target heads.

Also used was an automatic inverse calibration approach, whereby multiple iterations of parameter adjustments, selected by the modeler and constrained within a defined range, are run to determine parameter values that improve the modeled fit to the target data. PEST (Model-Independent Parameter Estimation and Uncertainty Analysis; Doherty, 2015) was used for this application and is a nonlinear parameter estimator which is well documented and commonly used for calibrating MODFLOW models. PEST also was used to identify parameters with the highest sensitivity, which aided in targeting parameters for refined calibration. When using automated calibration techniques, the modeler carefully considers the outputs from PEST and uses discretion as to the feasibility of model-generated parameter values. For instance, a modeler will not accept derived values outside the conceptual hydrogeologic range for the parameter in question. By using a combination of manual (trial and error) and automated PEST calibration techniques, the final calibration objectives were successfully achieved.

Model calibration acceptability is subjective, but the following general guidelines for judging calibration sufficiency for this model have included:

- Overall calibration quality is determined through statistical comparison of model results with field measurements at discrete points (wells).
- The primary statistics used in gauging and reporting goodness of fit are the root mean square (RMS) error, residual mean, residual standard deviation, absolute residual mean, and coefficient of determination ( $R^2$ ).
- Calibration continues until the following goals are achieved: 1) the residual mean is 5% or less of the range in observed (measured) water levels; 2) the residual standard deviation is 10% or less of the same range; and, 3) the absolute residual mean also is less than 10% of the same range. Calibration continues until the standard correlation coefficient between observed and computed values is at least 0.85.

These statistical goals are considered objectives for effective model calibration, and calibration continues until model statistics meet these requirements.

The comparison between modeled and observed (measured) data is achieved through the calculation of an error (called a residual) at each observation point (called a target). Calibration quality is further evaluated through visual inspection of the spatial bias of residuals, with an objective of determining the discrete distribution of residual highs and lows throughout the model domain, rather than spatially grouping error estimates. Finally, the calibrated model should reflect conceptual water budget parameters of recharge, discharge, and flows between defined hydrologic accounting areas, although modeling also may result in conceptual changes regarding uncertain parameters.

The calibration approach outlined above is based upon the concept that the model should be calibrated to discrete points where values are known rather than water level contour maps where known values are extrapolated. Many well-known researchers in the field, including Konikow (1978) and Anderson

and Woessner (1992), subscribe to this concept. The error statistics are then used to judge the quality of the calibration, and, thus, the model itself.

### 3.4.10 Simulated Heads and Calibration Quality

Simulated heads in the model reasonably duplicate field observations, as shown in Figures 11 and 12. A model is perfectly fitted if the plot of observed versus simulated water level elevations is a one-to-one line, with a corresponding  $R^2$  value of 1.00. The degree of scatter in the plots indicates the level of error present in the model. Any grouping of points above or below the 1-to-1 line indicates a spatial bias in the data. In the case of the model prepared for the project, spatial bias is low and the linear regressed  $R^2$  value is 0.97 (close to 1) for head targets.

Commonly used statistical criteria for judging model calibration fit and robustness are summarized in Table 10. The residual mean is near zero at 0.37 ft. The statistical values RMS error, residual mean, and residual standard deviation scaled by the range in target values meet the desired calibration objectives.

<b>Table 10 – Steady-State Model Calibration Summary Statistics</b>	
<b>Statistical Parameter</b>	<b>Value</b>
Residual Mean (ft)	0.37
Absolute Residual Mean (ft)	3.23
Residual Std. Deviation (ft)	4.38
Sum of Squares (ft)	193.03
RMS Error (ft)	4.39
Min. Residual (ft)	-6.10
Max. Residual (ft)	9.99
Number of Observations	10
Range in Observations (ft)	63.7
Scaled Residual Std. Deviation (ft/ft)	0.0687
Scaled Absolute Residual Mean (ft/ft)	0.0507
Scaled RMS Error (ft/ft)	0.0690
Scaled Residual Mean (ft/ft)	0.0058

### 3.4.11 Simulated Steady-State Flow of Groundwater

The resultant steady-state water table elevation contours for the steady-state model calibration are shown in Figure 11. The simulated potentiometric controls define flows of groundwater consistent with the conceptual flow system understanding. Groundwater flow west of the Pisgah Fault flows northerly toward Newberry Springs, being part of the Lower Mojave Valley Groundwater Basin flow system. Groundwater flows within the wedge between the Pisgah Fault and Fault B flows easterly, ultimately discharging across Fault B and continuing eastward toward Ludlow and the Broadwell Valley Groundwater Basin.

Potentiometric gradients across the wedge are notably steeper than outside the wedge, reflecting lower hydraulic conductivities of the older mudstone sediments as contrasted with the alluvium outside the wedge. Simulated eastern groundwater flow across the Pisgah Fault over its entire length in the model domain (~10 miles) and through the entire saturated thickness is 34 AFA, or approximately 30% of the recharge occurring to the southern model domain from the Lava Bed Mountains. Simulated subsurface flow through the saturated thickness of the mudstone and evaporate sediments near the ore body is 8 AFA, or approximately 7% of the recharge from to the southern model domain.

### 3.4.12 Parameter Sensitivity Testing

The purpose of a sensitivity analysis is to document relative sensitivity among the various input parameters and boundary conditions in the model. Such analysis provides information about which parameters are most important to the calibration.

To accomplish the sensitivity analyses, multiple model runs were made. In each run, the parameter of interest is adjusted by a certain percent lower or higher, and the statistical effect to the model calibration is reviewed. In each sensitivity simulation, the altered parameter was multiplied by a range in factors, and the sum of squared residual error was reported. The range of variation was not dependent on physical attribute ranges, but rather is established to distinguish sensitivity variation within the set of parameter values used. For example, variation in hydraulic conductivity sensitivity could be clearly distinguished in this model using a modest variation in the parameter values, while GHB conductance sensitivity required a more extreme variation to differentiate parameter sensitivities. GHB and HBF conductance terms were varied between 0.01 to 100, and the hydraulic conductivity and recharge rates were varied between 0.5 to 1.5, sufficient to gain clear definition of differences in sensitivity. The sensitivity runs were performed in the steady-state model with statistical calibration changes reported for the steady-state head target data set.

Results of sensitivity runs are summarized in Figures 13 to 15. Horizontal conductivity zones with the highest sensitivity are the mudstone/claystone unit (K Zone 1), and the shallow alluvium west of the Pisgah Fault (K Zone 9) (Figure 13). The parameter sensitivities indicate that the calibration could be improved mildly by decreasing the conductivity for Zone 2, which represents the layer 3 alluvium east of Fault B. However, the  $Kx-y$  value was desired to be maintained at or near to the computed value from the pumping test of well PW-1, and was not reduced below 2 ft/day.

Vertical conductivity values (Figure 13) show lower sensitivity as contrasted with horizontal conductivity values. The highest sensitivity was observed in Zones 6 and 3, representing upper alluvium west of the Pasgah Fault, and the bounding mountain blocks, respectively.

General Head Boundary conductance shows comparatively high sensitivity (Figure 14), with the most sensitivity observed for GHB Zone 2, the outflow boundary to the east to the Broadwell Valley basin. By contrast, the conductance values for the HFBs representing the Pisgah Fault and Fault B are less sensitive than the GHB conductance. The conductance of the Pisgah Fault has higher sensitivity than Fault B. The low sensitivity of Fault B to variance in conductance was noted during calibration, and therefore was left at a relatively high value so as to not overly constrain simulated flow through the fault.

Recharge rate is also a moderately sensitive parameter (Figure 15), with Zone 3 representing the recharge to the Lava Bed Mountains showing a little higher sensitivity as compared to Zone 2, representing recharge to the Cady Mountains.

## 4. PREDICTIVE MODELING

Since production-scale solution mining of the colemanite formation has not occurred to date, there are no time-series data to calibrate a transient model, such as observed extent and degree of propagation of pressure heads or acid solution migration or reaction. Future data collection during solution mining will allow for future transient calibration of the numerical flow model, which might include refinements of hydraulic conductivities, storage coefficient, dispersion, decay and reaction (none assumed in this model) coefficients. Values assigned for transient modeling are discussed below.

Two types of transient simulations were completed; one being a daily time step model extended out for 100 days – called the daily stress testing model, and the second being an annual stress period model – called the long-term model, which extends over the 25-year proposed mine life and a 50-year post mining period.

### 4.1 Transient Modeling Parameters

#### 4.1.1 Specific Storage Values

Storage coefficient, specific yield, and porosity distributions are made using the same zone areas as used for the hydraulic conductivity distribution. Very little data regarding regional storage coefficients are available, but a few coefficients have been determined via testing in the ore body, and from the pumping test at PW-1 in the alluvium east of Fault B.

The model input of the storage coefficient in MODFLOW2000 uses the specific storage ( $S_s$ ) value, which is the storage coefficient divided by the saturated thickness. In the ore body, this was calculated to be approximately  $2.5 \times 10^{-8}$ .  $S_s$  values assigned to hydraulic conductivity zones are summarized in Table 9.

For land subsidence modeling using the SUB package for MODFLOW2000 (Hoffman et al, 2003), the elastic and inelastic components of the specific storage are assumed to be partitioned into 10% elastic and 90% inelastic, for all model zones.

#### 4.1.2 Effective Porosity

Effective porosity is a variable used for solute transport simulations. The effective porosity is the total void space in the sediments or rocks, minus the pore space that is occupied by water absorbed on clay minerals or other grains. The effective pore space must additionally be interconnected for fluid conveyance. The effective porosity is therefore a value lower than the total pore space of the materials. Assumed effective porosities for lithologic units represented in the model are summarized in the Table 9. The ore body and anhydrite layer, together comprising stratigraphic Unit 3, is assumed to have an initial effective porosity that is low, reflecting hydraulically tight evaporite minerals and water absorbed to interbedded clays. As acid mining of colemanite occurs, it is assumed that the effective porosity of the ore body will increase to approximately 15%, based on the percentage of colemanite within the ore body that may be dissolved, and assuming the pore spaces will become interconnected. This effective porosity value assumes that interbedded clays and other evaporite minerals will be minimally affected by the solution mining.

#### 4.1.3 Pumping and Injection Wells

Well pumping and injection in the ore body, and process water supply pumping in the long-term transient model was simulated using the MODFLOW Well package. The Well package requires specified flow rates to be input for specified cells within the model. For solute transport modeling, the injection well fluid was simulated as having a concentration of 1, equal to 100% acid-containing injectate.

For the daily stress testing model, the MODFLOW Multi-Node Well package (MNW) was used. The MNW package enabled simulation of both pumping and injection based on pumping water levels or



injection pressure heads, rather than having specified flow rates. In the daily stress testing modeling, the hydraulic parameters of the ore body along with the pumping or injection parameters determine the well pumping or injection rates for each stress period. This approach was used to gain a preliminary understanding of the range in predicted flow rates and formation potentiometric water level responses under initial (low) hydraulic conductivity and progressing through mid-range and end-point hydraulic conductivity as the solution mining of the colemanite increases the permeability of the ore body. Results from this testing informed the long-term model simulation.

#### 4.1.4 Daily Test Modeling Injection and Pumping Cycle

The daily stress testing model was set up with 8-hour stress periods (1/3 of a day), progressing over 100 days (300 stress periods total) in a repeated cycle as summarized in Table 11. Pumping was simulated from wells placed only in sequential mining area A1. Each 250 ft by 250 ft model cell (100 ft thick) that contains ore material within the A1 area was assigned a pumping or injection well, with an equal number of pumping and injection wells being assigned in each model layer containing A1 ore. A total of 28 wells are utilized, as distributed as shown in Figure 16, with twenty wells in model layer 6, and eight wells are model layer 7. Each well uses the MNW functions to constrain the pumping and injections rates to what can be physically input or withdrawn from the model cell under a pressure of ~150 psi at land surface, or a drawdown of ~1100 ft from land surface (pumping water level elevation of 900 ft amsl).

The daily stress testing model was initially run using the native (pre-mining) hydraulic conductive of  $4.5 \times 10^{-3}$  ft/day and storage coefficient (Ss) estimates ( $5.7 \times 10^{-8}$ ) for the colemanite (K zone 20). This stress cycle modeling represents conditions at the start of mining before acid leaching of the colemanite has increased the localized permeability (termed the low-K scenario).

To gain a preliminary understanding of the bounding conditions near the end of mining, a high permeability model scenario was run, which increases the K and Ss to predicted values after solution mining (termed high-K scenario). A K value of 0.135 ft/day and a Ss of  $1.1 \times 10^{-7}$  were used, reflecting a 30x increase in storativity, as estimated by Hydro-Engineering (1996). An intermediate level of K ( $6.975 \times 10^{-2}$ ) and Ss ( $8.35 \times 10^{-8}$ ) values were also tested, termed the mid-K scenario.

Results of the daily stress test modeling informed inputs to the long-term modeling over the 25-year proposed mine life, and specifically examined two variables:

- the preliminary extent of observed pressure ranges / effects in the formations surrounding the ore body, and
- the potential range in injection and pumping rates over the course of solution mining.

The vertical K (Kz) was not modified over initial conditions, due to the thinly dispersed nature of the colemanite within anhydrite and other evaporites that will have limited dissolution during mining. The colemanite ore occurs in thinly bedded and discontinuous layers, and dissolution is assumed will occur in a preferential horizontal direction. This assumption could affect the degree of injectate simulated to influence the model layers immediately above or below each layer containing ore, but at the expense of lessening the lateral extent of influence. Given the presently available data, the assumption of limited vertical dissolution appears to be reasonable, and will result the greatest simulation of lateral extent of injection influence.

Table 12 summarizes the hydraulic properties for each test scenario and Table 13 summarizes total wellfield pumping and injection rates, for each scenario. Figures 17 to 19 show the predicted extent of potentiometric water level change (negative values = mounding, positive = drawdown) in model layer 6 after 100 days of the stress scenario pumping and injection. Potentiometric head increases are observed as the dominating change under all three injection and pumping scenarios, although to a lesser degree under the High K scenario. The increases in simulated potentiometric head are explained by

the longer times under pressurized conditions (injection time plus colemanite reaction time) as contrasted with simulated pumping time.

The outcome of the testing indicates that the maximum pressure response in the formation surrounding the ore body occurs under the medium K and S scenario. Under low K and S, the pressure response in the surrounding formation is constrained in part by the limited volume of fluids being injected and pumped. In the high K and S scenario, the increase in storativity and permeability in the ore body accommodates the injection and pumping more effectively as compared with the mid K and S scenario, resulting in a lower degree of formation pressure response outside the ore body. It is also notable that some pressure response is noticed beyond the Pisgah Fault and Fault B in the mid-K and S scenario (see Figure 18). This occurs because the faults are not represented as impermeable, rather as low permeability features that still allow of some groundwater flow across the structures. For long-term simulations of potential solution mining impacts to the hydrologic flow system, use of the mid-K and S will produce the greatest extent of pressure response in the surrounding formation, and is therefore a “conservative” selection for flow and transport modeling in long-term conditions.

Under the low K conditions, the average daily pumping rate of 11.3 gpm exceeds the average daily injection rate of 3.0 gpm (9.9 gpm in the injection phase), so there is a predicted net gain in fluid production from the well field. In the mid-K and high K conditions, the average daily injection exceeds the average daily pumping by 3.6 percent and 10.5 percent, respectively. This suggests that some injectate will be transmitted a short distance into the adjacent formation under medium to high (end-point) permeability conditions.

<b>Table 11 - Daily Injection and Pumping Cycles in the Stress Testing Model</b>				
<b>0-8 hours</b>	<b>Well Constraint</b>	<b>8-16 hours</b>	<b>16-24 hours</b>	<b>Well Constraint</b>
Injection	150 psi pressure head at land surface (water level elevation in well at 2350 ft amsl)	No injection or pumping	Pumping	Air lifting from 1100 ft in depth, maximum drawdown at 900 ft amsl

<b>Table 12 - Hydraulic Property Changes for Daily Stress Testing Model</b>				
<b>Ore Body Permeability</b>	<b>Kx-y</b>	<b>Kz</b>	<b>Ss</b>	<b>Porosity</b>
Low K	0.0045	0.0001	5.7e-08	0.010
Mid K	0.06975	0.0001	8.35e-08	0.075
High K	0.135	0.0001	1.1e-07	0.150

<b>Table 13 – Simulated MNW Pumping and Injection in Stress Test Modeling</b>						
<b>Test Scenario</b>	<b>Injection Rate (total from 14 wells)</b>			<b>Pumping Rate (total from 14 wells)</b>		
	<b>Daily Low (gpm)</b>	<b>Daily High (gpm)</b>	<b>Daily (24-hr) Average (gpm)</b>	<b>Daily Low (gpm)</b>	<b>Daily High (gpm)</b>	<b>Daily (24-hr) Average (gpm)</b>
Low K and Ss	0	9.9	3.0	0	34	11.3
Mid K and Ss	0	225	72.9	0	214	70.4
High K and Ss	0	350	116	0	335	105

### 4.1.5 Long-Term Mining Simulation

Simultaneous pumping and injection were simulated over the planned 25-year mine life using pairs of pumping and injection wells placed in model cells containing the ore body. Subareas of the ore body are assumed to be mined sequentially from areas A1 to A16 as shown in Figure 16 and Figure 20. Each mining subarea has ore body represented in one to three model layers, being layers 6 through 9. A pumping and injection well pair were placed into each layer containing ore for the subarea, thereby, there are one to three pumping and injection wells operating for each subarea. The pumping and injection well pairs represent, on a coarser-scale, the subarea wellfields that will be comprised of multiple wells. Twenty pumping and injection well pairs are used in the ore body mining simulation (40 wells total) distributed as shown in Figure 20.

The mining period for each subarea was simulated at three years, with one-year overlap in mining activities between sequential areas (see Table 14). Mining areas A15 and A16 were simulated pumping simultaneously during the last three years of mining. Each pumping and injection well was simulated at a flow rate of 25 gpm, therefore, at any given stress period in the 25 year mine life, there was between 25 gpm to 150 gpm of simultaneous pumping and injection simulated in the model.

Based on the daily stress testing, the ore body hydraulic parameters were set at the mid-range values which are representative of long-term expected average conditions. These mid-range values also produced the greatest extent of potentiometric head response to injection and pumping in the daily time-step test modeling. Hydraulic property values used are as follows:

- K<sub>x-y</sub> = 0.06975 ft/day
- K<sub>z</sub> = 0.0001 ft/day (no change from initial conditions)
- S<sub>s</sub> = 8.35 x 10<sup>-8</sup>
- Porosity = 0.075

Two water supply wells for processing and injectate make-up water are simulated as pumping at a rate of 100 gpm continuously over the 25-year mining period. The flow rates are distributed with 75 gpm assigned to well PW-1 from model layers 2 and 3, and 25 gpm assigned to well MWW-1 from model layer 2.

SP	Mining Yr	A1	A2	A3	A4	A5	A6	A7	A8	A9	A10	A11	A15	A16
1	0													
2	1	x												
3	2	x												
4	3	x	x											
5	4		x											
6	5		x	x										
7	6			x										
8	7			x	x									
9	8				x									
10	9				x	x								
11	10					x								
12	11					x	x							
13	12						x							
14	13						x	x						

Table 14 - Pumping Simulation in the Long-Term Model														
SP	Mining Yr	A1	A2	A3	A4	A5	A6	A7	A8	A9	A10	A11	A15	A16
15	14							x						
16	15							x	x					
17	16								x					
18	17								x	x				
19	18									x				
20	19									x	x			
21	20										x			
22	21										x	x		
23	22											x		
24	23											x	x	x
25	24												x	x
26	25												x	x
27	1	POST MINING												
28	10													
29	20													
30	30													
31	40													
32	50													

#### 4.1.6 Solute Transport Parameters

Injection wells were assigned an injectate concentration of 1, representing 100%. The model domain at the start of the transient simulation had an initial concentration of zero.

Non-reactive (no chemical reactions) advection-dispersion solute transport was used for the acid solute transport simulations. Density effects were not simulated, and were assumed to have limited influence on the model domain (limited density-driven interaction of higher salinity ore body water and fresh injection water). No removal of solute mass was assumed, other than pumping extraction by recovery wells. This set of simplifying assumptions is believed to be prudent since actual long-term injection and recovery mining and complementary monitoring data are not yet available to further refine or calibrate the contaminant transport simulation. As represented in this initial modeling effort, the set of parameters used can be viewed as “conservative” in that some additional mechanisms such as acid neutralization and solute attenuation by sorption and mineral precipitation will likely occur, thus limiting solute migration to no greater than the extent simulated in the model.

Assumed longitudinal dispersivity is 250 feet, transverse dispersivity is 25 ft, and vertical dispersivity is 2.5 ft. The grid Peclet number computed by dividing the grid dimension (250 to 1000 ft) by the longitudinal dispersivity (250 ft) is 1 to 4, sufficient to minimize numerical dispersion ( $\leq 2-4$ , and no greater than 10 is generally recommended). The GCG solver used an implicit finite difference solving technique and was implemented in MT3DMS.

A second solute transport test simulation was conducted using an increase in effective porosity of the ore body to 15%. The predicted extent of solute transport was slightly less under this scenario, but in general was similar to the base case (mid-range value of 7.5% effective porosity). This test simulation indicates that the effective porosity of the ore body is a low sensitivity parameter as it relates to the simulated extent of solute migration.

## 4.1.7 Land Subsidence Parameters

Subsidence is defined as the settling of the ground surface, or compaction of subsurface materials, when the intergranular pore pressures are reduced (Sneed, 2001). Several processes that cause subsidence include soil compaction, dissolution of soluble rocks such as limestone (or in the case of the proposed project – solution mining of the colemanite), hydro-compaction (wetting and drying of low-density soils), and groundwater withdrawal.

### 4.1.7.1 Physical Principals of Subsidence

Compaction of subsurface materials occurs differentially, depending largely on grain size and the compressibility of sediments or rocks comprising aquifers and aquitards. Aquifers refer to a volume of permeable rock or unconsolidated material where water can be stored and transmitted freely to wells, while an aquitard is a relatively low permeability zone that does not yield water freely to wells and is adjacent to an aquifer. In the project area, aquifers are identified in the upper basin-fill materials to the east and west of Fault B and the Pisgah Fault, respectively. Aquitards are composed of fine-grained material such as silt or clay, the extensive lacustrine mudstones, clays and evaporates presented within the up-lifted wedge, and within the deeper alluvial basin-fill behave as aquitards.

The potential for compressibility under potentiometric head changes is largely related to differences in elastic and inelastic storage coefficients of the materials. In general, bedrock has minimal compressibility, granular aquifer materials have moderate levels of compressibility, and the finer grained silt and clay materials comprising aquitards, or thinly interbedded within aquifers have relatively high compressibility. A detailed discussion of the mechanical properties of differential compaction due to differing elastic and inelastic properties of subsurface materials can be found in Terzaghi (1925) and in Sneed (2001). That discussion is summarized briefly below.

Changes in hydraulic head in saturated sediments cause changes in intergranular effective stress. Depressurization of an aquifer system induces stress that results in either elastic or inelastic strain. In a perfectly elastic system, changes in stress caused by the expansion or compaction of sediments, or the expansion and compaction of water, result in a proportional strain to the system. All deformation caused by elastic strain is, by definition, reversible. In inelastic systems, increases in effective stress result in a disproportional amount of strain and some degree of resulting deformation is not reversible. Although both aquifers and aquitards have elastic and inelastic properties, in coarse-grained aquifer units the inelastic component is generally negligible and may be ignored (Sneed, 2001). In fine-grained aquitard units, the inelastic component may be dominant if applied stress exceeds the maximum pre-consolidation stress of the system; that is, if the applied stress exceeds any other previous maximum hydraulic head decline. Thus, aquitard materials may behave elastically until a threshold strain is achieved and thereafter behave in an inelastic manner. The maximum effective stress is generally thought of as the greatest amount of stress applied to an aquifer/aquitard system which exceeds any previous maximum stress. It can be confidently assumed that a system has exceeded its previous maximum stress if water levels have consistently continued to decline as a result of continued groundwater withdrawals, particularly for a number of years or decades.

Mathematically, these concepts can be applied to an aquifer system as a whole by the following relationship (Sneed, 2001):

$$S^* = S^*k + S_k + S_w, \text{ where}$$

$S^*$  = aquifer storage coefficient of a compacting aquifer (see storativity, Section 3.6)

$S^*k$  = skeletal storativity of aquitard units,

$S_k$  = skeletal storativity of aquifer units, and

$S_w$  = storativity of water.

As indicated above, an important concept related to aquitards is that  $S'_k$ , the storativity (storage coefficient) of the aquitard unit, is composed of two components, elastic and inelastic. Once the maximum strain threshold is exceeded,  $S'_k$  will dominate, and the sediments will behave inelastically. Therefore, for subsurface materials undergoing compaction due to groundwater withdrawal, the maximum effective stress of the system has been exceeded, and the storage coefficient is then the sum of the inelastic storage coefficient of aquitard units, the storage coefficient of the aquifer units (elastic), and the storativity of water (elastic). Because the compressibility of water is very small (Freeze and Cherry, 1979), it can be ignored. Thus, the storage coefficient ( $S$ ) in compacting systems can be reasonably defined by two components: the elastic component of coarse-grained materials and the inelastic component of fine-grained materials.

The elastic storage coefficient, as used here, was defined by the volume of water taken into or released from storage per unit area of permeable material per unit of change in head. Water derived from this type of source was completely derived from the elastic compression of the aquifer. Typical values of elastic storage coefficients are not precisely known in the study area, but other detailed studies of land subsidence, particularly in the San Joaquin Valley of California, have indicated that specific elastic storage (the elastic storage coefficient divided by aquifer thickness) for coarse-grained materials can be in the range of  $1 \times 10^{-6}$ , although Morgan and Dettinger (1996) indicate that this value is generally higher than that derived from pumping tests. Hoffman and Zebker (2001) estimated the elastic storage coefficients to range between  $4.2 \times 10^{-4}$  and  $3.4 \times 10^{-3}$  from land deformation and extensometers placed at several well sites in the Las Vegas Valley. Bell et al. (2008) derived values ranging between  $2.0 - 3.7 \times 10^{-3}$  in the same area, using a variety of remote sensing and empirical techniques.

The inelastic component of the storage coefficient refers to the water released from storage as a result of compaction of fine-grained aquitards or fine-grained interbedded strata within an aquifer system (Morgan and Dettinger, 1996). During inelastic compaction, these fine-grained sediments may release large quantities of water from storage, particularly over prolonged periods of head decline (Morgan and Dettinger, 1996). In fact, the overall storage capacity of an aquifer system may be dictated more by the inelastic component than the elastic component (Jacob, 1940). In an evaluation of well logs, specific unit compaction, and volumetric analysis of subsiding sediments in the Las Vegas Valley, estimates of the inelastic storage coefficients for basin-fill materials ranged from  $9 \times 10^{-4}$  to  $1.4 \times 10^{-2}$  for shallow, near-surface aquitards and  $7 \times 10^{-4}$  to  $3.2 \times 10^{-4}$  for deeper aquifer/aquitard units (Morgan and Dettinger, 1996). In Las Vegas Valley, Bell et al. (2008) estimated inelastic storage coefficients ranging between  $9.0 \times 10^{-3}$  and  $2.0 \times 10^{-2}$  by analyzing ground displacement and pumping data, while Hoffman and Zebker (2001) provided estimates ranging from  $9.5 \times 10^{-4}$  to  $1.5 \times 10^{-3}$ .

Although the range of elastic and inelastic storage coefficients from San Joaquin Valley, California, and Las Vegas Valley, Nevada, may not correlate exactly to properties in the project area, they provide a general range in expected values. Comparisons of inelastic storage coefficient for two different studies indicate that the estimated values are 4.5 to 30 times greater than that estimated for the elastic component of storage (Helm, 1978; Morgan and Dettinger, 1996). This means that for analogous systems, subsidence is largely irreversible, and where caused by groundwater withdrawals, the area will not rise again once groundwater levels rebound.

#### **4.1.7.2 Documented Local Subsidence – Newberry Springs / Troy Lake Area**

Subsidence is commonly associated with groundwater withdrawals in basin-fill sediments, that have reduced the potentiometric water level in an aquifer. Subsidence is commonly quantified using InSAR (Interferometric Synthetic Aperture Radar) satellite imagery which can detect subtle changes in land surface elevation over time. InSAR data are available since the early 1990s. To the west of the project in the Newberry Springs and Troy Lake portion of the Lower Mohave River basin, InSAR has been used to quantify subsidence that has occurred (and is presently occurring) due to pumping by agriculture resulting in long-term declining groundwater levels. Sneed et al (2003) and Brandt and

Sneed, 2017) summarize the magnitudes and geographic extent of subsidence in the Newberry Springs - Troy Lake area. Between 1993-2009, there has been about 5 inches of land subsidence, with the rates of subsidence increasing from about 0.15 in/yr in the 1993-99 time period, to 0.45 in/yr during the 2004-09 time period. These levels of subsidence correspond to water level declines in the alluvial aquifer from which pumping occurs in the range of approximately 20 to 50 ft over the past 25 years (USGS NWIS water level data, 2019). The compaction of sediments is interpreted to be principally in thin to thickly bedded clays in the vicinity of the water level declines, and in thicker units of clay near Troy Lake. Using an average long-term subsidence rate of 0.03 ft/yr, the total subsidence over the past ~25 years is about 0.75 ft.

#### **4.1.7.3 Land Subsidence Model Parameters**

For the predictive subsidence modeling associated with potentiometric water level changes imposed by the project, the specific storage is assumed to be comprised of 90% inelastic storage and 10% elastic storage. This is a mid-range distribution of inelastic and elastic storage coefficients.

The MODFLOW SUB package assumes deformation and compaction within subsurface materials is caused by head or pore-pressure changes, thus by changes in effective stress within interbeds and aquitards comprised of compressible materials. The subsidence simulations are run assuming no delayed release of water from storage or uptake of water into storage by interbeds or aquitards.

## **4.2 Transient Long-term Modeling Results**

The simulated long-term mining impacts to groundwater and land surface are described in the following sections.

### **4.2.1.1 Predicted Potentiometric Head Responses**

Potentiometric water levels vary over time and with spatial changes in simulated injection and pumping. Appendix B1 shows the distribution of simulated potentiometric water level changes in each model layer at mine-year 25. Drawdown and mounding are shifted to the west side at that time, because pumping and injection is taking place in subareas A15 and A16 on the west side of the ore body. Water level drawdown is observed in the upper model layers outside the fault bounded wedge, as a result of process water supply pumping from wells PW-1 and MWW-1.

Appendix B2 shows the potentiometric water levels in model layer 7 (mid-depth in the ore body) at three-year time increments over the 25-year mine life. Potentiometric head changes are observed to take place up to approximately 20,000 feet outside the ore body at the 1 ft threshold level. At the 5 ft threshold, potentiometric water level change is observed up to approximately 4,000 ft outside the ore body. The potentiometric head change extends beyond the Pisgah Fault and Fault B, as these faults are not represented as impermeable, rather there are seepage changes across the faults and resultant potentiometric head changes across the faults.

Figures 21a to 21e are plots of simulated potentiometric head change at model observation points OP-1 to OP-5 located outside the ore body. The locations of the model observation points are shown in Appendix C. Head change varies within plus-minus approximately 25-35 feet over the 25-year mine life, and then trends back to within 1 foot of pre-mining potentiometric water levels by 50 years post-mining. Table 15 summarizes the predicted potentiometric water level changes at the observation points over the model simulation period.

Potentiometric head change at the monitoring wells and observation wells that were ultimately proposed in the UIC permit application are provided in Appendix D.

<b>Observation Point</b>	<b>Max Decrease in Head (ft)</b>	<b>Mine Year Occurs</b>	<b>Max Increase in Head (ft)</b>	<b>Mine Year Occurs</b>	<b>50 Year Residual Change in Head (ft)</b>
OP-1	7.1	19	8.8	16	0.6
OP-2	8.2	11	25.5	15	0.4
OP-3	17.1	16	11.1	19	0.2
OP-4	35.4	5	10.5	11	1.0
OP-5	11.0	16	15.4	19	1.0

#### 4.2.1.2 Predicted Solute Transport

Predicted solute transport of the injectate at Mine Year 25 is shown for each model layer, to a 0.0001 relative concentration threshold (effectively zero) in Appendix C1. The simulated lateral extent of injectate transport in model layer 7 (mid-depth in the ore body) is shown for 3-year increments in the mine life in Appendix C2.

Residual solute is observed across the ore body and in the adjacent formation immediately surrounding the ore body. The maximum lateral extent of simulated solute transport at the 0.0001 relative concentration threshold is shown in Figure 22. This solute transport modeling indicates that the migration of injection fluid solutes into the surrounding formation may occur, but is limited in lateral extent to an average distance of approximately 1,100 feet from the ore body.

Figure 23a and 23b present cross-sectional views showing the vertical extent of solute transport. The solute transport extends above the ore body (layers 6-9) into layers 4 and 5, and below into layer 10, but is not simulated to extend vertically into overlying layers 1-3, which contain the upper 1,100 feet of lakebed sediments, or underlying layers 11-13. No solute is predicted to migrate to the underlying layer 12, which represents a higher permeability basal conglomerate overlying the volcanic bedrock. No solute is predicted to migrate outside the wedge and beyond the bounding Pishgah Fault and Fault B to the shallower alluvium from which mining process water is produced from wells PW-1 and MWW-1.

Figures 24a to 24e are plots of predicted concentrations of residual injectate over the 25-year mine life and 50-year post mining period at the observation points OP-1 to OP-5. Up-gradient observation points OP-4 and OP-5 are not predicted to detect any solute. Observation points OP-1, OP-2 and OP-3 are predicted to experience very low levels of solute, between 0.0001 (0.01%) to 0.00043 (0.04%). Detections begin midway in the mine life, and continue post-mining due to a subtle flow gradient to the northeast as potentiometric water levels recover. The solute is essentially predicted to remain in the mining affected area presented at mine year 25 throughout the simulated 50-year post-mining period, with very little advective or dispersive movement. Table 16 summarizes solute transport simulation results. Table 17 presents the simulated rates of contaminant movement at the 0.01% concentration level and in the post-mining period. Rates of simulated transport range from approximately 0.5 to 5.5 ft/yr. The highest rate of transport occurs in the easterly direction, along the direction of natural groundwater flow.

Predicted concentrations of residual injectate at the monitoring wells and observation wells that were ultimately proposed in the UIC permit application are provided in Appendix D. The locations of these wells are provided in Figure 22.



The contaminant transport simulations do not reflect any rinsing of the formation after mining, and therefore may over predict the amount of residual injectate remaining in the ore body after mining. The model contaminant transport simulations also do not simulate any reaction, decay or absorption of the injectate solutes, which in reality is likely to occur. Lastly, the model simulates a very homogeneous environment. Future monitoring during mining activities will provide data upon which more sophisticated solute transport simulations may be made, and additional parameters governing solute transport may be calibrated to reflect observed conditions. However, this initial contaminant transport modeling which is based on advection and dispersion transport without decay or absorption is believed to be a conservative simulation that is helpful to provide constraint to expected outcomes and provide guidance to development of a monitoring network for the operation.

<b>Table 16 – Predicted Solute Transport Detection at Proposed Observation Wells</b>			
<b>Observation Point</b>	<b>Mine Year First Detection Occurs at 0.01% (0.0001)</b>	<b>Max Concentration Detected (% of initial concentration)</b>	<b>Year Occurs</b>
OP-1	NA	0.0085 (0.000085)	Post-mining Year 50
OP-2	65	0.014 (0.00014)	Post-mining Year 50
OP-3	44	0.043 (0.00043)	Post-mining Year 50
OP-4	NA	NA	NA
OP-5	NA	NA	NA

<b>Table 17 - Predicted Post-Mining Rate of Solute Transport</b>		
<b>Cardinal Direction</b>	<b>50-Year Distance of Movement of the 0.01% Concentration Front (ft)</b>	<b>Average Annual Transport Rate (ft/yr)</b>
North	100	2.0
South	25	0.5
East	275	5.5
West	210	4.2

#### 4.2.1.3 Predicted Land Surface Subsidence

The predicted land subsidence as a result of potentiometric head changes simulated due to solution mining ranges from approximately 0.1 ft to a maximum of 2.3 ft geographically distributed directly above the ore body. The process water supply pumping also produces a mild level of predicted land subsidence outside the faults bounding the up-lifted wedge, on the order of 0.1 to 0.2 ft after Mine Year 25. Figure 25 illustrates the extent and distribution of predicted land subsidence in Mine-Year 25.

The land subsidence is predicted to represent mostly a permanent compaction of sediments (inelastic compression), which will not rebound in post-mining conditions as potentiometric water levels recover to pre-mining levels. The simulated levels of land subsidence as a result of the project are similar to, but generally less than, the subsidence that is observed to the west of the project in the Newberry Springs / Troy Lake area (a result of agricultural pumping and drawdown), as documented in Section 4.1.6.2 of this report.

### 4.3 Development and Refinement of the AOR and ZEI Boundaries

The Zone of Endangering Influence (ZEI) and Area of Review (AOR) boundaries for the proposed mining project were developed and refined based on the model predictions. The ZEI corresponds to the predicted outer limit of injectate transport over the period of simulation. The AOR was developed as a buffer outside the ZEI, and was set at distance varying between 100 to 300 based on post-mining transport rates (Table 17). The smaller buffer distances were used in the directions of the slowest predicted transport rates. The AOR and ZEI boundaries are shown in Figure 22.

Observation wells (OW), monitoring wells (MW), and AOR confirmation wells were sited within the area between the proposed ore body and the AOR boundary (Figure 22). The intent of the OWs is to monitor predicted conditions for data collection and future modeling refinement, based on pressure and concentration measurements. The MW and AOR wells are sited at locations predicted to be outside the area of solute migration, as simulated in the model. These wells will provide confirmation of predicted conditions.

## 5. SUMMARY AND CONCLUSIONS

A numerical groundwater flow model has been prepared for the Fort Cady borate solution mining project. The steady-state model simulates existing groundwater flow conditions. Recharge to the local groundwater system occurs from the Cady Mountains to the north, and Lava Bed and Rodman Mountains to the south. Groundwater flow is significantly influenced by barrier conditions along the Pisgah Fault and Fault B, which bound a wedge of predominately sedimentary lakebed deposits, including the evaporates in which the colemanite ore body is located. Groundwater recharge from the southern bounding mountains flows westward to the Newberry Springs area and is considered tributary to the Lower Mohave River Groundwater Basin. A small amount of groundwater is simulated to seep easterly across the Pisgah Fault, through the uplifted wedge, through Fault B, and then outward to the east toward Ludlow and the Broadwell Valley Groundwater Basin. Simulated eastern groundwater flow across the Pisgah Fault through the length (~10 miles) and saturated full thickness (~1500 ft) of the fault-bounded wedge represented in the model is 34 AFA, and through the vicinity of the ore body simulated groundwater flow is 8 AFA.

Hydraulic conductivities of sedimentary deposits in the uplifted wedge are low, in the  $10^{-2}$  to  $10^{-4}$  ft/day range, as demonstrated by very low yield and injection capacities to wells, and hydraulic testing of the ore body materials. Groundwater quality in the evaporates within the uplifted wedge is poor, with baseline formation water TDS concentrations commonly in the range of approximately 30,000 mg/L.

Hydraulic conductivities are several orders of magnitude higher in the alluvium to the east and west of the bounding faults, and water quality is better, in the range of 1,000 to 3,000 mg/L. While not suitable as a drinking water supply, the quality is suitable for industrial-mining supply. Mining process water supply wells will be located in this alluvium, which is capable of yielding flow rates of several hundred gallons per minute.

The solution mining presents a unique combination of conditions to represent in a transient flow model, with cyclical injection and pumping into low conductivity materials that will develop increasing permeability as removal of the colemanite occurs. A daily stress testing model was initially set up to test potential responses, and gain an understanding of potential pumping and injection flow rates that may be possible over a range of hydraulic conductivities. The model operates on time steps of 1/3 of a day, cycling between injection under a pressure of 150 psi at land surface, residence time when the acid solution is allowed to dissolve the colemanite, followed by pumping (air-lifting extraction) which is simulated to permit fluid drawdown to 1,100 ft below ground surface. The low K stress-test scenario uses a native hydraulic conductivity of 0.0045 ft/day, and simulations permit only modest injection and pumping rates in a simulated wellfield in mining subarea A1. During the injection cycle, the formation accepts ~10 gpm total in the wellfield, and during the pumping cycle, the wellfield produces ~34 gpm total. There is a net fluid gain of water from the surrounding formation predicted in this scenario. However, the formation is under pressurized conditions for 2/3 of the day, and on balance there is a net pressure increase in the formation. However, over the long-term, very little water can be expected to be yielded from the formation surrounding the ore body being mined due to low hydraulic conductivity and low specific storage, making a long-term net fluid gain scenario unlikely to be sustainable.

The mid-K and high-K scenarios represent mid-point and end-point solution mining scenarios, when significant colemanite has been dissolved from the formation and permeabilities have increased. In these scenarios, the formation accepts a flow of approximately 200–350 gpm in the wellfield, and produces a similar quantity, however, the injection quantity exceeds the pumping quantity by about 3–10 percent. While the simulations are inexact representations of the highly variable process that will take place, they suggest that there will be net gains in fluid to the well field during early mining stages, transitioning to net losses in later stages. In reality, the net gains and losses can be managed in a balanced approach, with pumping and injection durations varying to achieve near balance. However,

it is important to acknowledge in the operations plans and permitting that the process of injection into and pumping from the low hydraulic conductivity environment will produce variable net flow gains and losses over the mine life, and some migration of barren or pregnant solution into the surrounding formation is anticipated.

Simulated solute (injectate) transport over of the proposed mine life of 25 years was made using mid-range permeability parameters and a sequential pumping and injection simulation over the entire ore body. Pumping and injection rates were balanced over the simulation period, and range from 25 to 75 gpm per mining subarea. Solution migration is simulated under advection and dispersion conditions, without simulation of reactions, decay, or absorption of the injectate. This set of assumptions is believed to be conservative, and as monitoring data are collected in the first few years of solution mining, more sophisticated transport representations may be developed that include reactions and decay of the acid solution used for mining. Refinements can also be made, if needed, to hydraulic conductivities and storage coefficients, and pumping and injection volumes based on measured rates, durations, and quantities.

This preliminary solute transport modeling indicates that the migration of injectate solution into the surrounding formation may occur, but will be limited in lateral extent to an average distance of approximately 1,100 feet from the ore body. No migration of injected solution is predicted to reach alluvium outside the wedge-bounding faults, nor down to a basal conglomerate layer that has been identified on top of underlying volcanic bedrock.

In the post mining portion of the simulation, the remaining residual injectate remains in place in the ore body and bounding formation, with very little migration due to low subsurface flow rates and the hydraulically tight bounding formation. In reality, residual injectate concentrations are expected to attenuate and decay because the formation will be rinsed to remove residual injectate after solution mining is completed in a subarea, and the residual acid injectate will react in alkaline environment and be neutralized.

Modeling indicates that injectate migration will be limited in extent and will not migrate outside the immediate area of mining. The limited extent of simulated migration of injectate is constrained primarily by the low hydraulic conductivities of the evaporate and mudstone formations surrounding the ore body, and to a lesser degree, the volumes being injected or pumped, and governing pressures or drawdown bounds assumed in the model. Therefore, conditions of permitting should not be linked to a net fluid removal scheme or limitations to injection/pumping rates, but rather should focus on demonstrating the desired end effect is accomplished, with migration of barren or pregnant acid solution remaining within near-proximity of the ore body, as demonstrated by monitoring / observation wells.

Land subsidence as a result of potentiometric water level changes during the solution mining process is predicted to range from 0.1 to 2.3 feet. The predicted land subsidence is geographically constrained to the land surface immediately above the ore body. Attempts to over-produce under a net-fluid gain scenario would result in greater durations and magnitudes of potentiometric water level drawdown, and therefore, would produce greater amounts of land subsidence. Mild land subsidence (<0.2 ft) is also predicted outside the bounding faults due to water level drawdown caused by process water supply.

As mining progresses, data collection on pressure heads, acid injectate migration, and operational information (pumping and injection rates and durations) can be input into the numerical groundwater flow model to provide an audit of predictive performance, and as needed, calibration update. An initial model audit and update is recommended at 2 years into mining, and sequent audits should be performed on a 3–5 year basis, or more frequently if notable deviations between observed and predicted conditions occur. Subsequent audits may show adequate match between observed and simulated conditions, therefore not requiring model calibration updates.

## 6. LIMITATIONS

The conclusions presented herein are partially based on information provided by MGA. MGA makes no warranties or guarantees as to the accuracy or completeness of information provided or compiled by others. The results reported herein are applicable to the time the sampling, measurement and testing occurred. Changes in site hydrogeology may occur as a result of rainfall, snowmelt, water usage, mining activities, or other factors.

It should be recognized that definition and evaluation of environmental conditions is a difficult and inexact science. Judgments and opinions leading to conclusions and recommendations are generally made with an incomplete knowledge of the conditions present. More extensive studies, including additional environmental investigations, can tend to reduce the inherent uncertainties associated with such studies. Additional information not found or available to MGA at the time of writing this report may result in a modification to the conclusions and recommendations contained herein.

The presentation of data presented herein is intended for the purpose of the visualization of environmental conditions. A greater degree of spatial and temporal data density may result in a more accurate representation of environmental conditions. Although such data visualization techniques may aid in providing a conceptual understanding of environmental conditions, such presentations are not intended to completely depict environmental conditions.

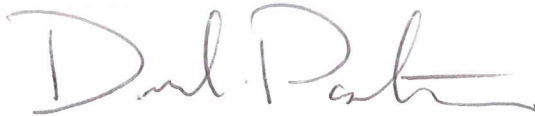
This report is not a legal opinion. The services performed by MGA have been conducted in a manner consistent with the level of care ordinarily exercised by members of our profession currently practicing under similar conditions. No other warranty, expressed or implied, is made.

The use of the word "certify" in this document constitutes an expression of professional opinion regarding those facts or findings which are the subject of the certification and does not constitute a warranty or guarantee, either express or implied.

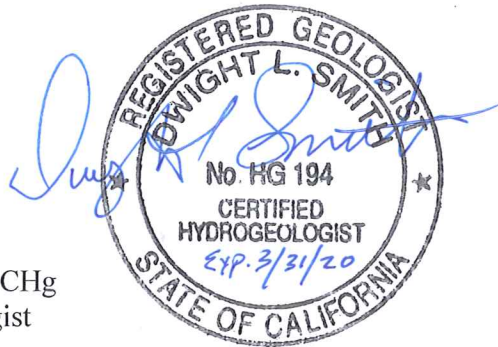
## 7. CLOSING

MGA trusts that the information provided herein will satisfy the needs of FCCC and the US EPA at this time. Should you have any questions regarding this report, or the recommendations provided herein, please contact the undersigned at (775) 829-2245.

**Respectfully submitted,**  
**McGinley and Associates, Inc.**

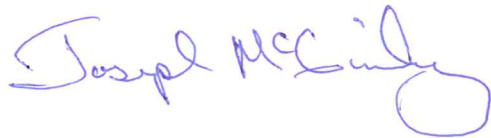


Daniel Pasteris, Ph.D.  
Hydrologist



Dwight L. Smith, PG, CHg  
Principal Hydrogeologist

**Reviewed by:**



Joseph M. McGinley, P.E., P.G.  
Principal

## 8. REFERENCES

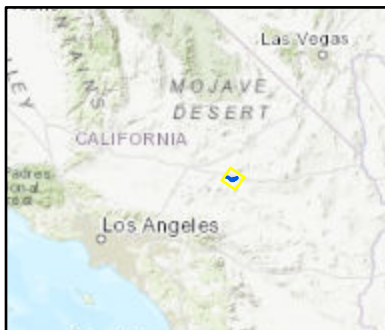
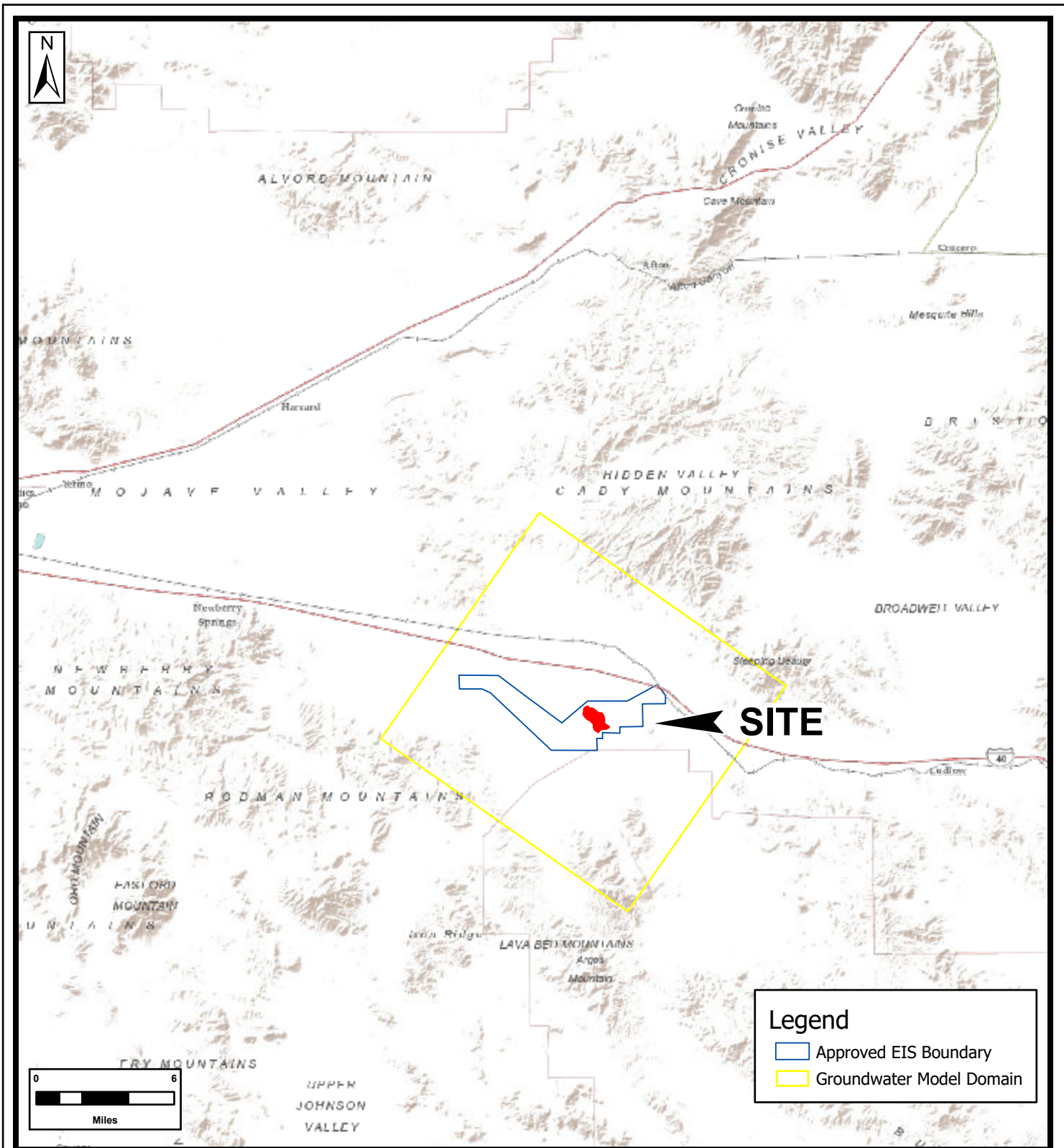
- Anderson, M.P., and Woessner, W.W., 1992, Applied groundwater modeling: Simulation of Flow and Advective Transport: Academic Press, San Diego, California, 381 p.
- Bell, J.W., F. Amelung, A. Ferretti, M. Bianchi, and F. Novali, 2008, Permanent scatterer InSAR reveals seasonal and long-term aquifer-system response to groundwater pumping and artificial recharge, Water Resources Research, vol. 44, W02407, 18 p.
- Brandt, J., and Sneed, M., 2017, Land Subsidence in the Southwestern Mojave Desert, California, 1992-2009; USGS Fact Sheet 2017-3053, 6 pages.
- California Department of Water Resources, Bulletin 118 – Interim Update 2016, Groundwater Basin Boundaries available at <https://water.ca.gov/Programs/Groundwater-Management/Bulletin-118>
- California Department of Water Resources, Water Data Library, Groundwater Level Data, available at <http://wdl.water.ca.gov/waterdatalibrary/>
- California Department of Water Resources, Well Completion Reports, available at <https://water.ca.gov/Programs/Groundwater-Management/Wells/Well-Completion-Reports>
- Confluence Water Resources, 2019. Fault B Program Technical Report, Fort Cady, San Bernardino County, March 2019.
- Cooper, H.H. and C.E. Jacob, 1946. A generalized graphical method for evaluating formation constants and summarizing well field history, Am. Geophys. Union Trans., vol. 27, pp. 526-534. Doherty, J., 2015. Calibration and Uncertainty Analysis for Complex Environmental Models. Watermark Numerical Computing, Brisbane, Australia. ISBN: 978-0-9943786-0-6.
- Core Laboratories, 1981, Special Core Analysis for Duval Corporation, Boron Analysis of Core Leachings, Well SMT-1, July 20, 1981.
- Deal, E. G., 1985. Geologic Summary of the Fort Cady Colemanite Deposit, modified and edited from summaries by P. A. K. Williamson and N. P. Krier, January 1985.
- Freeze, R.A., and J.A. Cherry, 1979, Groundwater, Prentice-Hall, Inc. Publishers, New Jersey, 604 p. Hantush, M.S., 1960. Modification of the theory of leaky aquifers, Jour. of Geophys. Res., vol. 65, no. 11, pp. 3713-3725.
- Harbaugh, A.W., Banta, E.R., Hill, M.C., and McDonald, M.G., 2000, MODFLOW-2000, the U.S. Geological Survey modular ground-water model -- User guide to modularization concepts and the Ground-Water Flow Process: U.S. Geological Survey Open-File Report 00-92, 121 p.
- Hart, E.W., 1987; Pisgah, Bullion and Related Faults, San Bernardino County, California, California Division of Mines and Geology, Fault Evaluation Report FER-188. April 17, 1987
- Helm, D.C., 1978, Field verification of a one-dimensional mathematical model for transient compaction and expansion of a confined aquifer system, American Society of Civil Engineers, Specialty Conference on Verification of Mathematical and Physical Models in Hydraulic Engineering, College Park, MD, August 1978, Proceedings, pp. 189 – 196.
- Hoffman, J., Leake, S., Galloway, D., and Wilson, A., 2003, MODFLOW-2000 Ground-Water Model User Guide to the Subsidence and Aquifer-System Compaction (SUB) Package; USGS Ground-Water Resources Program, Open-File Report 03-233.
- Hydro-Engineering, 1996. Aquifer Characteristics and Potential Well Field Geometry, February 1996.
- In-Situ, 1990, Fort Cady Injection Test, Ore zone wells, In-Situ Inc., April 1990.
- Jacob, C.E., 1940, On the flow of water in an elastic artesian aquifer, American Geophysical Union Transmittal 21st Annual Meeting, part 2, pp. 674-686.

- Jennings, C.W., with modifications by Gutierrez, C., Bryant, W., Saucedo, G., and Wills, C., 2010, Geologic map of California: California Geological Survey, Geologic Data Map No. 2, scale 1:750,000.
- Konikow, L.F., 1978, Calibration of Groundwater Models, in "Proceedings of the Specialty Conferences on Verification of Mathematical and Physical Models in Hydraulic Engineering": College Park, Maryland, August 9-11, 1978.
- Krier, N. P., 1981, Duval Corporation Memo - January Monthly Report, January 27, 1981.
- Leake, S.A., and Prudic, D.E., 1991, Documentation of a computer program to simulate aquifer-system compaction using the modular finite-difference groundwater flow model, USGS Techniques of Water Resources Investigations Report, Book 6, Chapter A2.
- Mann, J. F., 1981. Hydrogeologic Aspects of a Solution Mining Test, Hector, California September 9, 1981.
- Morgan, D.S., and M.D. Dettinger, 1996, Groundwater conditions in Las Vegas Valley, Clark County, Nevada, Part 2, hydrogeology and simulation of ground-water flow, U.S. Geological Survey Water-Supply Paper 2320-B, 124 p.
- Sneed, Michelle, 2001, Hydraulic and mechanical properties affecting ground-water flow and aquifer-system compaction, San Joaquin Valley, California, U.S. Geological Survey Open-File Report 01-35.
- Sneed, M., Ikehara, M., Stork, S., Amelung, F., and Galloway, D., 2003, Detection and Measurement of Land Subsidence Using Interferometric Synthetic Aperture Radar and Global Positioning System, San Bernardino County, Mojave Desert, California; USGS Water-Resources Investigations Report 03-4015.
- Simon Hydro-Search, 1993. Fort Cady Mineral Corporation Solution Mining Project Feasibility Report, San Bernardino, California, October 22, 1993.
- Terra Modelling Services (TMS), 2017. Resource Estimation for the Fort Cady Project, San Bernardino County, California, December 11, 2017.
- Terzaghi, K., 1925, Principles of soil mechanics, IV, Settlement and consolidation of clay, Engineering News-Record 95, no. 22:874-878.
- PRISM Climate Group, 30-Year Precipitation Normals, 800 meter resolution, available at <http://www.prism.oregonstate.edu/normals/>
- Theis, C.V., 1935. The relation between the lowering of the piezometric surface and the rate and duration of discharge of a well using groundwater storage, Am. Geophys. Union Trans., vol. 16, pp. 519-524.
- USGS, National Hydrography Dataset Watershed Boundaries, available at <https://www.usgs.gov/core-science-systems/ngp/national-hydrography/national-hydrography-dataset>.
- USGS, Quaternary Fault and Fold Database, Earthquake Hazards Program, Accessed October 2019 from <https://earthquake.usgs.gov/hazards/qfaults/>
- Zheng, C., and Wang, P.P., 1999, MT3DMS, A modular three-dimensional multi-species transport model for simulation of advection, dispersion and chemical reactions of contaminants in groundwater systems; documentation and user's guide, Vicksburg, Miss., U.S. Army Engineer Research and Development Center Contract Report SERDP-99-1, 202 p.



# FIGURES

---




**FIGURE 1**

TITLE:

**PROJECT LOCATION MAP  
-SHOWING-  
FORT CADY PROJECT  
SAN BERNARDINO COUNTY, CA**

JOB NO.:  
**APB003**

DATE:  
**10/19/2019**

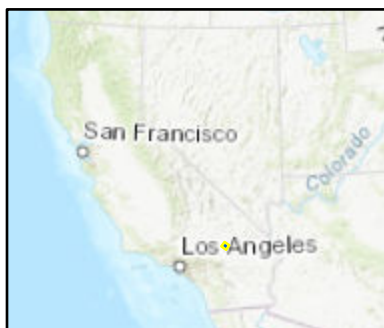
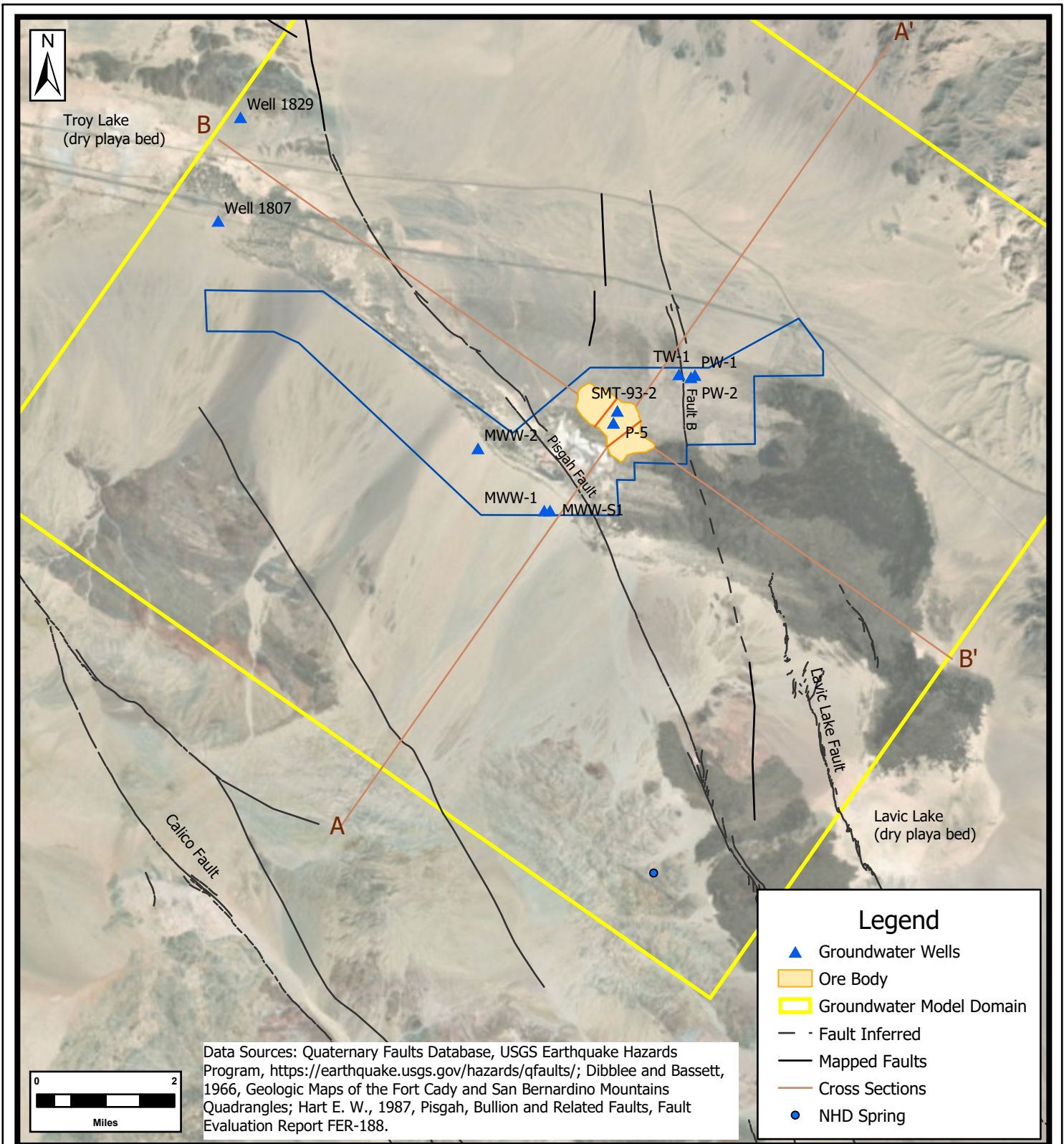


**McGinley & Associates**  
Environmental Engineering and Science  
RENO | LAS VEGAS | [www.mcgin.com](http://www.mcgin.com)

FILE:  
**FortCady3**

COORDINATE SYSTEM:  
**NAD 1983 UTM Feet**

DESIGNED	DRP	CHECKED	DRP	REVISION:
DRAWN	DRP	APPROVED	DRP	-



**FIGURE 2**

TITLE:  
**SITE MAP  
 -SHOWING-  
 FORT CADY PROJECT AREA AND  
 GROUNDWATER WELL LOCATIONS  
 SAN BERNARDINO COUNTY, CA**

JOB NO.:  
**APB003**

DATE:  
**11/11/2019**

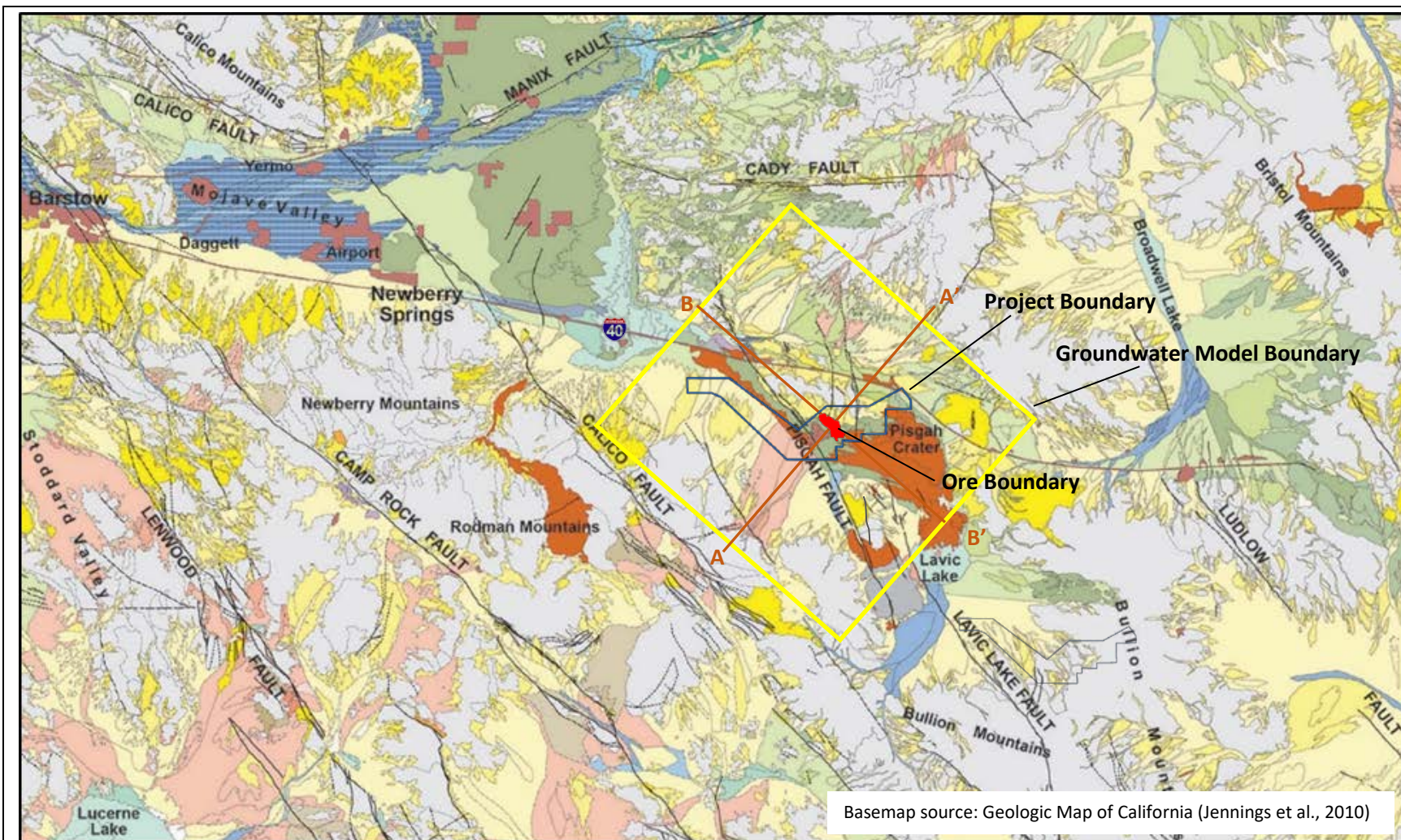
McGinley & Associates  
 Environmental Engineering and Science  
 RENO | LAS VEGAS | www.mcgin.com


FILE:  
**FortCady3**

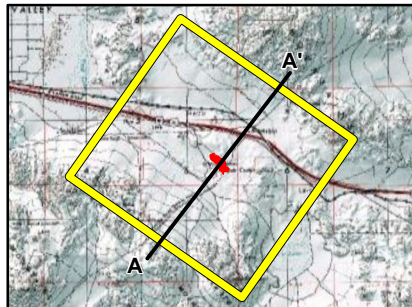
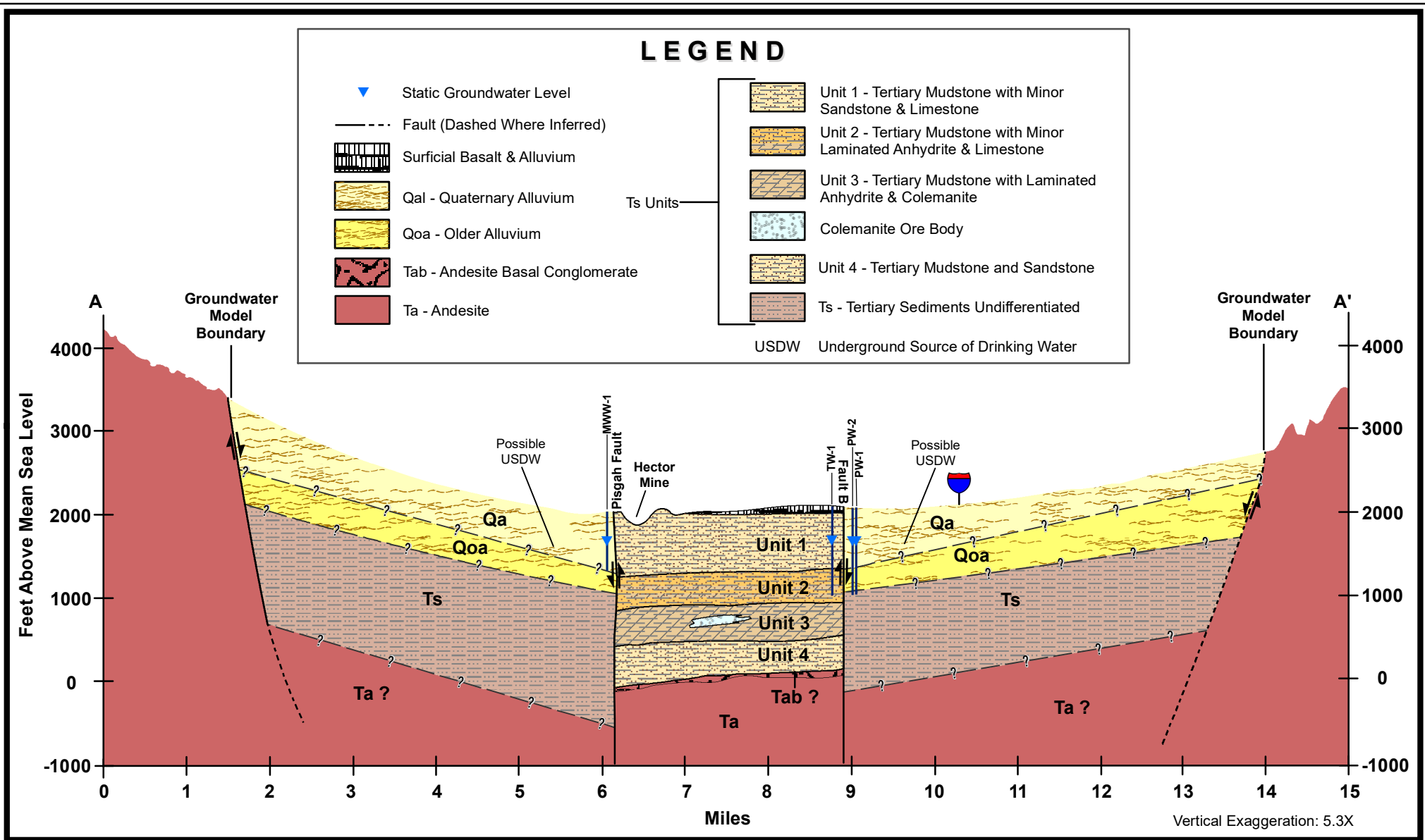
COORDINATE SYSTEM:  
**NAD 1983 UTM Feet**

DESIGNED	DRP	CHECKED	DRP	REVISION:
DRAWN	DRP	APPROVED	DRP	-





 <b>McGinley &amp; Associates</b> Environmental Engineering and Science	Title <b>Project Area Geologic Setting</b>			Figure  <b>3</b>
	Project Name Fort Cady Groundwater Flow Model	Project Number APB003		
	Client Name American Pacific Borate and Lithium	Date 10/18/19		



**FIGURE 4A**

TITLE:

**GEOLOGIC CROSS SECTION  
THROUGH ORE BODY  
FORT CADY PROJECT  
SAN BERNARDINO, CA**

JOB NO.:  
**APB003**

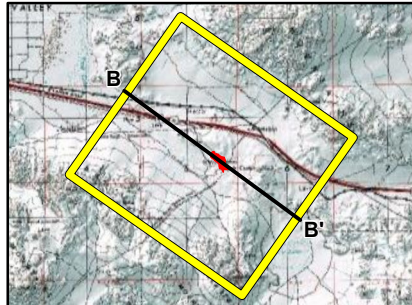
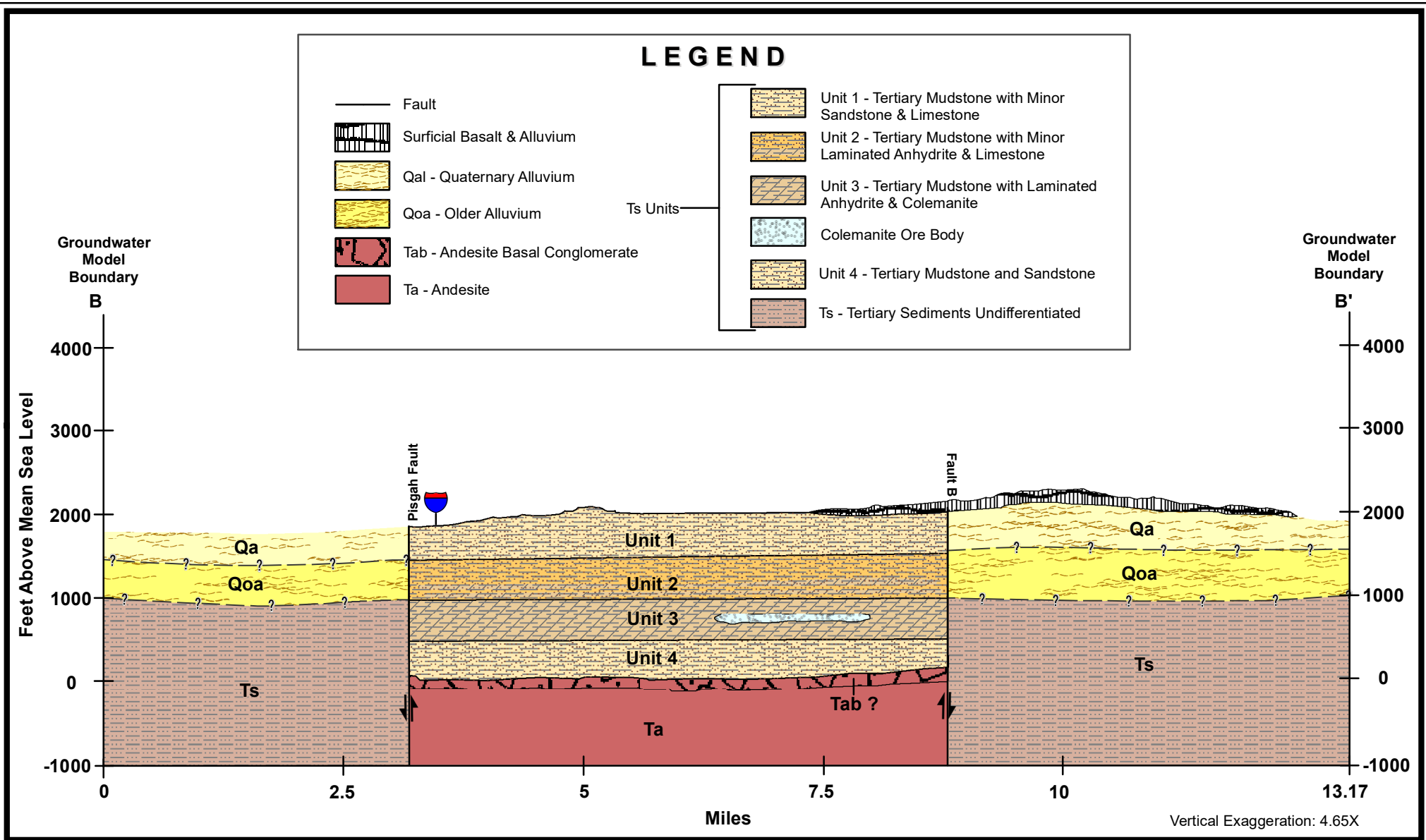
DATE:  
**10/21/2019**



FILE:  
**Fig 4A - Geologic Cross Section**

DESIGNED	DRP	CHECKED	DRP	REVISION:
DRAWN	HC	APPROVED	DRP	-





**FIGURE 4B**

TITLE:

**GEOLOGIC CROSS SECTION  
THROUGH ORE BODY  
FORT CADY PROJECT  
SAN BERNARDINO, CA**

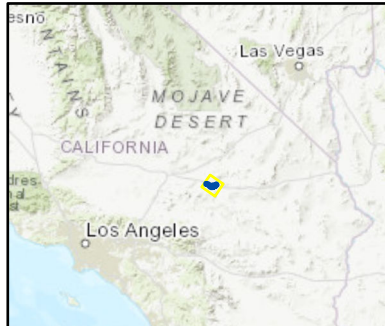
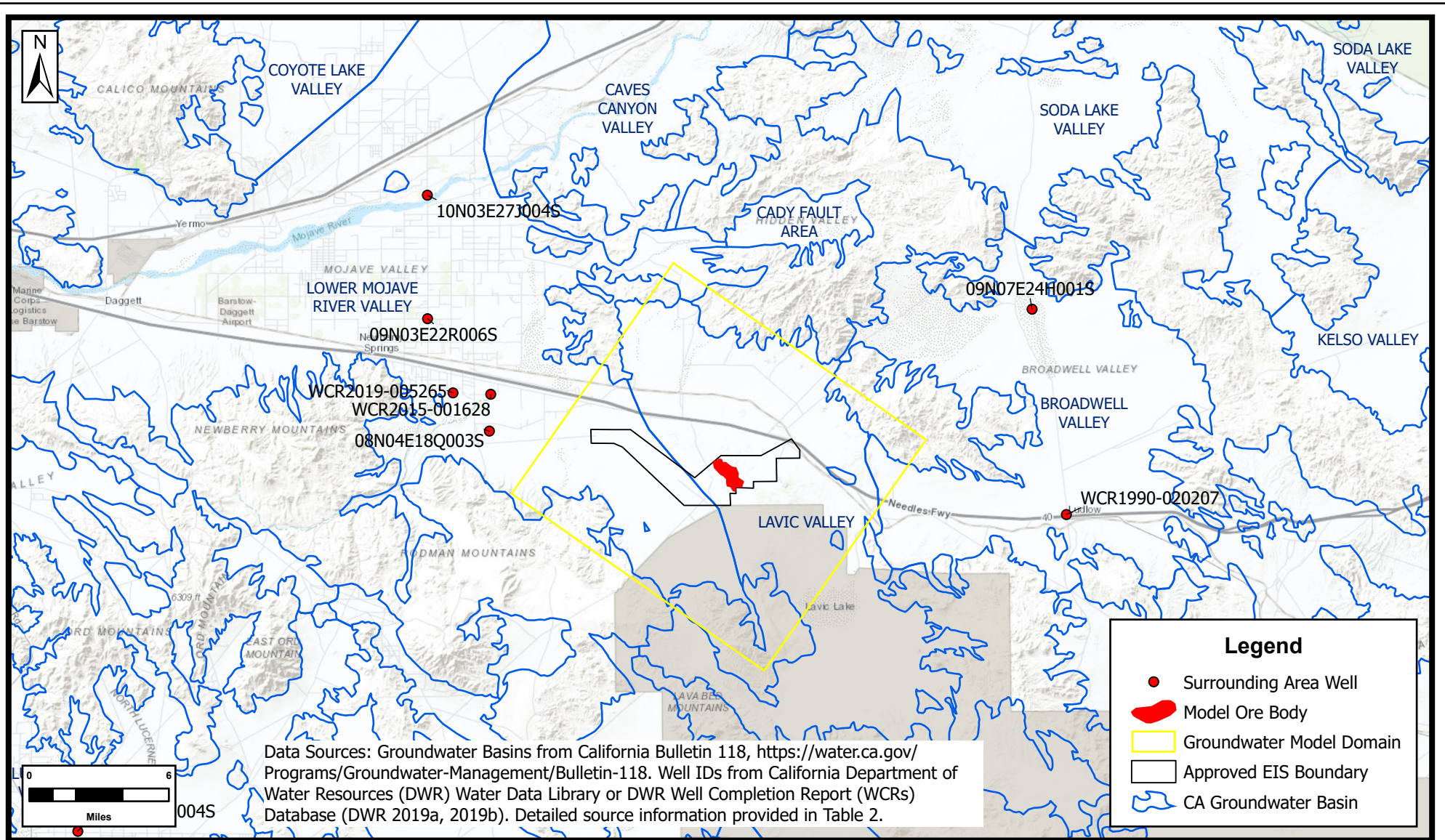
JOB NO.:  
**APB003**

DATE:  
**10/21/2019**



FILE:  
**Fig 4B - Geologic Cross Section**

DESIGNED	DRP	CHECKED	DRP	REVISION:
DRAWN	HC	APPROVED	DRP	-



**FIGURE 5**

TITLE:

**SITE VICINITY MAP  
-SHOWING-  
PROJECT AREA GROUNDWATER BASINS  
AND SURROUNDING AREA WELLS  
FORT CADY PROJECT  
SAN BERNARDINO COUNTY, CA**

JOB NO.:  
**APB003**

DATE:  
**2/24/2020**

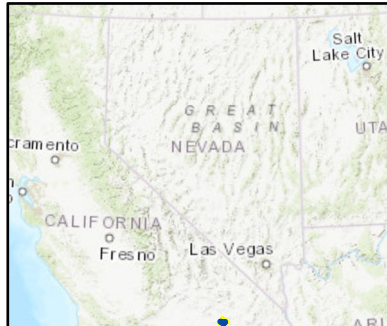
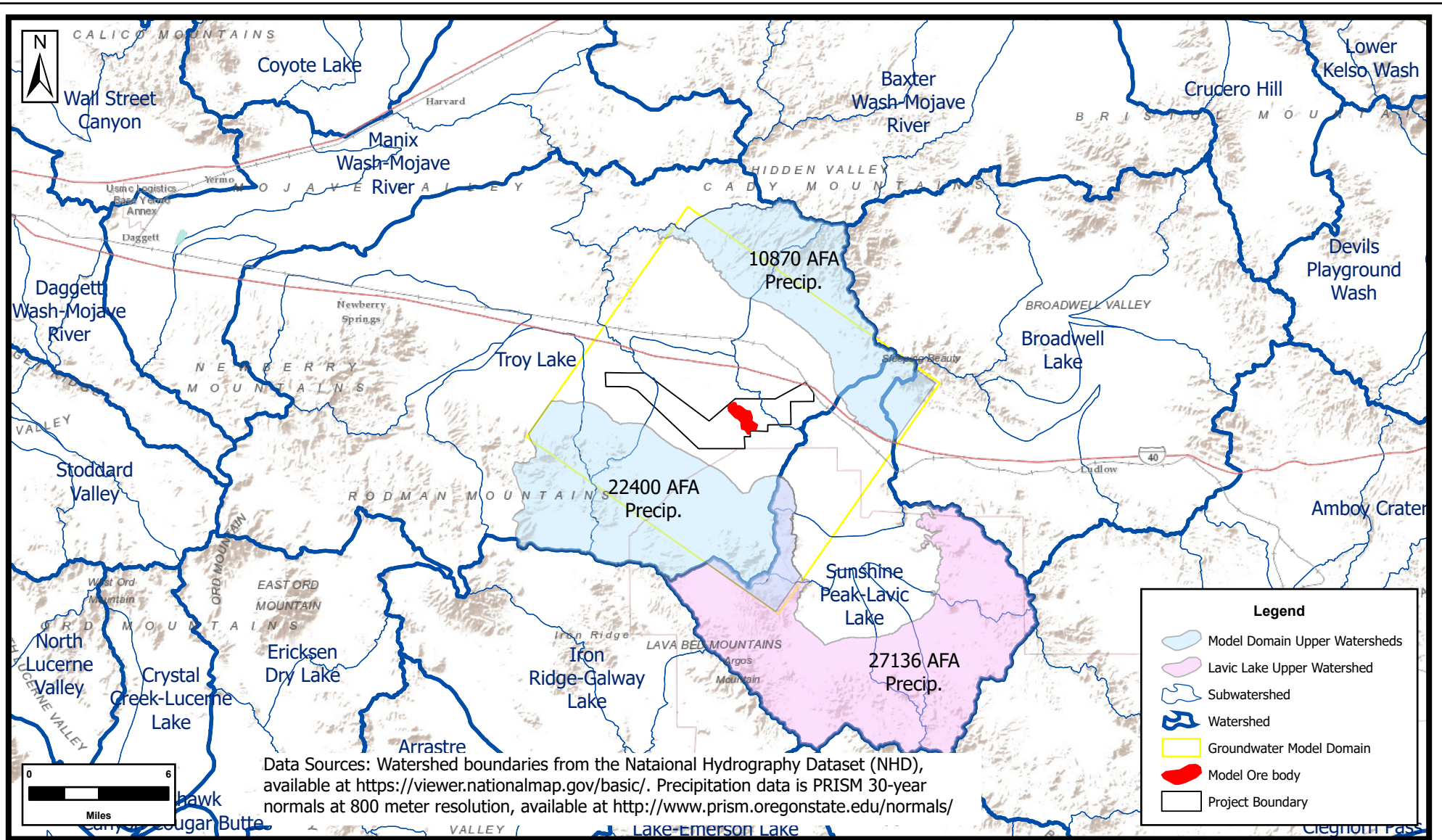


FILE:  
**FortCady3**

COORDINATE SYSTEM:  
**NAD 83 UTM Zone 11 Feet**

DESIGNED	DRP	CHECKED	DRP	REVISION: -
DRAWN	DRP	APPROVED	DRP	





**FIGURE 6**

TITLE:

**SITE VICINITY MAP  
-SHOWING-  
PROJECT AREA WATERSHEDS AND  
ANNUAL PRECIP AFFECTING MODEL DOMAIN  
FORT CADY PROJECT  
SAN BERNARDINO COUNTY, CA**

JOB NO.:  
**APB003**

DATE:  
**2/24/2020**

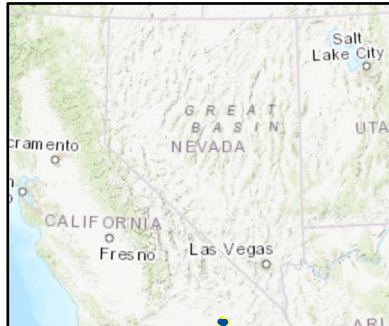
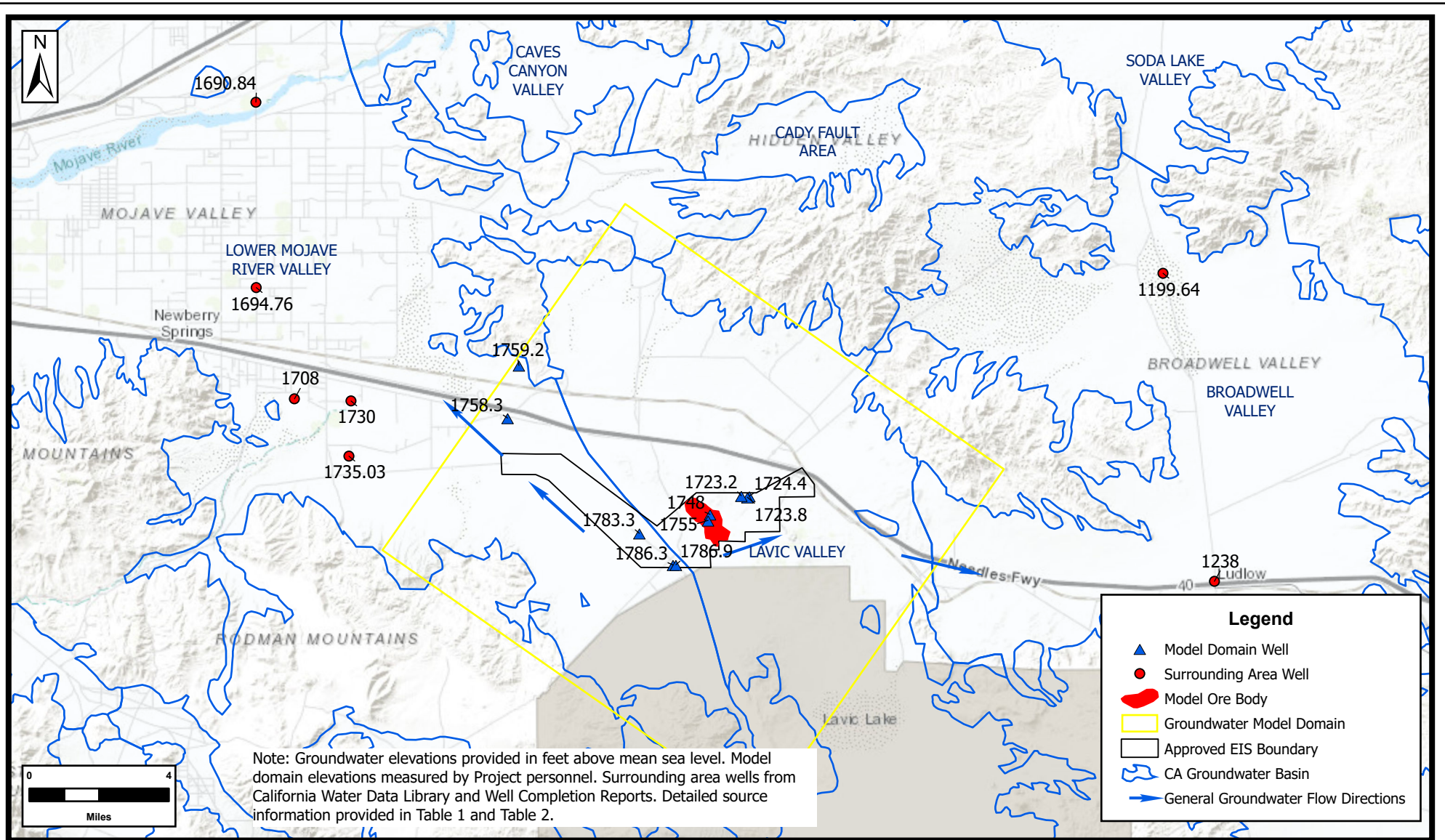


FILE:  
**FortCady3**

COORDINATE SYSTEM:  
**NAD 83 UTM Zone 11 Feet**

DESIGNED	DRP	CHECKED	DRP	REVISION:
DRAWN	DRP	APPROVED	DRP	-





**FIGURE 7**

TITLE:

**SITE VICINITY MAP  
-SHOWING-  
GROUNDWATER ELEVATIONS IN THE  
PROJECT AREA AND VICINITY  
FORT CADY PROJECT  
SAN BERNARDINO COUNTY, CA**

JOB NO.:  
**APB003**

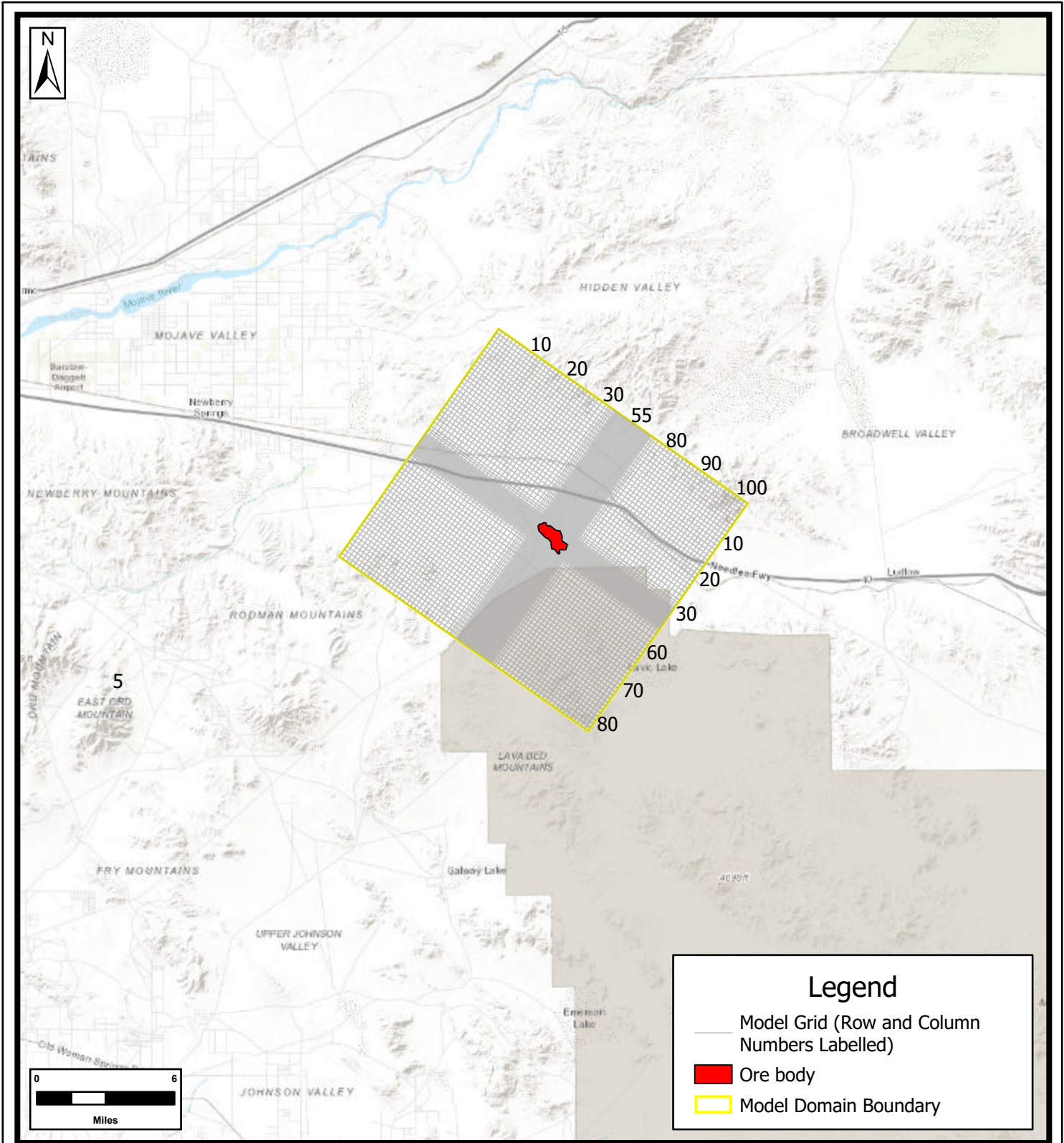
DATE:  
**2/24/2020**



FILE:  
**FortCady3**

COORDINATE SYSTEM:  
**NAD 83 UTM Zone 11 Feet**

REV:	DESIGNED	DRP	CHECKED	DRP	REVISION:
	DRAWN	DRP	APPROVED	DRP	



**Legend**

- Model Grid (Row and Column Numbers Labelled)
- Ore body
- Model Domain Boundary




**FIGURE 8**

TITLE:  
**SITE MAP  
 -SHOWING-  
 GROUNDWATER MODEL DOMAIN  
 FORT CADY PROJECT AREA  
 SAN BERNARDINO COUNTY, CA**

JOB NO.:  
**APB003**

DATE:  
**10/22/2019**



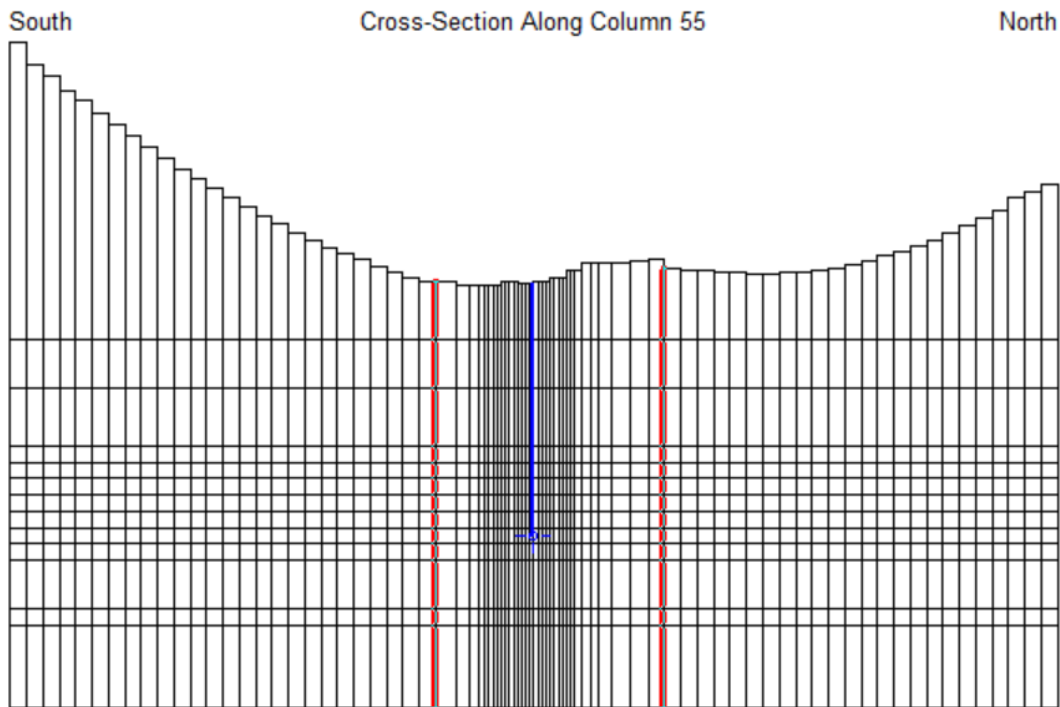
**McGinley & Associates**  
 Environmental Engineering and Science  
 RENO | LAS VEGAS | [www.mcgin.com](http://www.mcgin.com)

FILE:  
**FortCady3**

COORDINATE SYSTEM:  
**NAD 1983 UTM Feet**

DESIGNED	DRP	CHECKED	DRP	REVISION:
DRAWN	DRP	APPROVED	DRP	





Vertical Exaggeration = 10x



Title: **Representative Model Layers**

Project Name:  
Fort Cady Project

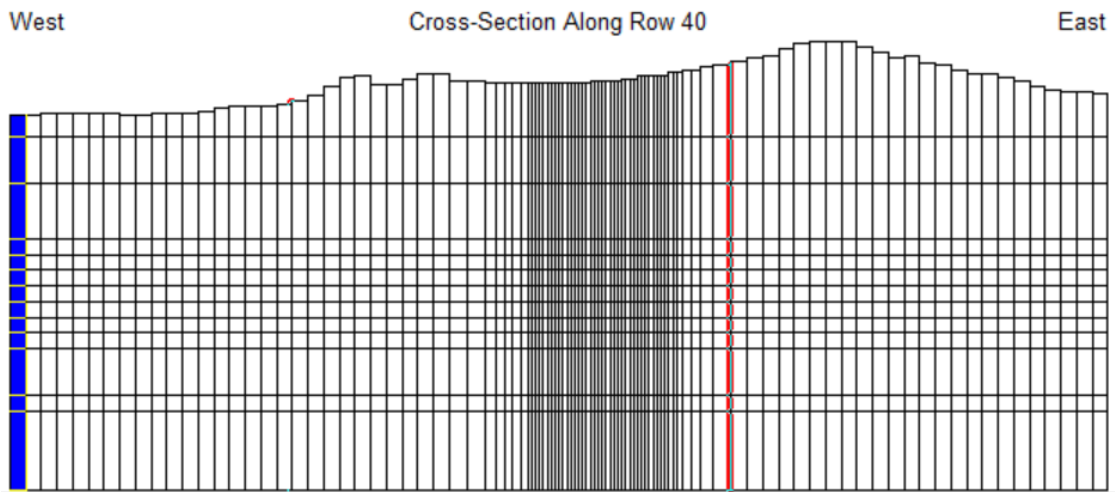
Project Number:  
APB003

Figure

Client Name:  
Fort Cady California Corporation

Date:  
7/31/2019

**9a**



Vertical Exaggeration = 10x



Title: **Representative Model Layers**

Project Name:  
Fort Cady Project

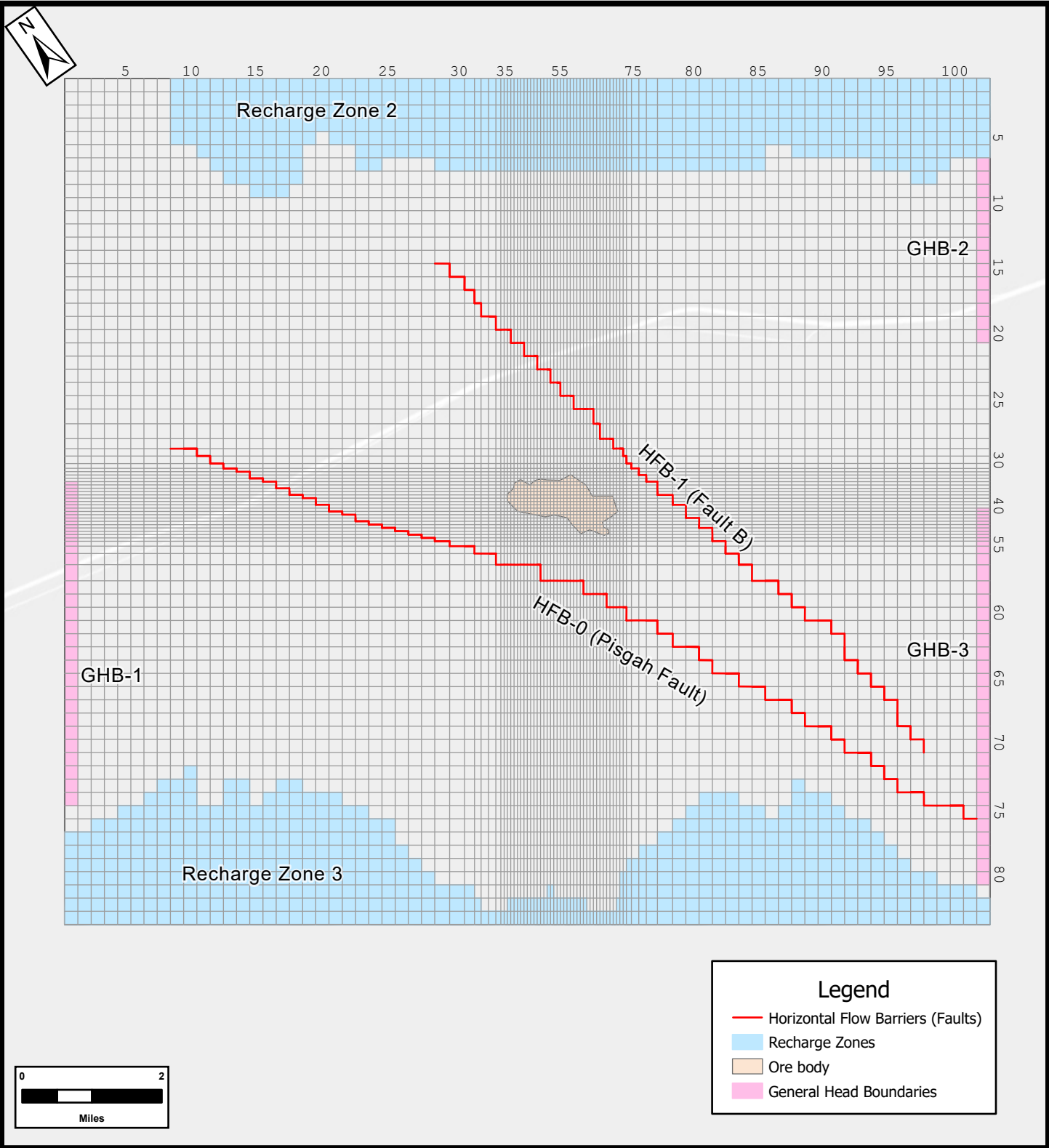
Project Number:  
APB003

Figure

Client Name:  
Fort Cady California Corporation

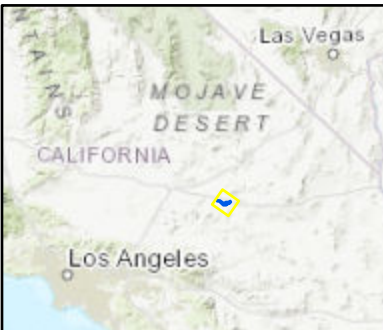
Date:  
7/31/2019

**9b**



**Legend**

- Horizontal Flow Barriers (Faults)
- Recharge Zones
- Ore body
- General Head Boundaries



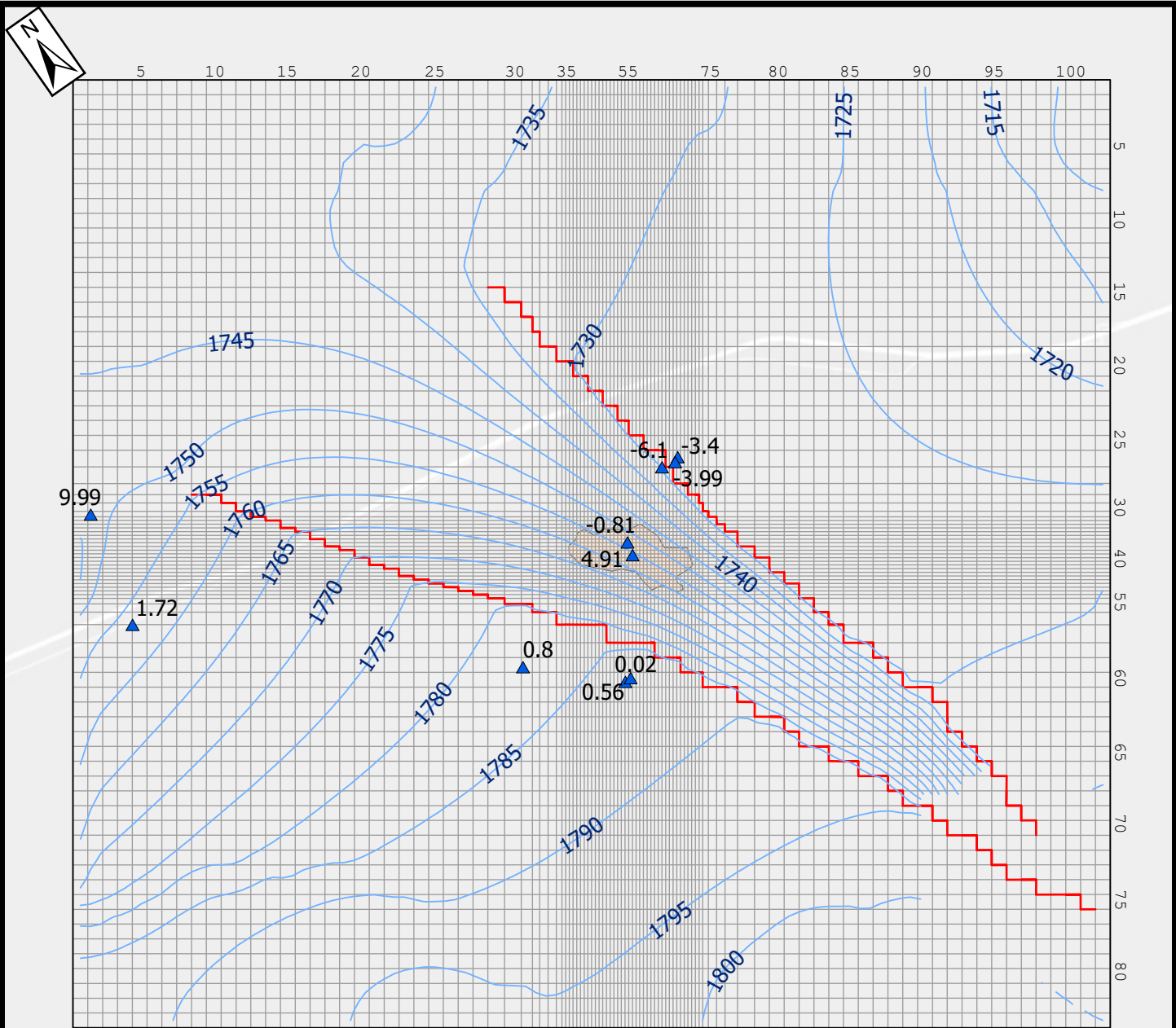
**FIGURE 10**

TITLE:  
**GROUNDWATER MODEL  
 BOUNDARY CONDITIONS  
 FORT CADY PROJECT  
 SAN BERNARDINO COUNTY, CA**

JOB NO.: <b>APB003</b>	DATE: <b>10/18/2019</b>
---------------------------	----------------------------

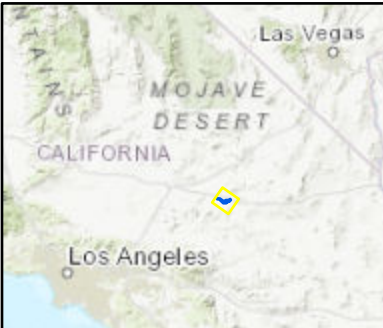
**McGinley & Associates**  
 Environmental Engineering and Science  
 RENO | LAS VEGAS | www.mcgin.com

FILE: <b>Fort Cady Model Figs</b>				
COORDINATE SYSTEM: <b>NAD 1983 UTM Feet</b>				
DESIGNED	DRP	CHECKED	DRP	REVISION:
DRAWN	DRP	APPROVED	DRP	-



**Legend**

- ▲ Steady State Head Targets with Residual (ft)
- Potentiometric Surface Contours
- Horizontal Flow Barriers (Faults)
- Ore body



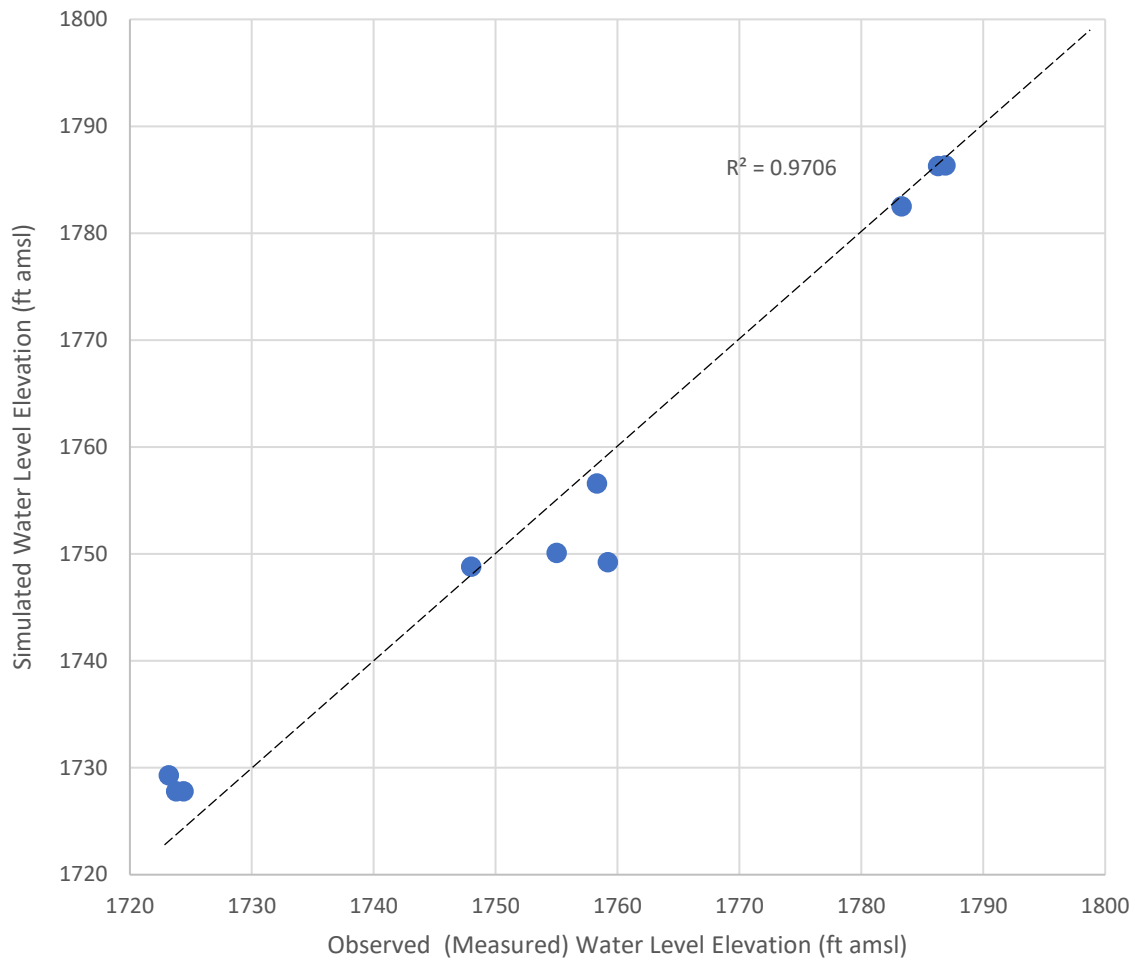
**FIGURE 11**  
 TITLE:  
**MODELED POTENTIOMETRIC  
 GROUNDWATER SURFACE  
 FORT CADY PROJECT  
 SAN BERNARDINO COUNTY, CA**



FILE:  
**Fort Cady Model Figs**  
 COORDINATE SYSTEM:  
**NAD 1983 UTM Feet**

JOB NO.:  
**APB003**  
 DATE:  
**10/21/2019**

DESIGNED	DRP	CHECKED	DRP	REVISION:
DRAWN	DRP	APPROVED	DRP	-



Title: **Simulated versus Measured Water Levels at Head Targets**

Project Name:  
Fort Cady Project

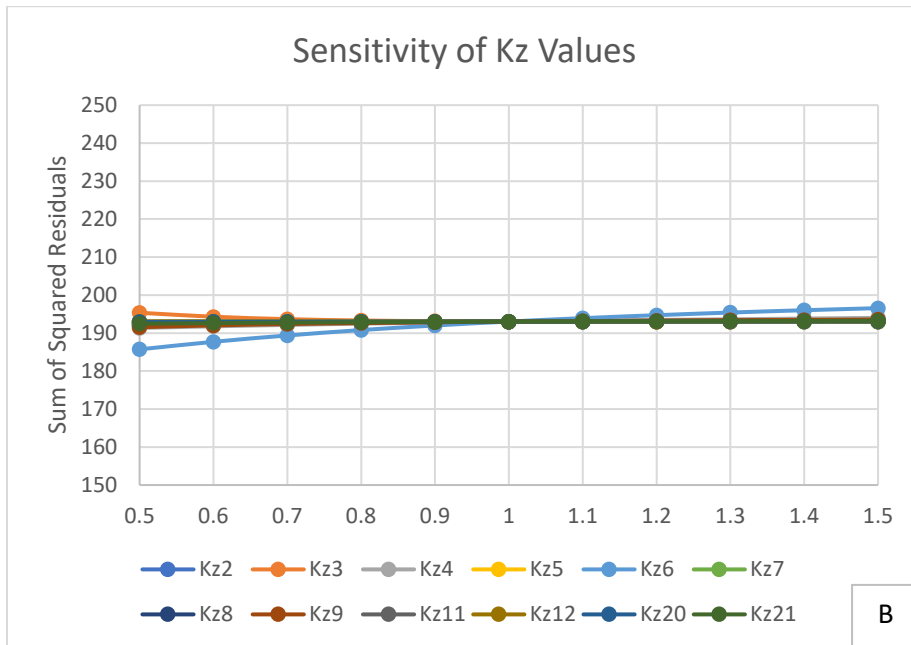
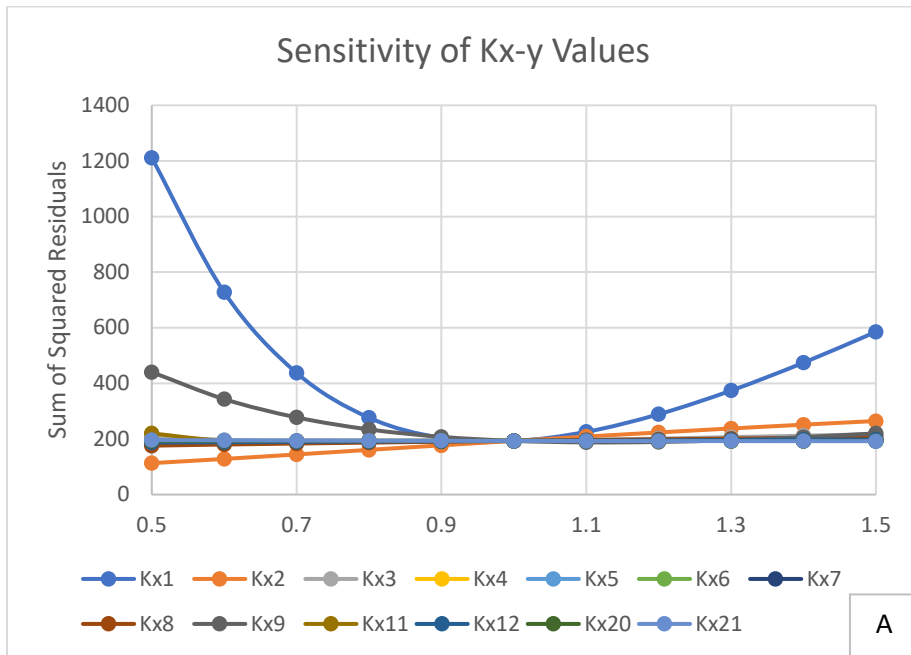
Project Number:  
APB003

Figure

Client Name:  
Fort Cady California Corporation

Date:  
7/31/2019

**12**



Title: **Results of Horizontal (A) and Vertical (B) Conductivity Sensitivity Analysis**

Project Name:  
Fort Cady Project

Project Number:  
APB003

Figure

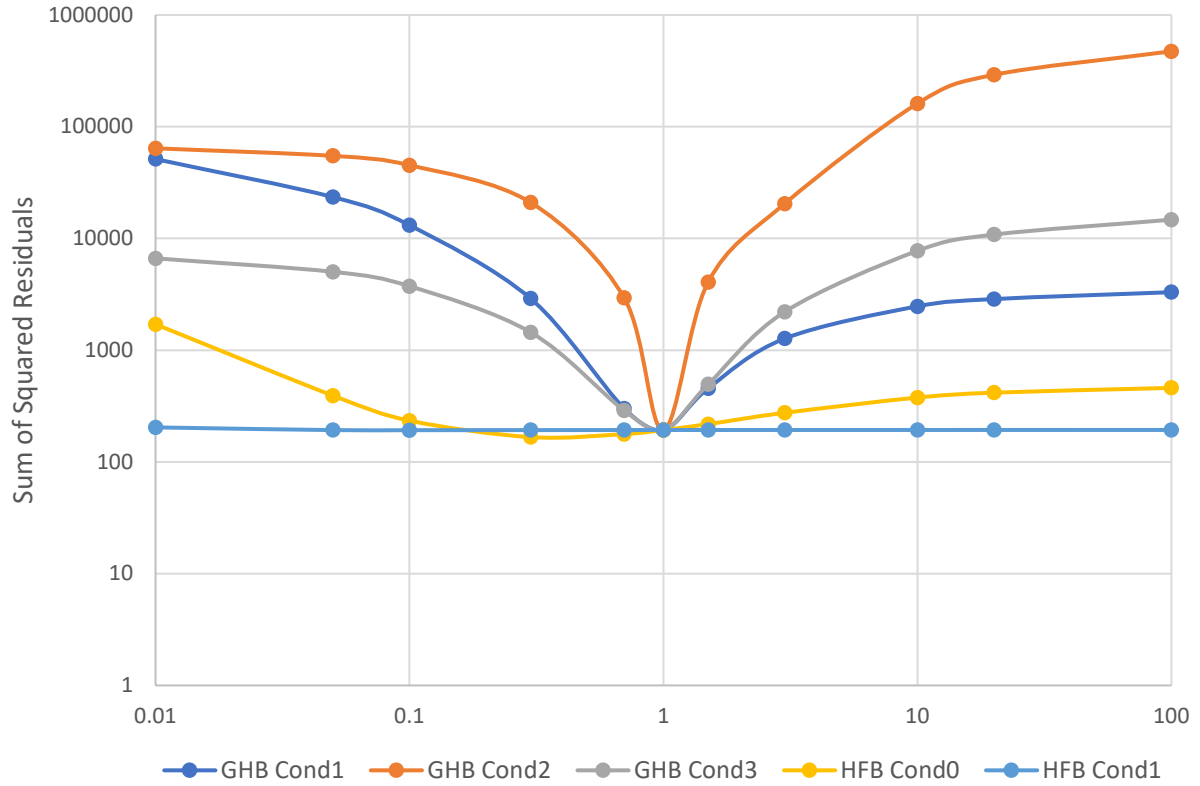
Client Name:  
Fort Cady California Corporation

Date:  
7/31/2019

**13A/B**



### Sensitivity of GHB and HFB Conductance Values



Title: **Results of General Head Boundary (GHB) and Hydraulic Flow Barrier (HFB Sensitivity Analysis**

Project Name:  
Fort Cady Project

Project Number:  
APB003

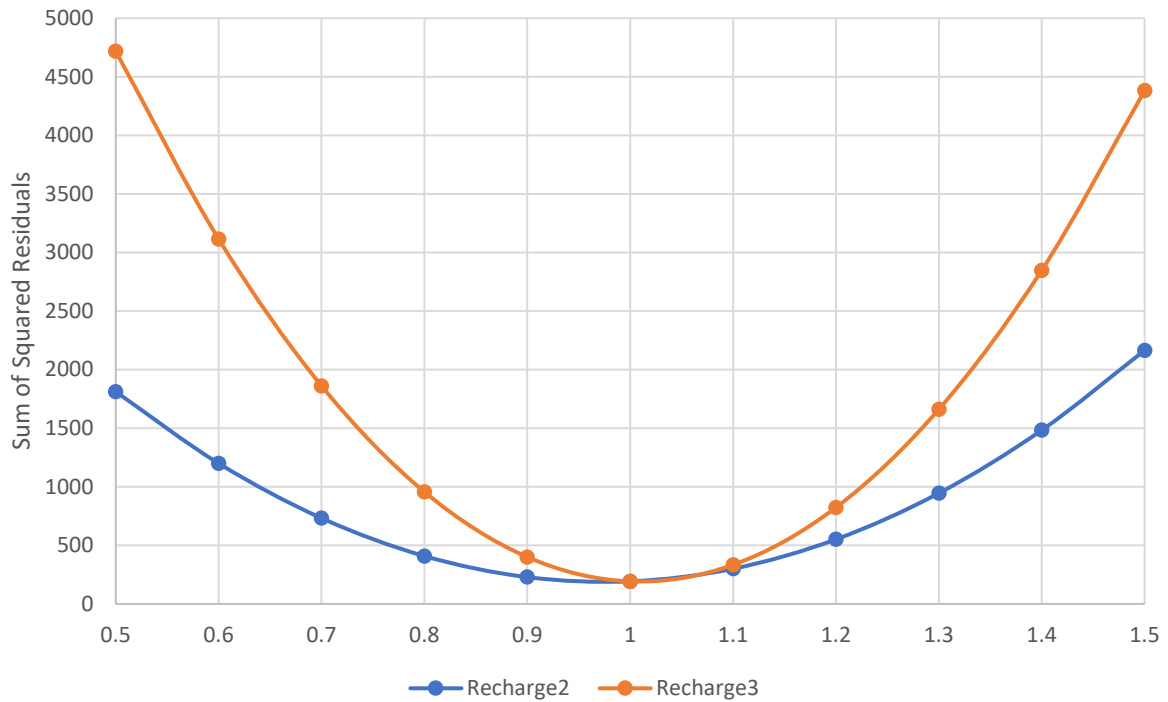
Figure

Client Name:  
Fort Cady California Corporation

Date:  
7/31/2019

**14**

### Sensitivity of Recharge Rates



Title: **Results of Recharge Rate Sensitivity Analysis**

Project Name:  
Fort Cady Project

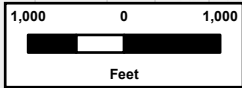
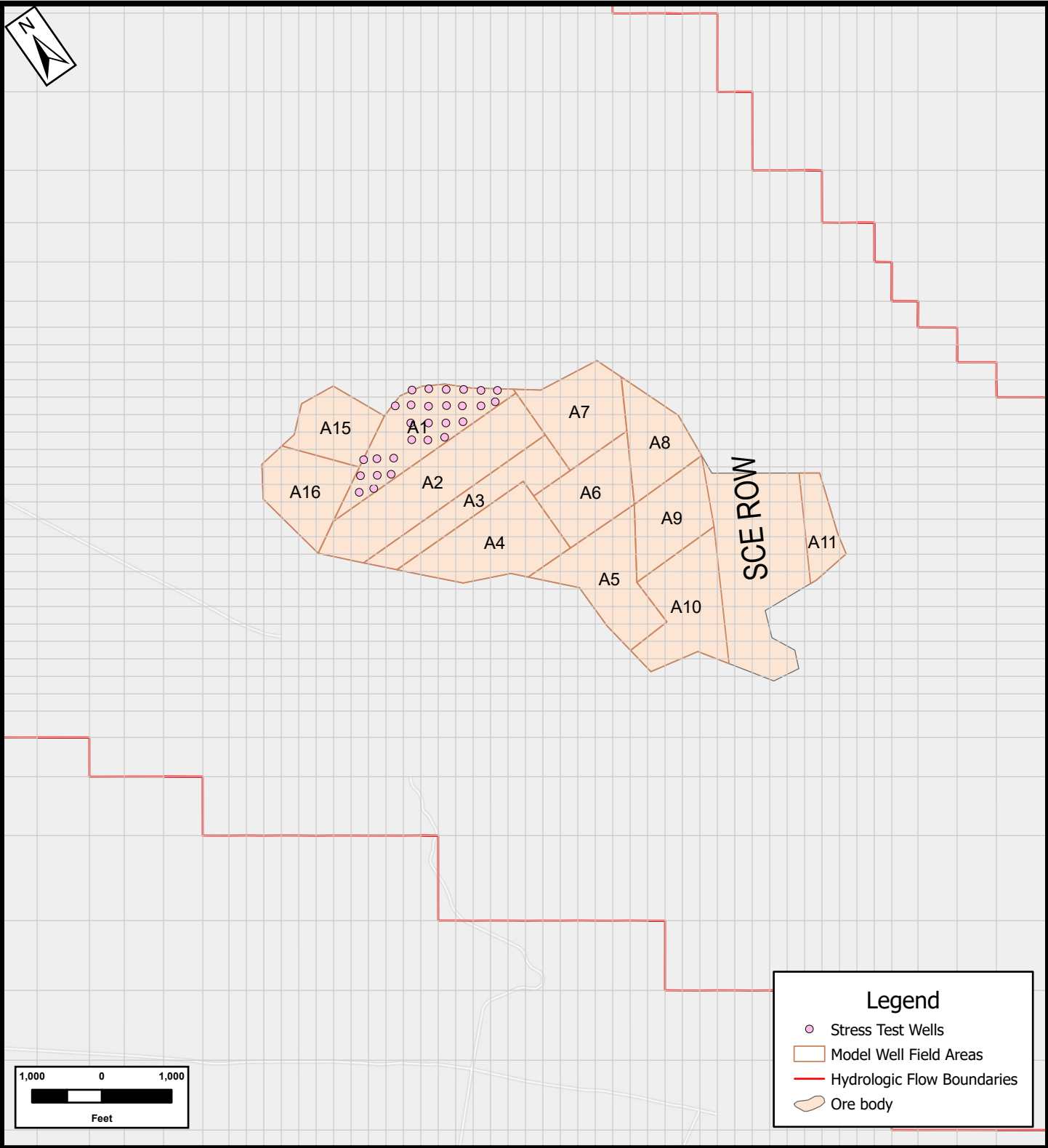
Project Number:  
APB003

Figure

Client Name:  
Fort Cady California Corporation

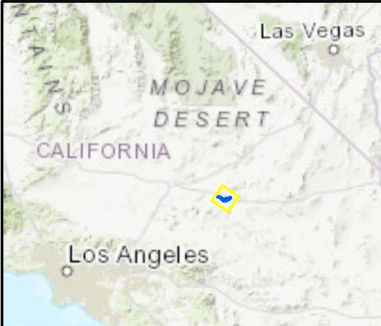
Date:  
7/31/2019

**15**



**Legend**

- Stress Test Wells
- Model Well Field Areas
- Hydrologic Flow Boundaries
- Ore body



**FIGURE 16**

TITLE:  
**PROPOSED WELL FIELD AREAS AND  
 DAILY STRESS TEST  
 WELL LOCATIONS  
 FORT CADY PROJECT  
 SAN BERNARDINO COUNTY, CA**

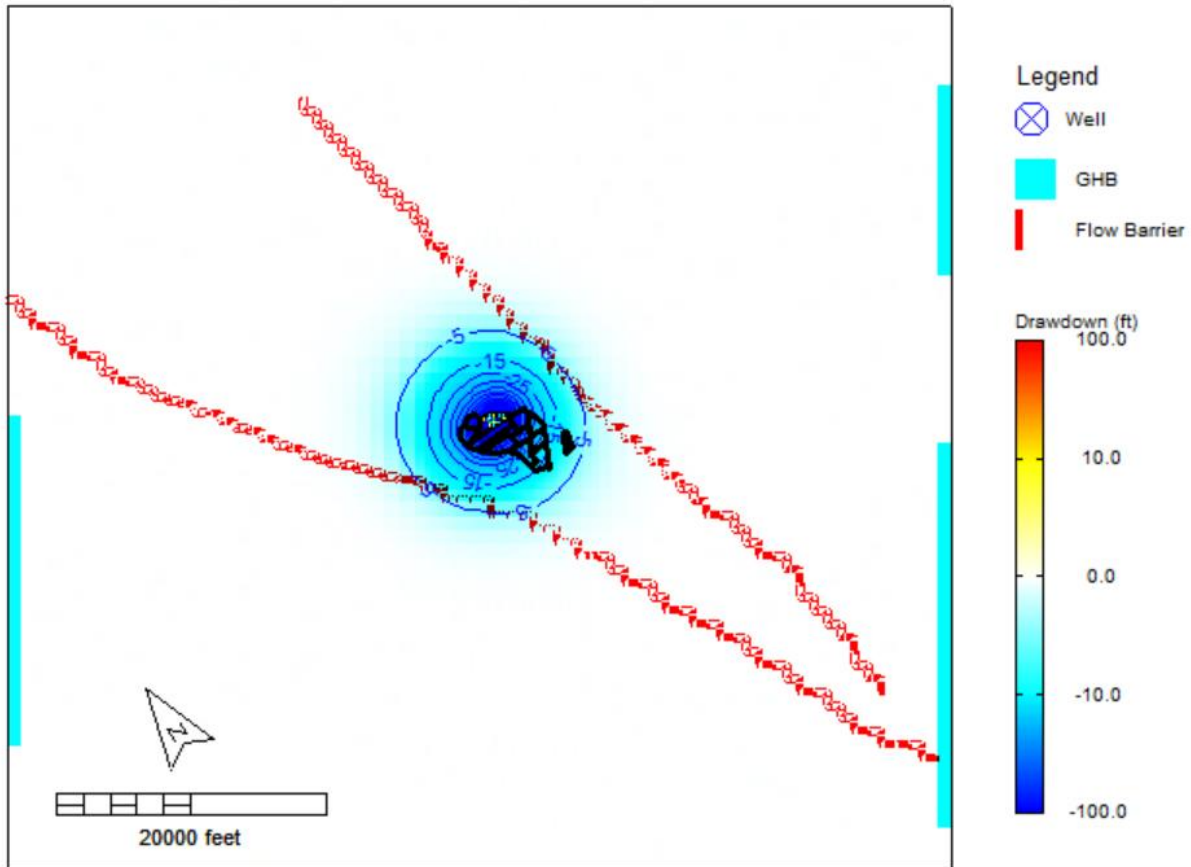
JOB NO.: **APB003**      DATE: **2/24/2020**




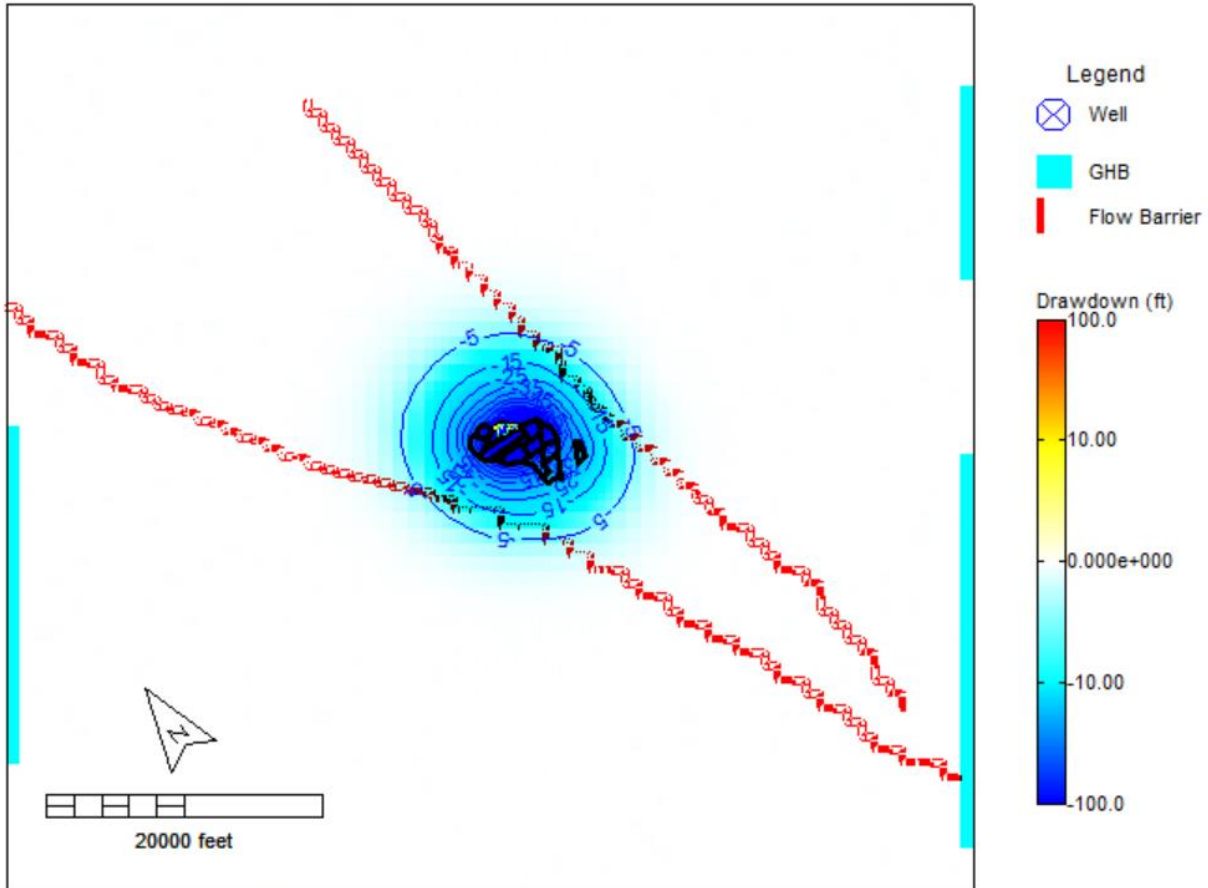
FILE:  
**Fort Cady Model Figs**


COORDINATE SYSTEM:  
**NAD 1983 UTM Feet**

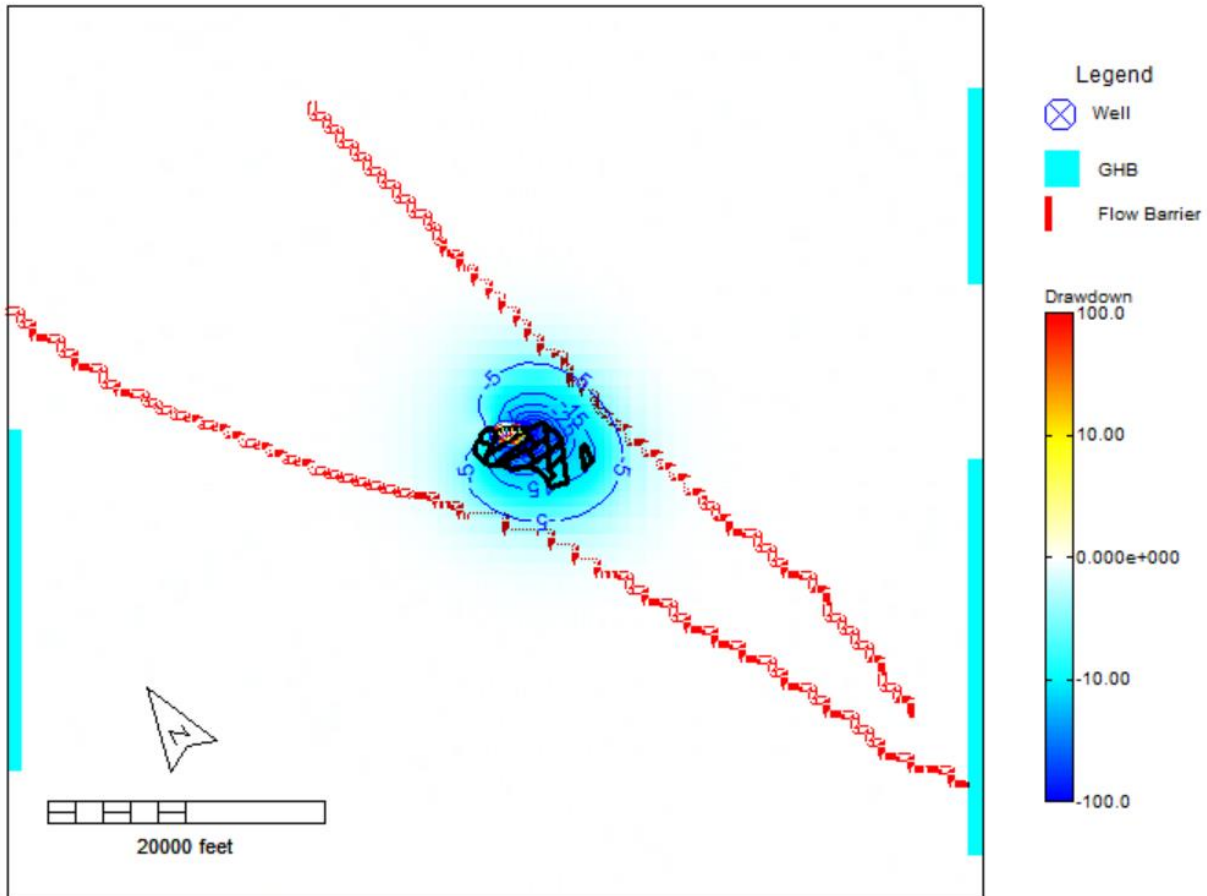
REV:	DESIGNED	DRP	CHECKED	DRP	REVISION: -
	DRAWN	DRP	APPROVED	DRP	




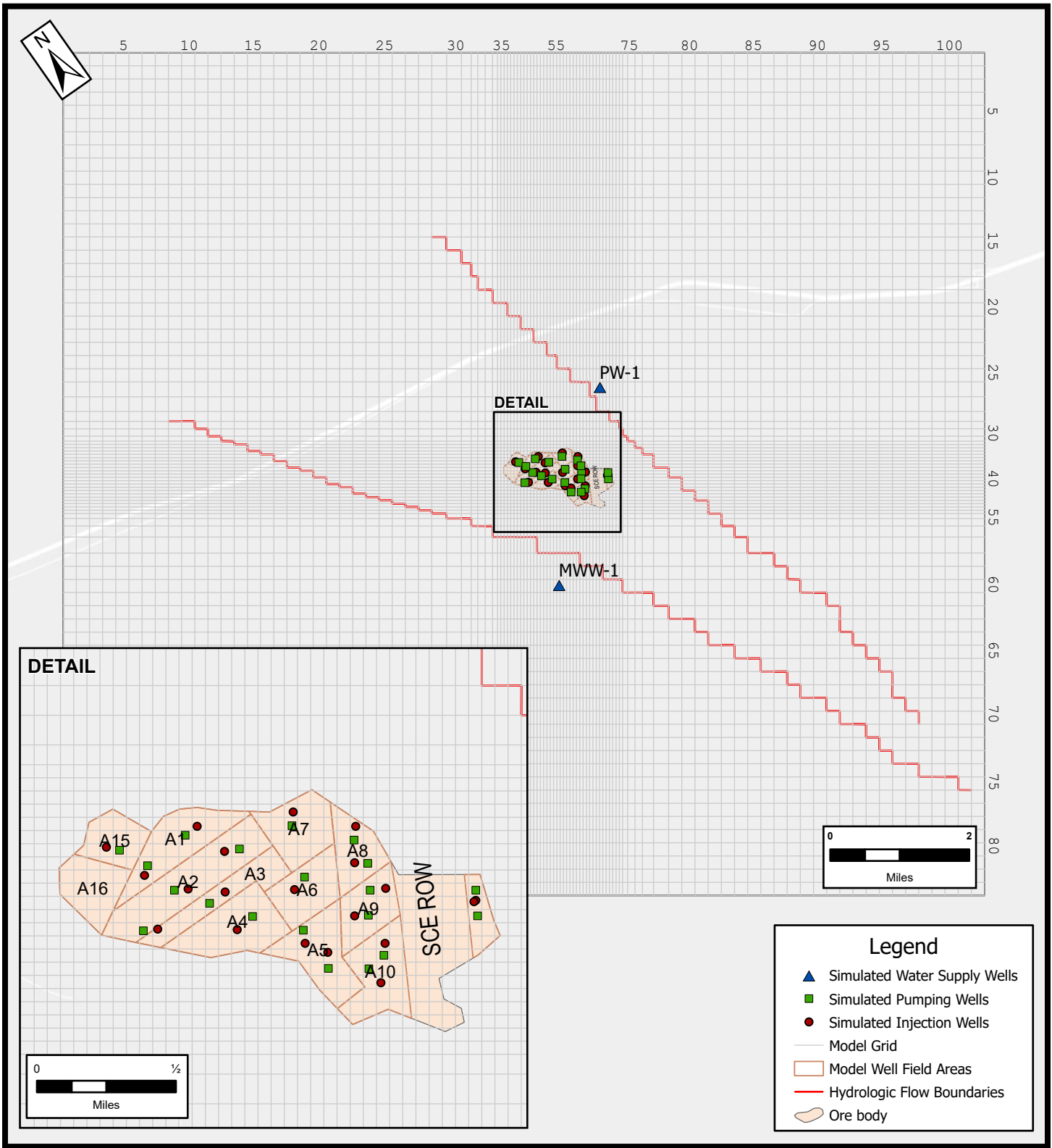
 <b>McGinley &amp; Associates</b> Environmental Engineering and Science	Title: <b>Low K Scenario - Simulated Potentiometric Drawdown / Mounding at 100 Days in Layer 6</b>		
	Project Name: Fort Cady Project	Project Number: APB003	Figure  <b>17</b>
	Client Name: Fort Cady California Corporation	Date: 7/31/2019	



 <b>McGinley &amp; Associates</b> Environmental Engineering and Science	Title: <b>Mid K Scenario - Simulated Potentiometric Drawdown / Mounding at 100 Days in Layer 6</b>		
	Project Name: Fort Cady Project	Project Number: APB003	Figure  <b>18</b>
	Client Name: Fort Cady California Corporation	Date: 7/31/2019	



 <b>McGinley &amp; Associates</b> Environmental Engineering and Science	Title: <b>High K Scenario - Simulated Potentiometric Drawdown / Mounding at 100 Days in Layer 6</b>		
	Project Name: Fort Cady Project	Project Number: APB003	Figure  <b>19</b>
	Client Name: Fort Cady California Corporation	Date: 7/31/2019	




**FIGURE 20**

TITLE:

**MINING SIMULATION  
WELL LOCATIONS  
FORT CADY PROJECT  
SAN BERNARDINO COUNTY, CA**

JOB NO.:  
**APB003**

DATE:  
**2/24/2020**

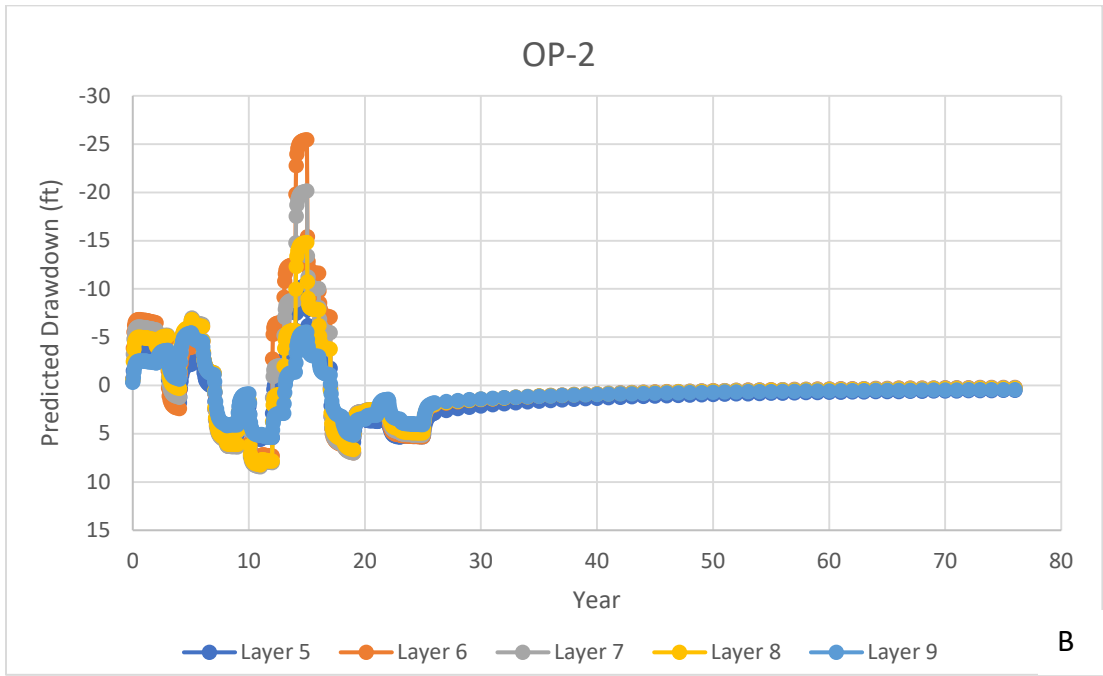
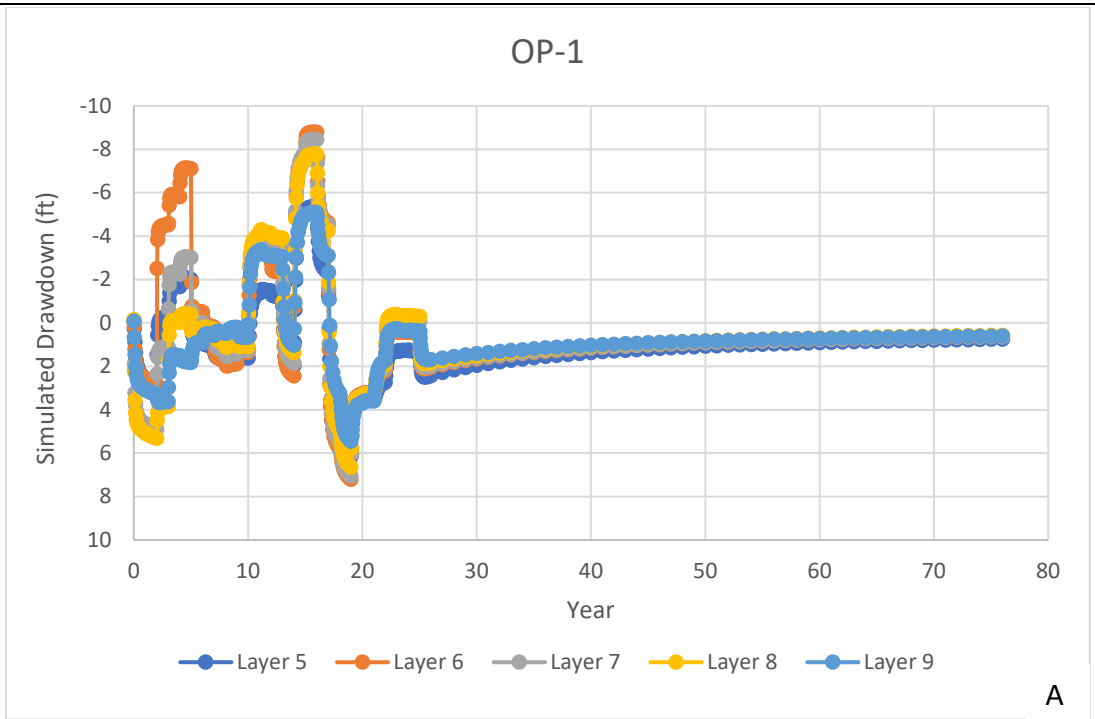


**McGinley & Associates**  
Environmental Engineering and Science  
RENO | LAS VEGAS | www.mcgin.com

FILE:  
**Fort Cady Model Figs**

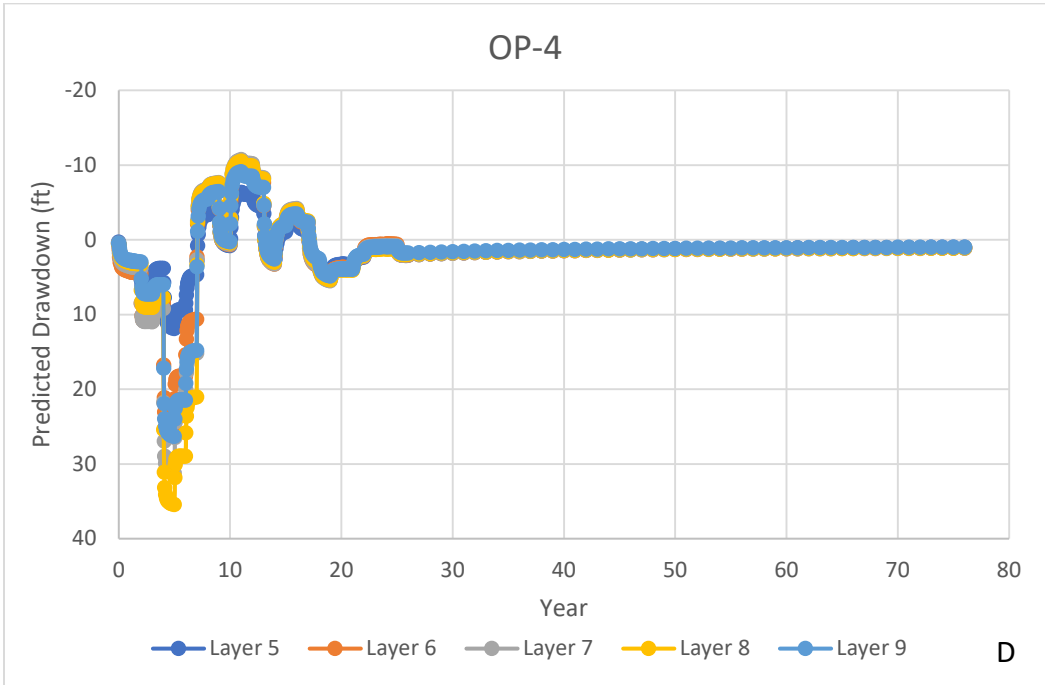
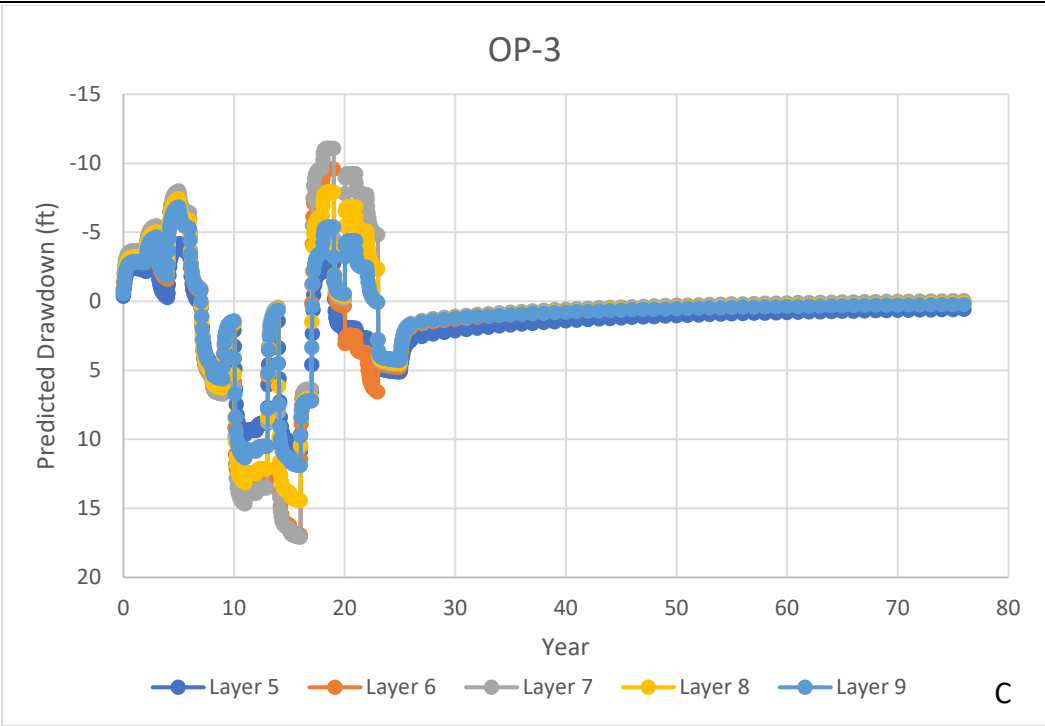
COORDINATE SYSTEM:  
**NAD 1983 UTM Feet**

REF:	DESIGNED	DRP	CHECKED	DRP	REVISION: -
	DRAWN	DRP	APPROVED	DRP	



<p><b>McGinley &amp; Associates</b> Environmental Engineering and Science</p>	<b>Title: Simulated Drawdown at Model Observation Points</b>		
	Project Name: Fort Cady Project	Project Number: APB003	<b>21 A/B</b>
	Client Name: Fort Cady California Corporation	Date: 8/7/19	





Title: **Simulated Drawdown at Model Observation Points**

Project Name:  
Fort Cady Project

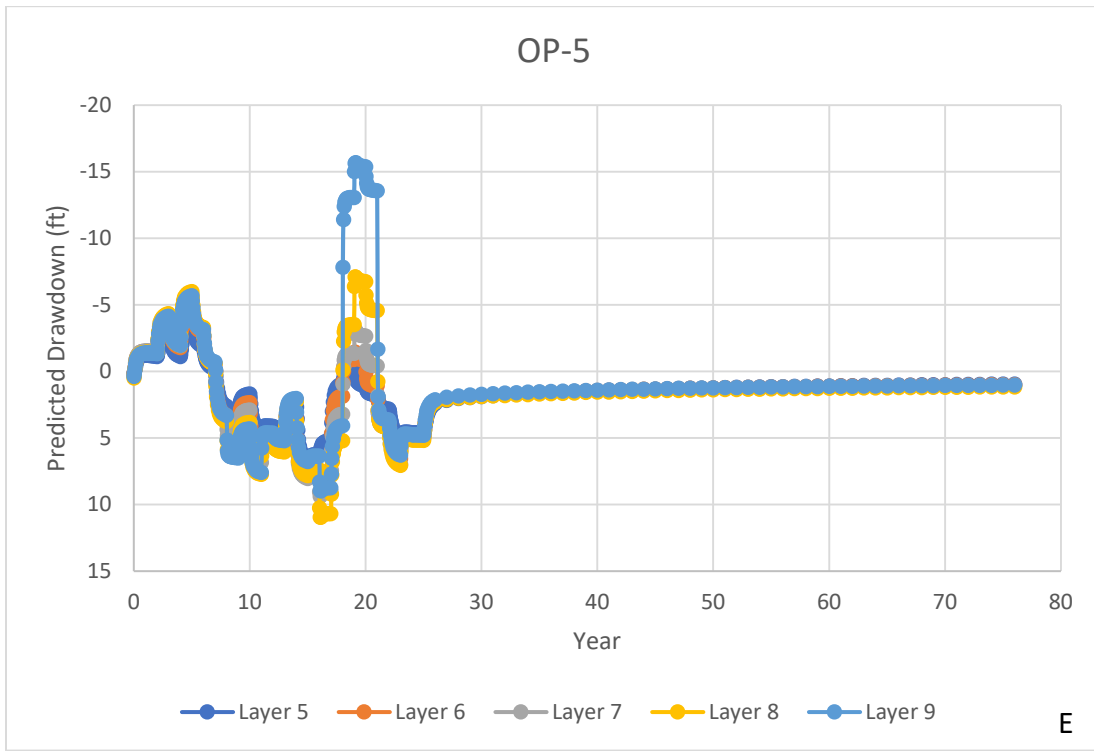
Project Number:  
APB003


Figure

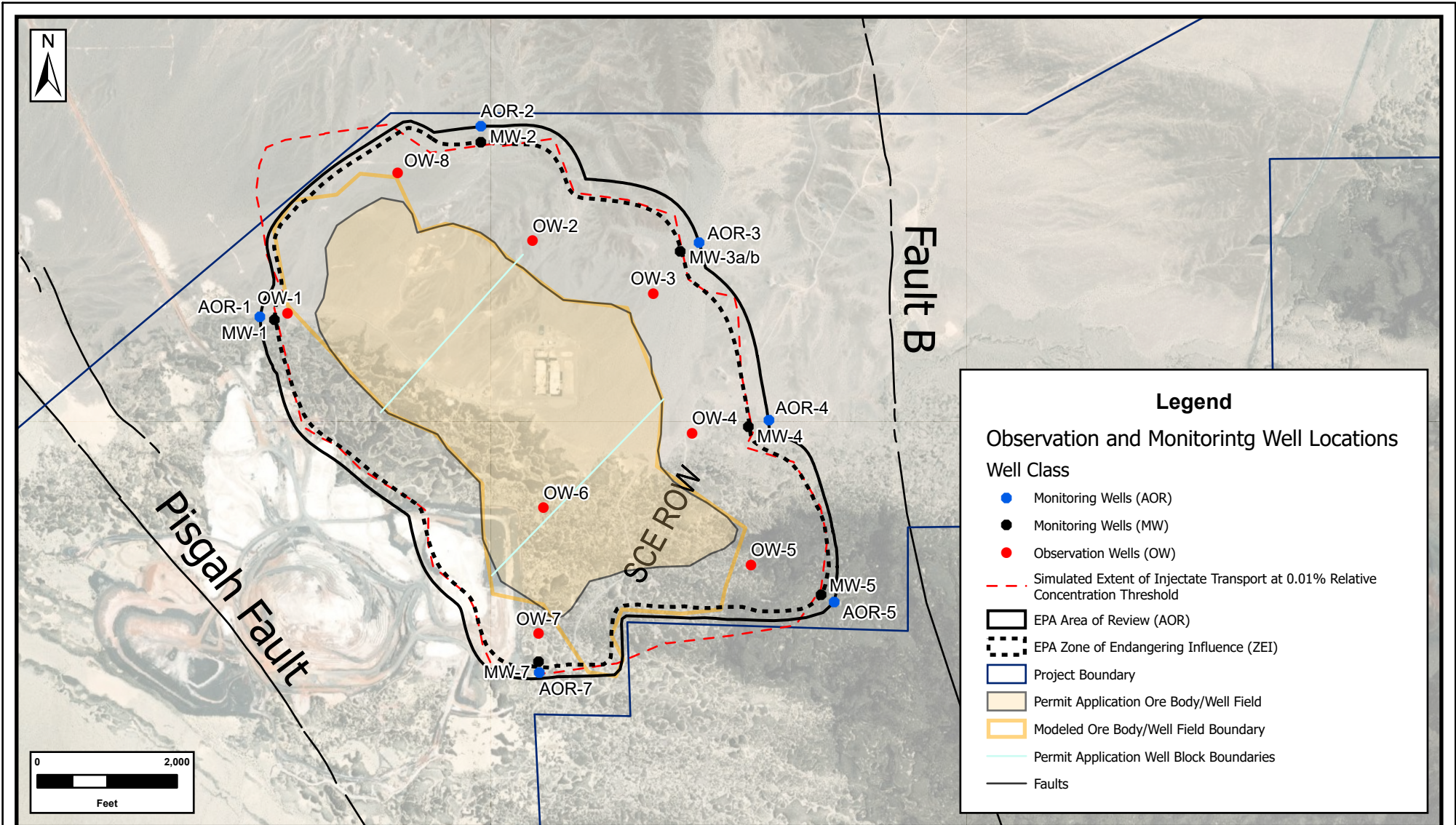
Client Name:  
Fort Cady California Corporation

Date:  
8/7/19

**21 C/D**



 <b>McGinley &amp; Associates</b> Environmental Engineering and Science	Title: <b>Simulated Drawdown at Model Observation Points</b>		
	Project Name: Fort Cady Project	Project Number: APB003	Figure  <b>21 E</b>
	Client Name: Fort Cady California Corporation	Date: 8/7/19	



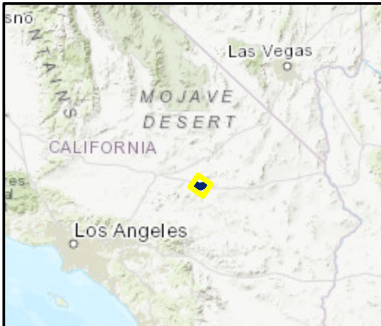
### Legend

**Observation and Monitoring Well Locations**

**Well Class**

- Monitoring Wells (AOR)
- Monitoring Wells (MW)
- Observation Wells (OW)

- Simulated Extent of Injectate Transport at 0.01% Relative Concentration Threshold
- EPA Area of Review (AOR)
- EPA Zone of Endangering Influence (ZEI)
- Project Boundary
- Permit Application Ore Body/Well Field
- Modeled Ore Body/Well Field Boundary
- Permit Application Well Block Boundaries
- Faults



**FIGURE 22**

TITLE:

**SITE MAP  
-SHOWING-  
SIMULATED EXTENT OF SOLUTE TRANSPORT,  
AREA OF REVIEW BOUNDARY AND PROPOSED MONITORING WELLS  
FORT CADY PROJECT  
SAN BERNARDINO COUNTY, CA**

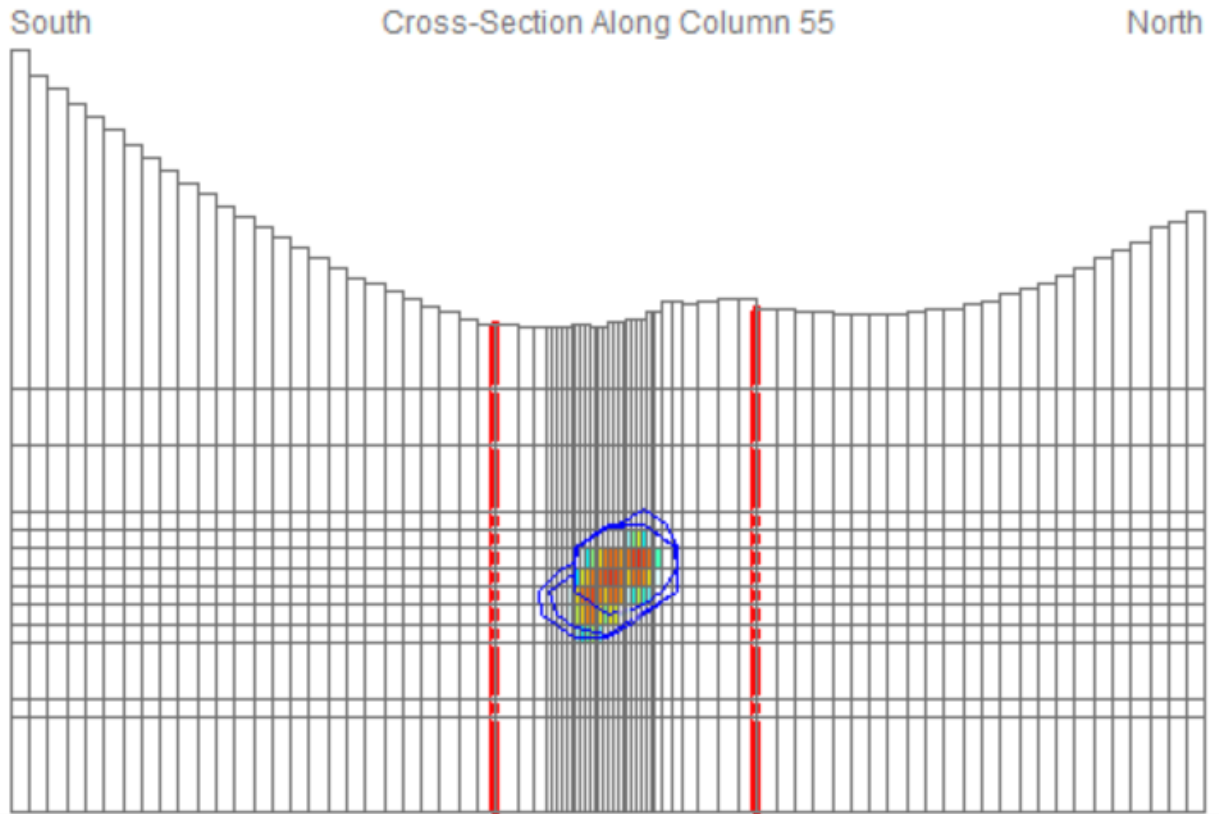
JOB NO.: **APB003**      DATE: **6/12/2020**

**McGinley & Associates**  
Environmental Engineering and Science  
RENO | LAS VEGAS | www.mcgin.com

FILE: **APB\_Concentrations**

COORDINATE SYSTEM:

REV:	DESIGNED	DRP	CHECKED	DRP	REVISION:
	DRAWN	DRP	APPROVED	DRP	



Title: **Cross-Section Showing Vertical and Lateral Extent of Predicted Solute Transport at Mine Year 25**

Project Name:  
Fort Cady Project

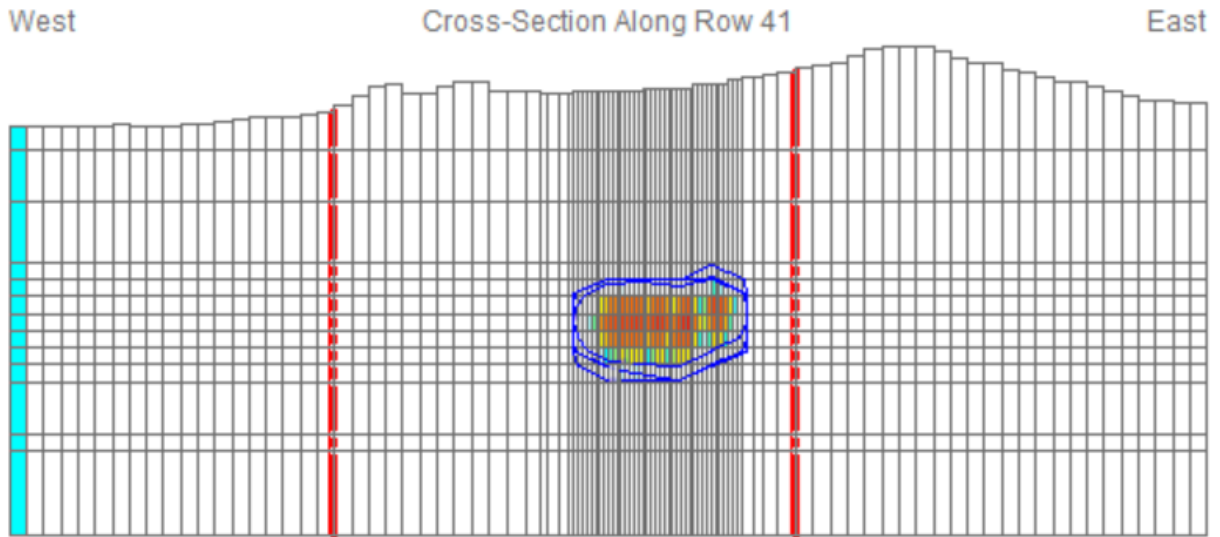
Project Number:  
APB003

Figure

Client Name:  
Fort Cady California Corporation

Date:  
7/31/2019

**23a**



Title: **Cross-Section Showing Vertical and Lateral Extent of Predicted Solute Transport at Mine Year 25**

Project Name:  
Fort Cady Project

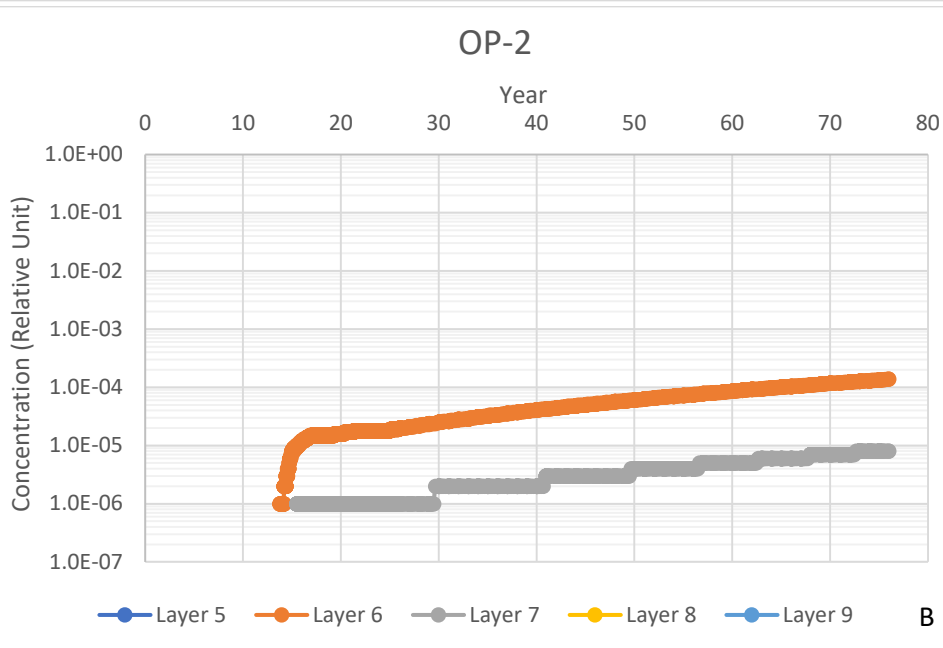
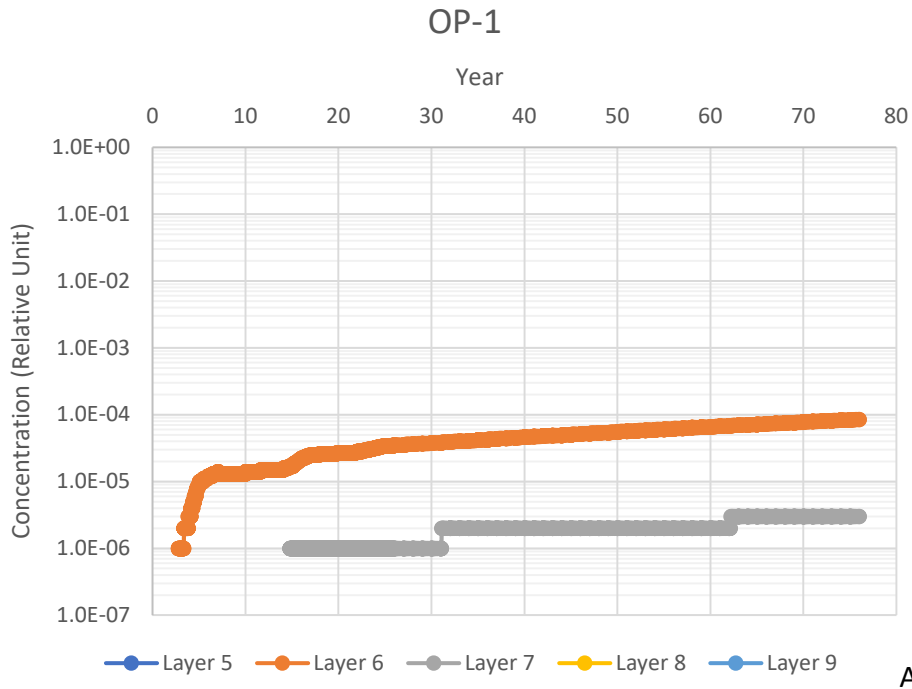
Project Number:  
APB003

Figure

Client Name:  
Fort Cady California Corporation

Date:  
7/31/2019

**23b**



Title: **Simulated Particle Concentrations at Model Observation Points**

Project Name:  
Fort Cady Project

Project Number:  
APB003

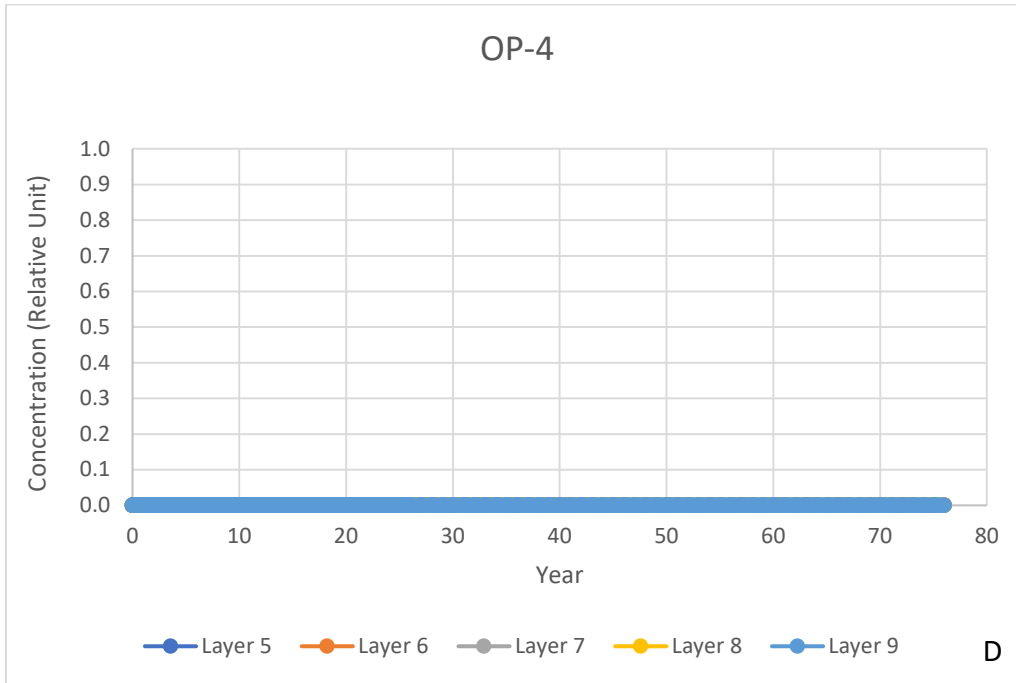
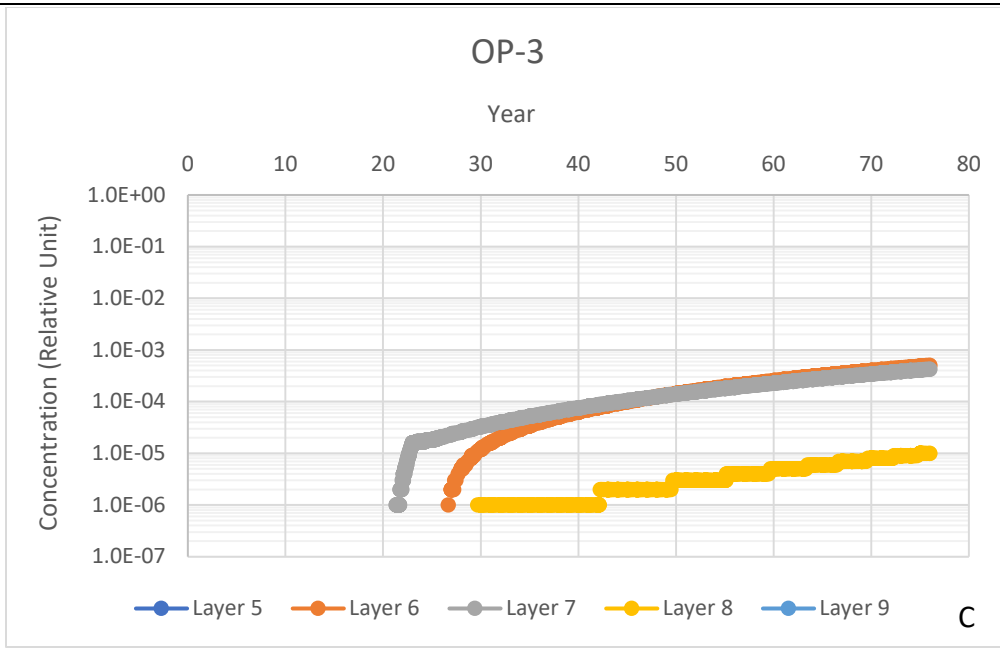
Figure

Client Name:  
Fort Cady California Corporation

Date:  
8/7/19

**24 A/B**





Title: **Simulated Particle Concentrations at Model Observation Points**

Project Name:  
Fort Cady Project

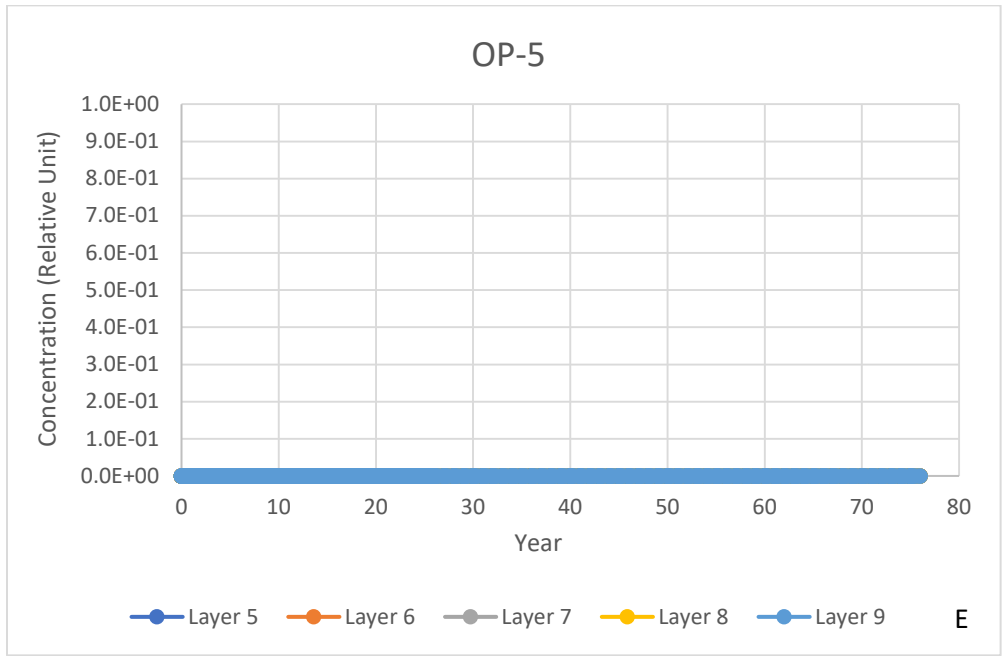
Project Number:  
APB003

Figure

Client Name:  
Fort Cady California Corporation

Date:  
8/7/19

**24 C/D**



Title: **Simulated Particle Concentrations at Model Observation Points**

Project Name:  
Fort Cady Project

Project Number:  
APB003

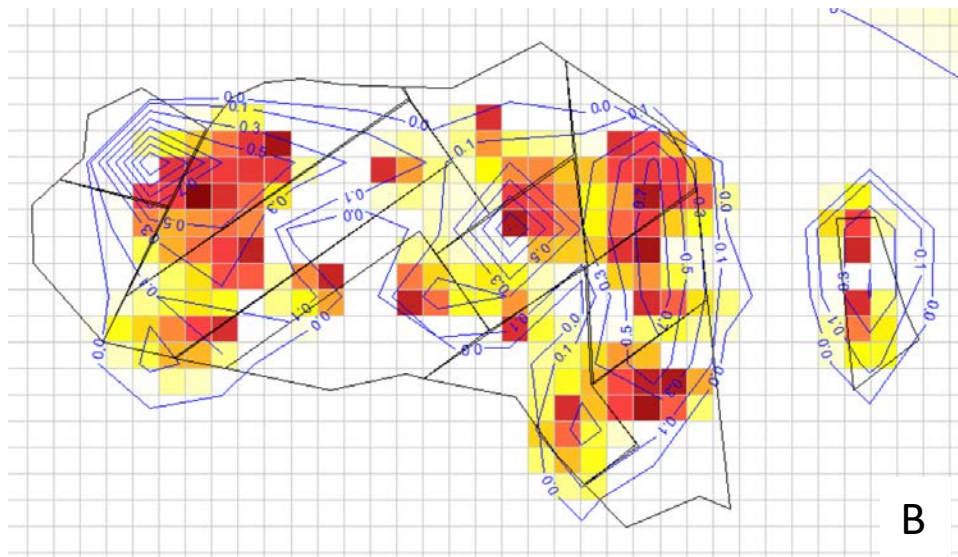
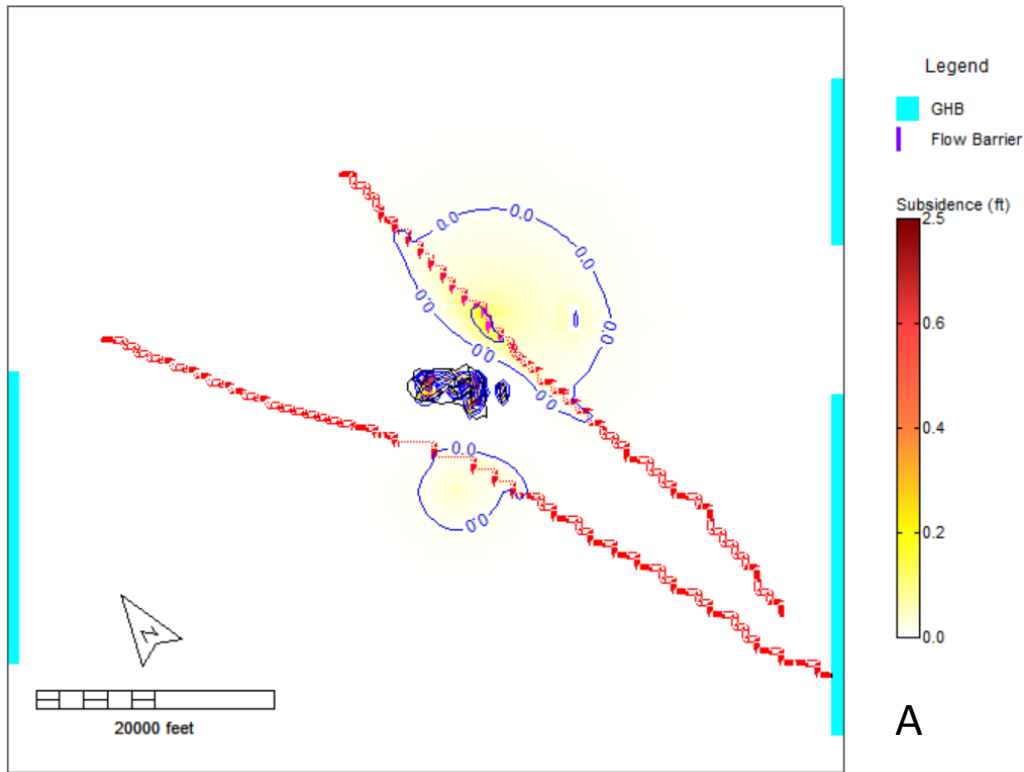
Figure

Client Name:  
Fort Cady California Corporation

Date:  
8/7/19

**24 E**





Title: **Predicted Land Subsidence at Mine Year 25 for A) Full Model Domain B) Ore Body Footprint.**

Project Name:  
Fort Cady Project

Project Number:  
APB003

Figure

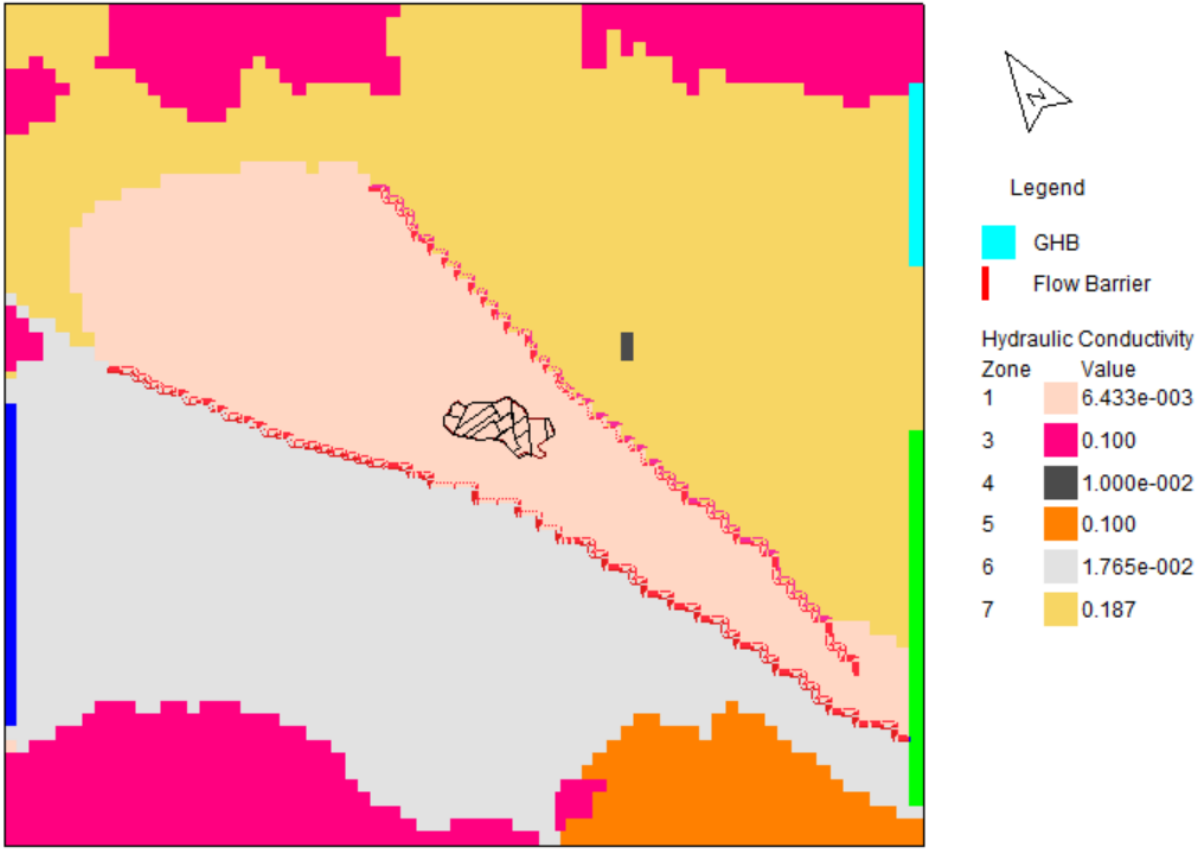
Client Name:  
Fort Cady California Corporation

Date:  
7/31/2019

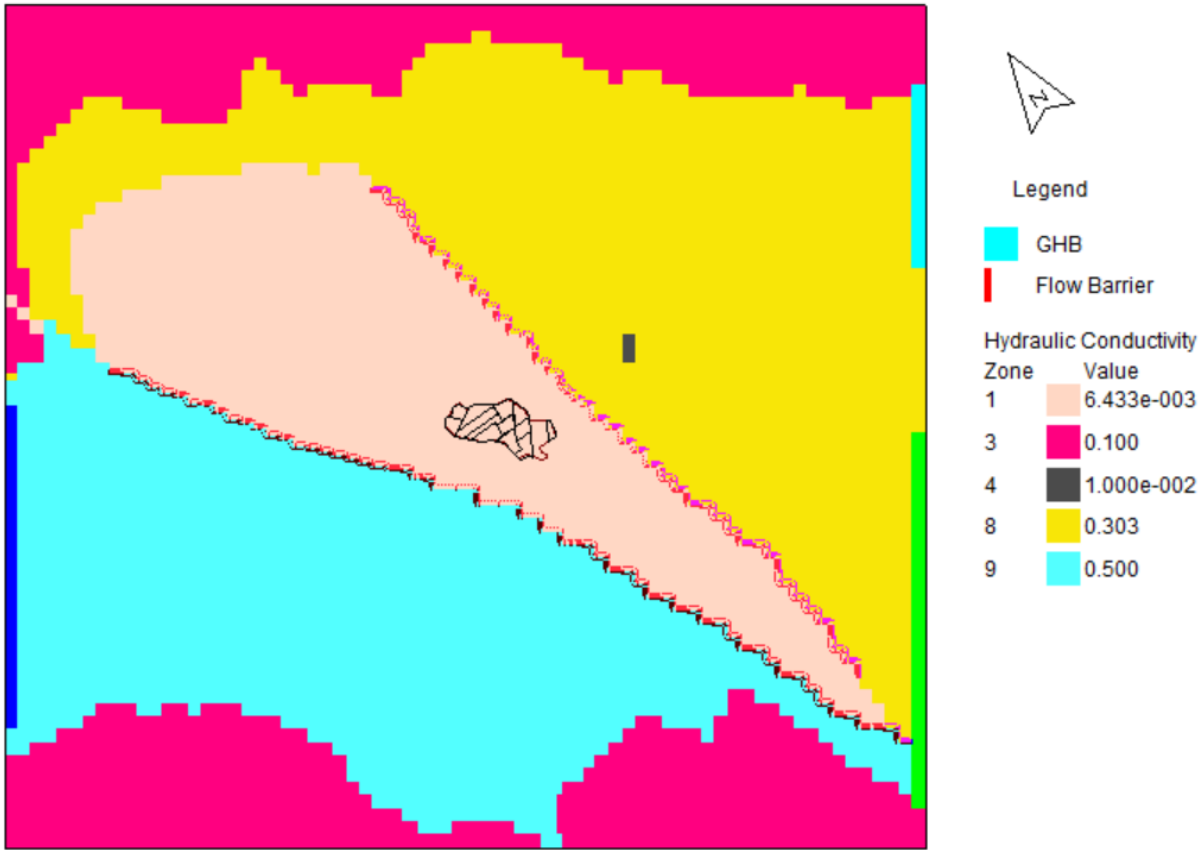
**25**

# APPENDIX A

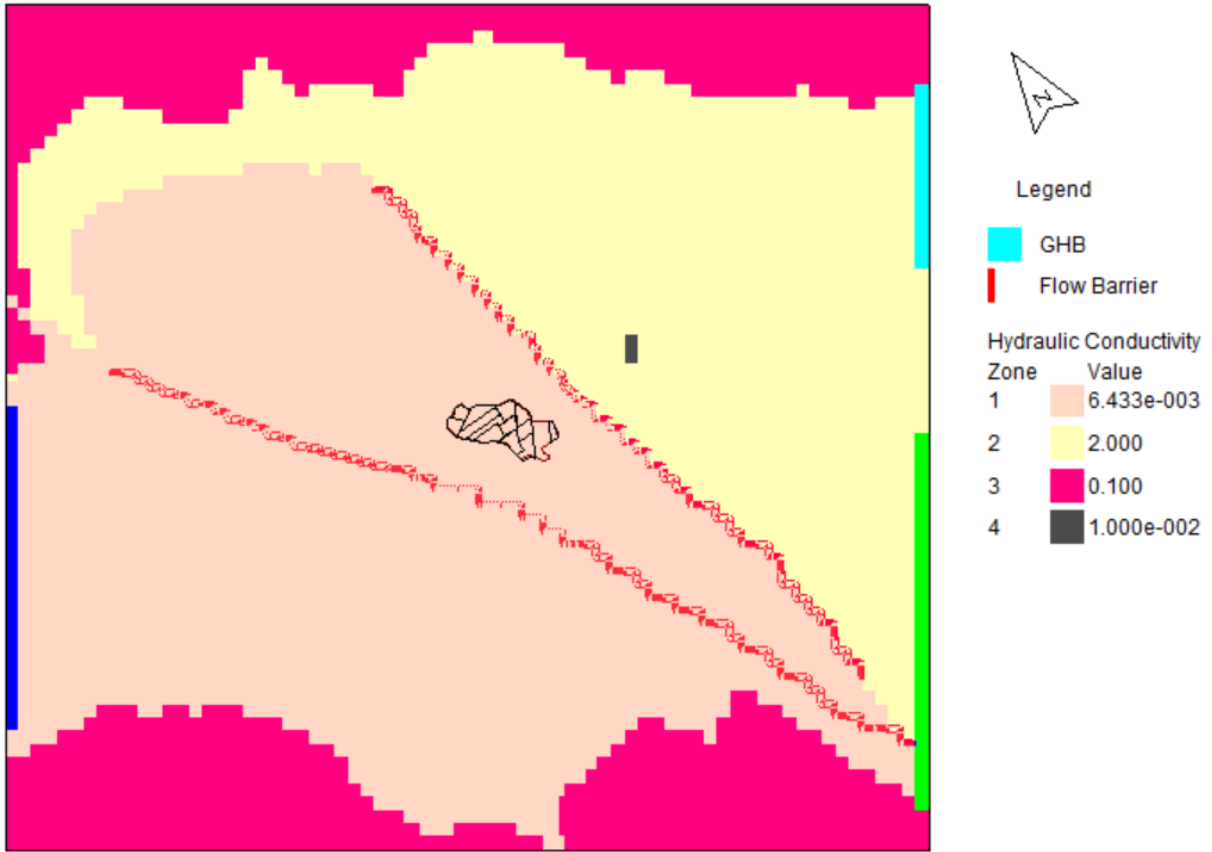
---



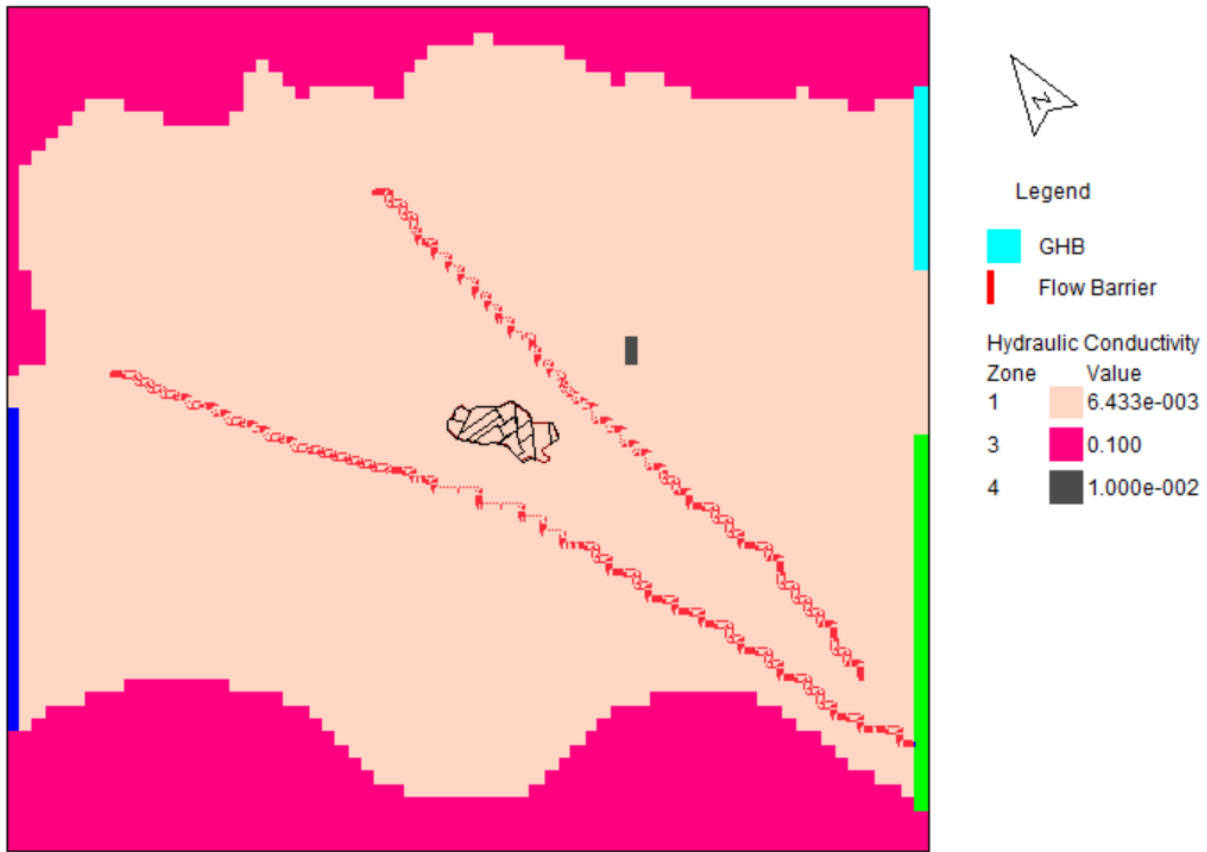
Layer 1



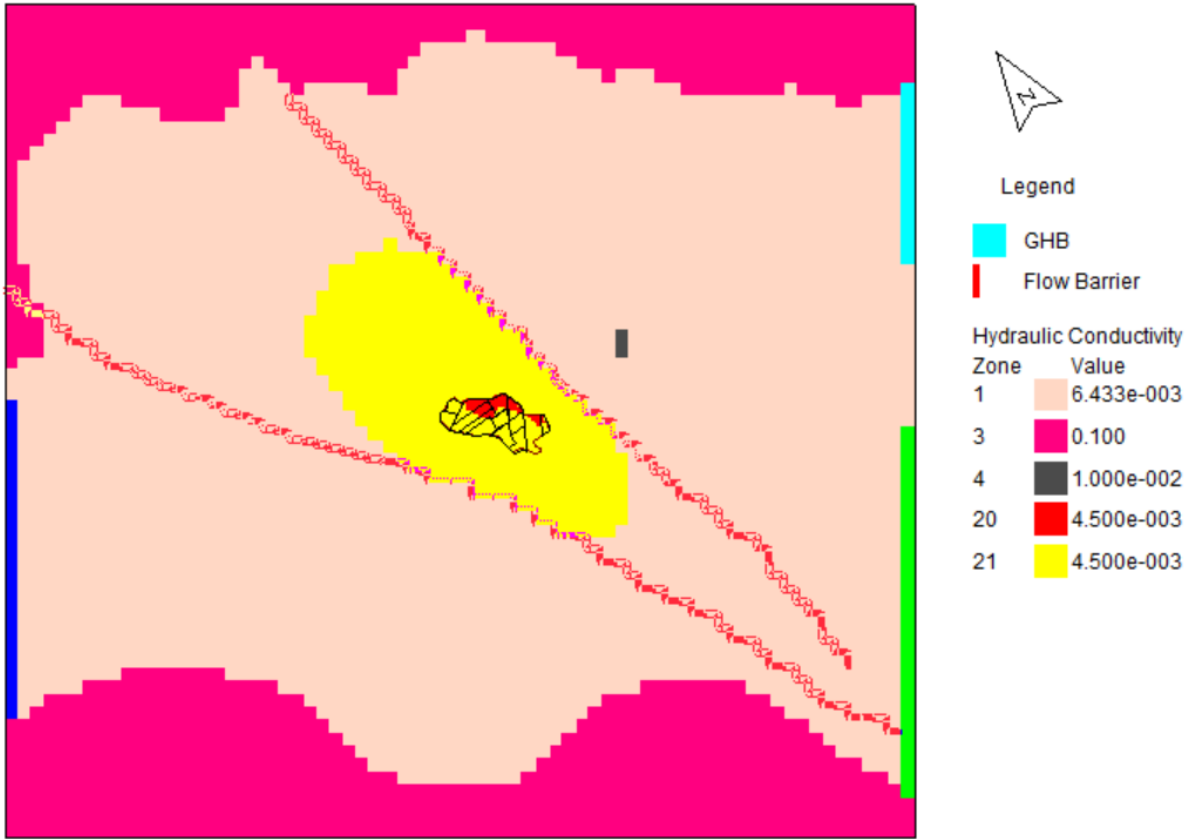
Layer 2



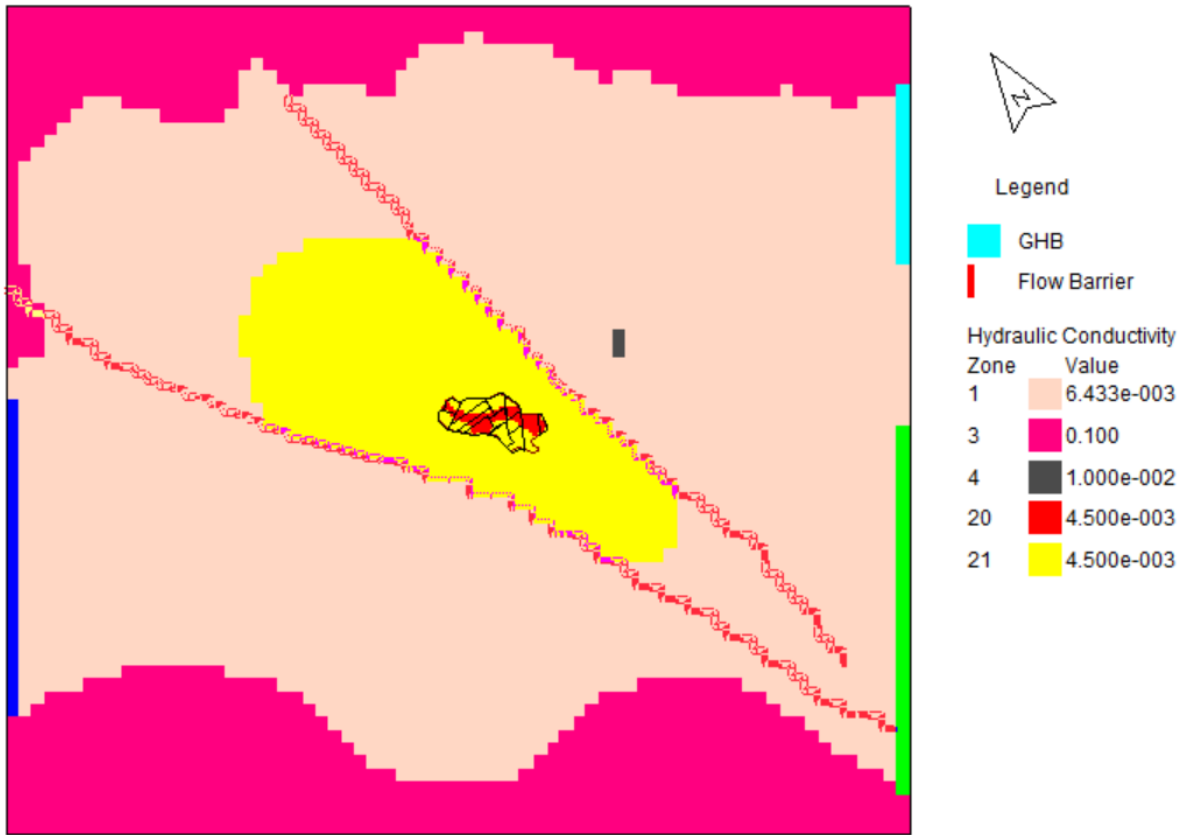
Layer 3



Layer 4 and 5

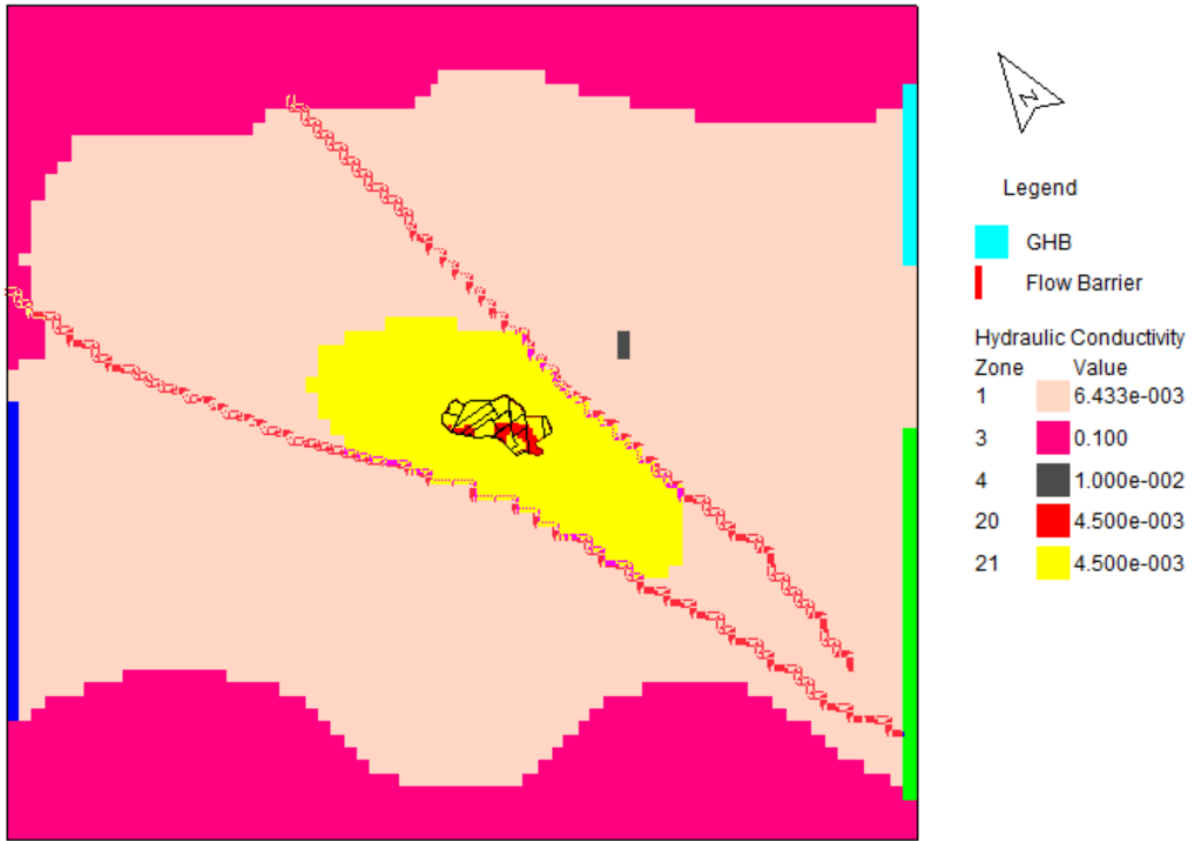


Layer 6

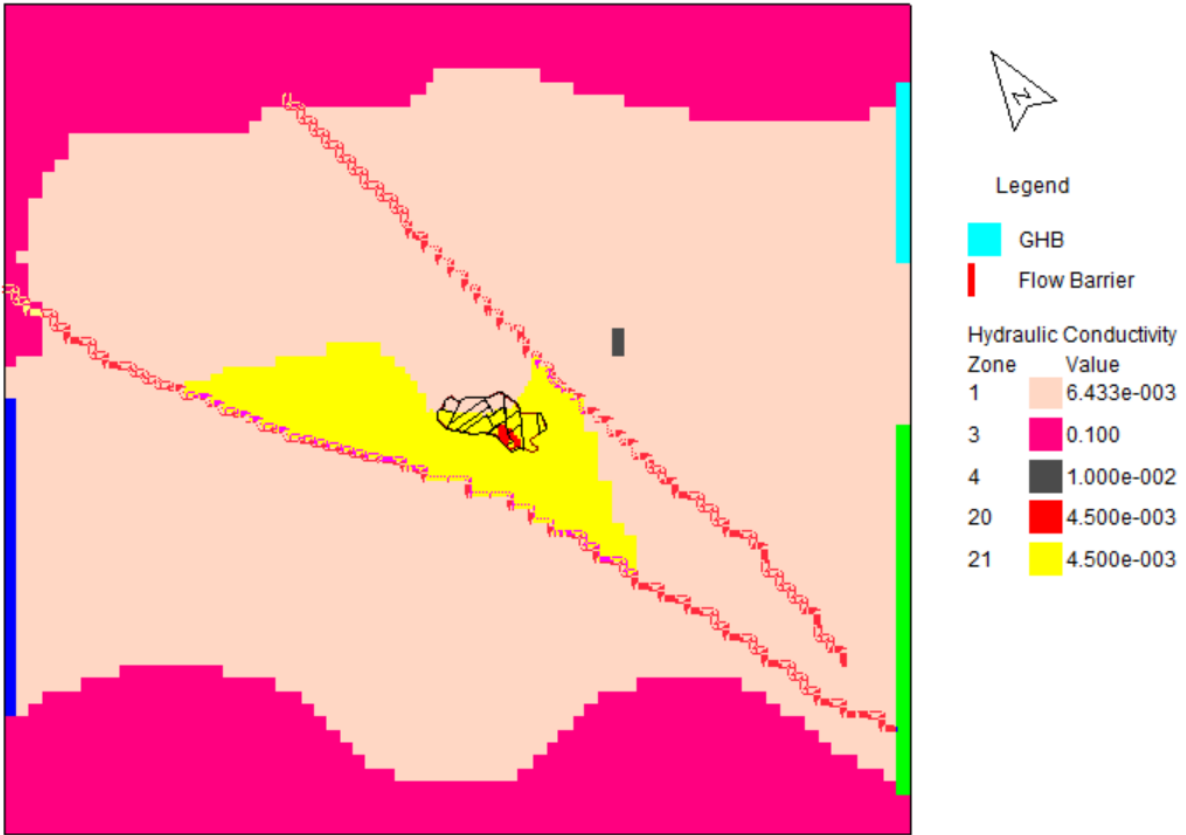


Layer 7

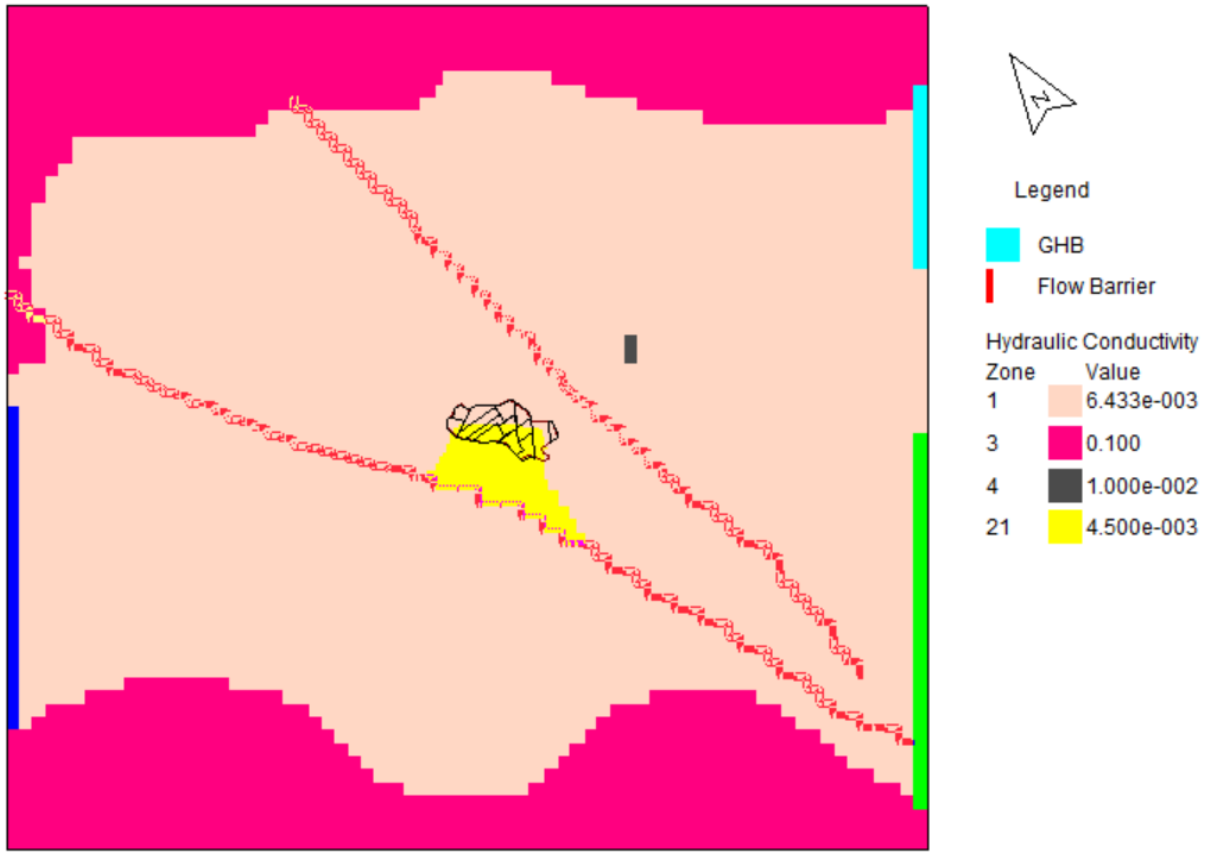




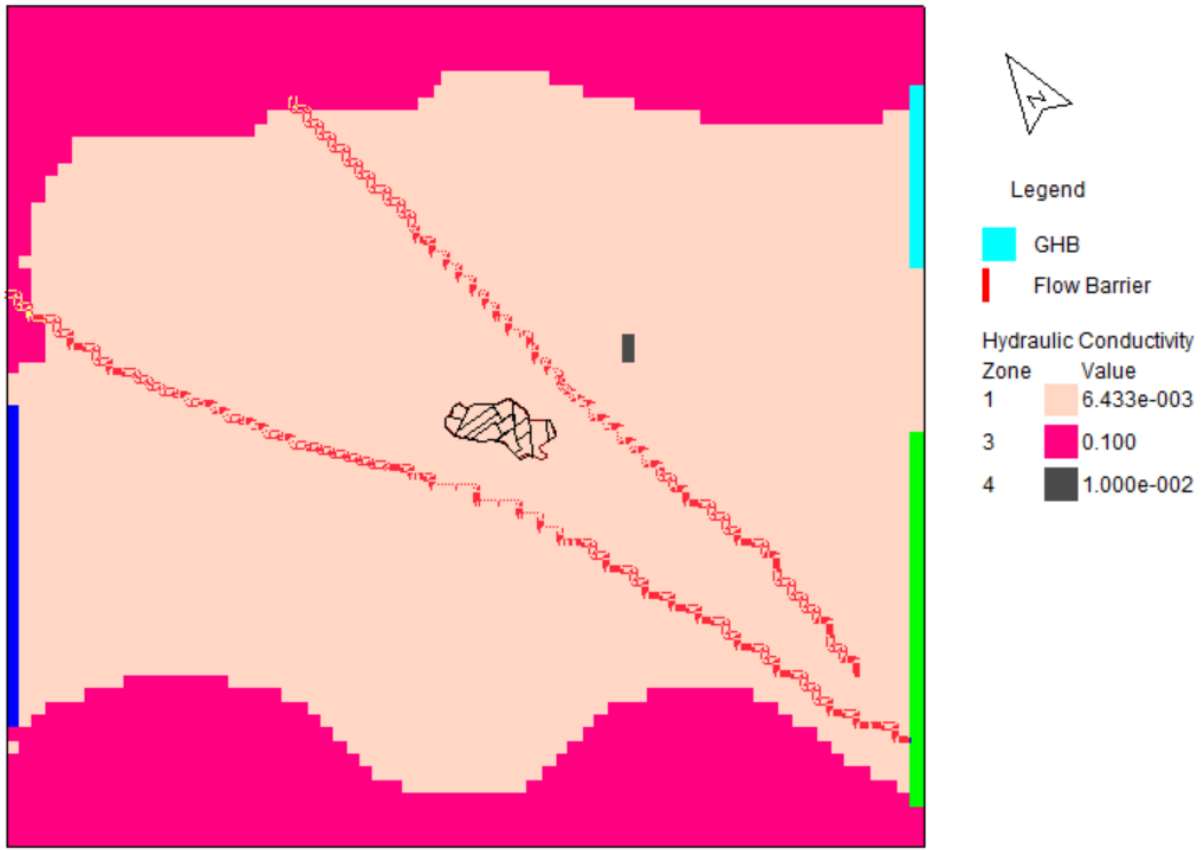
Layer 8



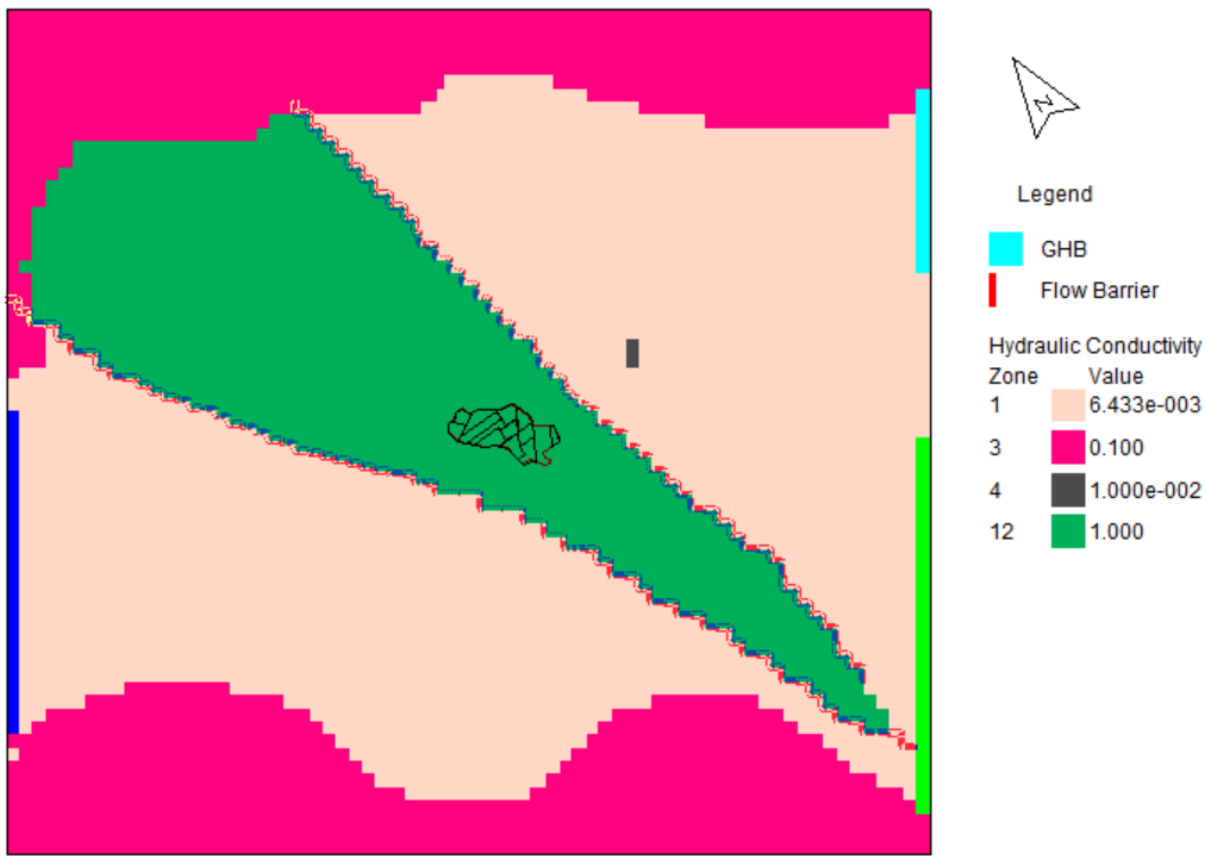
Layer 9



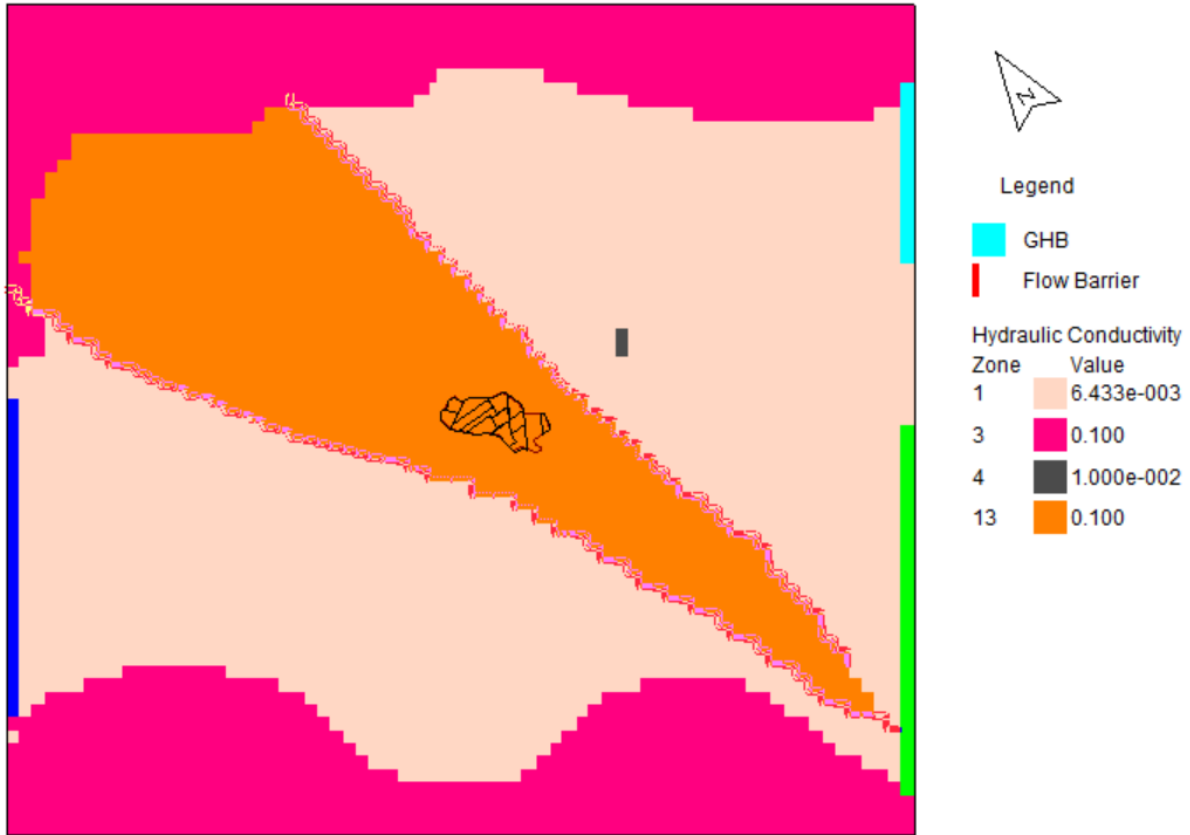
Layer 10



Layer 11



Layer 12



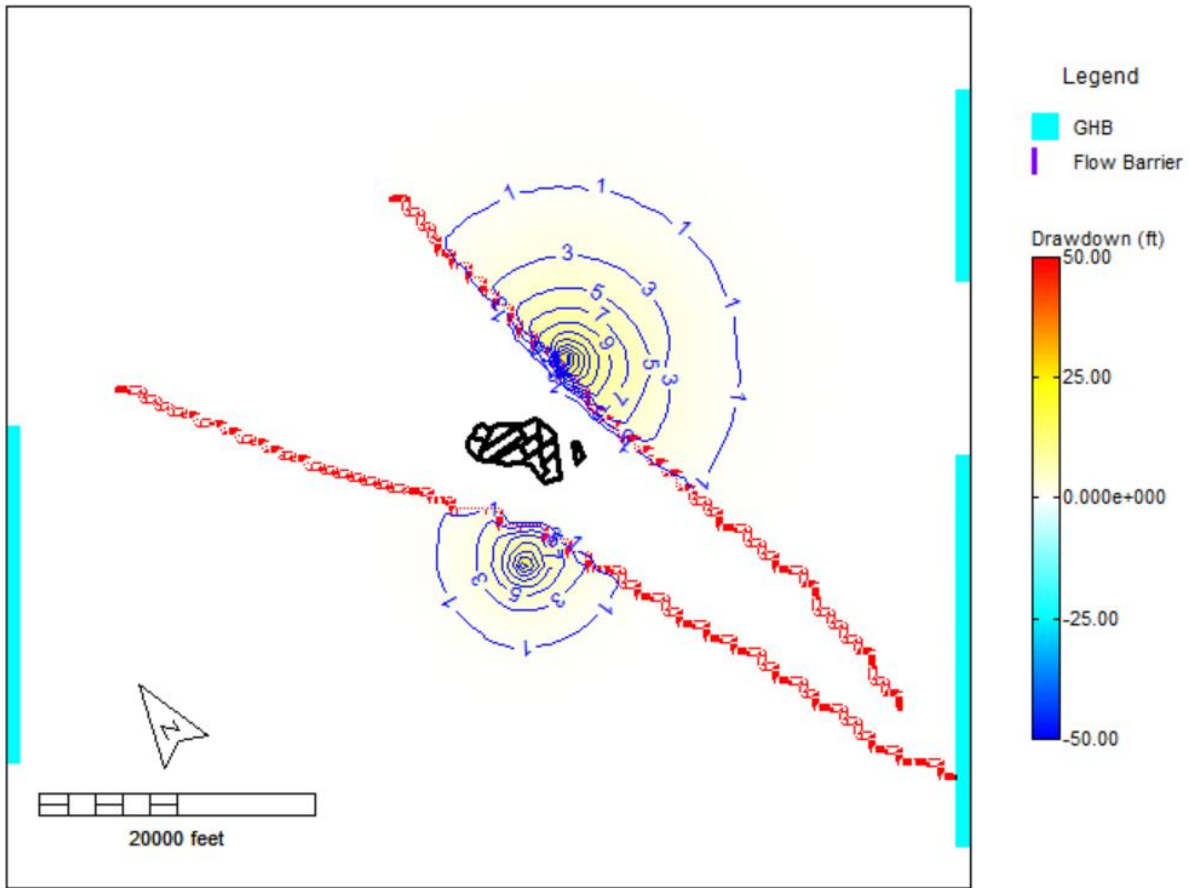
Layer 13



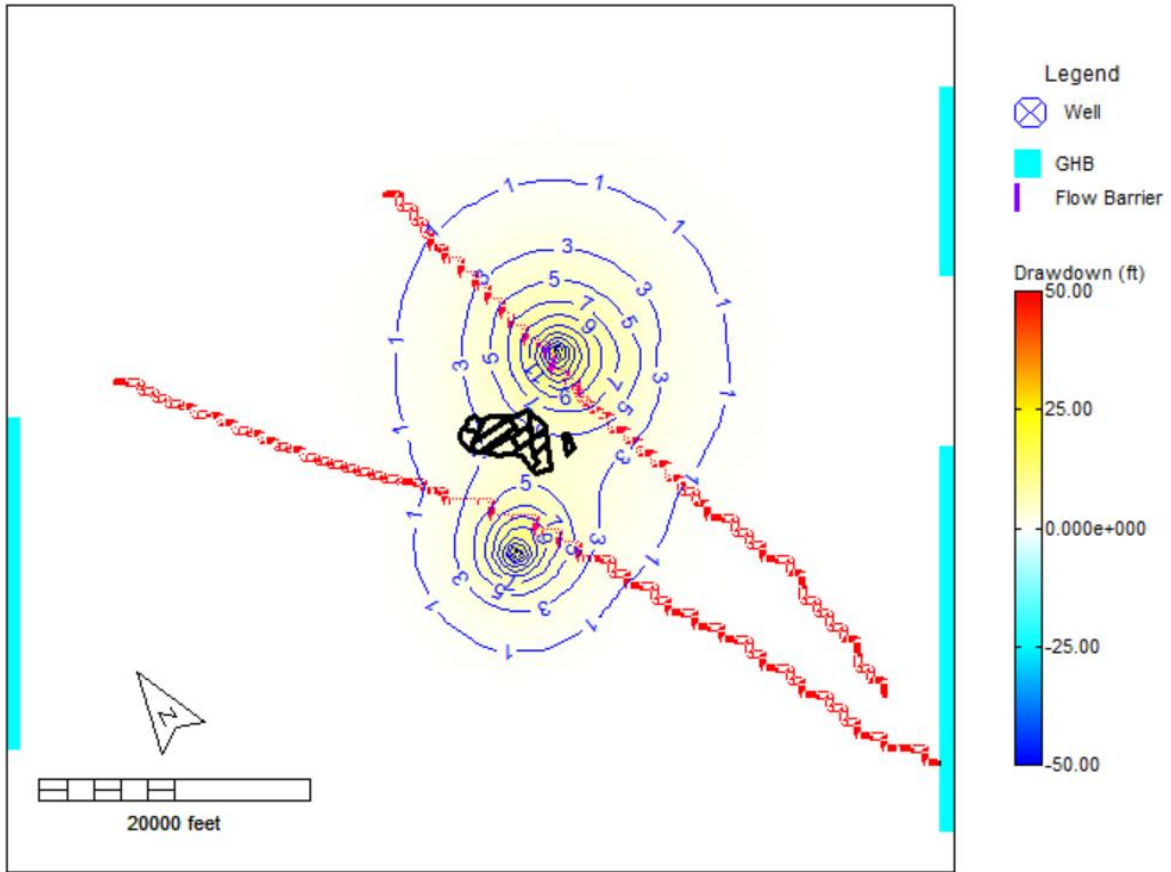
# APPENDIX B1

---

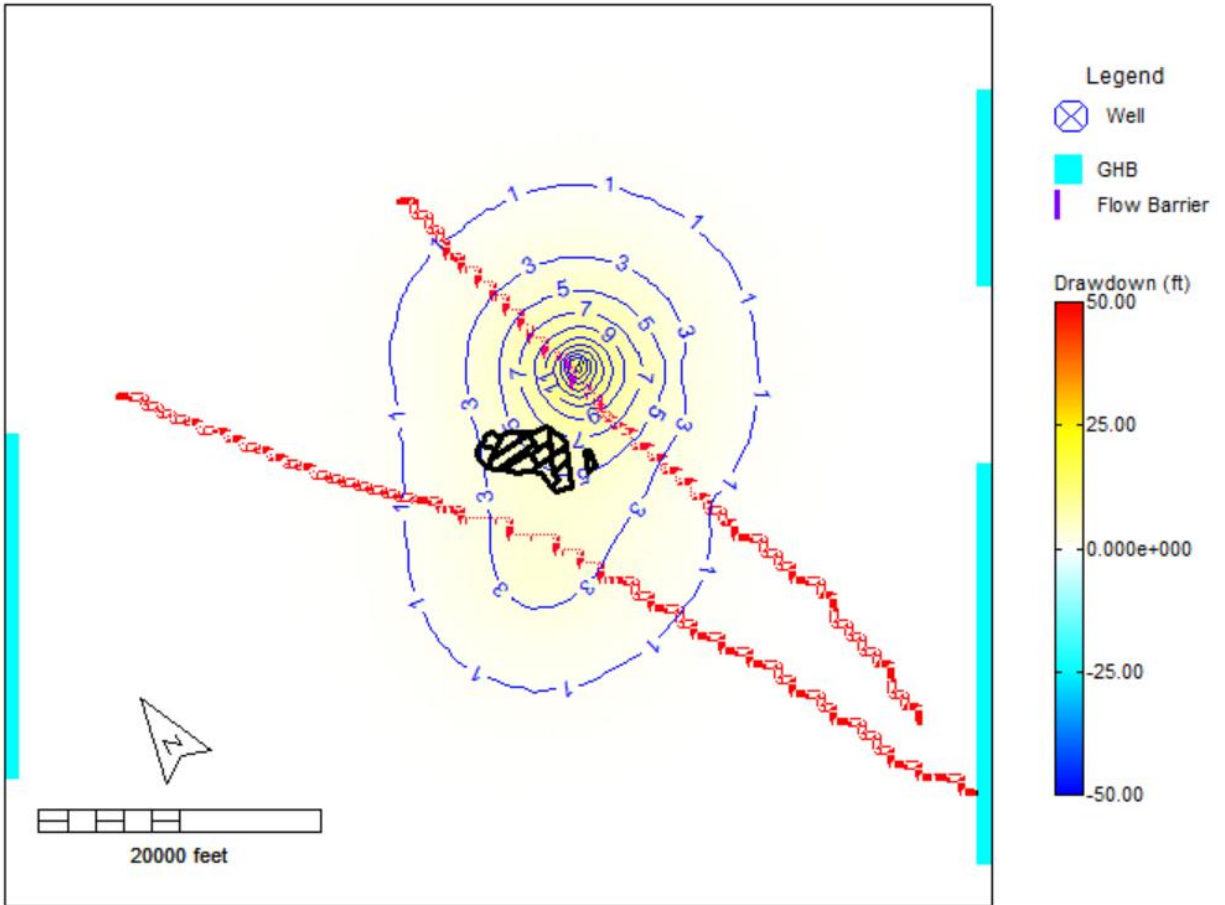




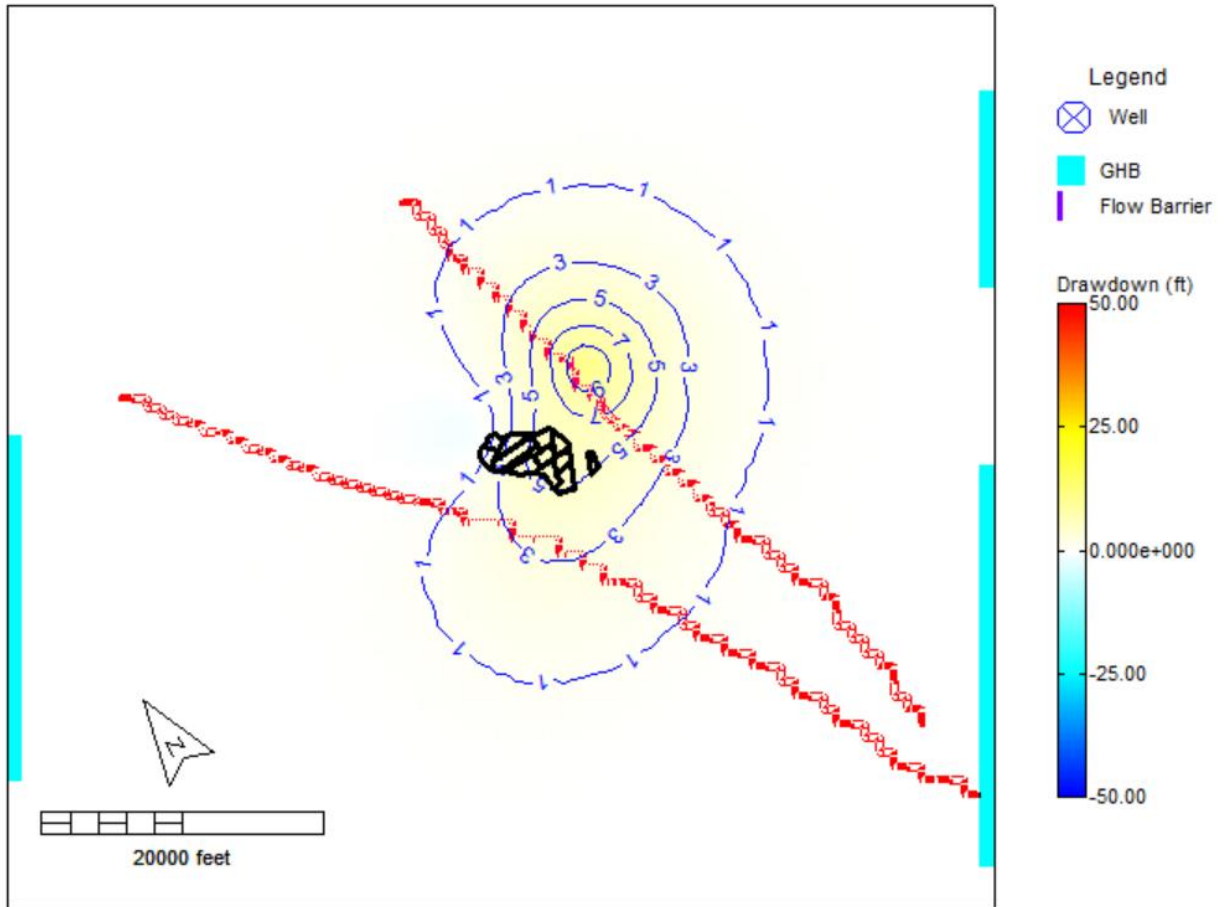
Layer 1



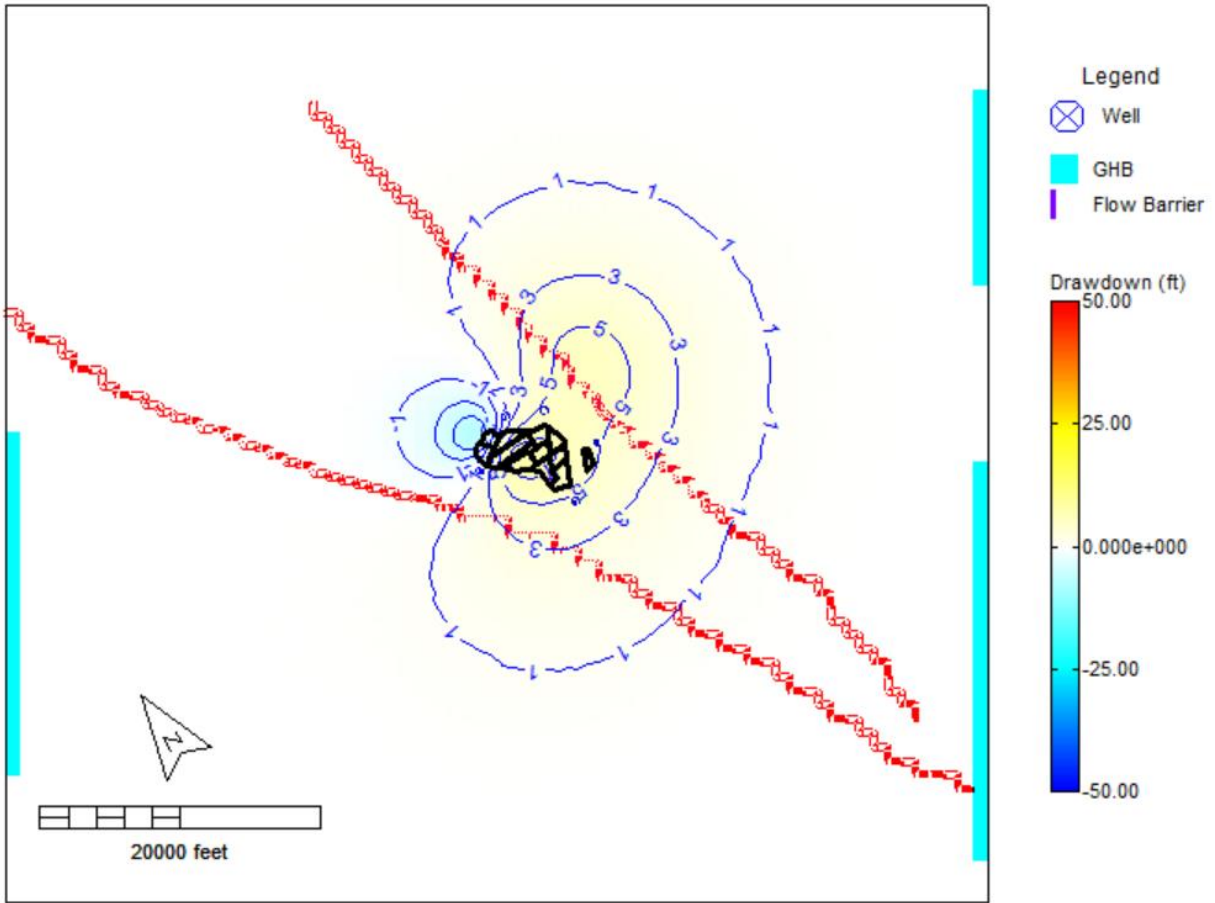
Layer 2



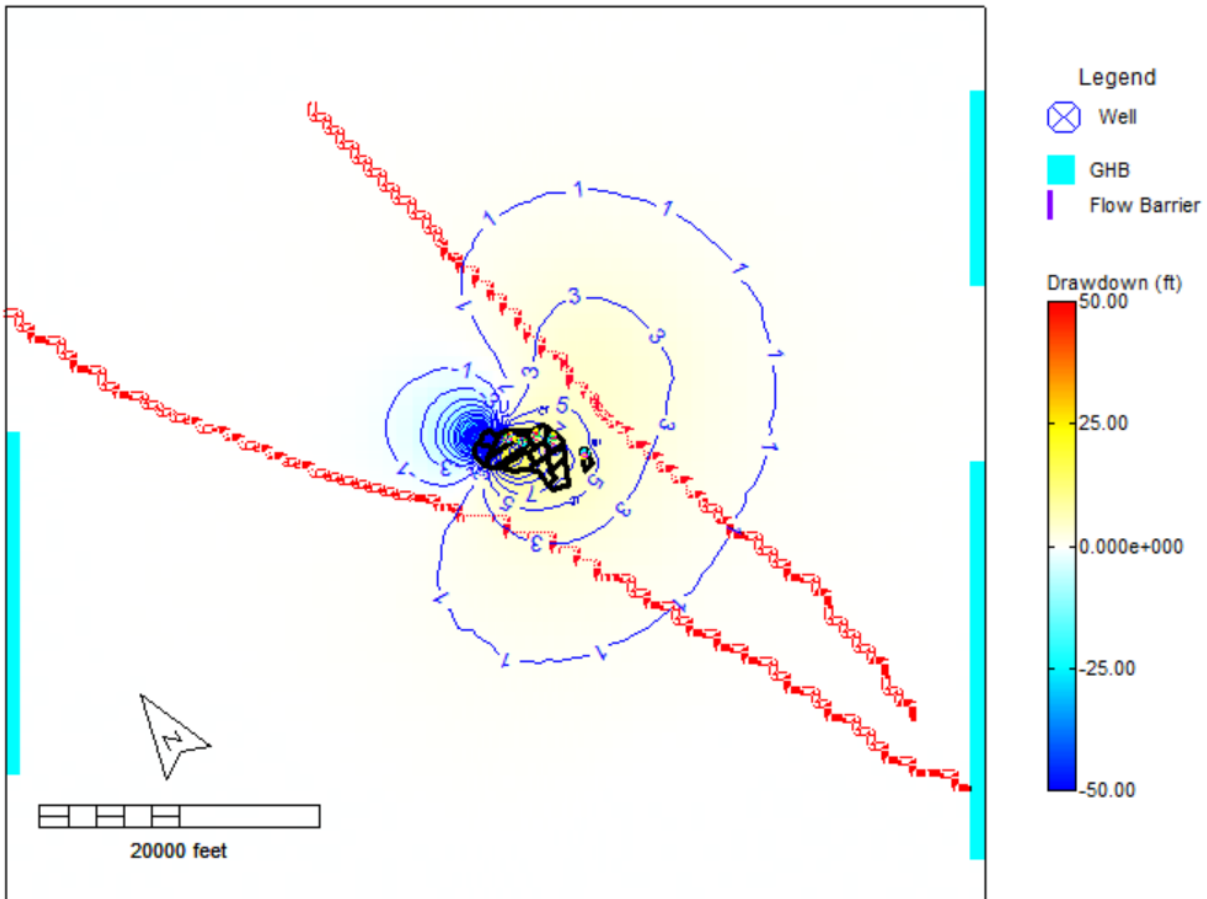
Layer 3



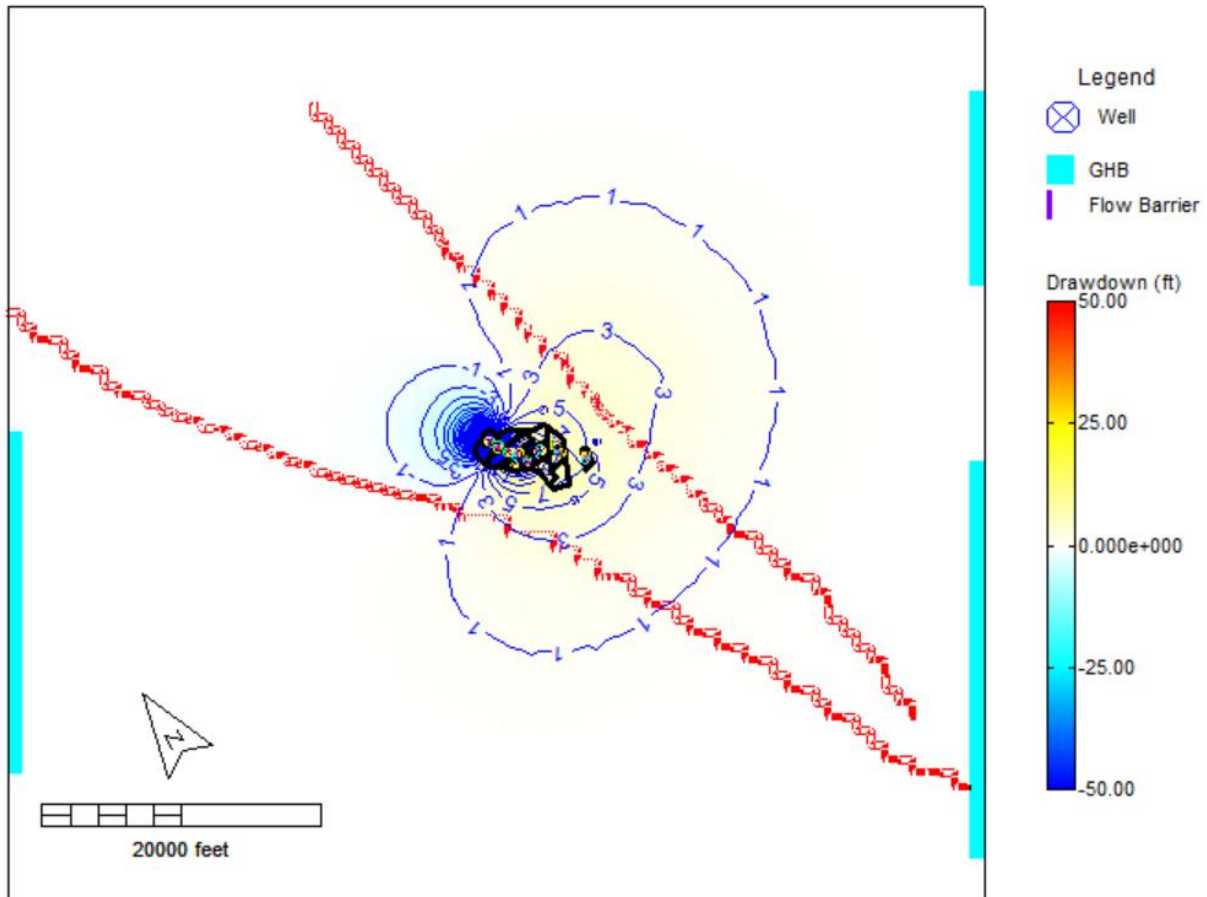
Layer 4



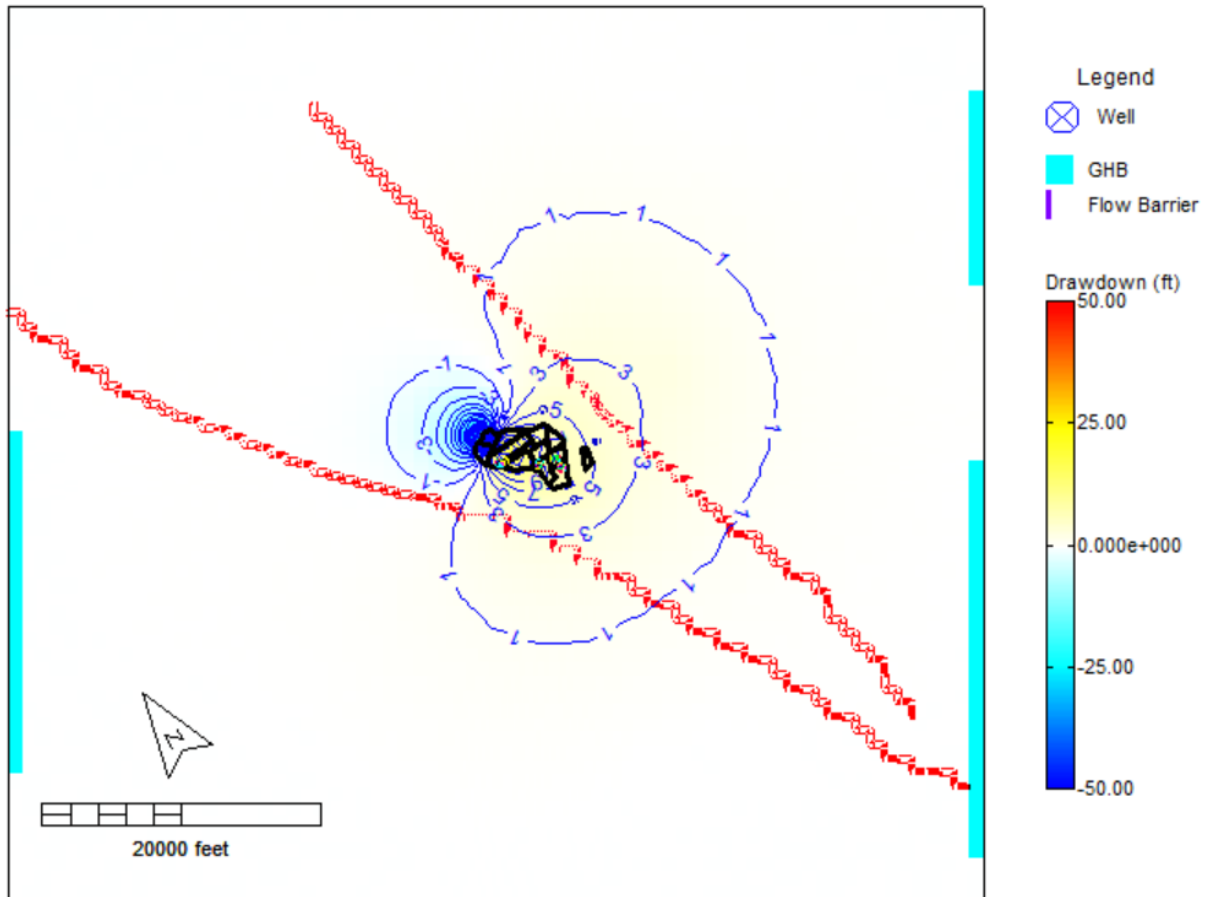
Layer 5



Layer 6

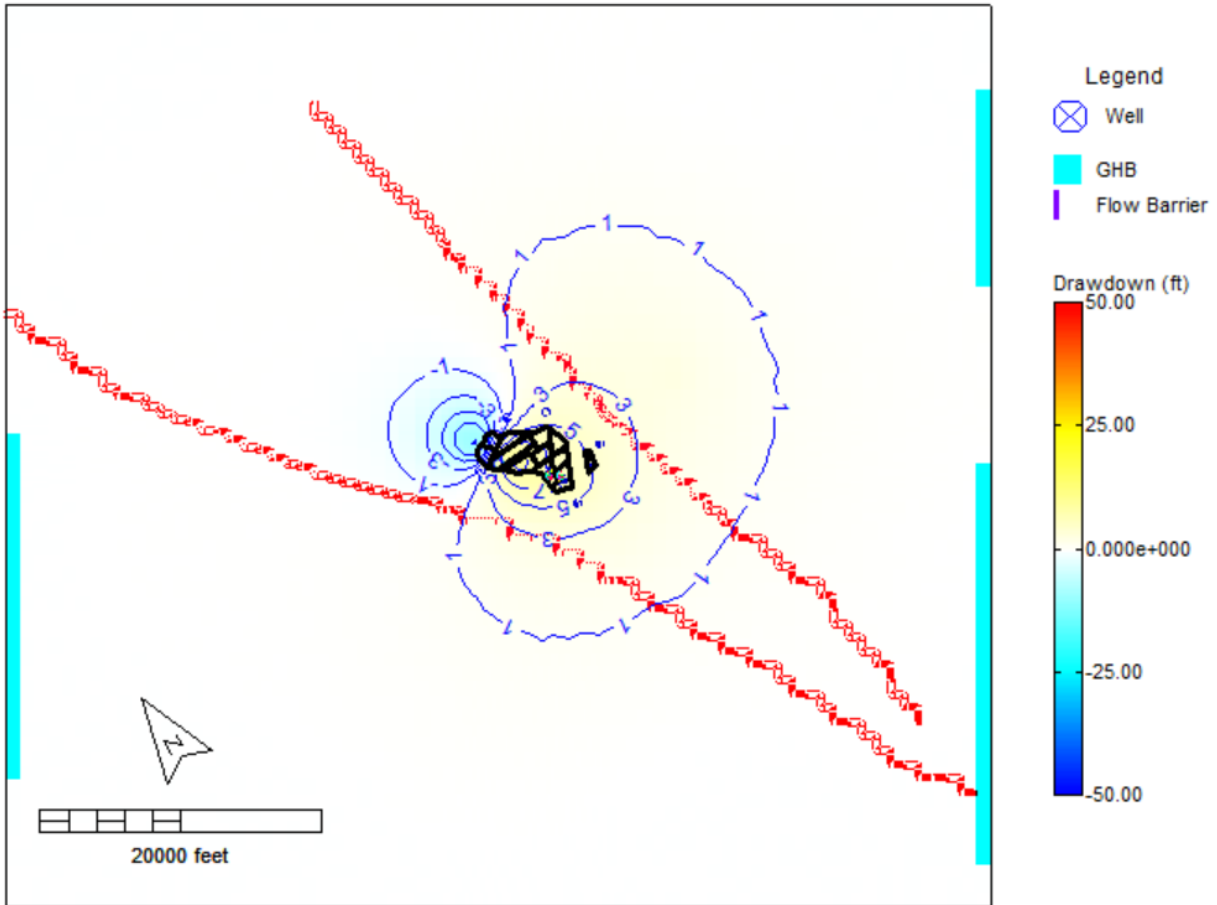


Layer 7

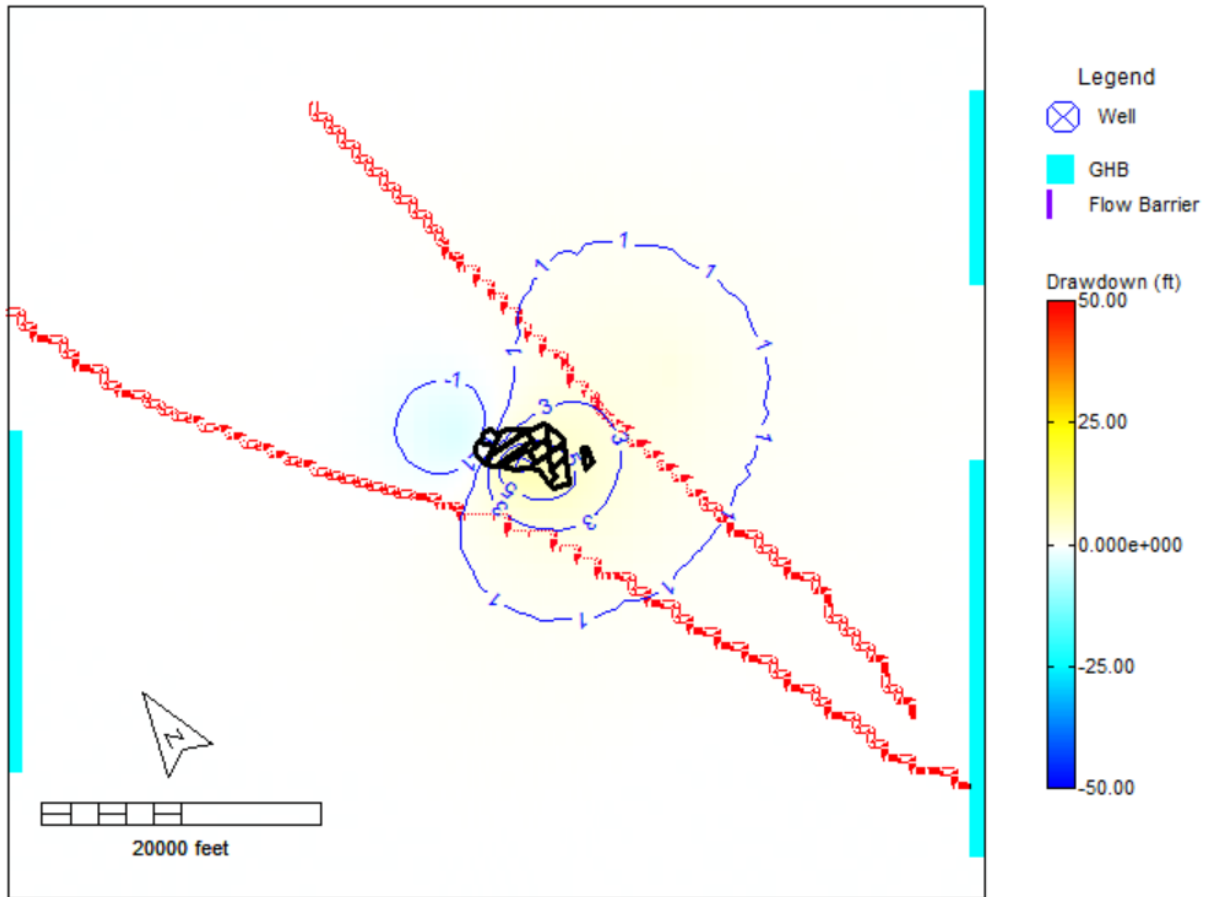


Layer 8

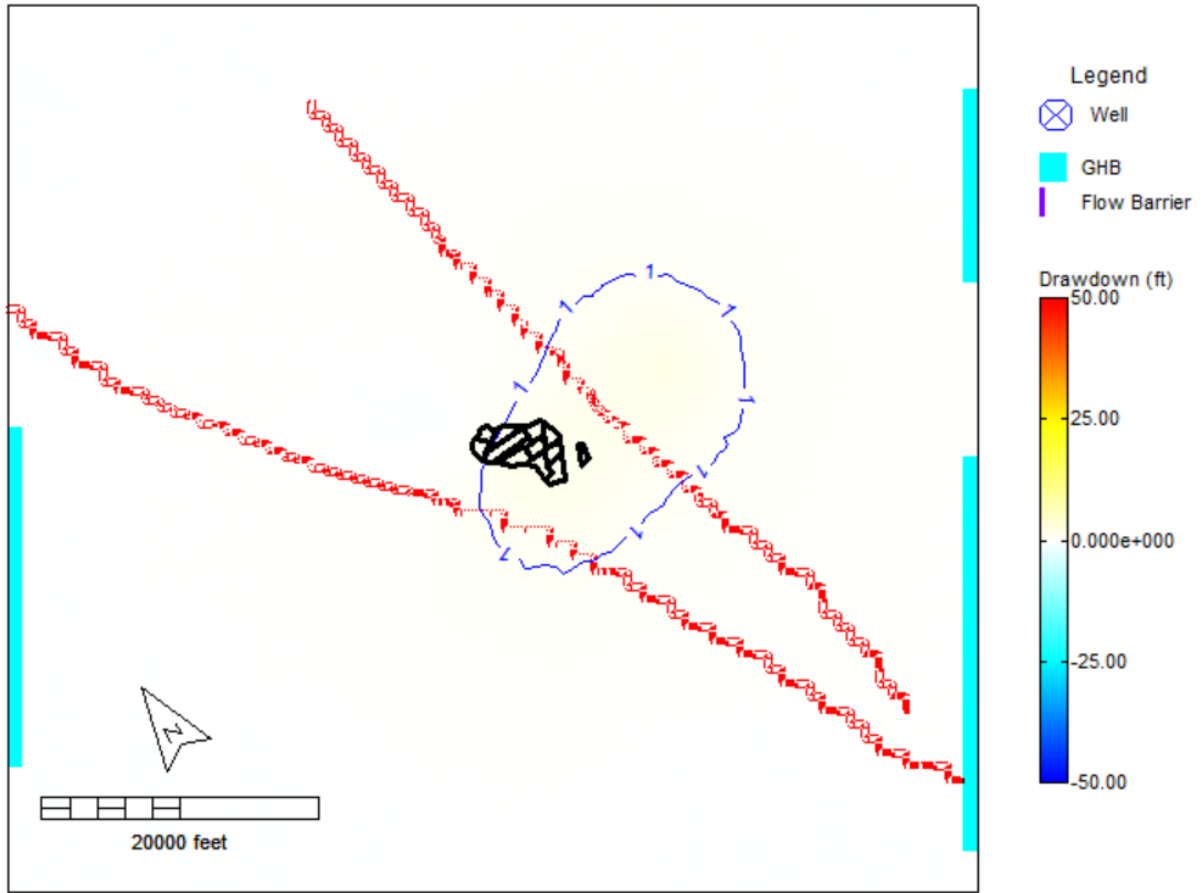




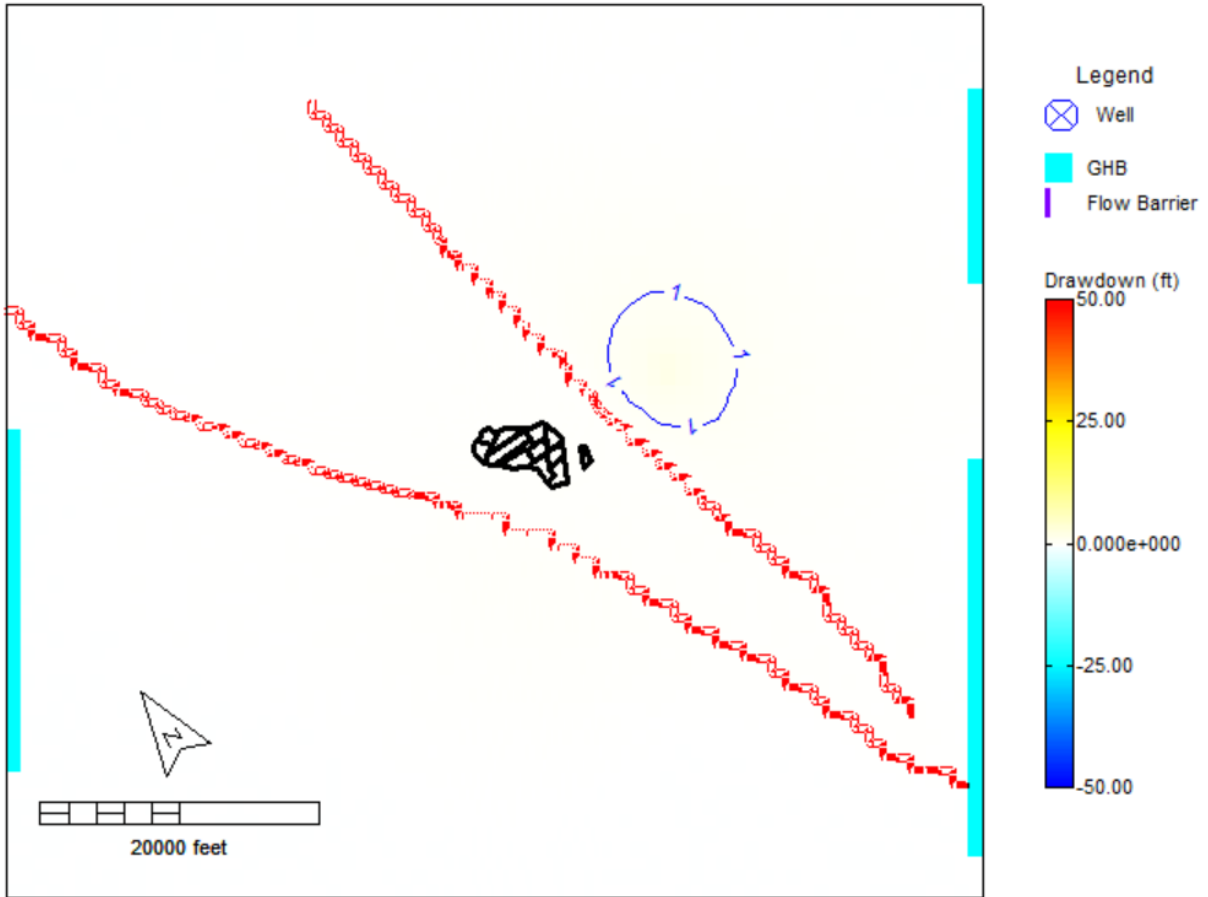
Layer 9



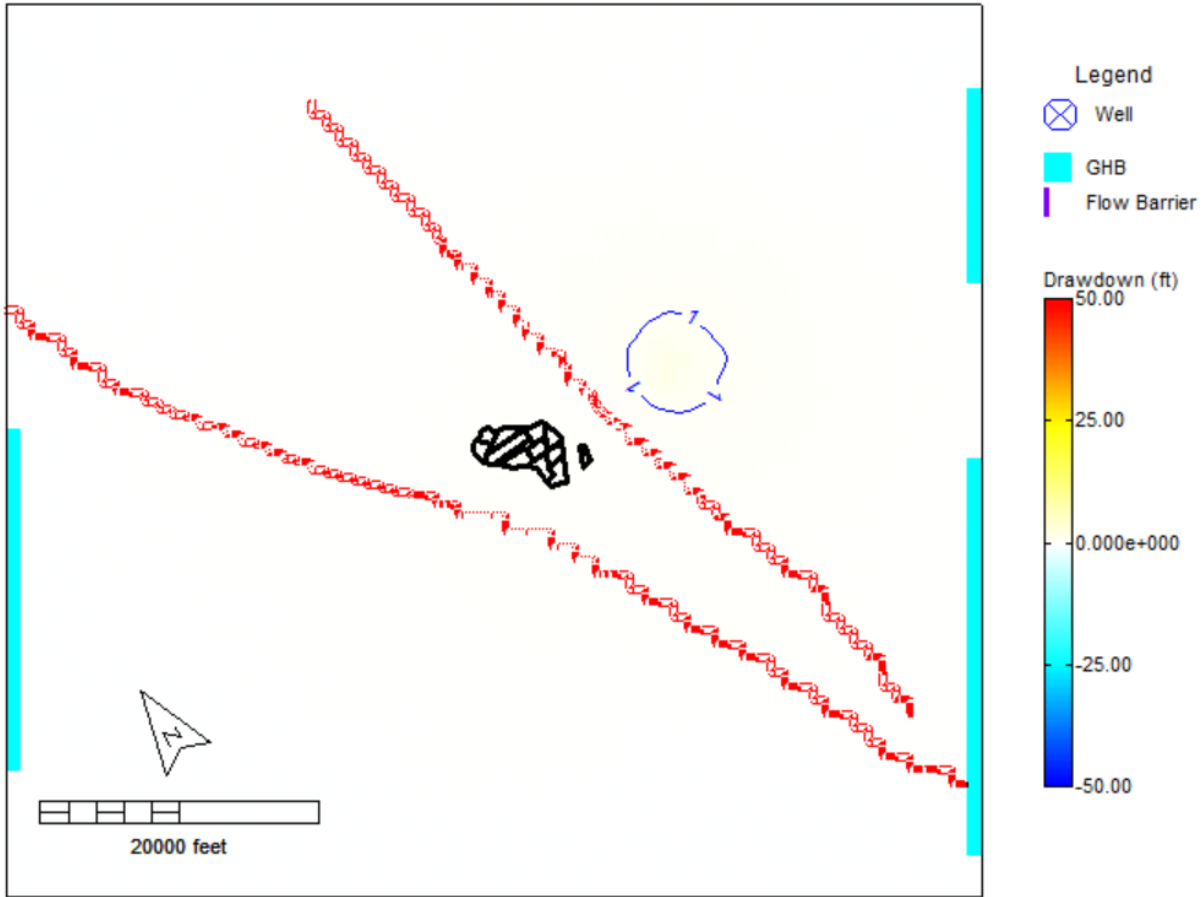
Layer 10



Layer 11



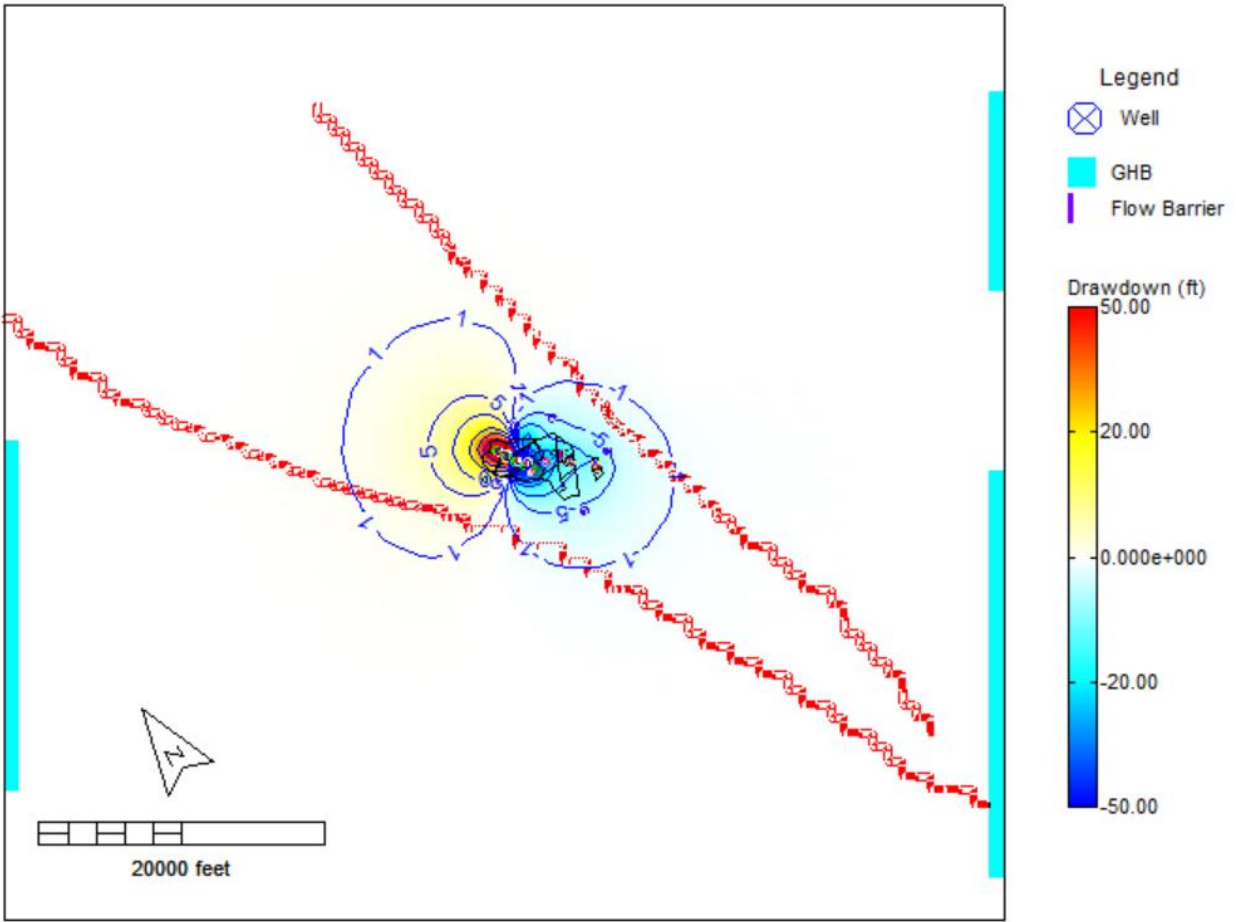
Layer 12



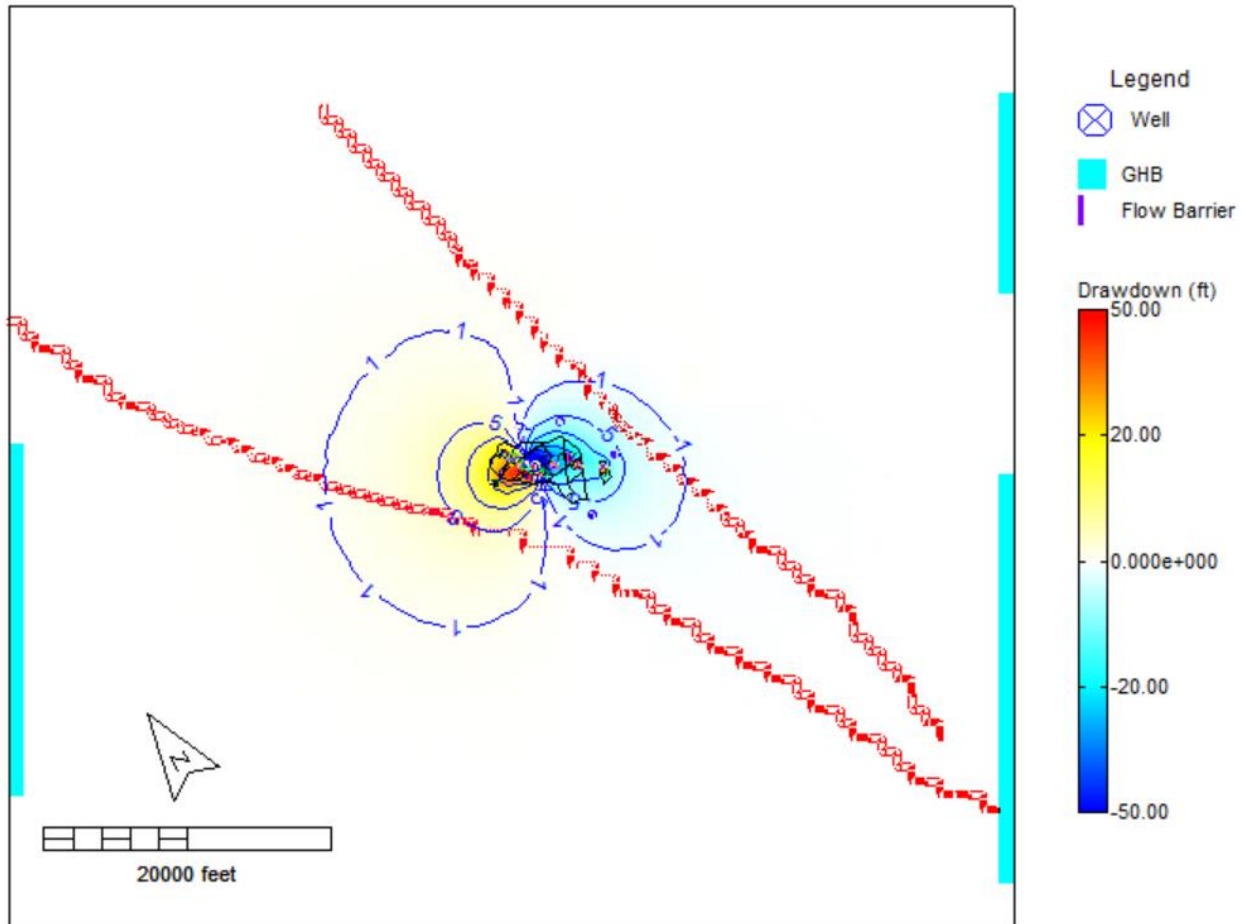
Layer 13

# APPENDIX B2

---

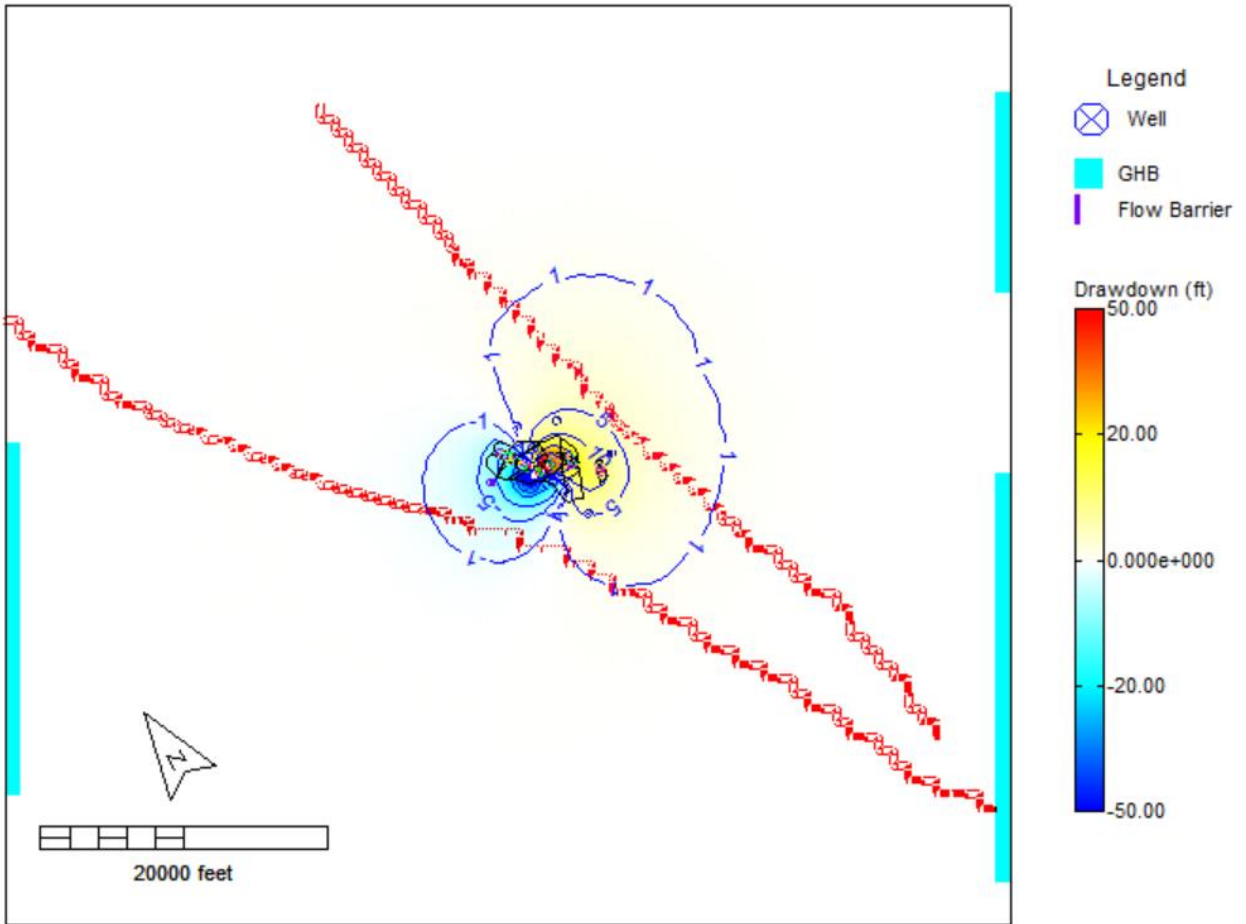


Mine Year 3

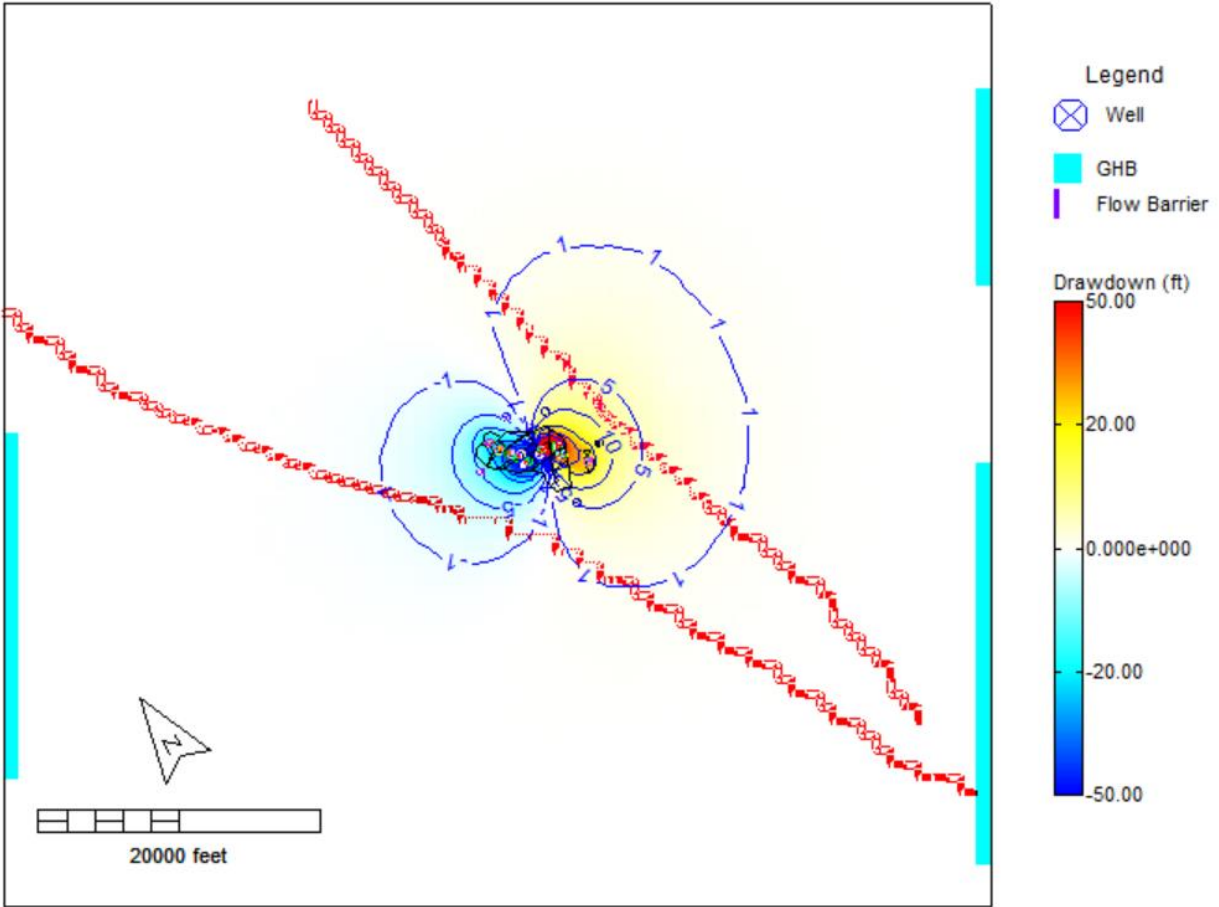


Mine Year 6

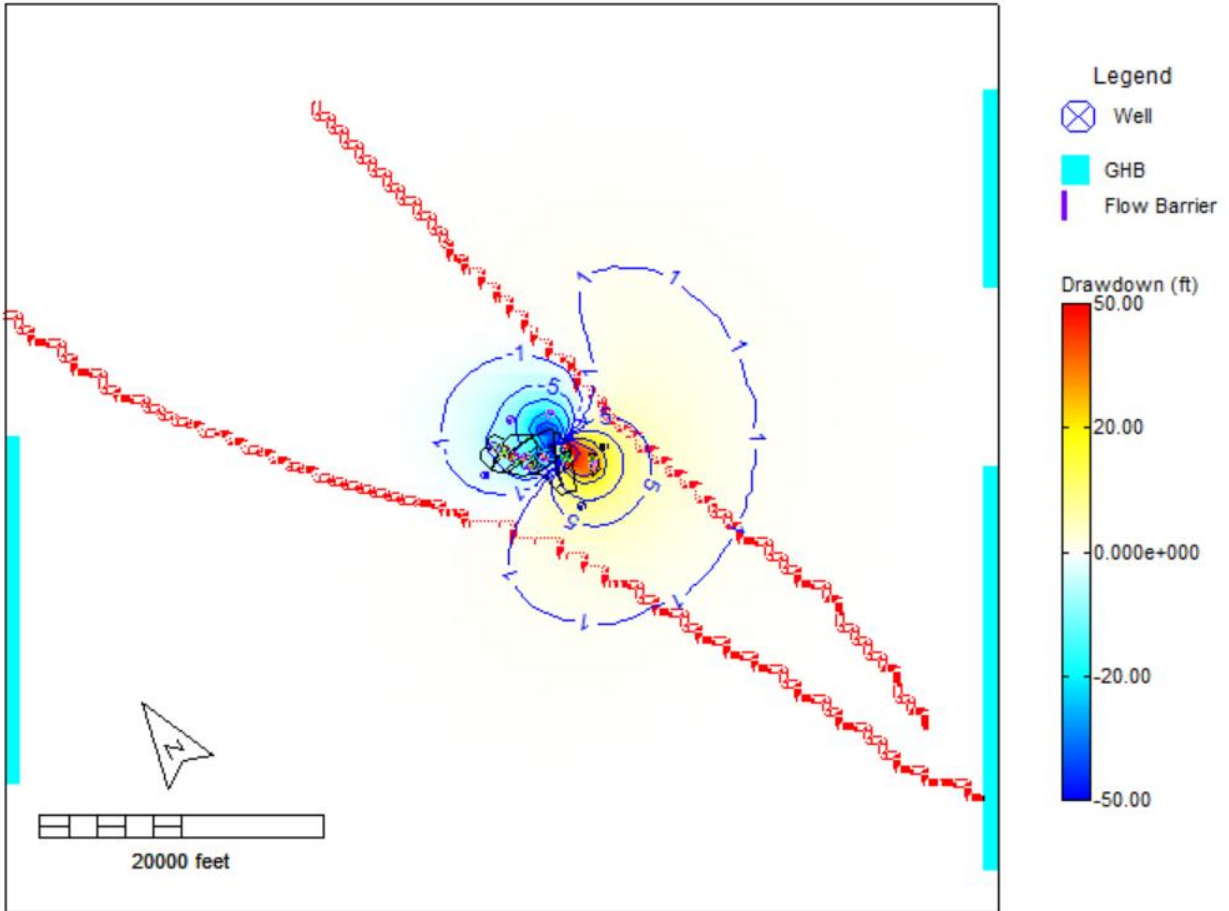




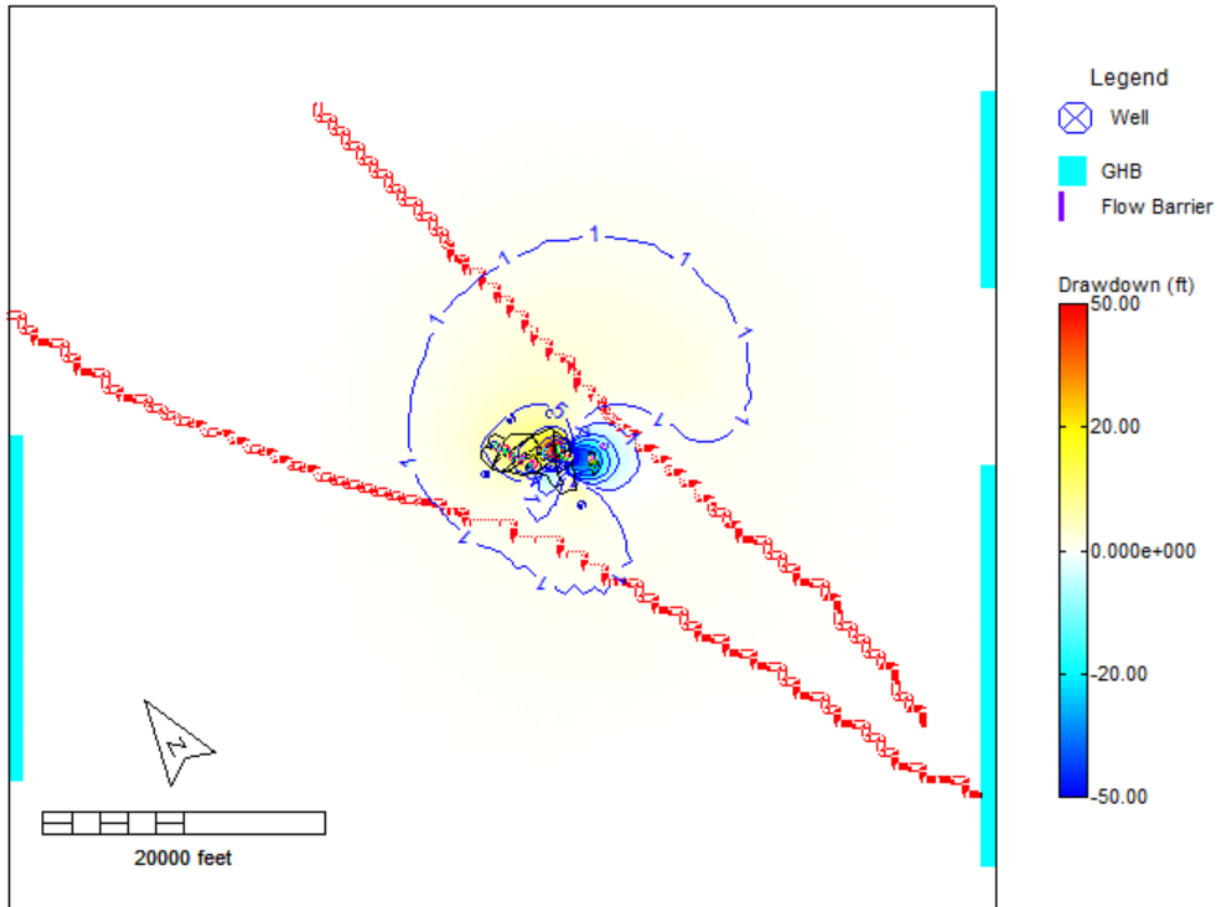
Mine Year 9



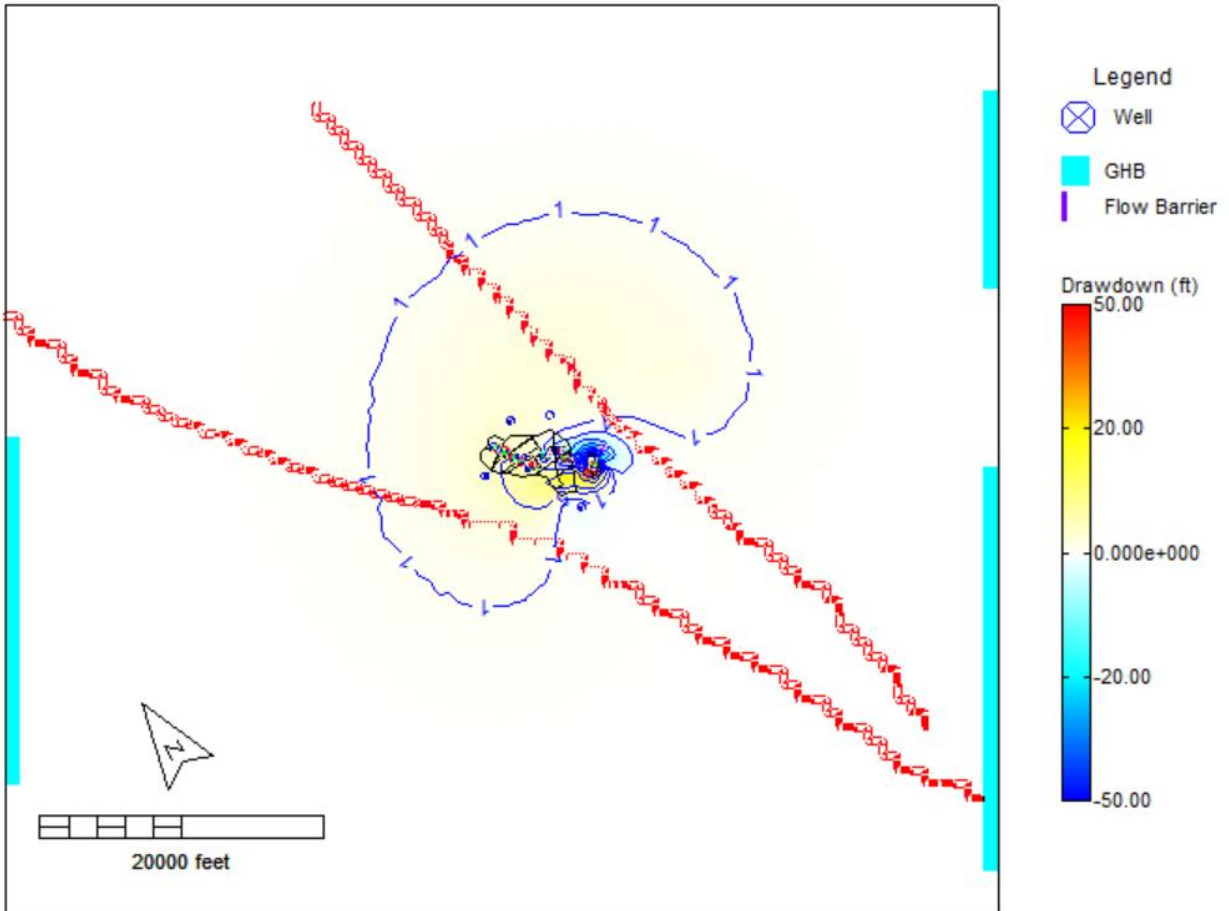
Mine Year 12



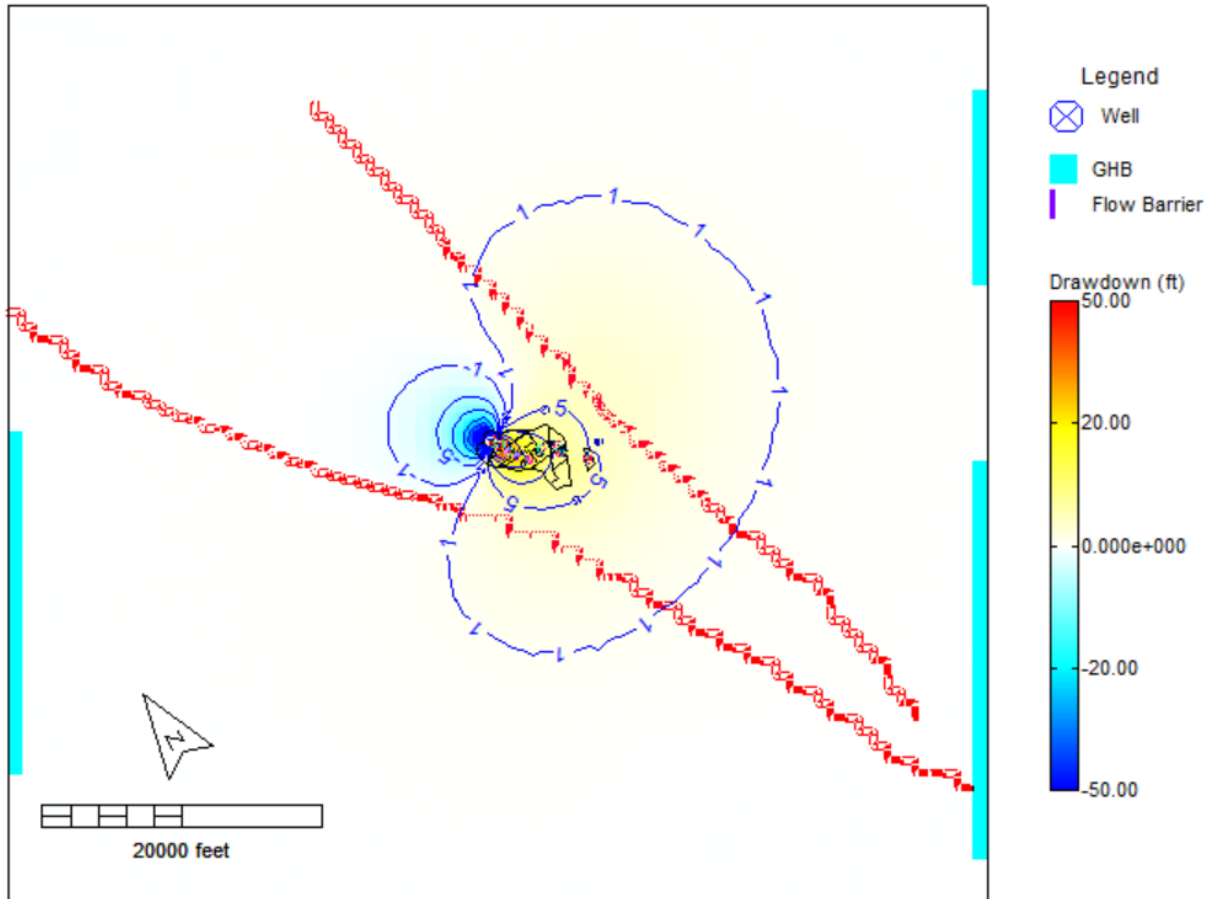
Mine Year 15



Mine Year 18



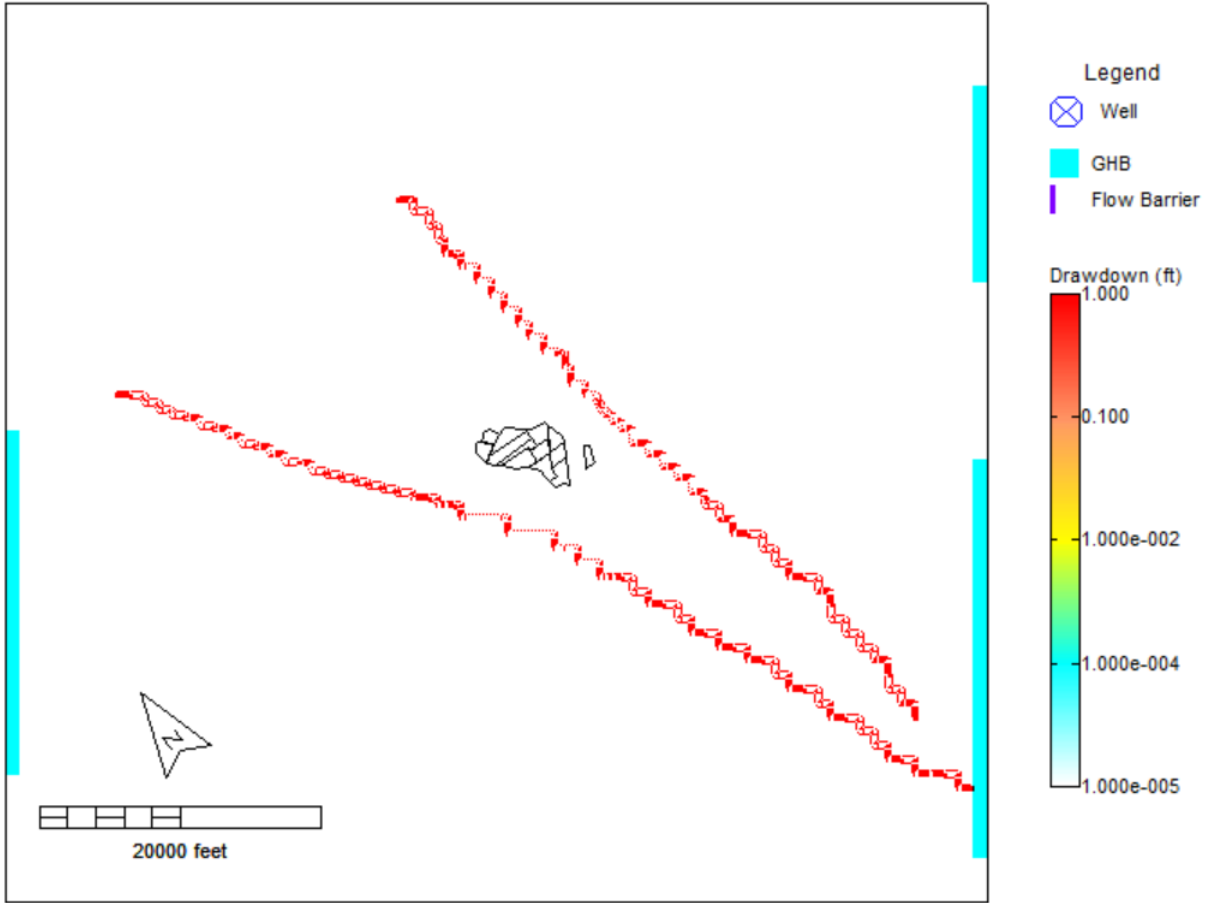
Mine Year 21



Mine Year 25

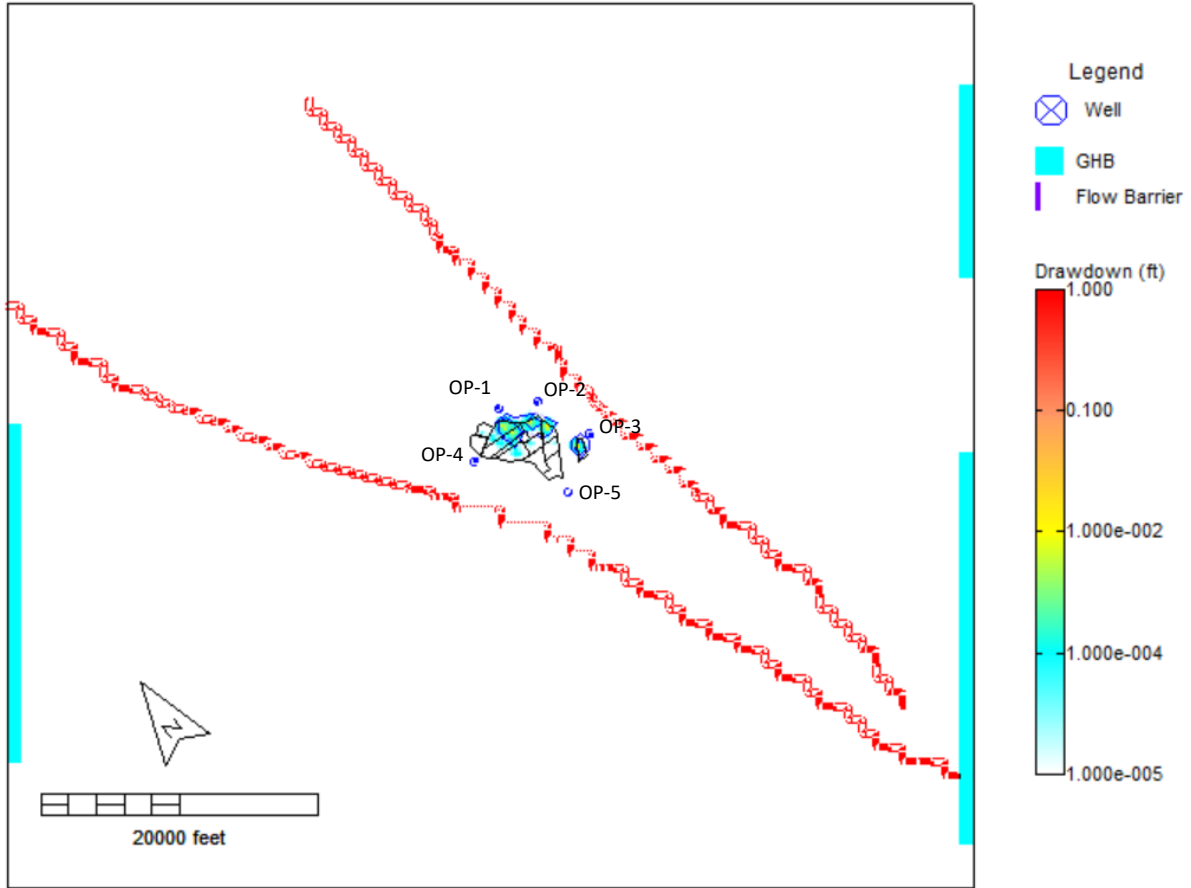
# APPENDIX C1

---

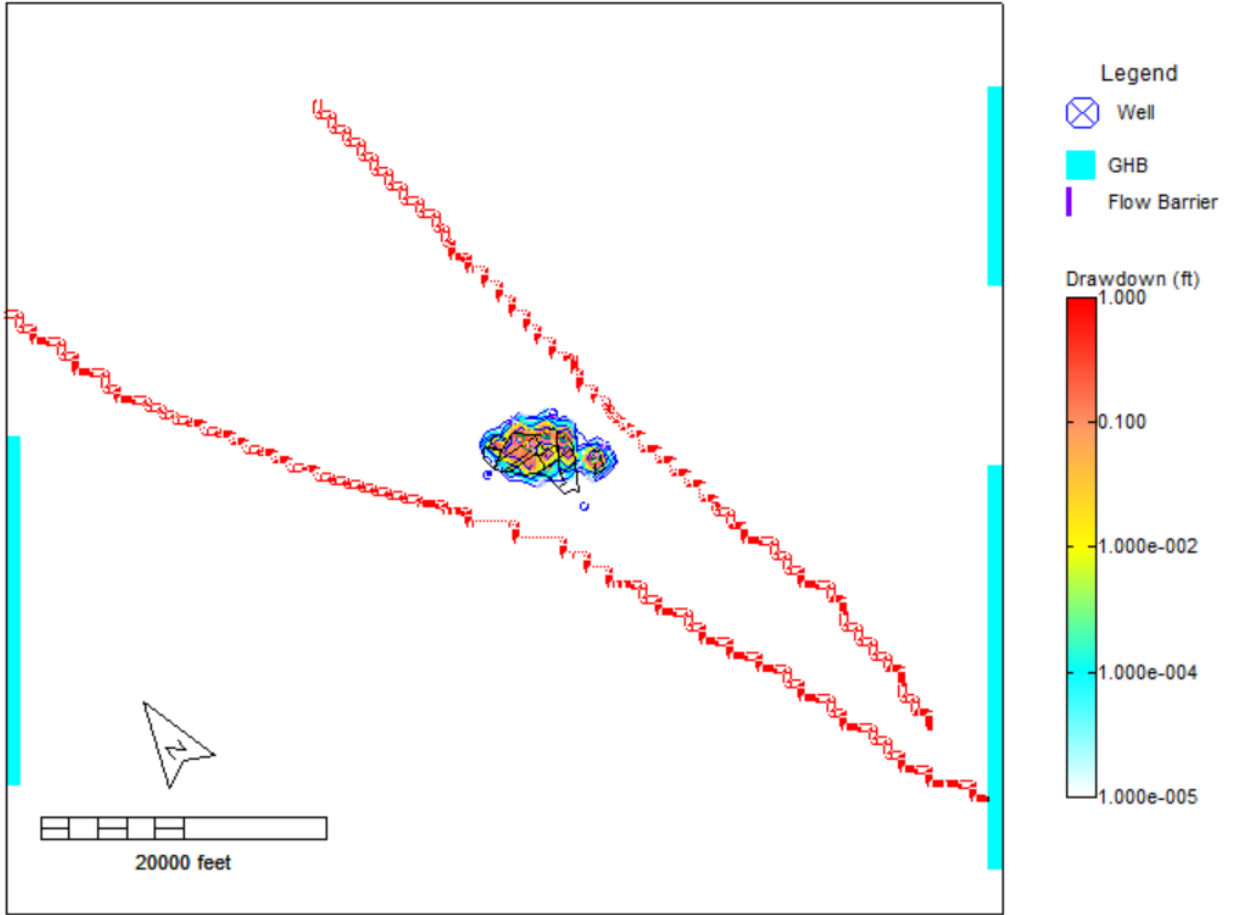


Layer 4

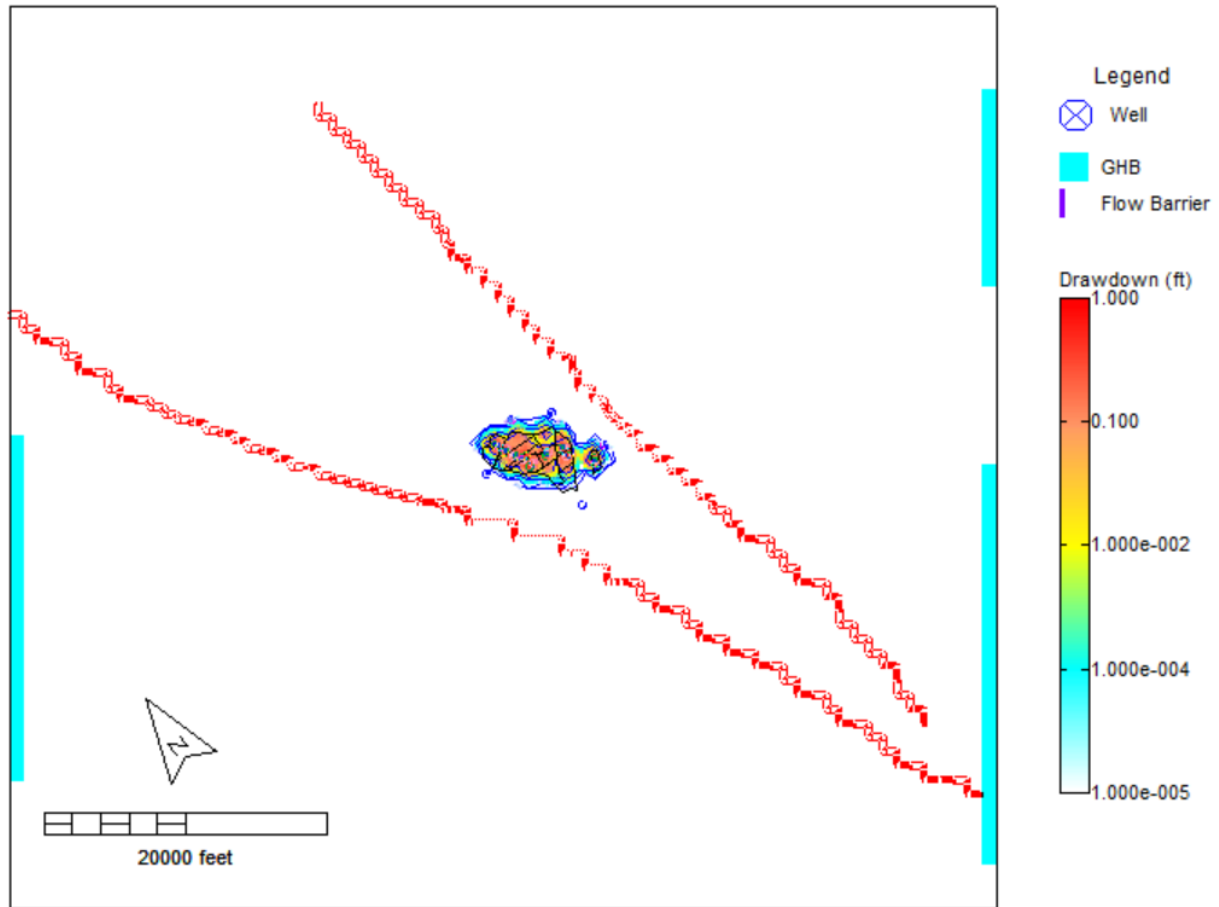




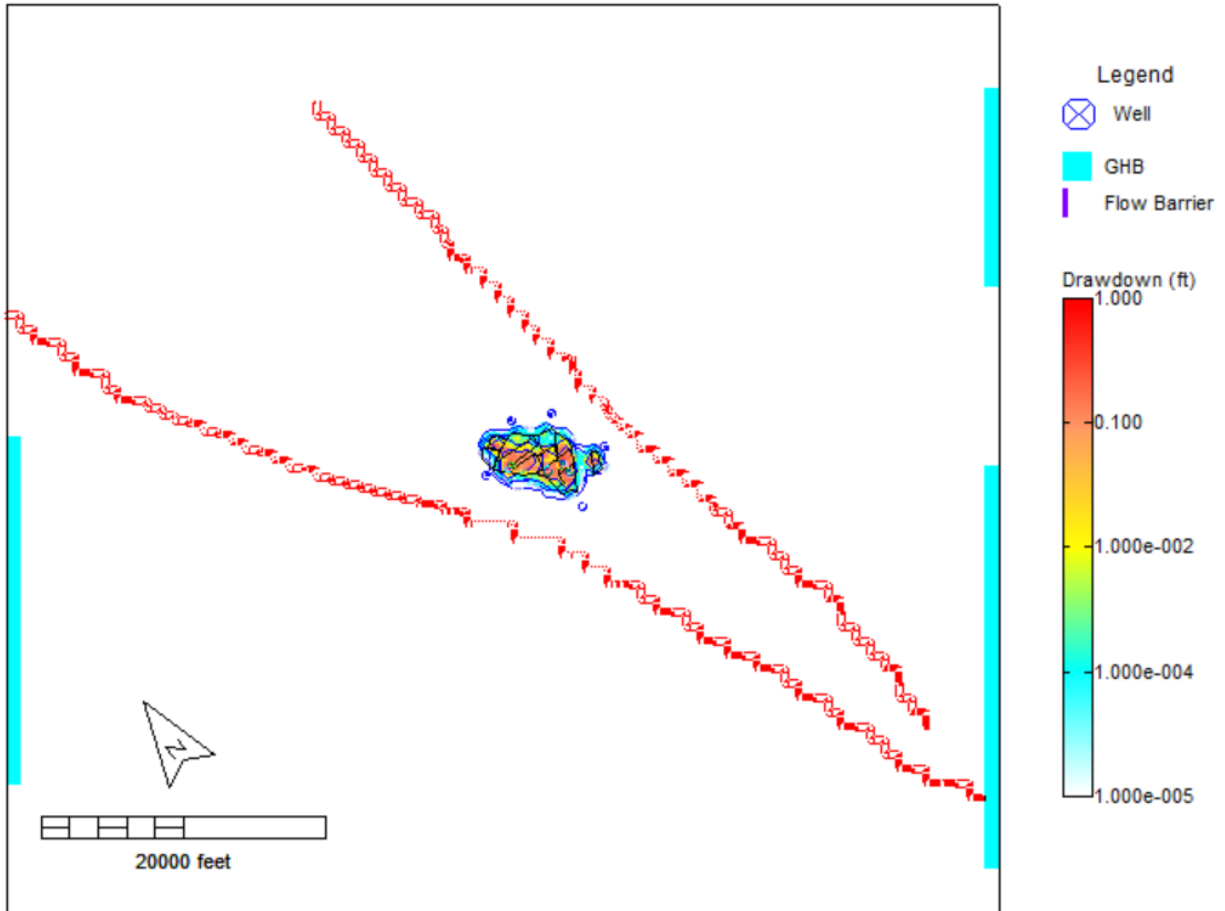
Layer 5



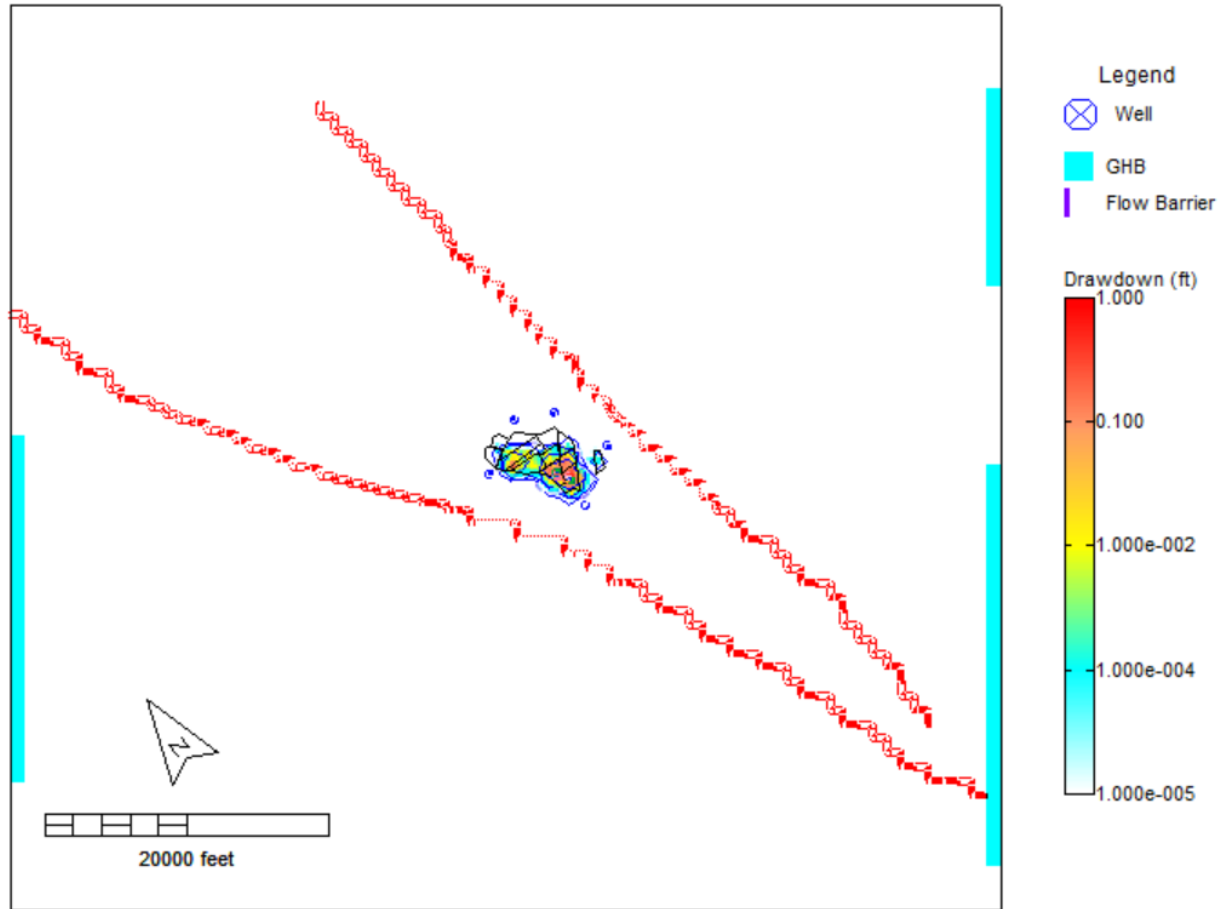
Layer 6



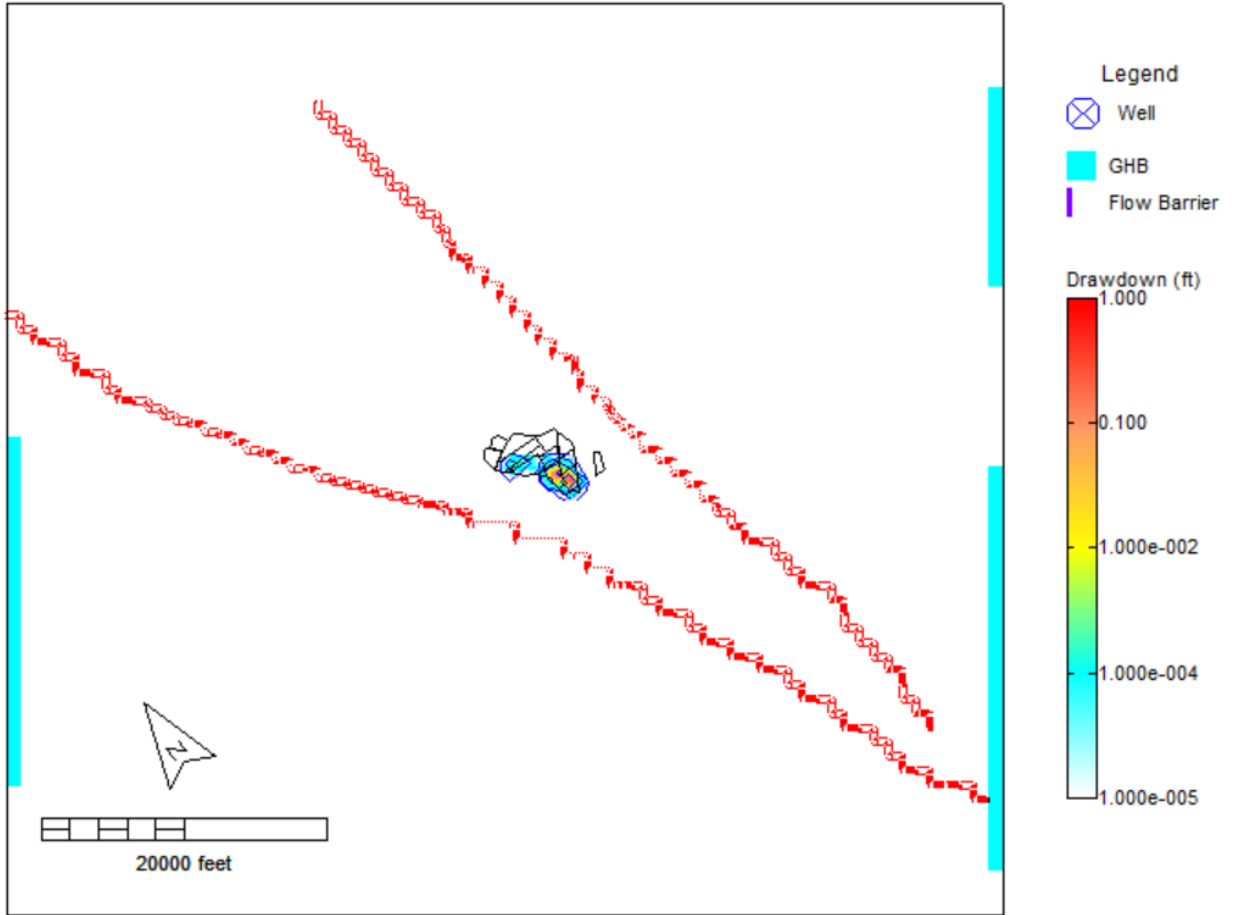
Layer 7



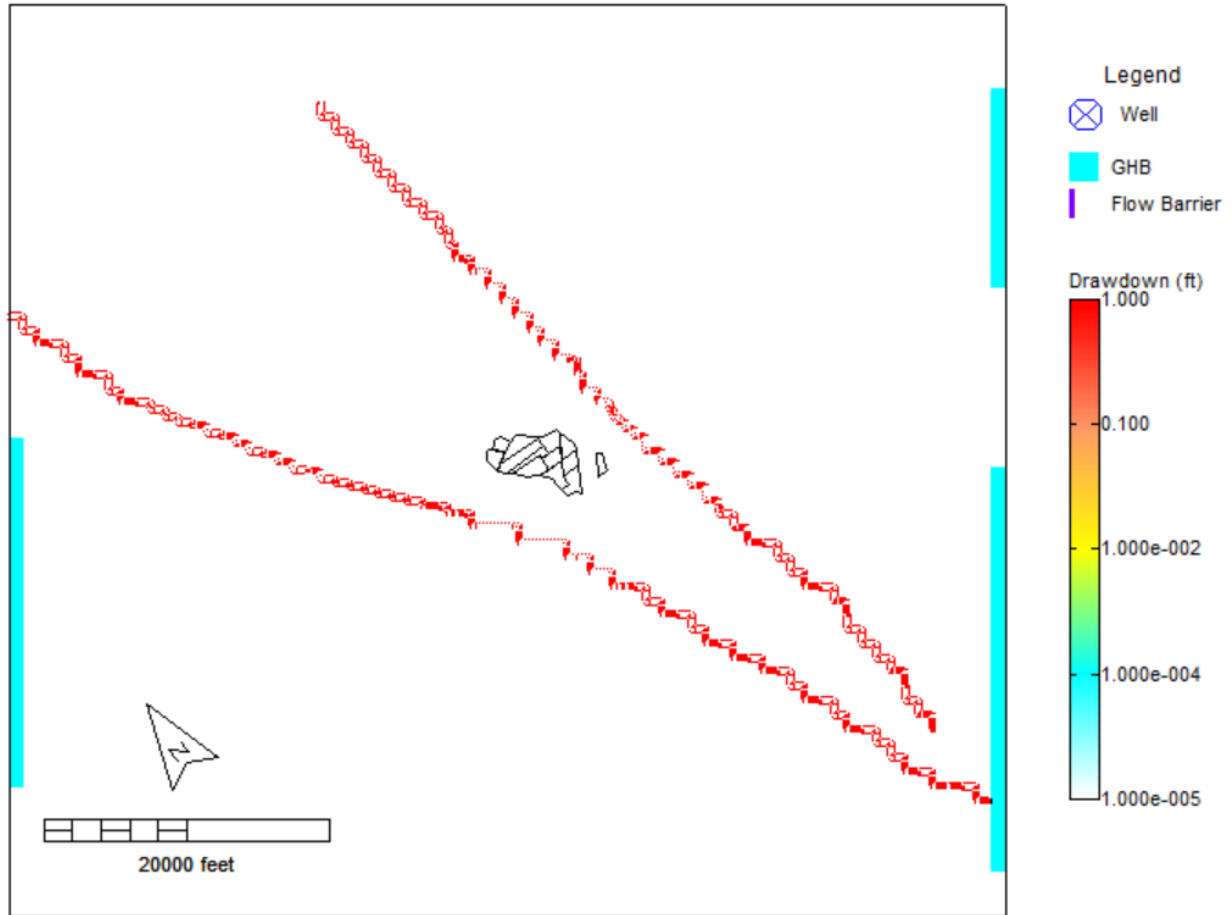
Layer 8



Layer 9



Layer 10

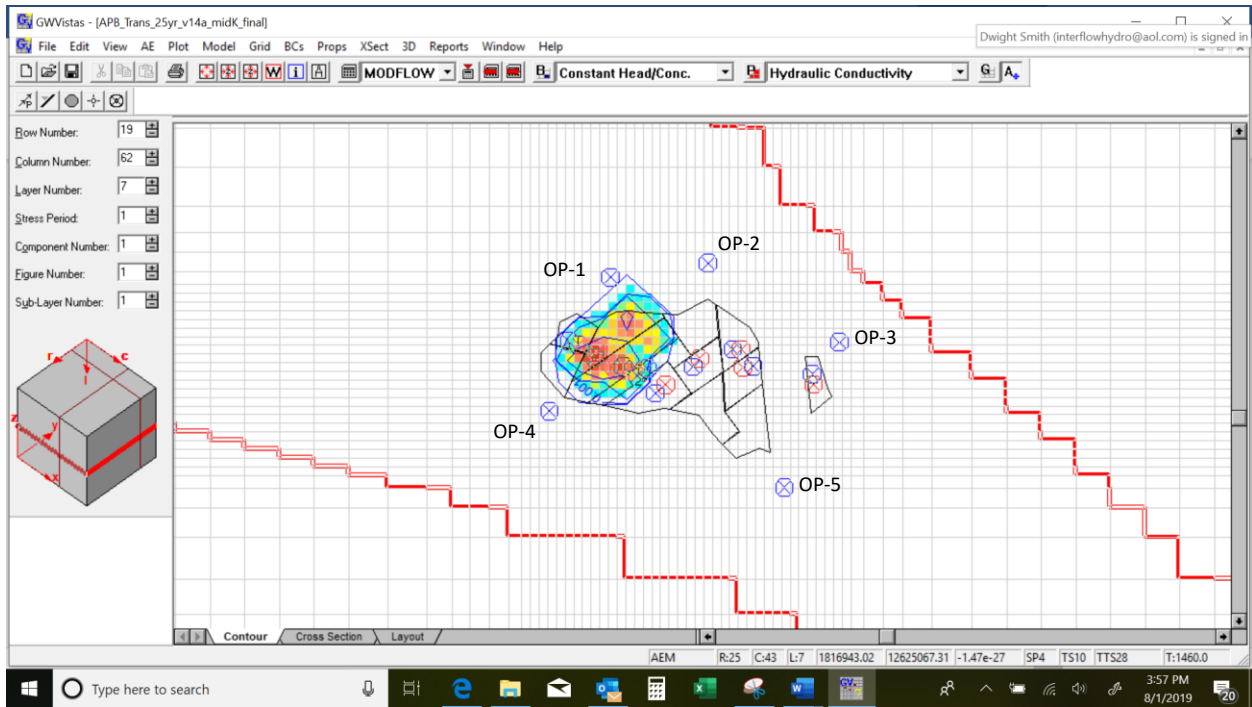


Layer 11

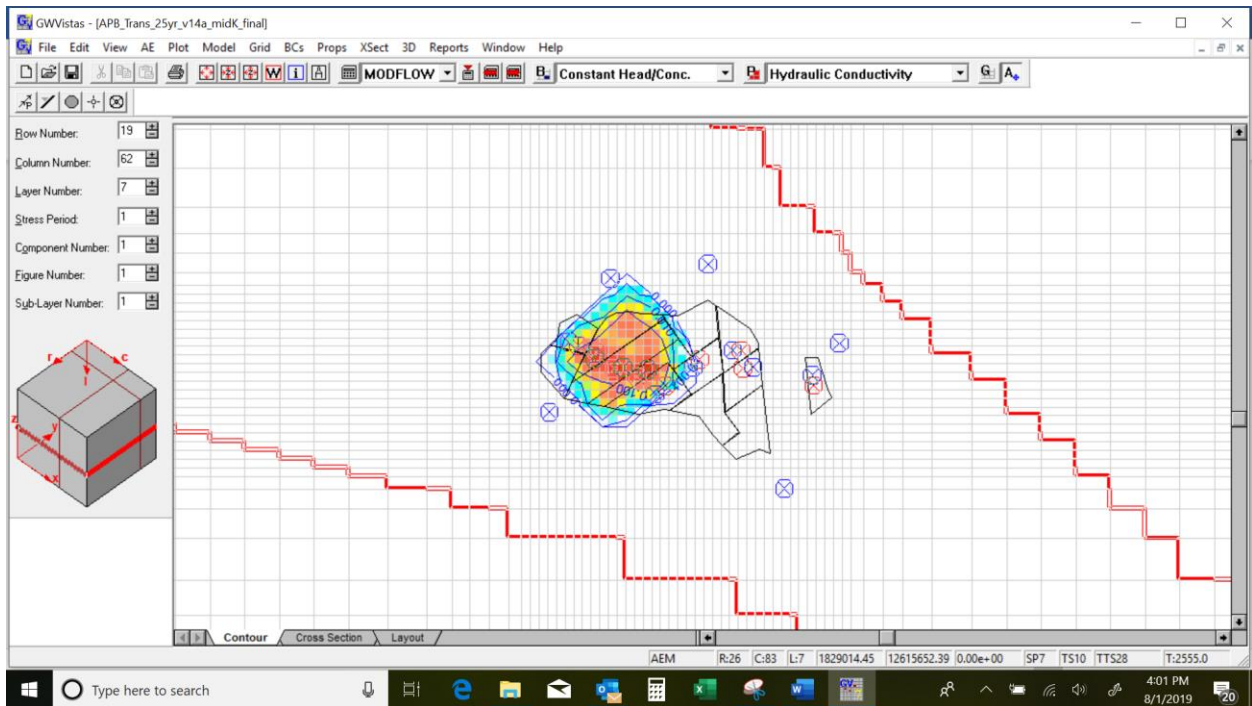
# APPENDIX C2

---

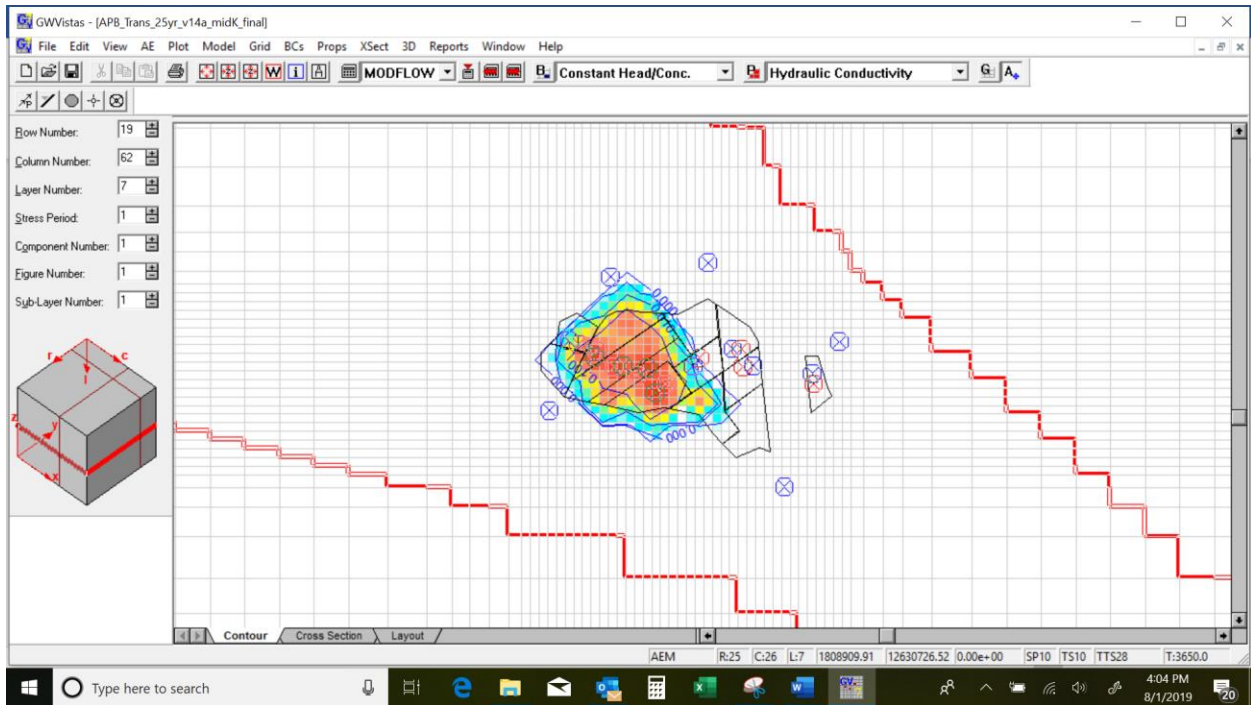




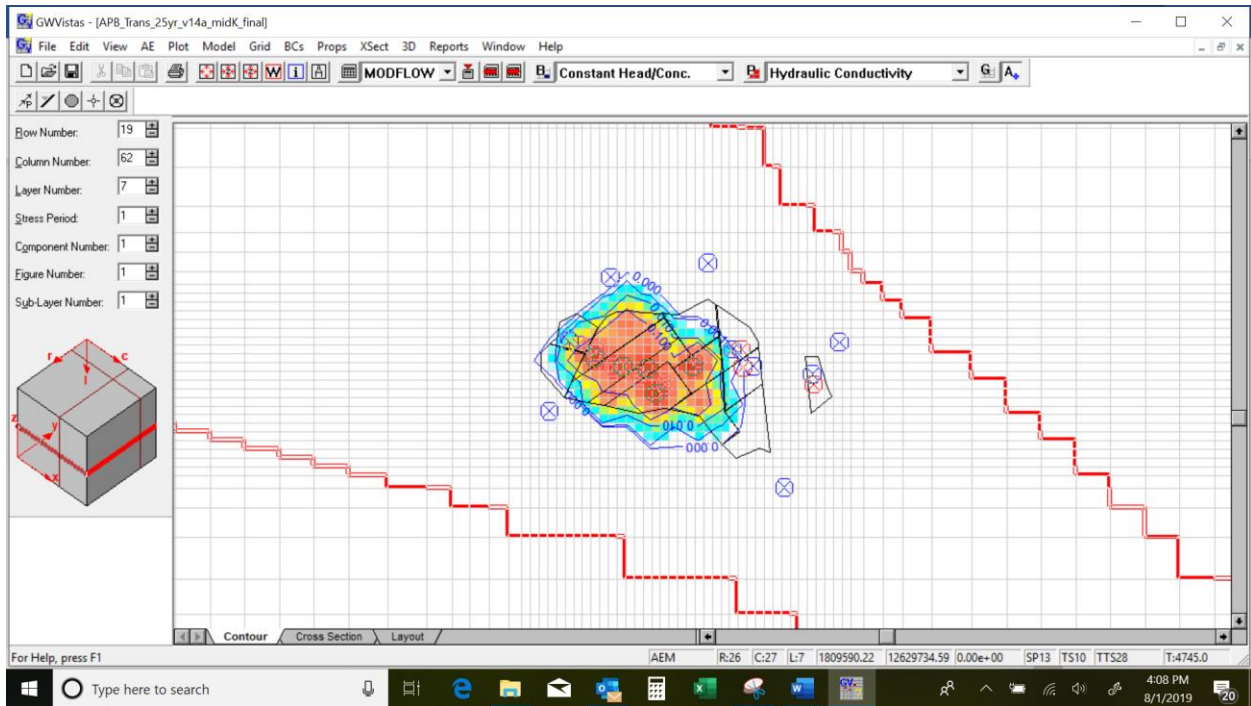
Mine Year 3



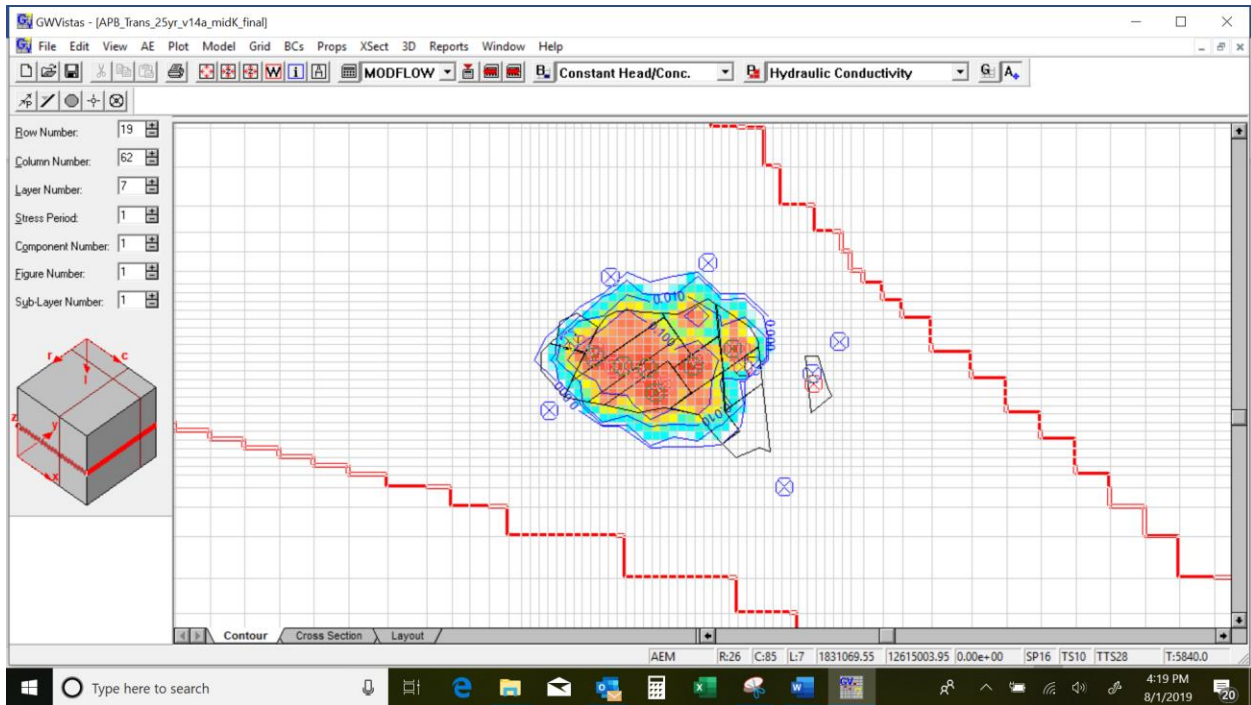
Mine Year 6



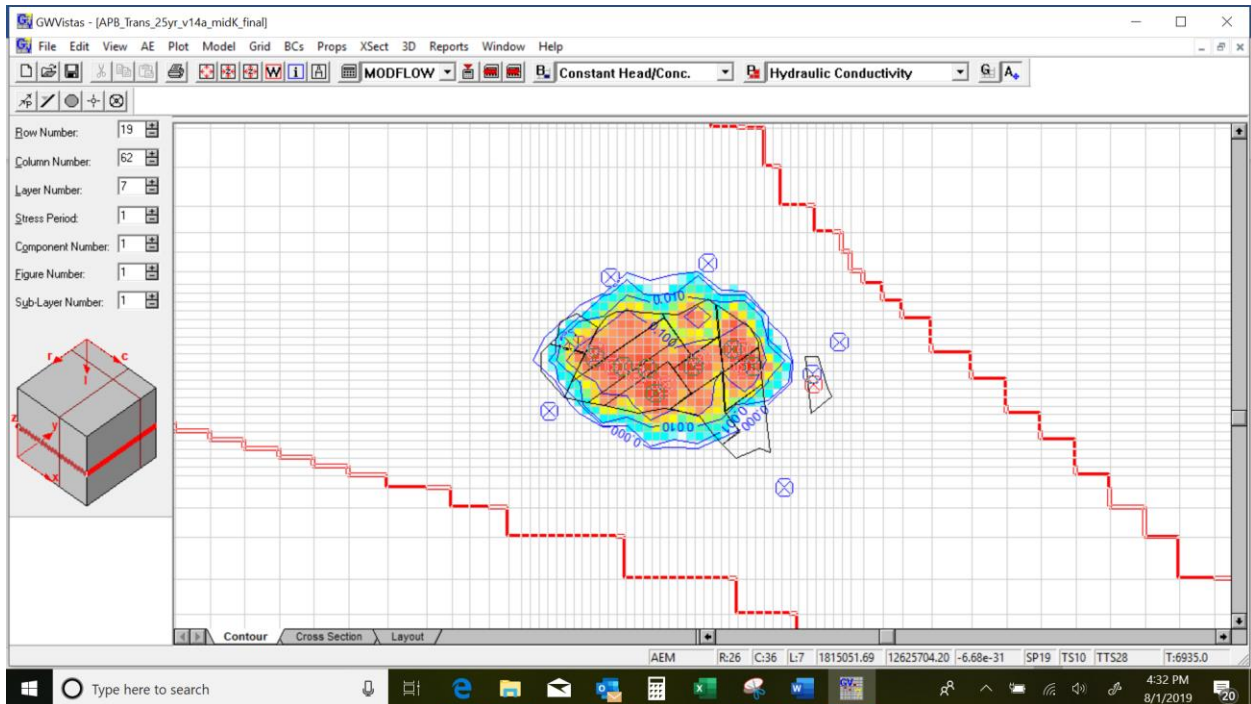
### Mine Year 9



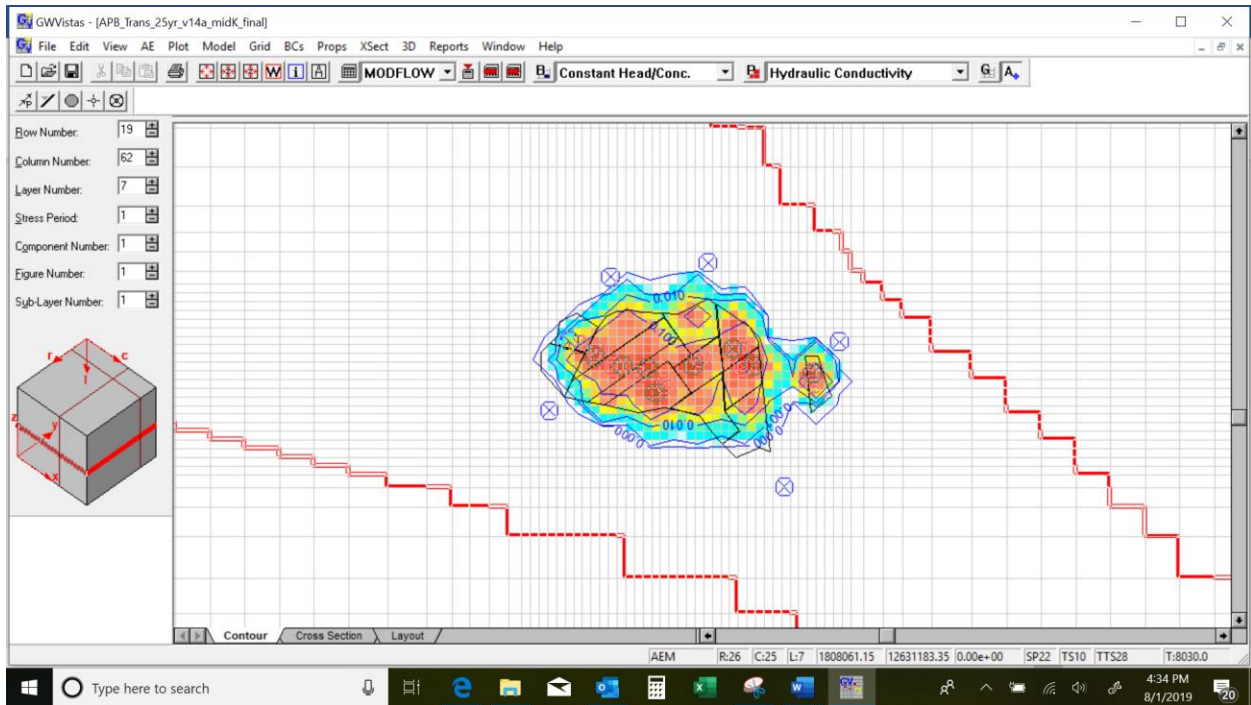
### Mine Year 12



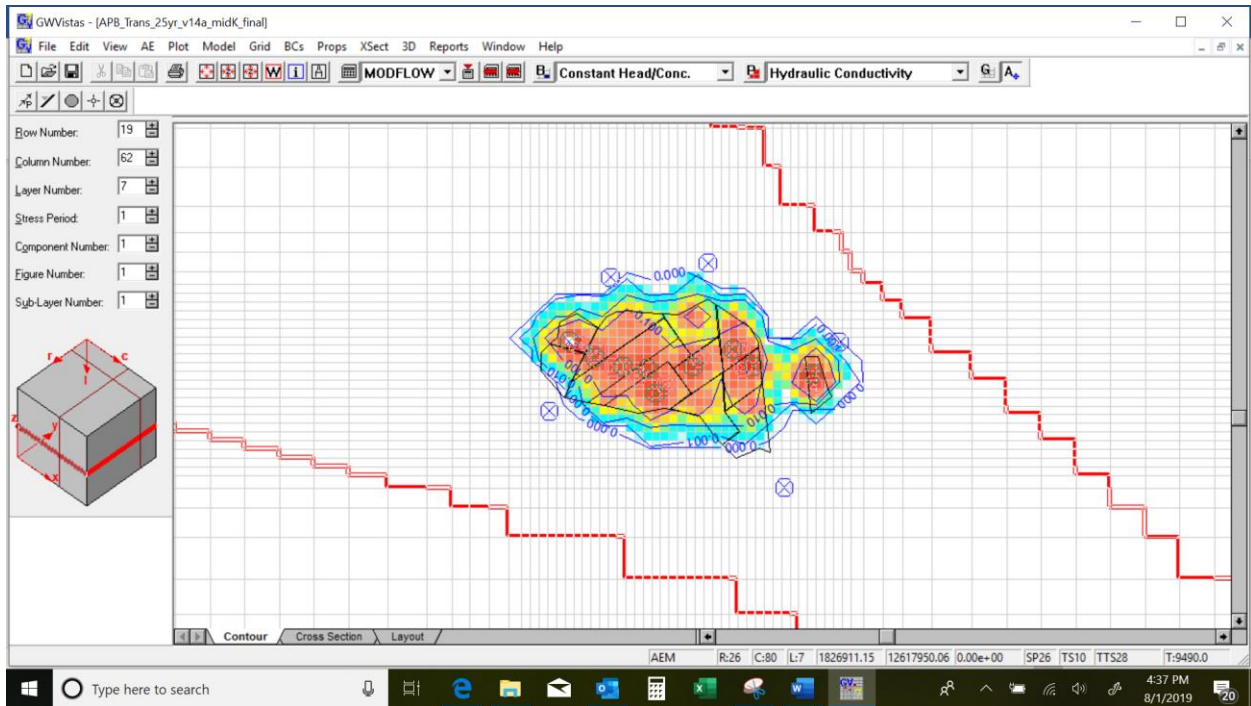
Mine Year 15



Mine Year 18



Mine Year 21



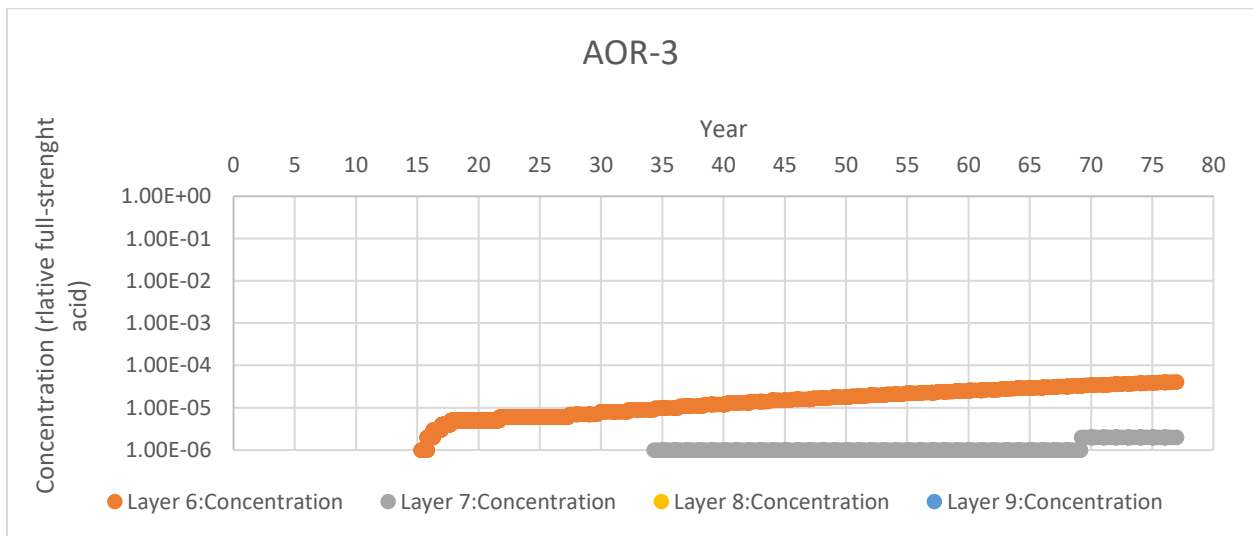
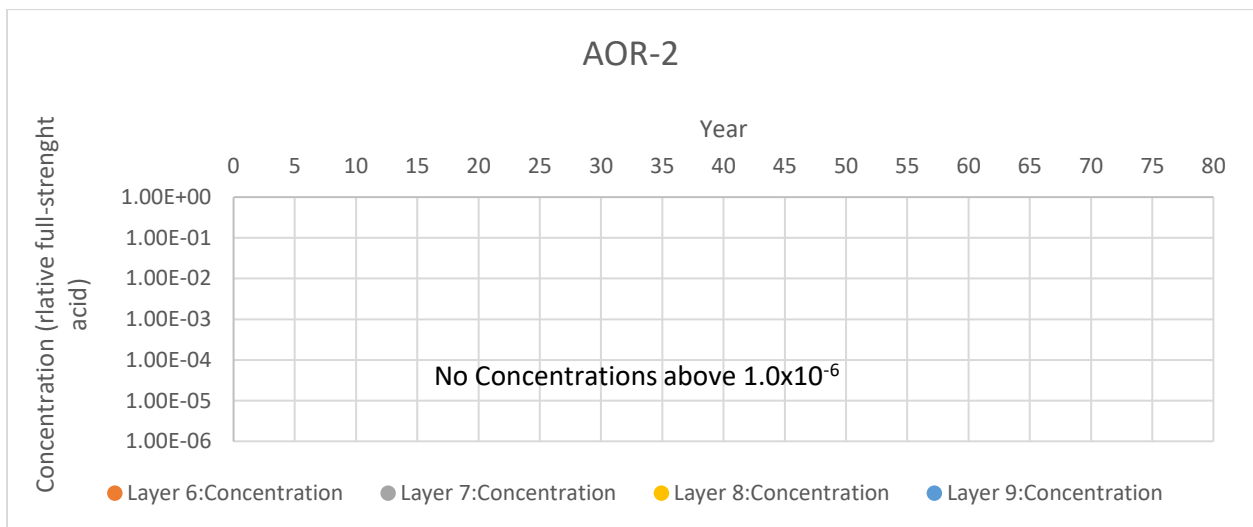
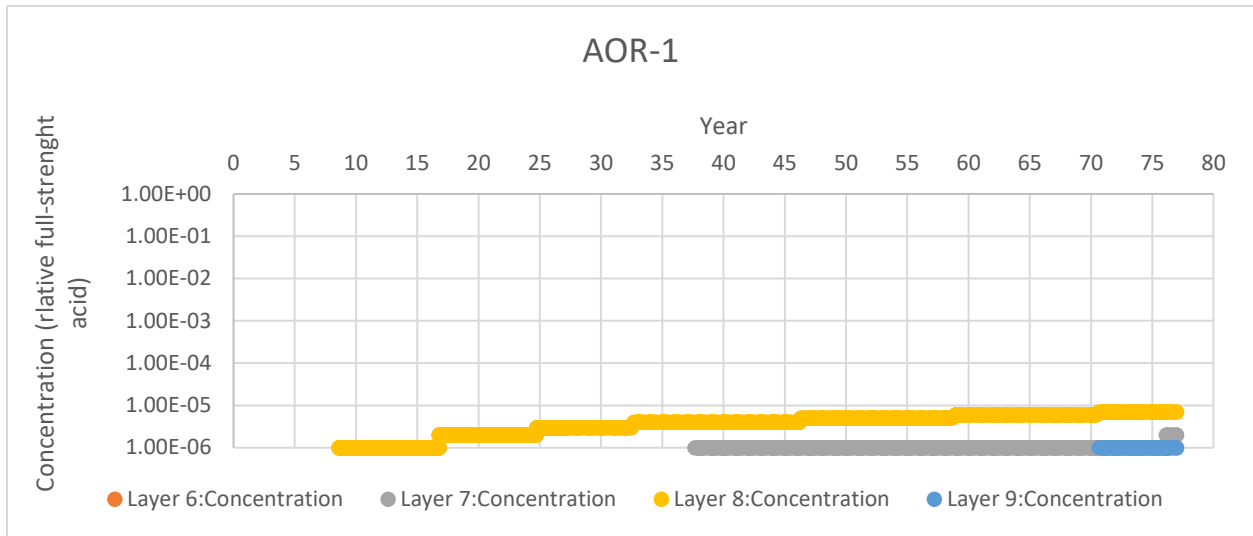
Mine Year 25

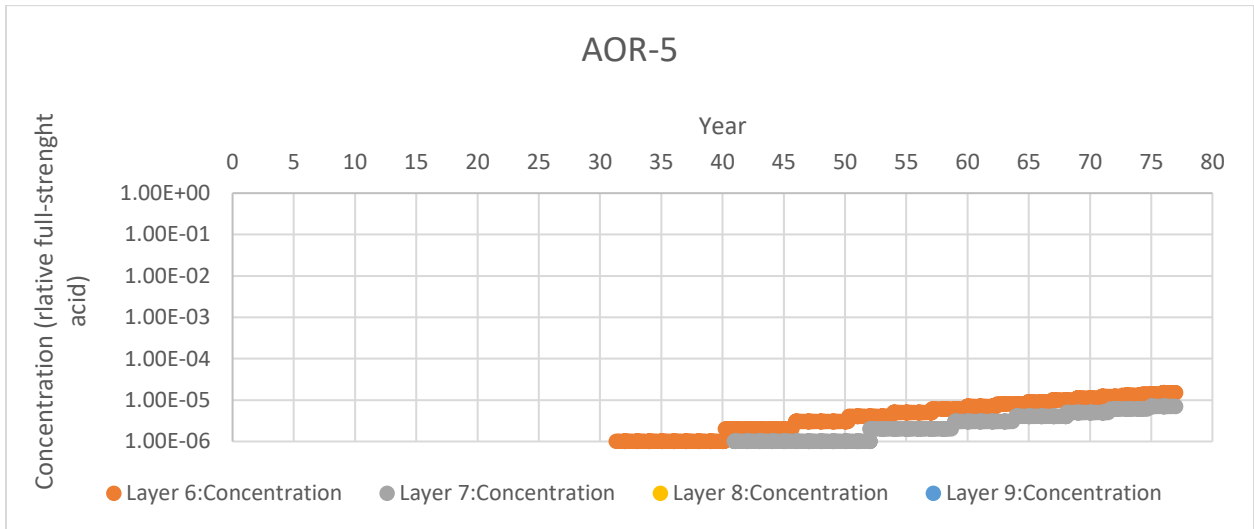
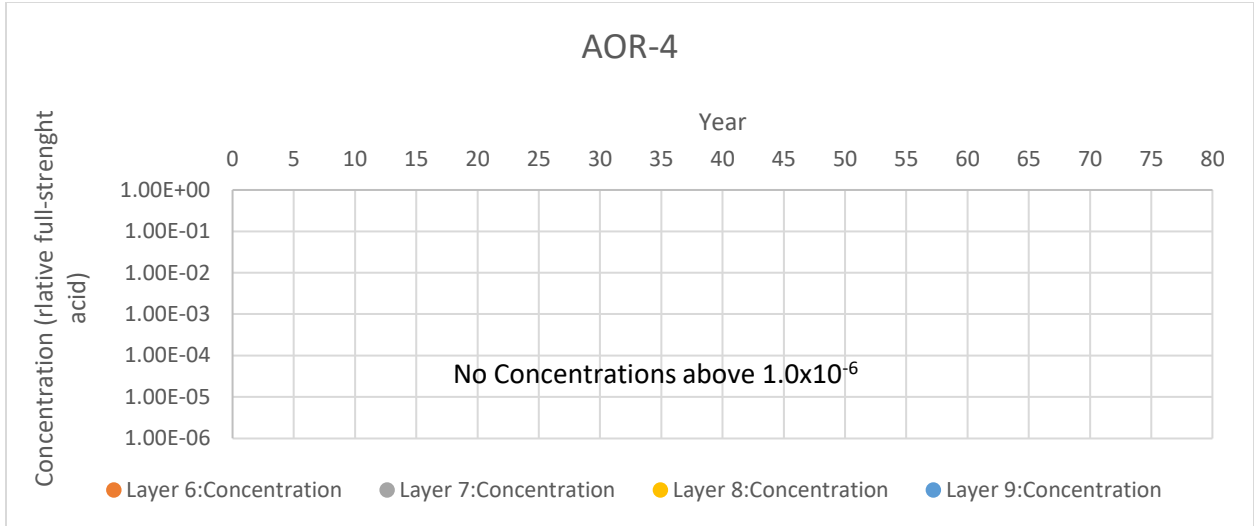
# APPENDIX D

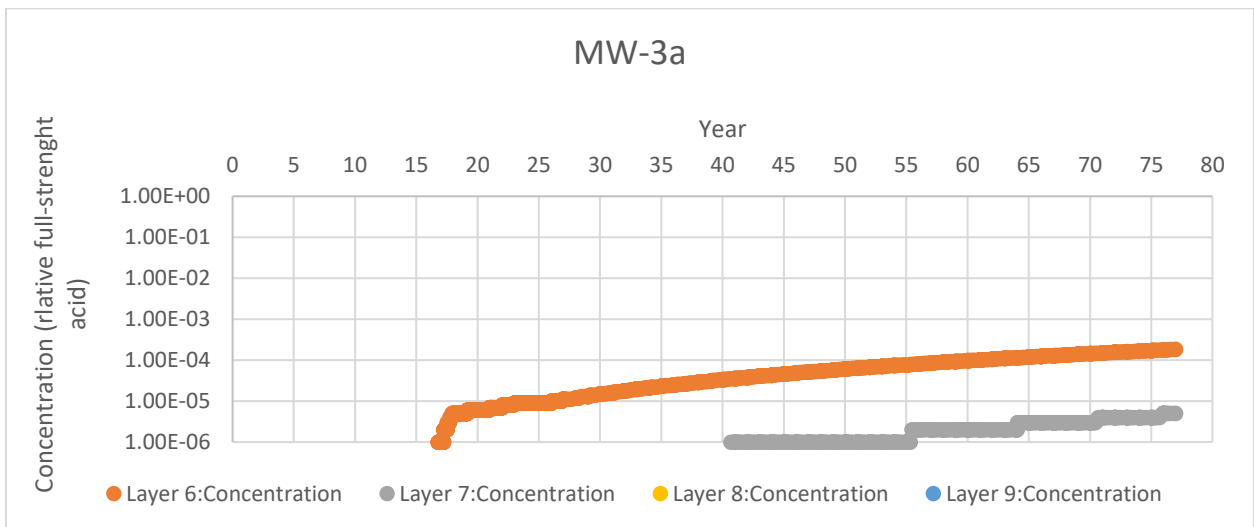
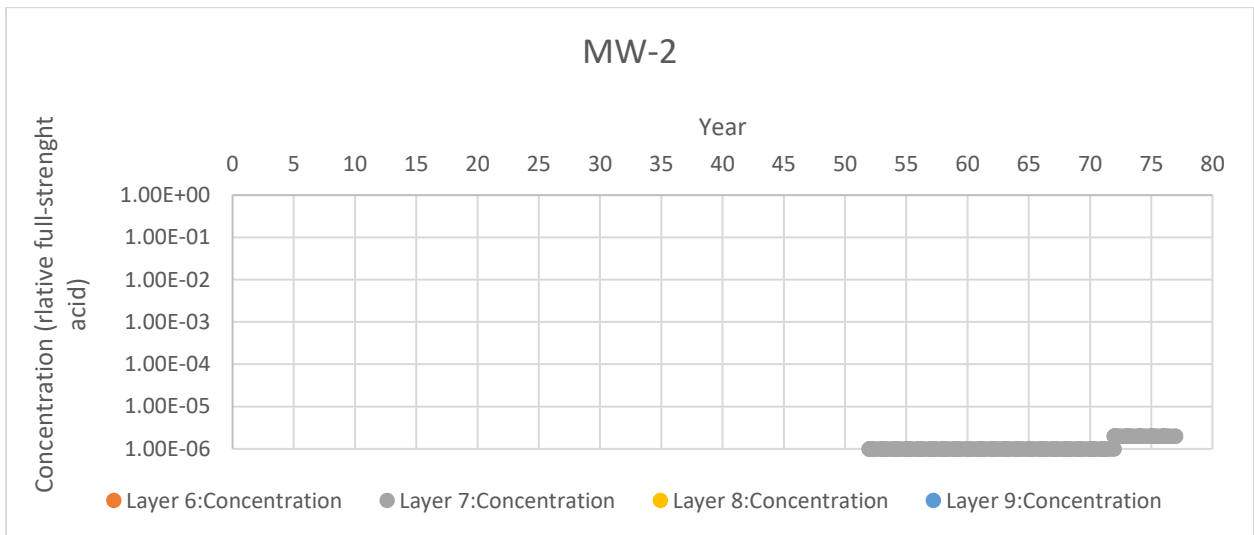
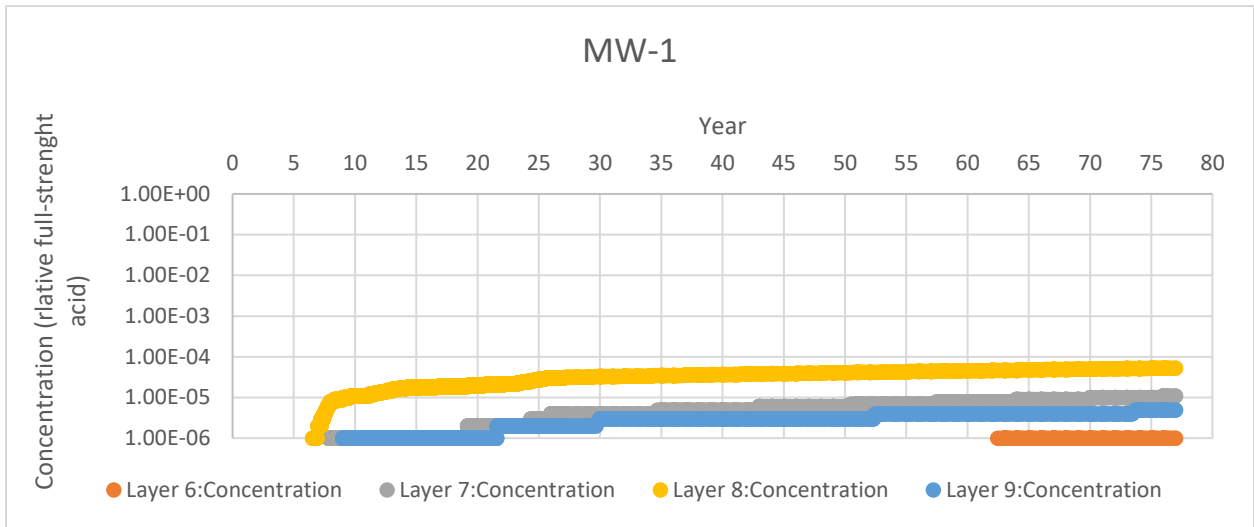
---



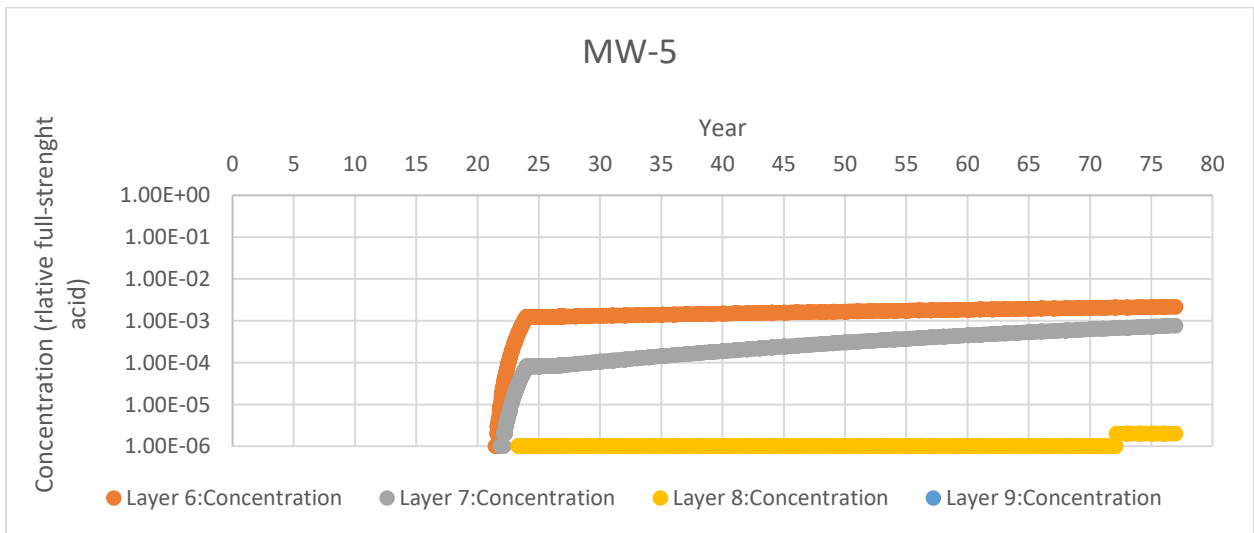
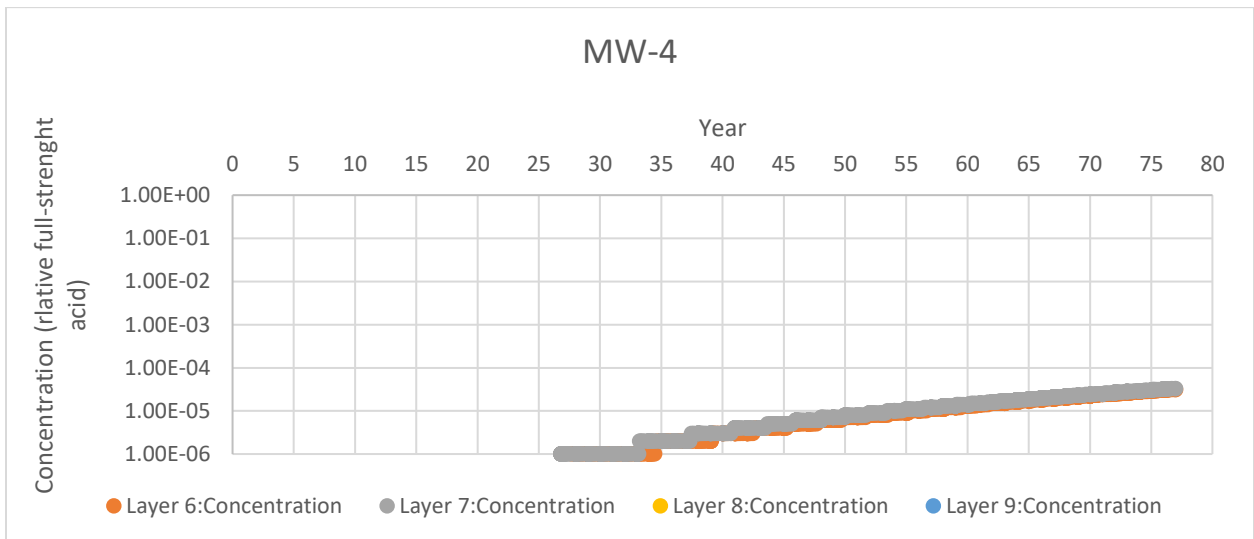
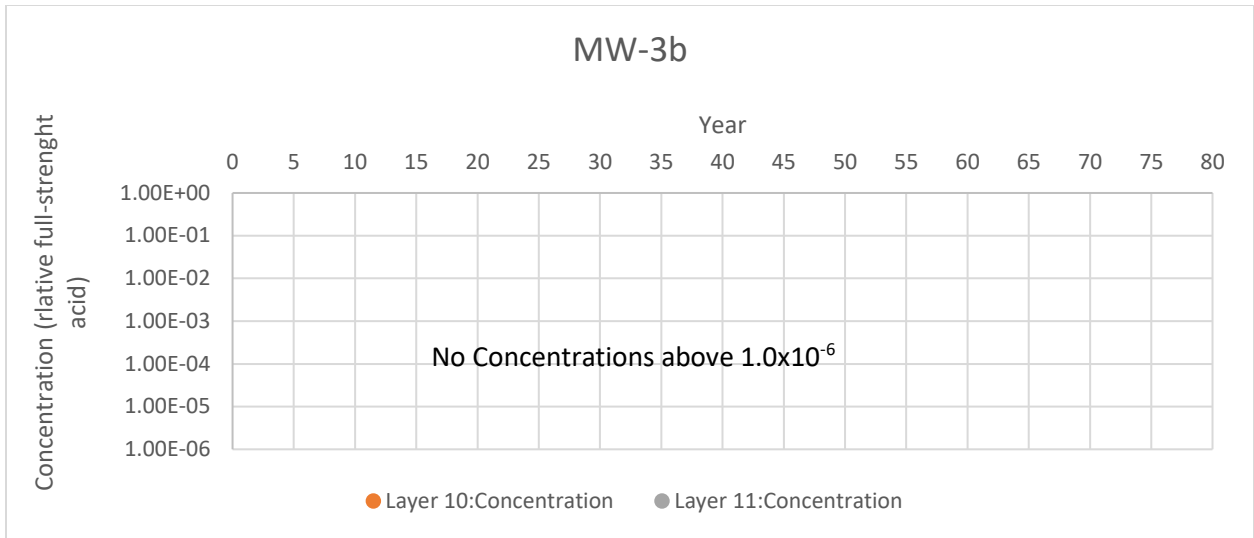
**Predicted Concentrations at AOR and ZEI Monitoring Wells and Observation Wells**

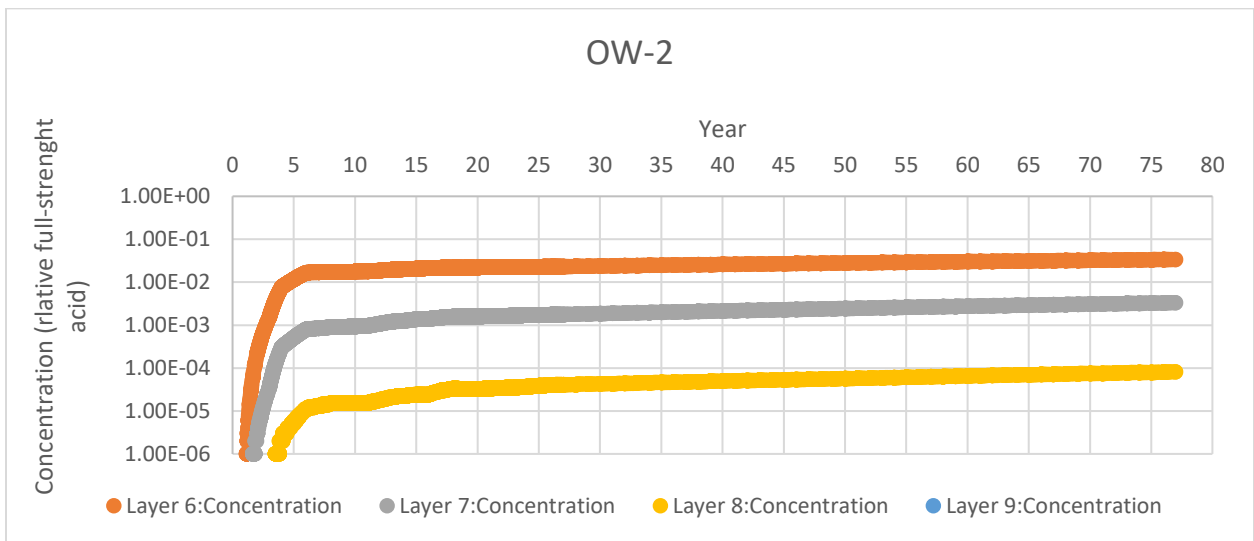
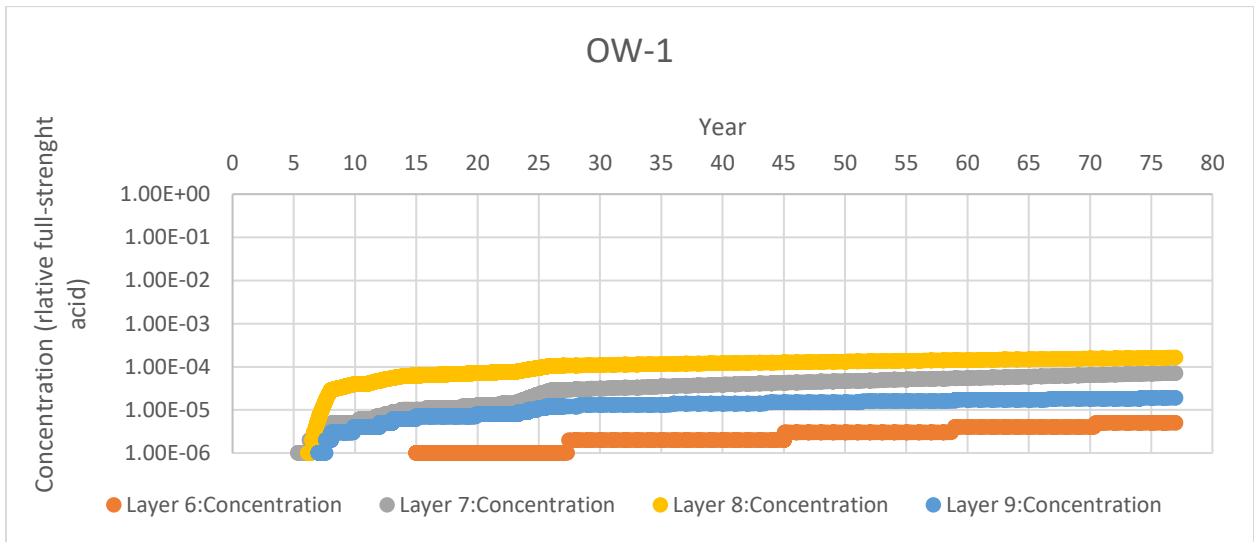


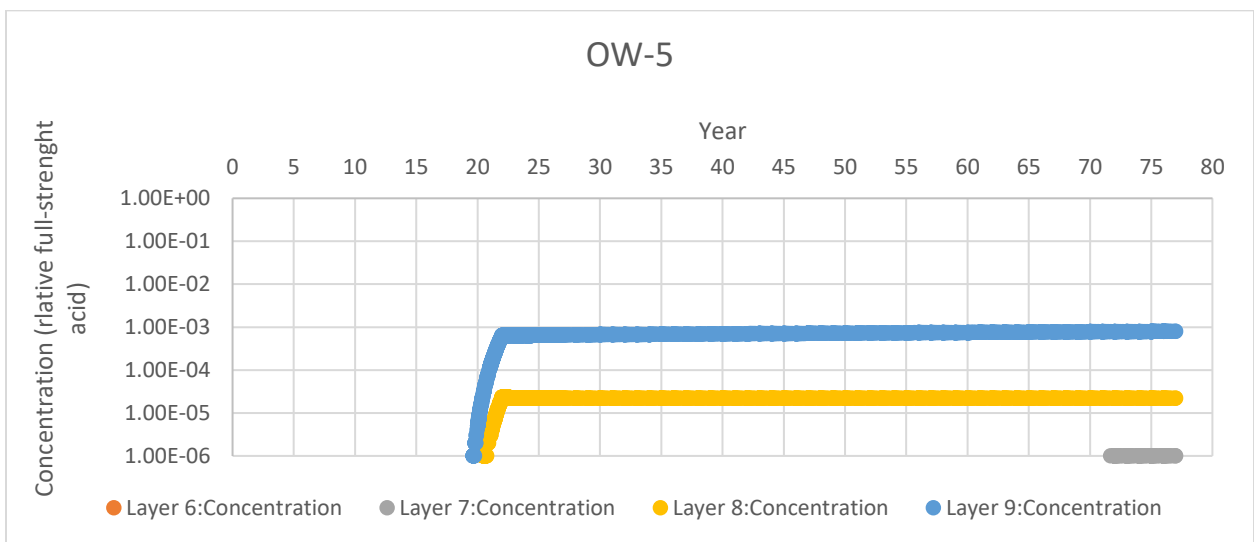
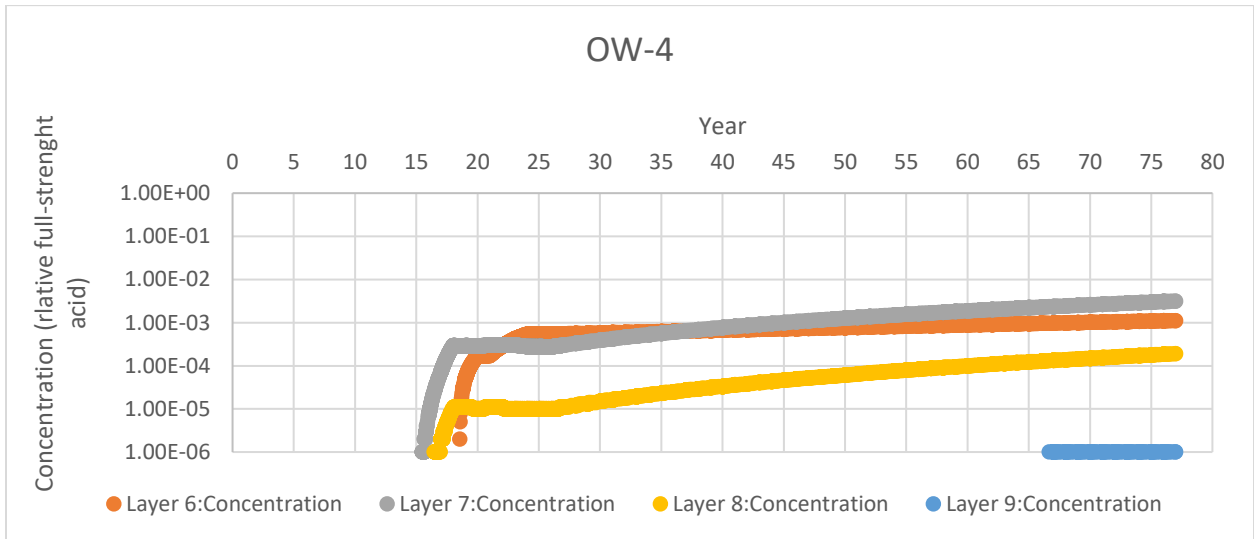
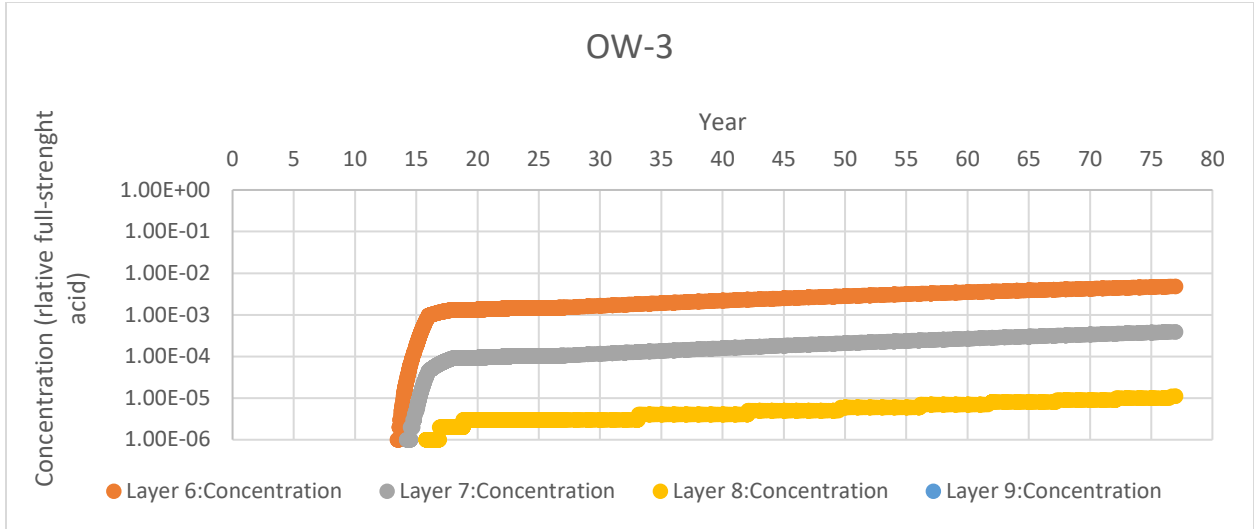


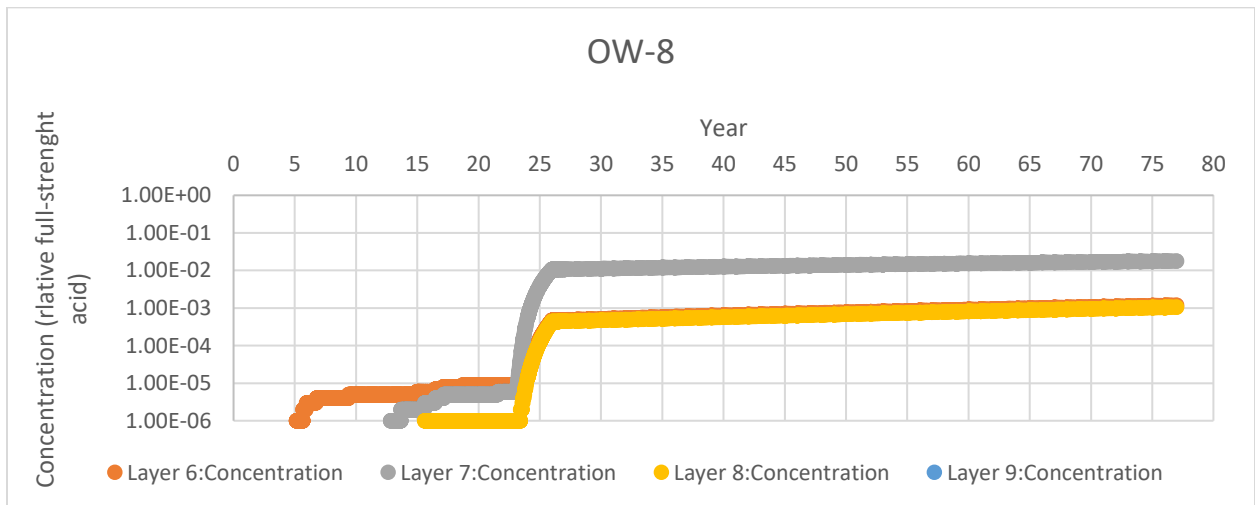
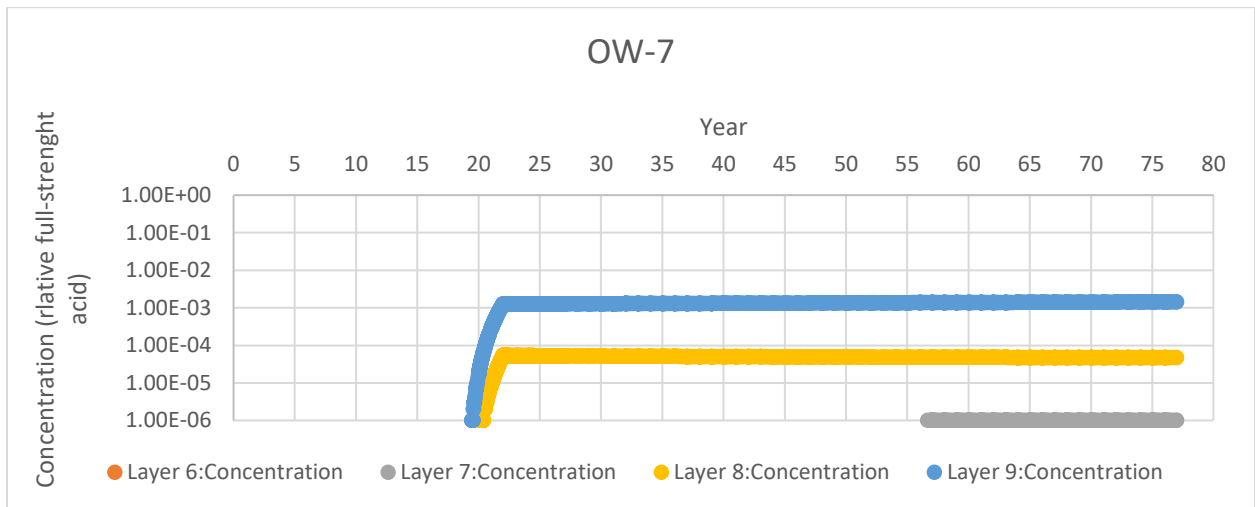
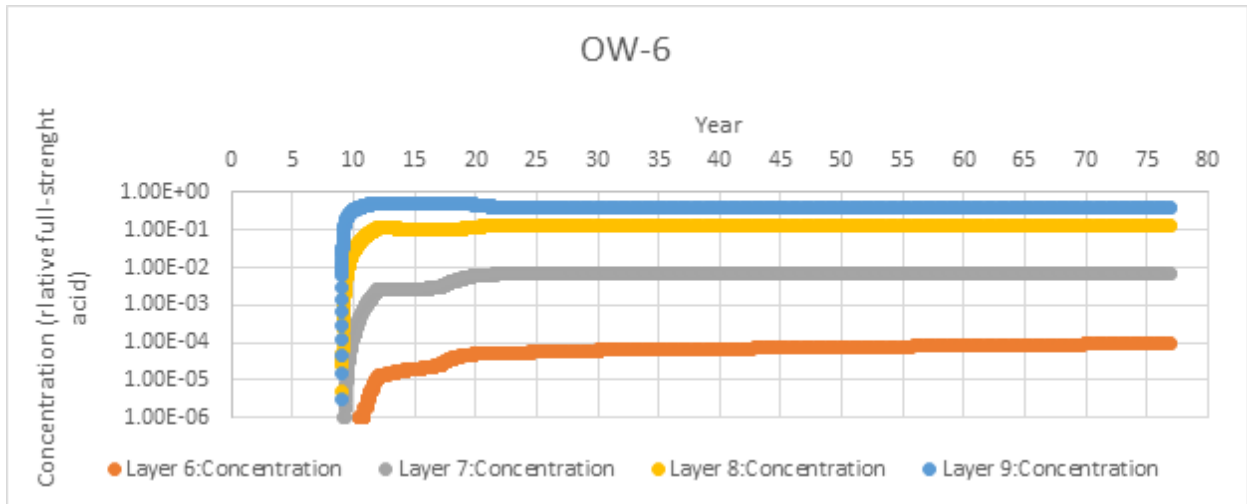












Predicted Potentiometric Head at AOR and ZEI Monitoring Wells and Observation Wells

